Prestressed Concrete Design

Second edition

M.K. Hurst

E & FN SPON
An Imprint of Routledge

Prestressed Concrete Design

This page intentionally left blank.

Prestressed Concrete Design

Second edition

M.K.Hurst MSc, DIC, MICE, MIStruct.E

E & FN SPON
An Imprint of Routledge
London and New York

To Alice and Maurice Hurst
and to my wife, Jeannie

This page intentionally left blank.

Contents

Preface

The purpose of this book is to explain the fundamental principles of design for prestressed concrete structures, and it is intended for both students and practising engineers. Although the emphasis is on design—the problem of providing a structure to fulfil a particular purpose—this can only be achieved if the designer has a sound understanding of the behaviour of prestressed concrete structures. This behaviour is described in some detail, with references to specialist literature for further information where necessary.

Guidance on the design of structures must inevitably be related to a code of practice and the one followed here is Eurocode 2: Design of concrete structures, Part 1 *General rules and rules for buildings,* DD ENV 1992–1–1:1992 (referred to below as EC2) which will supersede British Standard BS 8110:1985 *Structural Use of Concrete* covering the design of the buildings. The main purpose of this second edition is to outline the provisions of the new code as they relate to prestressed concrete design. The code is intended for use throughout Europe, although some clauses which relate specifically to practice in the UK are included in a National Application Document which accompanies the code and which is followed here. However, engineers are now able to design structures for acceptance in many countries other than their own. The basic design philosophy contained in the earlier codes, that of limit state design, has also been adopted in EC2 and the overall design of a given structure to the new code will be similar to that according to BS8110. Other aspects of design covered in BS8110 are yet to appear in EC2. In these cases reference is made to the relevant provisions of BS8110.

Strictly speaking, Part 1 of EC2 is a draft of the full code. However, it is unlikely that there will be any significant changes to Part 1 when the full code is finally published.

Part 2 of EC2 will cover the design of prestressed concrete bridges. The basic philosophy and nomenclature of Part 2 will be the same as Part 1. However, there will be some differences of detail, such as the requirements for the serviceability limit state.

No guidance is yet given in EC2 on the design of prestressed flat slabs, and reference is made to the Concrete Society Technical Report TR43 (1994): *Post-tensioned Concrete Floors—Design Handbook.* However, the

provisions of Part 1–3 of EC2, dealing with precast concrete structures, and Part 1–5 for unbonded tendons are described.

Most of the applications of prestressed concrete in buildings are in the form of simply supported beams, and this is reflected in the many examples throughout the book. Although some of these examples are of bridge decks, the subject of bridge design in general is beyond the scope of this book. Torsion of prestressed concrete members in buildings is rarely a problem and has not been covered here. Information on both of the above topics may be found by reference to the Bibliography. The Bibliography also refers to other types of prestressed concrete structures, such as axial tension and compression members, storage tanks and pressure vessels.

The calculations involved in prestressed concrete design are well suited to implementation by computer, with which most design offices are now equipped. In recognition of this, examples of the designs of the two basic types of prestressed concrete members, namely cracked and uncracked, have been included in Chapter 13 in the form of computer spreadsheets. Listings are given for the formulas contained in each cell, and these can be adapted for use with most of the spreadsheet programs currently available.

An overall view of the behaviour of prestressed concrete structures is given in Chapter 1. Chapter 2 deals with material properties, while limit state design is outlined in Chapter 3. The detailed considerations in the analysis and design of statically determinate prestressed concrete structures are dealt with in Chapters 4–10. Chapter 11 gives an introduction to statically indeterminate prestressed concrete structures and Chapter 12 outlines the design principles for the most important application of such structures in buildings, namely flat slabs, based on the provisions of TR43. Finally, Chapter 13 contains the computer spreadsheets noted above.

Problems are given at the ends of many of the chapters for further exercise. For rapid solution, some of these require the use of simple structural analysis or spreadsheet computer programs, which are widely available.

The extracts from British Standards are included by permission of the British Standards Institution, Linford Wood, Milton Keynes MK14 6LE, from whom complete copies of the Standards may be obtained.

Finally, thanks are due to Bill Mosley for his initial encouragement in the writing of this book and to Nick Clarke and Sarah Tester for all their help in the many aspects of the book's production.

Symbols

The symbols used in this book are in accordance with EC2 wherever possible. They, and other symbols used, are defined below and in the text where they first appear.

A_c	Cross-sectional area of member
A_{co}	Cross-sectional area of anchorage plates
A_{c1}	Maximum area corresponding to A_{co}
A_{ct}	Area of concrete in tension prior to first crack
$A_{c,beam}$	Cross-sectional area of beam in composite construction
$A_{c,slab}$	Cross-sectional area of slab in composite construction
A_p	Area of prestressing steel
A_s	Area of reinforcing steel
A_{sv}	Cross-sectional area of shear reinforcement across a horizontal joint
A_{sw}	Cross-sectional area of shear reinforcement
$A_{\bar{y}}$	First moment of area
b	Breadth of section
b_j	Width of interface
b_v	Length of side of critical perimeter
b_w	Minimum width of section
C	Compression
d	Effective depth
d_g	Nominal aggregate size
d_r	Drape of tendons
e	Eccentricity
e_s	Distance between centroids of slab and composite section
e_x	Eccentricity in x direction
e_y	Eccentricity in y direction
E_{ceff}	Effective modulus of elasticity of concrete
E_{cm}	Secant modulus of elasticity of concrete
E_{cmt}	Long-term modulus of elasticity of concrete
$E_{c,slab}$	Modulus of elasticity of slab concrete
E_s	Modulus of elasticity of steel
f_c	Maximum compressive stress
f_{ck}	Characteristic concrete cylinder strength

f_{ct}	Concrete tensile strength at time when cracks first expected to form
f_{ctm}	Characteristic concrete tensile strength
f_k	Characteristic strength
f_m	Mean strength
$(f_{max})_{qp}$	Maximum allowable concrete stress under quasi-permanent load
$(f_{max})_{ra}$	Maximum allowable concrete stress under rare load
f'_{max}	Maximum allowable concrete stress at transfer
f_{min}	Minimum allowable concrete stress under rare load
f'_{min}	Minimum allowable concrete stress at transfer
f_{pk}	Characteristic strength of prestressing steel
f_{yk}	Characteristic strength of reinforcement
f_{yv}	Characteristic strength of shear reinforcement
F_t	Total tensile force in a section
h	Overall depth of section
l_b	Second moment of area of beam
I_c	Second moment of area of concrete section
I_{comp}	Second moment of area of composite section
k	Profile coefficient
k_c	Stress distribution coefficient
l_{bp}	Transmission length
l_{bpd}	Design transmission length
L	Span
m	Modular ratio
M	Bending moment
M_{cr}	Bending moment to cause cracking
M_d	Bending moment due to beam and slab self weight
M_{des}	Design load bending moment
M_F	Fixed-end moment
M_{fr}	Frequent load bending moment
M_{max}	Maximum bending moment
M_o	Self weight bending moment
M_p	Prestress moment
M_{qp}	Quasi-permanent load bending moment
M_r	Moment of resistance for design load
M_{ra}	Rare load bending moment
M_{sd}	Ultimate bending moment at point of maximum shear
M_t	Ultimate bending moment transmitted from slab to column
M_u	Ultimate moment of resistance
M_{ult}	Ultimate bending moment
M_z	Bending moment to produce zero stress at tension face
M'	Moment due to unit point load
p	Loss of prestress force per unit length

P Prestress force

ΔP_A Loss of prestress force due to anchorage draw-in

P_e Effective prestress force after elastic shortening

P_o Initial force in tendons

P_x Prestress force in x direction

p_y Prestress force in y direction

P^* Prestress force across side of critical perimeter

P' Initial small force in tendons

r Radius of gyration

r_{ps} Radius of curvature of tendons

$1/r$ Curvature

$1/r_b$ Curvature at midspan of beam or support of cantilever

$1/r_m$ Effective curvature

$1/r_1$ Curvature of uncracked section

$1/r_2$ Curvature of cracked section

s_{rm} Average crack spacing

s_v Spacing of links

T Tension

T_d Force in longitudinal reinforcement

T_f Final cable tension

T_o Initial cable tension

u Critical perimeter

v_c Allowable ultimate concrete shear stress

V Shear force

V_{cr} Ultimate shear resistance along one side of critical perimeter

V_{eff} Effective shear force in a slab

V_{Rd1} Shear resistance of section without reinforcement

V_{Rd2} Maximum shear resistance of a section

V_{sd} Ultimate shear force

V_t Ultimate support reaction at a column

w Uniformly distributed load

w_d Dead load

w_{fr} Frequent uniform load

w_k Characteristic crack width

w_o Self weight

w_{qp} Quasi-permanent uniform load

w_{ra} Rare uniform load

w_{ult} Ultimate uniform load

W Point load

x Neutral axis depth

x_A Length of anchorage draw-in effect

y Displacement

$\bar{y}$ Depth to centroid of section

z Lever arm

Z_b	Section modulus for bottom fibre
$Z_{b,beam}$	Section modulus for bottom of beam in composite section
$Z_{b,comp}$	Section modulus for bottom of composite section
Z_t	Section modulus for top fibre
$Z_{t,comp}$	Section modulus for top of composite section
Z^*	Section modulus for top fibre over length of side of critical perimeter
α	Short-term prestress loss factor
β	Long-term prestress loss factor
β_1	Bond coefficient
β_2	Load duration coefficient
β_b	Transmission length factor
γ_f	Partial factor of safety for load
γ_m	Partial factor of safety for materials
γ_P	Partial factor of safety for prestressing
δ	Ratio of bending moments at a section after and before redistribution
δ	Beam deflection
δ_{ad}	Anchorage draw-in
δ_d	Dead-load deflection
δ_e	Expected elongation of tendon
δ_{ex}	Extra elongation of tendon after taking up of slack
δ_{qp}	Quasi-permanent load deflection
δ_M	Deflection of beam due to end-moments
δ_o	Deflection at transfer
δ_R	Deflection of beam due to point load
δ_{sh}	Deflection due to shrinkage
ε_c	Concrete strain
ε_{cu}	Ultimate concrete strain
ε_P	Total strain in tendons
ε_{pb}	Strain in tendons due to bending
ε_{pe}	Effective prestrain in tendons
ε_{pk}	Characteristic ultimate strain in tendons
ε_s	Steel strain
ε_{sh}	Shrinkage strain
ε_{sm}	Average concrete strain at level of tendons
ζ	Distribution coefficient
μ	Coefficient of friction
ϱ	Shear reinforcement ratio across a joint
ϱ_l	Tension reinforcement ratio
ϱ_w	Minimum shear reinforcement ratio
$\Delta\sigma_p$	Reduction in tendon stress due to elastic shortening
$\Delta\sigma_{pr}$	Variation in tendon stress due to steel relaxation
σ	Standard deviation

σ_b	Stress at bottom of section
$\sigma_{b,beam}$	Stress at bottom of beam in composite section
$\sigma_{b,slab}$	Stress at bottom of slab in composite section
σ_{b25}	Stress at point 25 mm below lowest tendon
σ_{cg}	Stress in concrete at level of tendons
σ_{cp}	Axial stress in concrete
σ_{cpo}	Stress in concrete at level of tendons due to prestressing
σ_d	Stress in longitudinal reinforcement
σ_p	Total stress in tendons
σ_{pb}	Stress in tendons due to bending
σ_{pe}	Effective prestress in tendons
σ_{po}	Initial stress in tendons
σ_{pu}	Ultimate stress in tendons
σ_N	Normal stress across a joint
σ_s	Steel stress under frequent load
σ_{sr}	Steel stress under load to cause cracking
σ_t	Stress at top of section
$\sigma_{t,beam}$	Stress at top of beam in composite section
$\sigma_{t,slab}$	Stress at top of slab in composite section
τ_{Rd}	Basic concrete shear strength
τ_{Rdj}	Shear resistance across horizontal joint
τ_{sdj}	Shear stress across horizontal joint
φ	Creep coefficient

This page intentionally left blank.

1

Basic principles

1.1 INTRODUCTION

Prestressed concrete is the most recent of the major forms of construction to be introduced into structural engineering. Although several patents were taken out in the last century for various prestressing schemes, they were unsuccessful because low-strength steel was used, with the result that long-term effects of creep and shrinkage of the concrete reduced the prestress force so much that any advantage was lost. It was only in the early part of the twentieth century that the French engineer Eugène Freyssinet approached the problem in a systematic way and, using high-strength steel, first applied the technique of prestressing concrete successfully. Since then prestressed concrete has become a well-established method of construction, and the technology is available in most developed, and in many developing, countries. An account of some of the early developments in prestressed concrete is given in Walley (1984).

The idea of prestressing, or preloading, a structure is not new. Barrels were, and still are, made from separate wooden staves, kept in place by metal hoops. These are slightly smaller in diameter than the diameter of the barrel, and are forced into place over the staves, so tightening them together and forming a watertight barrel (Fig 1.1). Cartwheels were similarly prestressed by passing a heated iron tyre around the wooden rim of the wheel. On cooling, the tyre would contract and be held firmly in place on the rim (Fig. 1.2), thus strengthening the joints between the spokes and the rim by putting them into compression.

The technique of prestressing has several different applications within civil engineering, often being used to keep cables taut when subjected to compressive forces. However, by far the most common application is in prestressed concrete where a prestress force is applied to a concrete member, and this induces an axial compression that counteracts all, or part of, the tensile stresses set up in the member by applied loading.
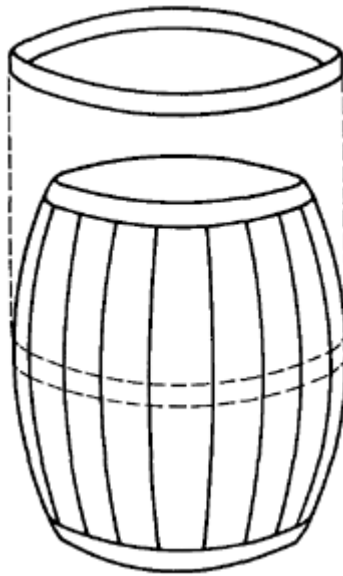
Figure 1.1 Barrel staves compressed with hoops.
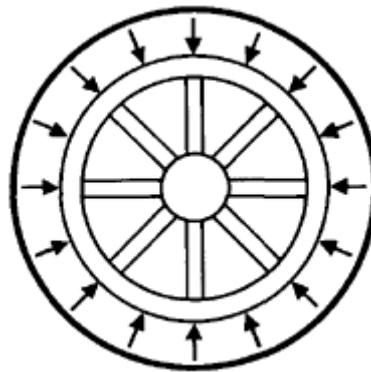
Figure 1.2 Cartwheel compressed by contracting tyre.

Within the field of building structures, most prestressed concrete applications are in the form of simply supported precast floor and roof beams (Fig. 1.3). These are usually factory-made, where the advantages of controlled mass production can be realized. Where large spans are required, *in situ* prestressed concrete beams are sometimes used, and *in situ* prestressed concrete flat slab construction is increasingly being employed. This last technique is often associated with that of the lift slab, whereby whole floor slabs are cast and tensioned at ground level, and then jacked up into their final position.

In the field of bridge engineering, the introduction of prestressed

concrete has aided the construction of long-span concrete bridges. These often comprise precast units, lifted into position and then tensioned against the units already in place, the process being continued until the span is complete. For smaller bridges, the use of simply supported precast prestressed concrete beams has proved an economical form of construction, particularly where there is restricted access beneath the bridge for construction. The introduction of ranges of standard beam sections has simplified the design and construction of these bridges (Fig. 1.4).

Some further examples of the many applications of prestressed concrete are shown in Fig 1.5–1.8.
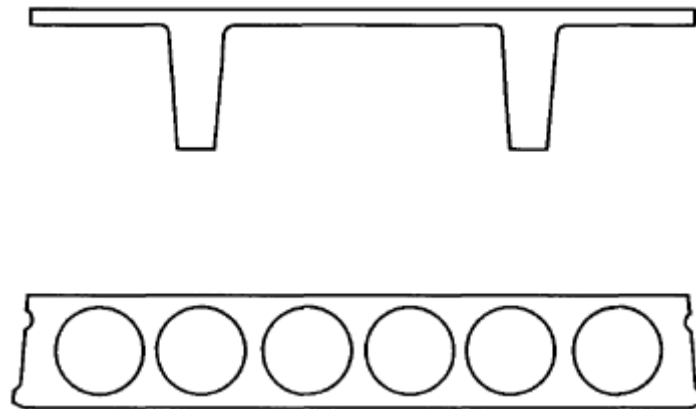
Figure 1.3 Examples of precast beams.
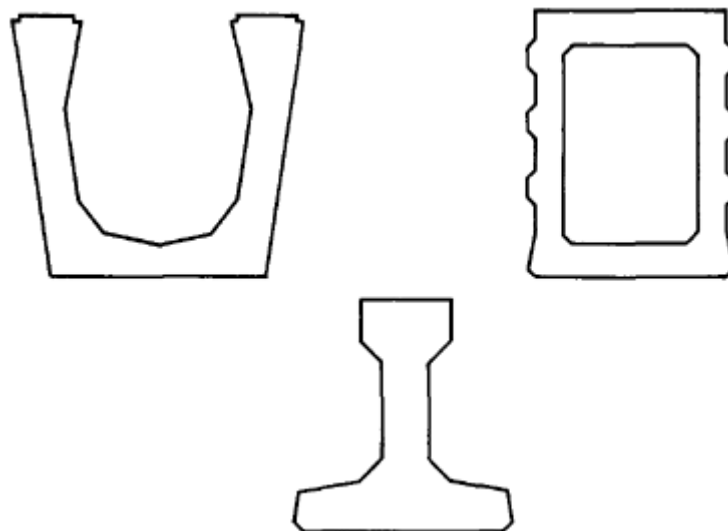
Figure 1.4 Examples of standard bridge beams.

Figure 1.5 Externally prestressed bridge deck *(courtesy VSL International)*.

Figure 1.6 Prestressed flat slab construction *(courtesy VSL International)*.
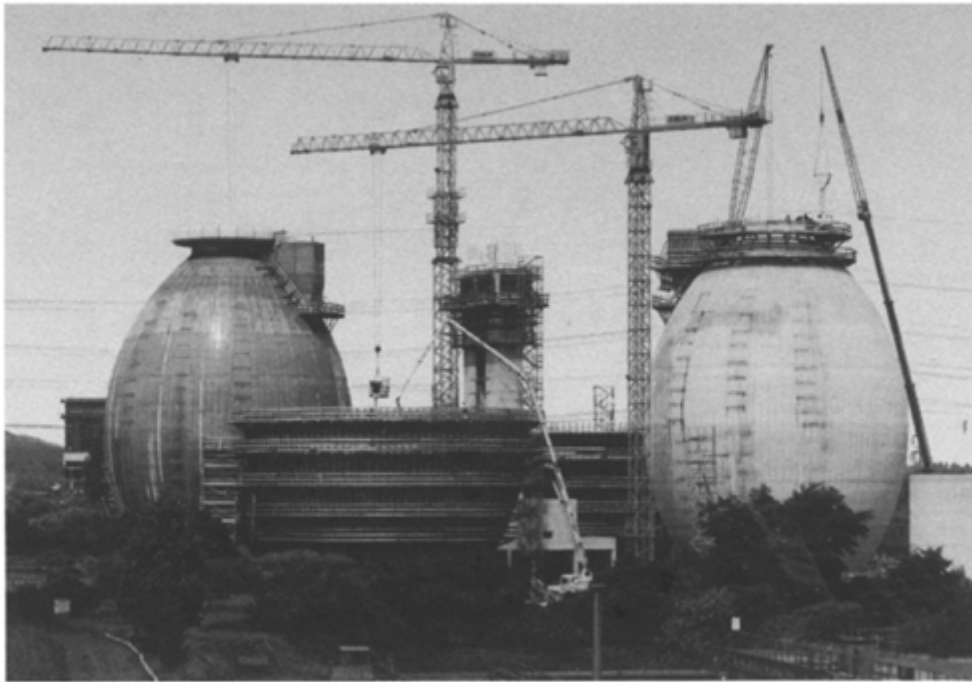
Figure 1.7 Prestressed liquid retaining structures *(courtesy VSL International)*.
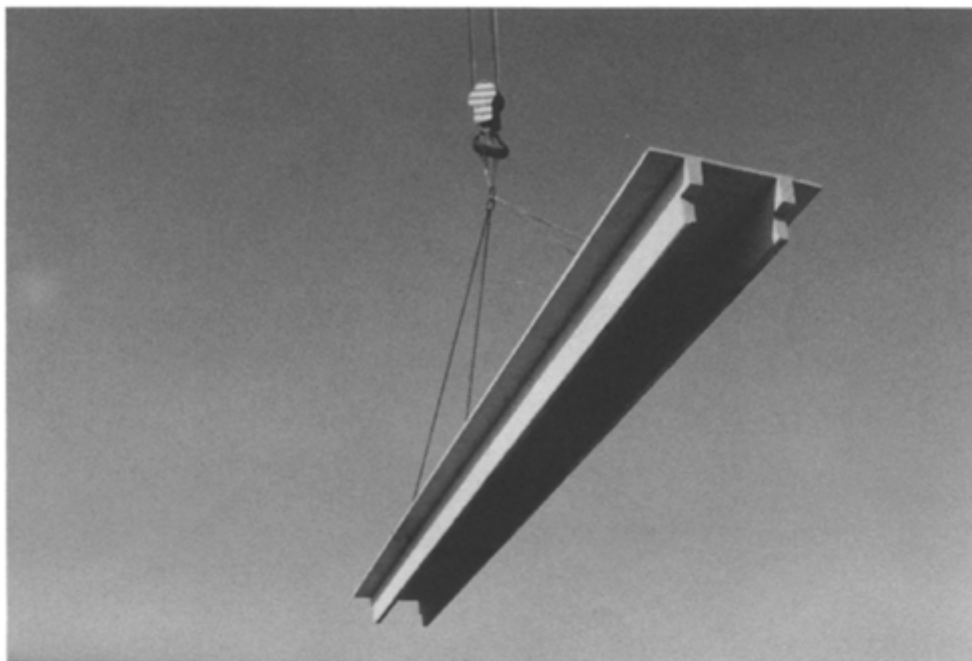
Figure 1.8 Prestressed double-tee roof beam.

One of the main advantages of prestressed over reinforced concrete is that, for a given span and loading, a smaller prestressed concrete member is required. This saving of the dead load of the structure is particularly important in long-span structures such as bridges, where the dead load is a large proportion of the total load. As well as a saving in concrete material for members, there is also a saving in foundation costs, and this can be a significant factor in areas of poor foundation material.

Another important advantage of prestressed concrete is that by suitable prestressing the structure can be rendered crack-free, which has important implications for durability, especially for liquid-retaining structures.

A third advantage is that prestressing offers a means of controlling deflections. A prestress force eccentric to the centroid of a member will cause a vertical deflection, usually in the opposite direction to that caused by the applied load. By suitable choice of prestress force, the deflections under applied load can be reduced or eliminated entirely.

Against the advantages listed above must be listed some disadvantages of using prestressed concrete. The fact that most, if not all, of the concrete cross-section is in compression under all load conditions means that any inherent problems due to long-term creep movements are increased. From the point of view of construction, a high level of quality control is required, both for material production and for locating the tendons within the structure.

The technology required for prestressing concrete may not be available in many developing countries, and, if specified, may prove to be uneconomical since all equipment and personnel would have to be imported.

1.2 METHODS OF PRESTRESSING

Methods of prestressing concrete fall into two main categories: *pretensioning* and *post-tensioning*.

(a) Pretensioning

In this method steel *tendons,* in the form of wires or strands, are tensioned between end-anchorages and the concrete members cast around the tendons. Once the concrete has hardened sufficiently, the end-anchorages are released and the prestress force is transferred to the concrete through the bond between the steel and concrete. The protruding ends of the tendons are then cut away to produce the finished concrete member. Pretensioned members usually have a large number of wires or strands to provide the prestress force, since the force

in them is developed by bond to the surrounding concrete, and as large an area of surface contact as possible is desirable.

This method is ideally suited to factory production since large anchorages are required to anchor all the tendons, and several members can be cast along the same set of tendons (Fig. 1.9). It is important to ensure that the members are free to move along the prestressing bed, otherwise undesirable tensile stresses may be set up in them when the end-anchorages are released.

It is interesting to note the use of *in situ* prestressing in cable-stayed and suspension bridge construction. In the former, the stays are tensioned in order to reduce the deflections of the bridge and also to optimize the deck cross-section. Pretensioning of suspension bridge cables has also been employed to ensure that the grout used to protect them from corrosion remains in compression, and therefore crack-free, under all load conditions.

Some examples of pretensioned members, other than beams, which are commonly produced are shown in Fig. 1.10.

(b) Post-tensioning

The prestress force is applied in this case by jacking steel tendons against an already-cast concrete member. Nearly all *in situ* prestressing is carried out using this method. The tendons are threaded through ducts cast into the concrete, or in some cases pass outside the concrete section. Once the tendons have been tensioned to their full force, the
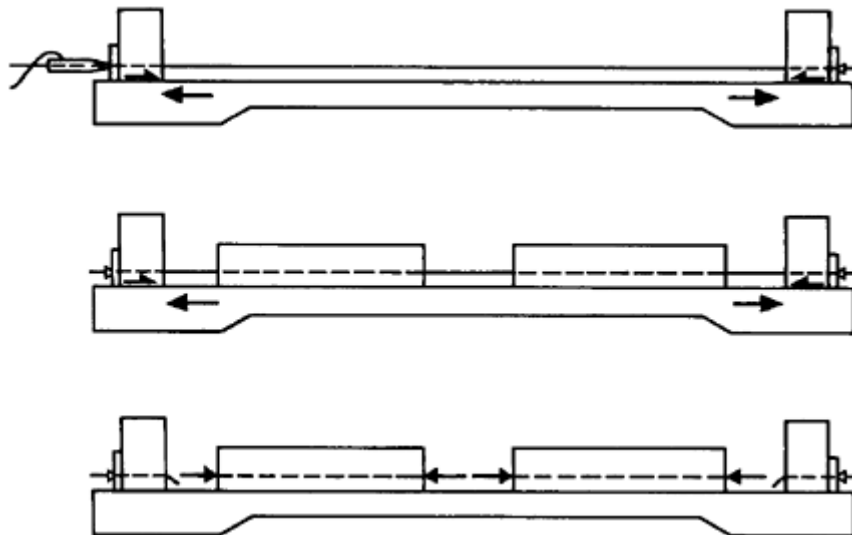
Figure 1.9 Pretensioning.
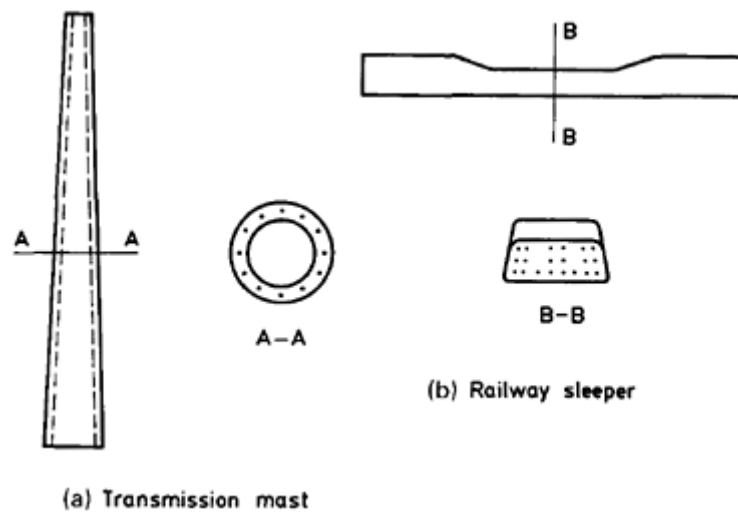
Figure 1.10 Examples of pretensioned members: (a) transmission mast; (b) railway sleeper.

jacking force is transferred to the concrete through special built-in anchorages. There are various forms of these anchorages and they are considered in detail in Chapter 8. The prestress force in post-tensioned members is usually provided by many individual wires or strands grouped into large tendons and fixed to the same anchorage. The concentrated force applied through the anchorage sets up a complex state of stress within the surrounding concrete, and reinforcement is required around the anchorage to prevent the concrete from splitting.

In most post-tensioned concrete applications the space between the tendon and the duct is injected with a cement grout. This not only helps to protect the tendons, but also improves the ultimate strength capacity of the member.

One advantage of post-tensioning over pretensioning is that the tensioning can be carried out in stages, for all tendons in a member, or for some of them. This can be useful where the load is applied in well-defined stages.

An important different between pretensioned and post-tensioned systems is that it is easy to incorporate curved tendons in the latter. The flexible ducts can be held to a curved shape while the concrete is poured around them (Fig. 1.11). The advantages of having curved tendons will become apparent later. With pretensioned members, it would be extremely difficult to arrange for a pretensioned curved tendon, although it is possible to have a sharp change of direction, as shown in Fig. 1.12. This involves providing a holding-down force at the point of deflection, and this is another reason why such members are nearly

Figure 1.11 Post-tensioning.
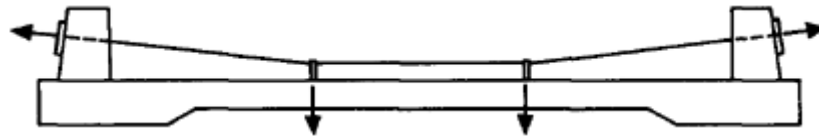
Figure 1.12 Deflected pretensioning tendons.
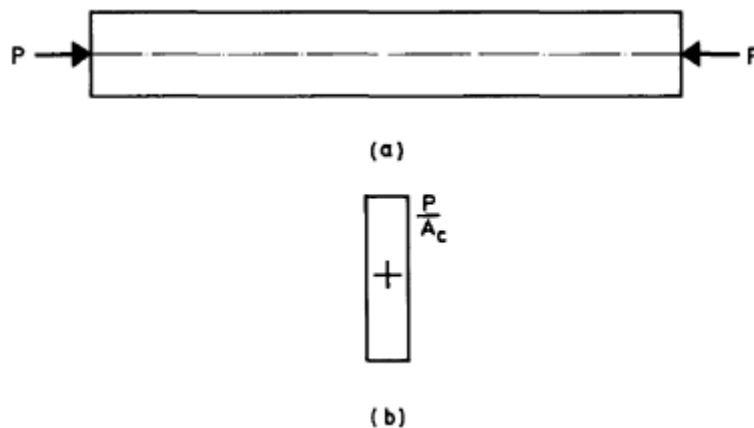
Figure 1.13 Axially loaded member.

always cast in a factory, or precasting yard, where the holding-down force can be accommodated more easily.

There are other methods available for prestressing concrete (Ramaswamy, 1976) but the ones described above are by far the most common.

1.3 STRUCTURAL BEHAVIOUR

Consider a rectangular concrete member with an axial load P applied through its centroid (Fig. 1.13(a)). At any section of the member, the stress at each point in the section is P/A_c, where A_c is the cross-sectional area of the member (Fig. 1.13(b)). The external force is now to be supplied by a tendon passing through a duct along the member centroid. The tendon is stretched by some external means, such as a

hydraulic jack, the stretching force is removed and the force required to keep the tendon in its extended state is transferred to the concrete *via* bearing plates (Fig. 1.14).

As far as the concrete is concerned, the effect is the same as in Fig. 1.13; the stress at each point in a section is P/A_c. (This is not strictly true near the ends of the member where the tendon force is concentrated, but by St Venant's principle it is reasonably true for sections further away from the end.) What has just been described is the situation in a post-tensioned member. In all of the following, the same is also true for a pretensioned member.

If the location of the duct is now moved downwards so that it no longer coincides with the member centroid, but is at a distance *e* from the centroid (Fig. 1.15(a)) then the stress distribution at any section is no longer uniform. It would be the distribution given by treating the section as though it had an axial force *P* and a moment *Pe* acting on it. On the assumption that the member behaviour can be approximated as linearly elastic, the stress distribution can be determined from ordinary bending theory and is shown in Fig. 1.15(b), where Z_t and Z_b are the member section moduli for the top and bottom fibres of the beam respectively, and compressive stresses are positive.

Figure 1.14 Axially prestressed member.
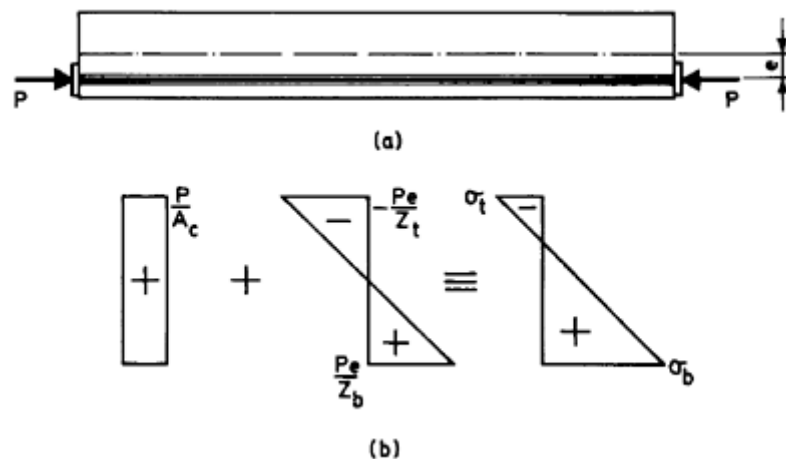
Figure 1.15 Eccentrically prestressed member.

If the member is now mounted on simple supports at either end and subjected to a uniform load in addition to its own weight (Fig. 1.16(a)) then the stresses at midspan can be determined for a bending moment, *M,* which is due to the total uniform load. The resulting stress distribution is shown in Fig. 1.16(b).

Note that the resulting stress distribution has been shown with a net tensile stress at the beam soffit. However, by a suitable adjustment of the values of *P* and *e,* this tension can be eliminated and a crack-free member produced. This is the key to the use of prestressed concrete. With reinforced concrete, a certain degree of cracking of the concrete is inevitable. With prestressed concrete it can be eliminated entirely, which has the advantages mentioned earlier.

The use of the terms 'top' and 'bottom' is appropriate with horizontal members such as beams. With vertical members such as masts or tank walls, however, it is more appropriate to consider Z_t and Z_b as the section moduli for the faces of the member with the greater and lesser compressive stresses, respectively, under applied load.

There is another important difference between prestressed and reinforced concrete. With reinforced concrete simply supported beams the minimum load on the beam is of minor importance; it is the maximum load which governs the structural design. However, with prestressed concrete members the minimum load is an important loading condition. Figure 1.17 shows the stresses due to the combination of prestress force and the self weight of the beam. A net tension may occur at the top of the beam, rather than at the soffit as is the case with the maximum load. This is particularly important since the minimum
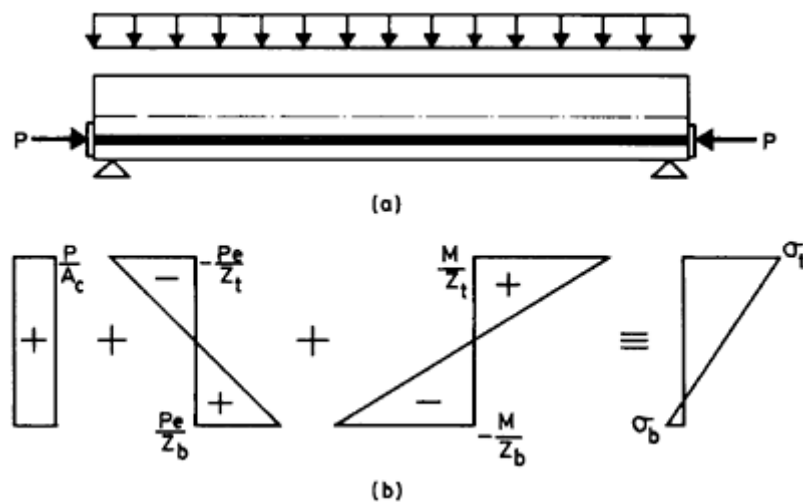
Figure 1.16 Stresses due to prestress and applied load.
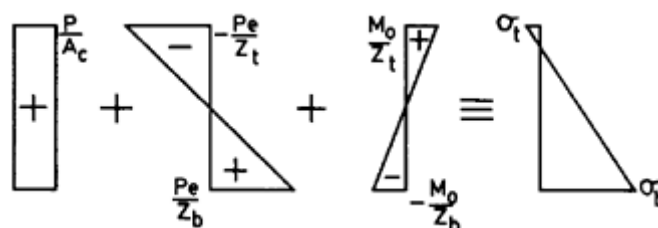
Figure 1.17 Stresses due to prestress and self weight.

load condition usually occurs soon after *transfer,* the point when the prestress force is transferred from the tensioning equipment to the concrete and is at its maximum value. Transfer is often carried out soon after the casting of the member (in precast work it is important that transfer is achieved as soon as possible in order to allow rapid re-use of the beds), and the strength of the concrete at this age is usually lower than it is when the total load acts on the member.

1.4 INTERNAL EQUILIBRIUM

If a vertical cut is taken along the beam shown in Fig. 1.15 and the member is separated into free bodies, one containing the steel tendon and one containing the concrete, the forces acting on the free bodies are as shown in Fig. 1.18(a). The respective forces in the concrete and steel are a compressive force P and a tensile force T.

The location of the compressive force in the concrete must, in order to maintain equilibrium, be at the location of the tendon. This may seem obvious for this simple example, but in Section 1.5 a more general treatment is given, where the location of the concrete compressive force is not so obvious. Thus, considering the composite member of steel and concrete, internal equilibrium of forces is maintained, and there is no net internal moment, the two forces P and T being equal and opposite, and coincident. This is to be expected from consideration of overall equilibrium, since there is no external axial load on the member.

If, as in Fig. 1.16, the member is mounted on simple supports and a uniform load is applied, there is now a bending moment M at midspan, which can be found by considering equilibrium of the beam as a whole. The resultants of the steel and concrete stresses across the midspan section form an internal resisting moment which must balance the bending moment M. Since the force in the tendon is fixed in position, defined by the location of the tendon at midspan, it must be the force in the concrete which moves in order to provide an internal resisting couple with lever arm z (Fig. 1.18(b)). The locus of the concrete force
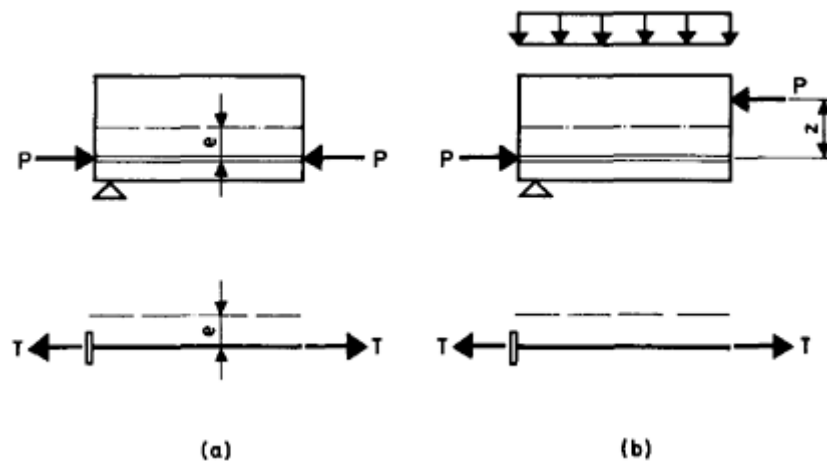
Figure 1.18 Internal equilibrium.
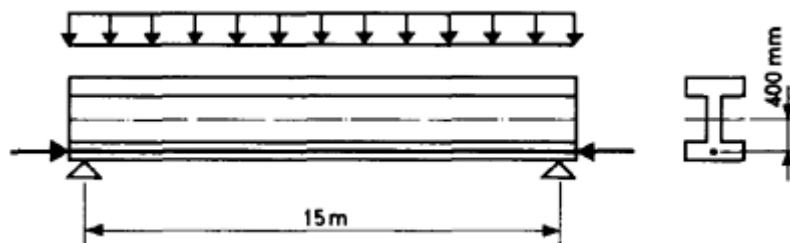
Figure 1.19

along a member is often referred to as the *line of pressure,* a concept which will be useful in dealing with statically indeterminate structures (Chapter 11).

If the section were analysed under the action of a force *P* acting at a lever arm *z* from the tendon location, the resulting stress distribution would be that shown in Fig. 1.16(b).

The relationship between prestress force, lever arm and applied bending moment described above is valid right up to the point of collapse of a member and will be used to find the ultimate strength of sections in Chapter 5.

Example 1.1 ▪▪

A simply supported beam with a cross-section as shown in Fig. 1.19 spans 15 m and carries a total uniform load, including self weight, of 50 kN/m. If the beam is prestressed with a force of 2000 kN acting at an

eccentricity of 400 mm below the centroid, determine the stress distribution at midspan.

Maximum bending moment at midspan=$50 \times 15^2/8 = 1406.3$ kNm.

Section properties:

$Z_b = Z_t = 70.73 \times 10^6$ mm^3
$A_c = 2.9 \times 10^5$ mm^2.

Thus the stresses at midspan are:

Top:

$$\sigma_t = \frac{P}{A_c} - \frac{Pe}{Z_t} + \frac{M}{Z_t}$$

$$= \frac{2000 \times 10^3}{2.9 \times 10^5} - \frac{2000 \times 10^3 \times 400}{70.73 \times 10^6} + \frac{1406.3 \times 10^6}{70.73 \times 10^6}$$

$$= 6.90 - 11.31 + 19.88$$
$$= 15.47 \text{ N/mm}^2.$$

Bottom:

$$\sigma_b = \frac{P}{A_c} + \frac{Pe}{Z_b} - \frac{M}{Z_b}$$

$$= 6.90 + 11.31 - 19.88$$
$$= -1.67 \text{ N/mm}^2.$$

The resulting stress distribution is shown in Fig. 1.20.

The alternative approach is to consider the location of the line of pressure in the concrete. From Fig. 1.18(b)

$z = M/P = 1406.3/2000 = 0.703$ m.

Thus the location of the force in the concrete is $(703-400) = 303$ mm above the centroid. The stresses may be determined by considering the
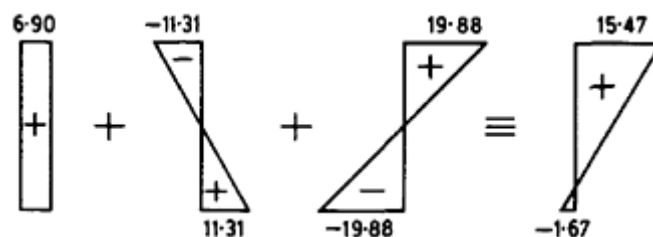
Figure 1.20 Stresses at midspan of beam in Example 1.1 (N/mm^2).

section under the action of an axial load of 2000 kN and a moment of 2000×0.303=606.0 kNm.

The stresses at midspan are thus:

$$\sigma_t = \frac{2000 \times 10^3}{2.9 \times 10^5} + \frac{606.0 \times 10^6}{70.73 \times 10^6}$$

$$= 6.90 + 8.57$$
$$= 15.47 \text{ N/mm}^2$$

$$\sigma_b = 6.90 - 8.57$$
$$= -1.67 \text{ N/mm}^2.$$

■■

It is useful to consider what happens at the supports. The bending moment there is zero, and therefore the stress distribution is as shown in Fig. 1.21. A large net tensile stress is produced at the top of the beam. It is thus undesirable to have the same eccentricity at the ends of the member as at the midspan section. This can be overcome by reducing the eccentricity near the supports, as described in the next section. For pretensioned members an alternative is to destroy the bond between the steel and the surrounding concrete by greasing the tendons, or by providing sleeves around them in the form of small tubes, or an extruded plastic coating.

The preceding description of the internal equilibrium of a prestressed concrete member still applies when the prestress force is not actually applied within the section. Figure 1.22(a) shows a beam with a prestressing tendon situated such that, at midspan, it is outside the concrete section. Nevertheless, the free-body diagram for the concrete in one half of the beam, shown in Fig. 1.22(b), indicates that the concrete section would still behave as though a prestressing force were acting on it with an eccentricity *e*.

The situation shown in Fig. 1.22 is known as *'external prestressing'* and has been used in several modern bridge projects. In practice the
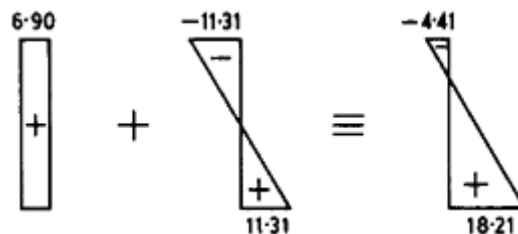
Figure 1.21 Stresses at the supports of beam in Example 1.1 (N/mm^2).
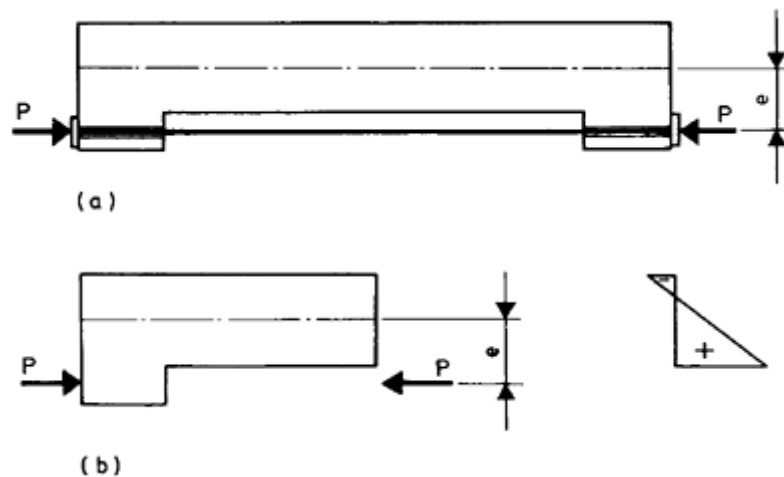
Figure 1.22 Externally prestressed beam (a) elevation (b) free-body diagram.

tendons are usually contained within the space inside a box-section bridge deck (Fig. 1.5), so that they are protected from the outside environment but still available for inspection and, if necessary, replacement.

For sections near to the end of the beam in Example 1.1, the tendon is still in the same location in the section, but the bending moment is smaller than at the midspan. Thus the value of the lever arm z must change in order to provide a reduced internal resisting moment. The pressure line for a member with no applied load must be coincident with the tendon in order to satisfy internal equilibrium. Once a load is applied, however, the pressure line must move away from the tendon location in order to provide the internal couple necessary to resist the applied bending moment.

1.5 DEFLECTED TENDONS

So far all the prestressed concrete members considered have had straight tendons. Consider now a member with a tendon that is deflected at the third-points along its length as shown in Fig. 1.23. The prestress force is no longer horizontal at the ends of the member. The angle θ is usually small, however, and the prestress force may be considered horizontal for design purposes. The vertical component of the force at the ends of the member is resisted directly by the supports.

In order to determine the stress distribution at midspan, the location of the pressure line is required. To find this, consider free bodies of the concrete and steel respectively (Fig. 1.24) for the left-hand half of the member. The actual direction of the prestress force at the end of the
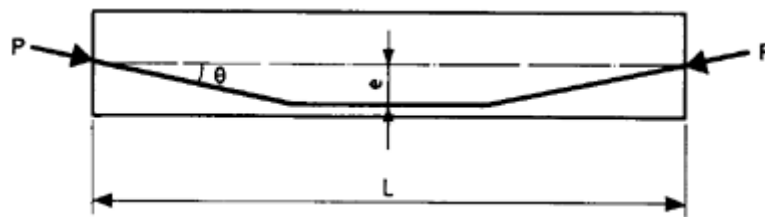
Figure 1.23 Member with deflected tendons.
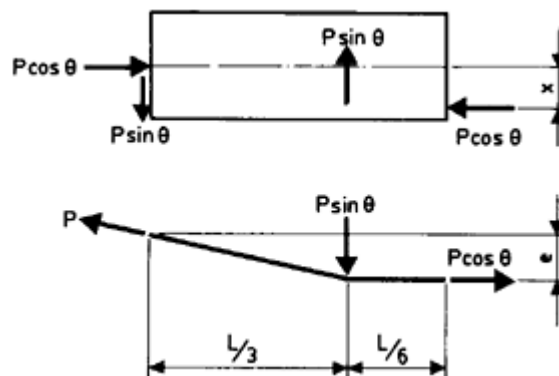
Figure 1.24 Free bodies of concrete and steel.

member must now be considered, giving a horizontal component of $P\cos\theta$ and a vertical component of $P\sin\theta$. By considering the free body of the steel tendon, it is clear that there must be a vertical force of $P\sin\theta$ at the deflection point.

The location of the pressure line at the midspan section can be determined by considering equilibrium of the free body of the concrete.

Taking moments about the left-hand support:

$P\sin\theta(L/3)=(P\cos\theta)x$
$\therefore x=(L/3)\tan\theta.$

But

$\tan\theta=e/(L/3)$
$\therefore x=e.$

The important conclusion is thus that the pressure line in a prestressed concrete member with a deflected tendon, and with no external applied load, is located at the position of the steel tendon for any section along the member. That is, the pressure line is coincident with the tendon profile, as with the case of a straight tendon. Although the above example shows a straight tendon deflected in two places, the same

argument applies in the case of a continuously deflected, or draped, tendon as found in most post-tensioned members.

If a cut is made in the beam shown in Fig. 1.23 at a third-point along its length, the free body of the concrete in the left-hand portion will be as shown in Fig. 1.25. Also shown is a shear force V transferred to the left-hand section by the remainder of the beam to the right of the cut. The force in the concrete at the cut is not horizontal and thus there is a vertical component that counteracts the shear force V at the cut section. The shear stresses at that section will therefore be reduced. The determination of the shear resistance of prestressed concrete members is discussed in detail in Chapter 7.

1.6 INTEGRAL BEHAVIOUR

The fact that the pressure line is coincident with the tendon profile for an unloaded member affirms the view of a prestressed concrete member as a single structural element, rather than treating the steel and concrete separately. This aspect is emphasized by considering a vertical concrete member, *prestressed* is a force P through the centroid of the section, Fig. 1.26(a), and comparing it with a similar vertical concrete member loaded with an *external force P* applied through the centroid of the section, Fig. 1.26(b). In the first case, as the force P is increased from zero, there is no possibility of the member buckling due to the prestress force alone, whatever the dimensions of the member; failure will eventually occur by crushing of the concrete. In the second case, as the applied force is increased from zero, there may come a time when buckling occurs before crushing of the concrete, depending on the dimensions of the member.

The difference between these two examples is important because it illustrates the fundamental behaviour of prestressed concrete. In the first example, if the vertical member is given a small lateral displacement, at any section the pressure line is still coincident with the tendon position, and a uniform stress distribution is obtained. In the second example, if the vertical member is given a small lateral displacement,
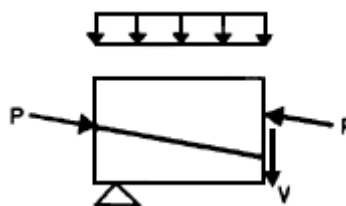
Figure 1.25 Free body of concrete near a support.
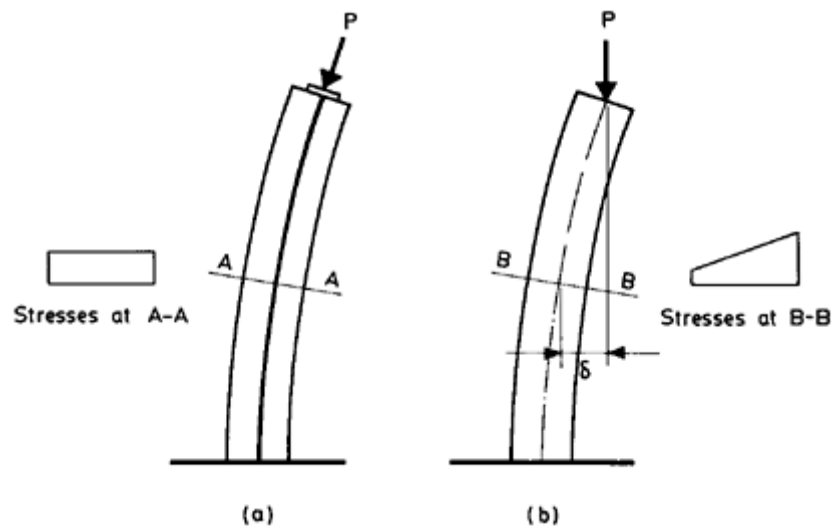
Figure 1.26 (a) Prestressed and (b) axially loaded vertical members.
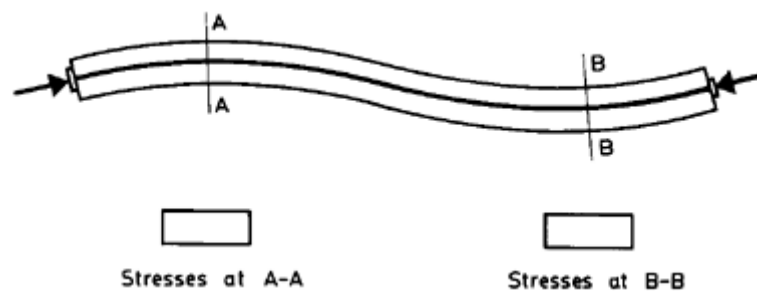
Figure 1.27 Curved prestressed member.

there is a bending moment induced at any section, and the resulting stress distribution is no longer uniform. In the case of the prestressed vertical member, the effect of the axial force can never be to increase the lateral deflections and so lead to buckling.

Another example is illustrated in Fig. 1.27 where the tendon profile follows the member centroidal axis and the stress at any section along the curved member is always uniform, under prestress force only.

1.7 FORCES EXERTED BY TENDONS

From Fig. 1.24 it can be seen that, by deflecting a tendon from the straight position, a downwards force is required to maintain the tendon in the deflected position, and this force is transmitted to the concrete as an upwards force. In the case of a continuously curved tendon, there

must be a distributed force applied to the concrete to maintain the tendon in position (Fig. 1.28).

In order to determine the value of this force, consider a small, but finite, section of the tendon (Fig. 1.29(a)). If the frictional forces between the tendon and the surrounding concrete are ignored, the force in the tendon at either end of the element Δs is equal to T. If w is the uniformly distributed load on the tendon required to maintain it in position, then, from the triangle of forces Fig. 1.29(b):

$w\Delta s=2T\sin(\Delta\theta/2)$.

For small changes of angle, $\sin(\Delta\theta/2)=\Delta\theta/2$. If the element is made smaller and smaller, in the limit the force at a point on the tendon is given by

$w=Td\theta/ds$.
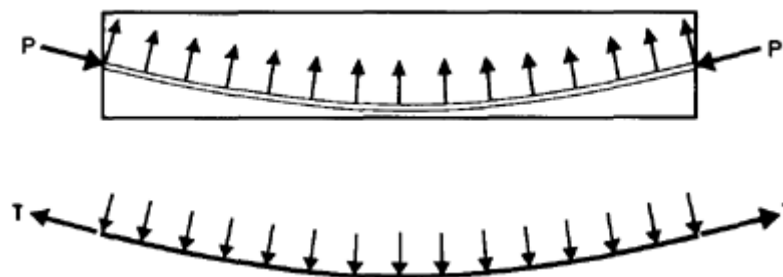
Figure 1.28 Free bodies of concrete and curved tendon.
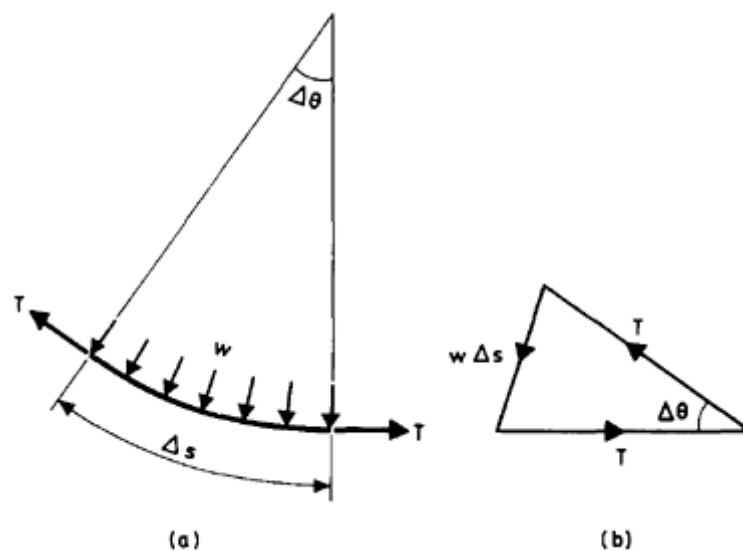
Figure 1.29 Small length of tendon.

Now, $d\theta/ds=1/r_{ps}$, where r_{ps} is the radius of curvature, so that

$w=T/r_{ps}$.

Although this force is theoretically directed towards the centre of curvature at any given point, in practice most tendon profiles are reasonably flat and it can be assumed that the force at any point is vertical.

The vertical force produced by a sharp change of profile, such as that found in pretensioned beams, is shown in Fig. 1.30. In this case

$W=T(\sin\theta+\sin\varphi)$.

Example 1.2 ■■

A simply supported beam of length L has a parabolic tendon profile with maximum eccentricity e, as shown in Fig. 1.31. Determine the upwards force on the beam exerted by the tendon and draw the shear force and bending moment diagrams due to the prestress force.

If the parabolic curve is given a set of x and y coordinates with the origin at the left-hand end, the equation of the tendon profile is

$y=4ex\,(L-x)/L^2$.

For a reasonably flat curve, $1/r_{ps}$ may be approximated by d^2y/dx^2.

Therefore

$1/r_{ps}=-8e/L^2$
$\therefore\ w=P/r_{ps}=-8Pe/L^2$,
(1.1)

where w is an upwards force.
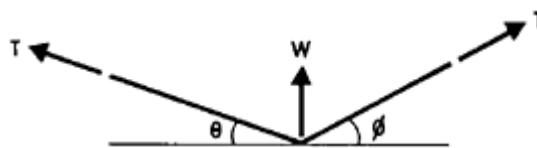
Figure 1.30 Sharp change of tendon profile.
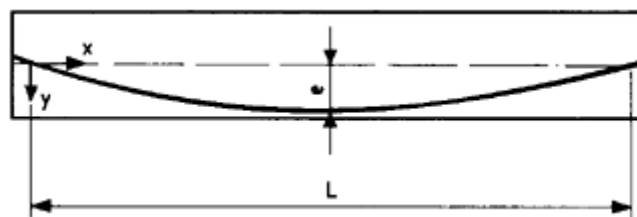
Figure 1.31

The maximum bending moment in the beam is given by

$$M_{max}=wL^2/8=(-8Pe/L^2)(L^2/8)$$
$$=-Pe.$$

■■

The prestress moment and shear force diagrams are shown in Fig. 1.32(a) and (b) respectively. Note that the prestress moment diagram is a scaled version of the shape of the tendon profile. The moments are negative because the prestress force is below the centroid at midspan, causing a hogging moment in the beam.

The observation that the prestress moment diagram is of the same shape as the tendon profile is true of all statically determinate members. It is particularly useful in drawing the prestress moment diagram, and for determining the deflections (see Chapter 6) for the member shown in Fig. 1.33(a), which has a varying section but a straight tendon. There can be no vertical loads in this case, since the tendon is straight, but the prestress moment diagram can be drawn simply by considering the distance between the tendon location and the centroid of the member at any section, Fig. 1.33(b).

The fact that a deflected tendon must exert a force on the surrounding concrete is the basis of the load balancing method which has useful application in the design of indeterminate structures, and in particular for designing prestressed concrete flat slabs (Chapter 12). However, it is not applicable for members with straight tendons, and account must be taken of any moments due to eccentricity at the ends of the member.
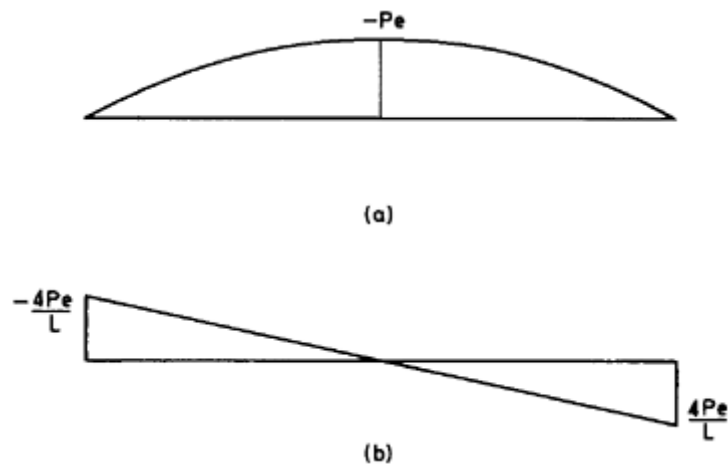
Figure 1.32 (a) Prestress moment and (b) shear force diagrams.
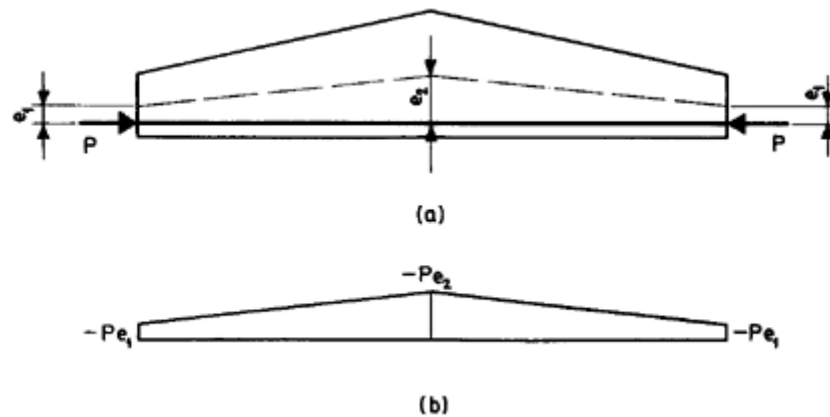
Figure 1.33 Member with varying section.
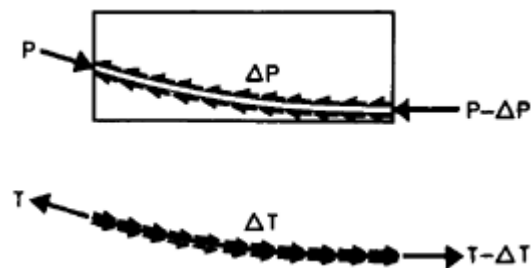
Figure 1.34 Loss of prestress due to friction.

1.8 LOSS OF PRESTRESS FORCE

In all the prestressed concrete members considered so far, it has been assumed that the force in the tendon is constant. However, during tensioning of a post-tensioned member, there is friction between the tendon and the sides of the duct. This is caused by changes in curvature of the tendon profile along its length. However, even in a straight tendon there is friction present since the tendon does not lie exactly along the centreline of the duct, and there is contact at points along its length.

The effect of friction on the behaviour of post-tensioned members is that, at any section away from the tensioning end, the force in the tendon is less than that applied to the tendon through the jack. This is shown by considering once again the free bodies of the steel tendon and concrete in a portion of a member (Fig. 1.34).

Friction is only one of the causes of loss of prestress force, and applies to post-tensioned members only. Another cause of loss which applies to both pretensioned and post-tensioned members is initial elastic

shortening of the concrete which also shortens the steel tendon, reducing the prestress force. Long-term changes in length of the concrete member due to creep and shrinkage also cause reduction of prestress force. All these effects will be considered in more detail in Chapter 4.

1.9 DEGREES OF PRESTRESSING

When the idea of prestressing concrete was first introduced it was considered that all cracking should be avoided under service load, and, further, that the whole section should be in a permanent state of compression. This is often referred to as *'full prestressing'*. However, at a later stage, experiments were carried out using small amounts of tensioned steel to control cracking and larger amounts of untensioned reinforcement, which together provided the necessary ultimate strength. This combination of tensioned and untensioned steel is often referred to as *'partial prestressing'*.

In EC2 the distinction is made between a concrete member that is uncracked and one that is cracked in tension. In the former case, some tension is allowed, but the amount is kept below the tensile strength of the concrete. In the latter case, cracks are allowed but must be limited in width so as not to affect adversely the durability of the member. The stress distributions in each type of member are shown in Fig. 1.35. Uncracked and cracked members are described more fully in Chapters 5 and 9.

The distinction made in EC2 can be seen as a way of relating prestressed concrete members to non-prestressed, reinforced concrete members. Many of the clauses in EC2 relate to both types of member. In particular, the clauses on their behaviour at the point of collapse and on the respective analysis procedures are similar.

(a) Uncracked   (b) Cracked
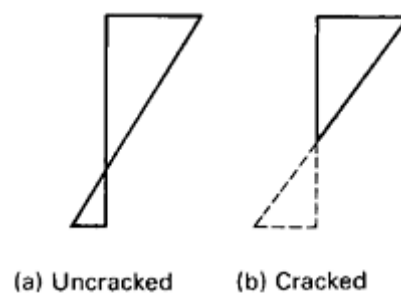
Figure 1.35 Stress distributions in (a) uncracked and (b) cracked concrete members.

1.10 SAFETY

Since high stresses exist in prestressed concrete members at both maximum and minimum load conditions, there must be careful control of the quality of the materials used. In reinforced concrete or steelwork structures these high stresses occur only under maximum load conditions, and are rarely reached. In prestressed concrete structures they are present at all stages of loading. In one sense it can be said that a prestressed concrete structure has been pre-tested, in that the presence of low-standard concrete or steel will generally be detected before the structure enters service.

Since a small change in tendon eccentricity can have a large effect on the stresses induced in a prestressed concrete member, care must be taken during construction that the correct profile for the prestressing steel is maintained during casting of the concrete.

Another important feature of the construction of prestressed concrete structures is the very large jacking forces that are required. Adequate provision must be made to protect site personnel against sudden failure of a steel tendon during tensioning, a not-uncommon occurrence, large amount of strain energy suddenly released is potentially lethal.

An aspect of prestressed concrete structures that is beginning to concern engineers is how to demolish them. As the early structures reach the end of their useful lives, the problem arises of how to break up prestressed concrete members which have such large amounts of energy stored in them. In some cases it is possible to reduce the force in the tendons to allow safe demolition. The problem, however, will assume greater significance as more prestressed concrete structures require demolition.

PROBLEMS

1.1 A set of books, measuring 300 mm long by 210 mm wide, of total length 600 mm, is to be held at the centre of the ends of the set. If the weight of the books is 60 kg/m determine the force necessary to prevent a bookmark, inserted between the bottom edges of the two centremost books of the set, from just falling away. (It may be assumed that the books do not slide against each other.)

1.2 A long children's party balloon with a membrane thickness of 0.1 mm is inflated to a uniform external diameter of 100 mm with a pressure of 0.2 N/mm^2. It is placed on supports 600 mm apart. Determine the maximum weight that can be placed on the balloon at its centre without the top surface crumpling. (Local effects may be ignored.)

1.3 A metal tyre is heated to 200 °C and placed so that it just fits over a wooden wheel rim of outside diameter 1 m. The tyre is then cooled by quenching to 20 °C. If the thicknesses of the tyre and rim are 5 mm and 50 mm respectively, and they are both 50 mm wide, determine the tensile stress in the tyre and the compressive stress in the rim. The coefficient of thermal expansion of the tyre may be taken as 10^{-5}/°C, and the moduli of elasticity of the tyre and rim $200{\times}10^3$ and $8{\times}10^3$ N/mm^2 respectively.

1.4 Two steel beams, with second moments of area 0.01 m^4 and self weights of 20 kN/m, are placed on supports as shown in Fig. 1.36. The level of the central support is raised by an amount Δ, and a welded connection made between the beams. The support is then lowered to its original position. Determine the value of Δ such that the midspan and support self weight bending moments are equal. Assume that $E_s{=}205{\times}10^3$ N/mm^2. (A similar method to this was used in the construction of Robert Stephenson's Britannia Bridge over the Menai Straits, completed in 1850.)

1.5 Equation 1.1 (page 21) is only an approximation of the radius of curvature of a parabolic curve. The exact expression is

$$1/r_{ps} = \frac{(d^2y/dx^2)}{[1 + (dy/dx)^2]^{3/2}}$$

(1.2)

For the prestressing tendon in Fig. 1.37, with initial force 1000 kN, show, by using Equation 1.1, that the uniform load does not exactly
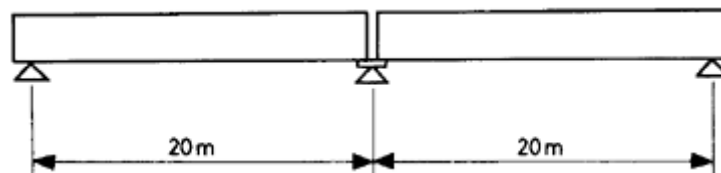
Figure 1.36
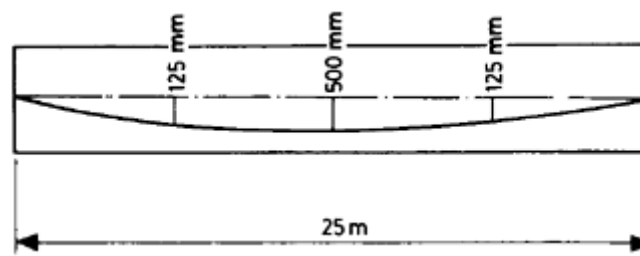
Figure 1.37

balance the vertical components of the end forces. Also show, by using Equation 1.2 and Simpson's rule, that the forces do balance.

1.6 A simplified model of a cable-stayed bridge is shown in Fig. 1.38. If the self weight of the bridge deck is 50 kN/m, its cross-sectional area 0.1 m² and second moment of area 0.5 m⁴, the cross-sectional area of the cables 0.01 m² and $E_s=205\times10^3$ N/mm² for all members, determine the prestress to be applied to the cables, as indicated on jacks located at the supports, such that the maximum sagging and hogging self weight bending moments within the span are equal. What then is the deflection
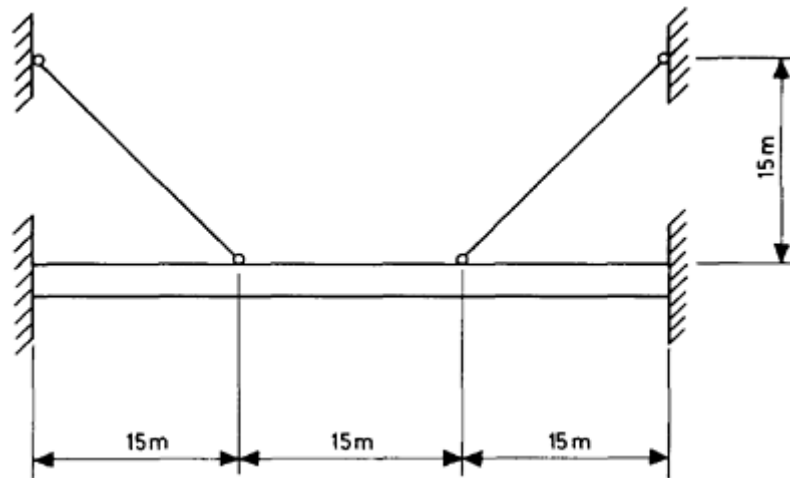
Figure 1.38
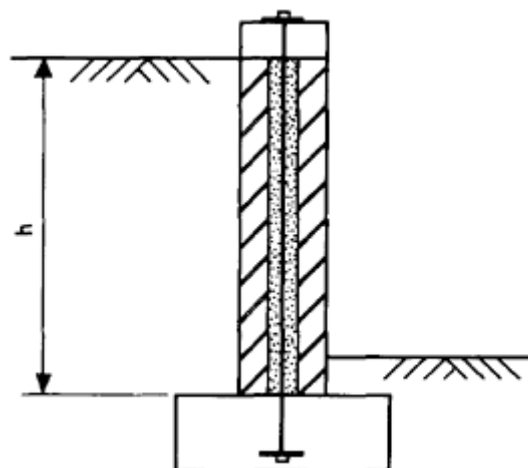
Figure 1.39

of the beam at the cable support point? (Prestressing of the cables may be modelled in a structural analysis computer program either by imposing a lack of fit or a temperature change, depending on the facilities available in the program.)

1.7 A prestressed masonry retaining wall is shown in Fig. 1.39, comprising hollow blocks filled with mortar to ensure a composite section. The section properties are: section modulus $Z=6.67\times 10^6$ mm^3/m, cross-sectional area $A=2\times10^5$ mm^2/m. If the prestress force is 700 kN/m applied through the centroid of the wall, determine the maximum height of the retaining wall, h, such that the joint between the wall and the base is just put into tension. Assume, for the soil, $\gamma=18$ kN/m^3 and $\varphi=35°$, and ignore passive resistance in front of the wall.

REFERENCES

Ramaswamy, G.S. (1976) *Modern Prestressed Concrete Design,* Pitman, London.
Walley, D. (1984) The Childhood of Prestressing, *The Structural Engineer,* **62A**, No. 1.

2

Properties of materials

2.1 STRENGTH OF CONCRETE

The strength of concrete is primarily affected by the water/cement ratio, that is the ratio of the weights of mixing water and cement used in a mix. The lower the water/cement ratio the higher the strength, and typical relationships between water/cement ratio and compressive cylinder strength at different ages are shown in Fig. 2.1.

A major factor affecting strength is the amount of voids left in the concrete after compaction. The more air contained in the concrete, the more compressible it becomes and the less the strength. It is thus important that the concrete is compacted as fully as possible. It is often the case that the concrete at the top of a horizontally cast member is less well-compacted than at the bottom, leading to lower strength. Another property of concrete affected by poor compaction is the bond developed between the concrete and any steel placed within it. This is particularly important for pretensioned members, where reliance is made on this bond to transfer the prestress force to the concrete.

The strength of concrete increases with age, but the rate at which it increases is greatly affected by the curing conditions. Ideally, the concrete should be kept in a moist condition to allow as much hydration of the cement as possible to take place. Most concrete members are cured for the first few days under moist covering and then cured in air.

In EC2 the standard compressive strength test is that of a 350 mm×150 mm diameter cylinder after 28 days. The cylinder strength, f_{ck}, of a given mix is between 70 and 90% of the cube strength, the criterion used in BS8110. The usual range of concrete cylinder strengths used in prestressed concrete is 25–50 N/mm^2, with values at the lower end of the range used for slabs, and those at the upper end for beams. Details of the design of mixes to achieve these strengths are given by the Department of the Environment (1975).

Whilst in reinforced concrete it is important to know the compressive
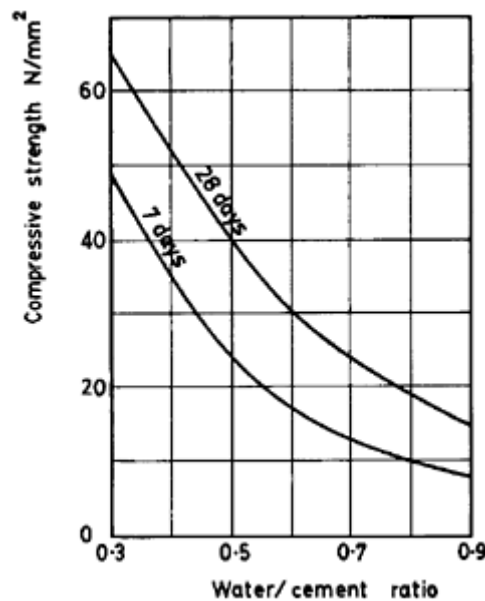
Figure 2.1 Strength of OPC concrete.

Table 2.1 Allowable concrete tensile stresses (N/mm^2)

	Concrete grade						
	C20/25	C25/30	C30/37	C35/45	C40/50	C45/55	C50/60
f_{ctm}	2.2	2.6	2.9	3.2	3.5	3.8	4.1

strength only, since the contribution of tensile strength to bending resistance is ignored, in prestressed concrete it is important to know both. Values for allowable tensile stresses, f_{ctm}, of various strength classes or grades of concrete are given in Table 2.1, where the classes refer to cylinder/cube strengths.

2.2 MODULUS OF ELASTICITY OF CONCRETE

The modulus of elasticity of concrete is important, not only in estimating deflections of prestressed concrete members but also because some of the losses of prestress force are influenced by it. This is discussed further in Chapter 4.

A typical stress-strain curve for concrete tested in a compression testing machine is shown in Fig. 2.2. The initial portion of the curve is approximately linear, and the modulus of elasticity may be approximated by the slope of the line *O A*. This is known as the *secant modulus,* and

point A is defined at a given concrete stress of $0.4f_c$, where f_c is the maximum stress achieved, for a rate of load application of 15 N/mm^2 per minute. This last requirement is important, since the stress-strain curve is dependent on the rate of loading. This is due to the time-dependent deformation of concrete under stress, known as creep (see Section 2.3). An idealized version of the stress-strain curve shown in Fig. 2.2 used for design purposes is shown in Chapter 3.

Values of the secant modulus given in EC2 for concretes of varying strengths are shown in Table 2.2. They may be used for determining the short-term deflections of prestressed concrete members and the initial losses of prestress force due to elastic shortening. For long-term deflections, the time-dependent effects of creep and shrinkage should be taken into account (see Chapter 6).
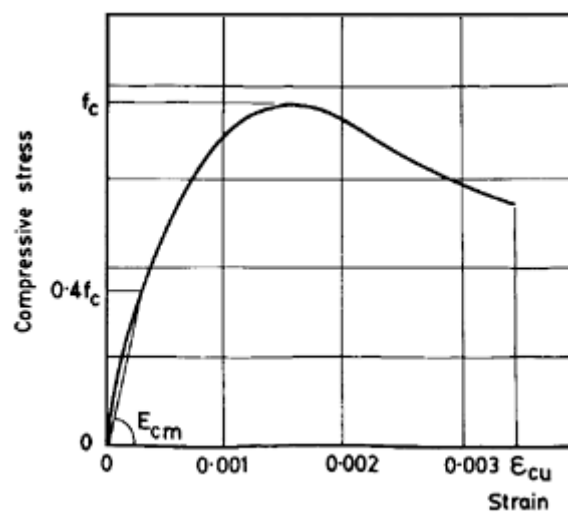
Figure 2.2 Stress-strain curve for concrete.

Table 2.2 Modulus of elasticity of concrete

Concrete grade	Mean value (10^3 N/mm^2)
C20/25	29.0
C25/30	30.5
C30/37	32.0
C35/45	33.5
C40/50	35.0
C45/55	36.0
C50/60	37.0

2.3 CREEP OF CONCRETE

A phenomenon which affects most materials to some extent is that of *creep,* or time-dependent deformation under constant load. Creep is particularly important in concrete, and affects both the long-term deflections and loss of prestress force in prestressed concrete members. The basic mechanism of creep in concrete is that of gradual loss of moisture, causing contraction in the structure of the cement paste in the concrete. The effects of creep in prestressed concrete members are more pronounced than in reinforced concrete members since, in the former, a greater proportion of the cross-section of the member is in compression. A typical curve of creep strain with time is shown in Fig. 2.3. Since creep over a given time interval varies with the level of stress in the concrete, a useful parameter is the *specific creep,* defined as the creep strain per unit stress.

The long-term (30-year) specific creep strain may be determined from the relationship

$$\text{specific creep} = \varphi/E_{cmt}$$
(2.1)

where E_{cmt} is the modulus of elasticity of the concrete in the long term and φ is a creep coefficient determined from Table 2.3. The cross-sectional area of the concrete member is A_c and u its perimeter.

2.4 SHRINKAGE OF CONCRETE

Concrete contains a significant proportion of water, and as the surplus water that has not been used to hydrate the cement evaporates, the concrete member shrinks. The amount of shrinkage is dependent on the environmental conditions surrounding the concrete, and is independent of the external load on the member. If the concrete is in a dry windy
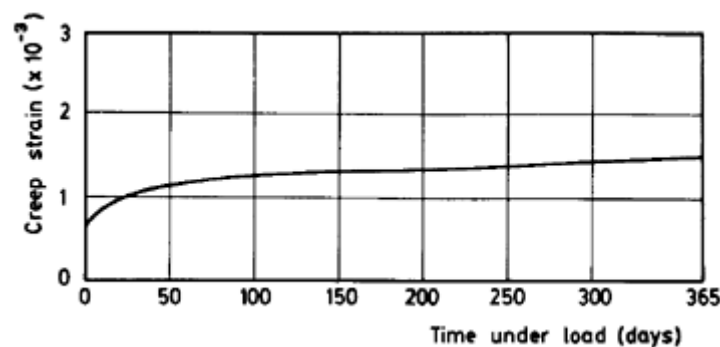
Figure 2.3 Creep of concrete stored at 21 °C with stress/strength ratio 0.7 (Neville, 1996).

Table 2.3 EC2 creep coefficients

| | Notional size $2A_c/u$ (mm) | | | | | |
| | 50 | 150 | 600 | 50 | 150 | 600 |
Age at transfer (days) days	Dry atmospheric conditions (inside) (relative humidity 50%)			Humid atmospheric conditions (outside) (relative humidity 80%)		
1	5.5	4.6	3.7	3.6	3.2	2.9
7	3.9	3.1	2.6	2.6	2.3	2.0
28	3.0	2.5	2.0	1.9	1.7	1.5
90	2.4	2.0	1.6	1.5	1.4	1.2
365	1.8	1.5	1.2	1.1	1.0	1.0
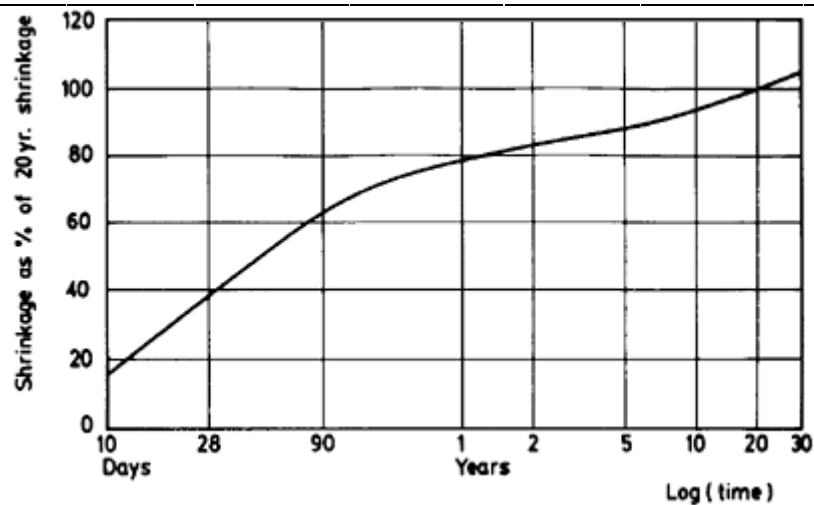
Figure 2.4 Average shrinkage of concretes stored at 50–70% RH (Neville, 1996).

climate, the loss of moisture will be much greater than if the concrete is kept in a moist condition.

Shrinkage of concrete varies with time, and a typical relationship is shown in Fig. 2.4. The initial rate of shrinkage decreases, and by the end of one year approximately 80% of the long-term shrinkage will have taken place. The values of long-term shrinkage strain for normal concrete mixes to be used for design purposes may be taken from Table 2.4.

The effects of creep and shrinkage on loss of prestress force and long-term deflections will be discussed in Chapters 4 and 6 respectively. Further information on both these effects may be found in Neville (1996) and in Appendix 1 to EC2.

Table 2.4 EC2 shrinkage strains

Shrinkage strain ($\times10^{-6}$)	Typical relative humidity %	Notional size ($2A_c/u$) (mm)	
		≤150	600
Inside	50	600	500
Outside	80	330	280

2.5 LIGHTWEIGHT CONCRETE

Several notable prestressed concrete structures have been built in recent years with concretes made from lightweight aggregates. Apart from the primary advantage of a saving in weight, these concretes also offer better fire resistance and insulation properties.

The aggregates used may be naturally occurring, such as pumice, or manufactured, such as expanded blast furnace slag. The density of the concretes produced with these aggregates is in the range 1300–2000 kg/m^3, compared with 2400 kg/m^3 for normal-density concretes.

For lightweight concretes the strength is usually dependent on the strength of the aggregates. The 28-day cylinder strengths obtainable range from 1 N/mm^2, using expanded clay aggregate, to 50 N/mm^2, using pulverized-fuel-ash aggregate. The modulus of elasticity of lightweight concrete is between 50 and 70% of that of normal-density concrete. Shrinkage and creep effects are usually greater, and, in the absence of more detailed information from the aggregate supplier, the shrinkage strain may be taken as 400–600$\times10^{-6}$ and the specific creep as 0.7−0.9$\times10^{-4}$ per N/mm^2 (Abeles and Bardhan-Roy, 1981).

2.6 STEEL FOR PRESTRESSING

There are several different types of steel used for prestressing, covered by respective British Standards:

  (i) wire, to BS5896:1980;
 (ii) strand, to BS5896:1980;
(iii) bars, to BS4486:1980.

Wires vary in diameter from 3 to 7 mm, and have a carbon content of 0.7–0.85%. The wires are drawn from hot-rolled rods, which have been subsequently heated to 1000 °C and then cooled to make them suitable for drawing. After several drawing operations which reduce the diameter of the wire and increase the tensile strength, the wires are wound on to capstans with diameter 0.6–0.7 m. This is known as the

'as-drawn' condition, and the steel is supplied in mill coils, suitable for pretensioning.

However, as-drawn wires will not pay out straight from the coils, but they can be pre-straightened, to make them suitable for threading through post-tensioning ducts, by heating them for a short time, or heating them while subjected to high tension. Both these processes also increase the elastic range of the wires over the as-drawn condition. The former type of wire is known as *'stress-relieved'* wire, and the latter as *'stabilized'* wire. Stress-relieved wire is also termed *'normal-relaxation'* wire, while stabilized wire is also known as *'low-relaxation'* wire, since its relaxation properties (see Section 2.7) are much better than for either as-drawn or stress-relieved wire.

For pretensioned concrete members, the prestress force is transferred to the concrete by bond between the steel and concrete. This bond is substantially increased if indentations are made on the wire surface, and also if the wire is *'crimped'*, that is given an undulating, instead of a straight, shape. These two processes are shown in Fig. 2.5. The crimp pitch varies between five and twelve times the wire diameter, and the wave height varies between 5 and 12% of the diameter for helical crimping and between 10 and 25% of the diameter for uniplanar crimping.

Strand is produced by spinning several individual wires around a central core wire. Modern strands comprise seven wires with overall diameters ranging from 8 to 18 mm. A strand can be spun from as-drawn wires to produce an *as-spun* strand, or it can be heat treated after spinning to produce either normal- or low-relaxation strand.

In order to make the strands, six wires are helically wound round a central straight wire (Fig. 2.6(a)). They can be produced as either
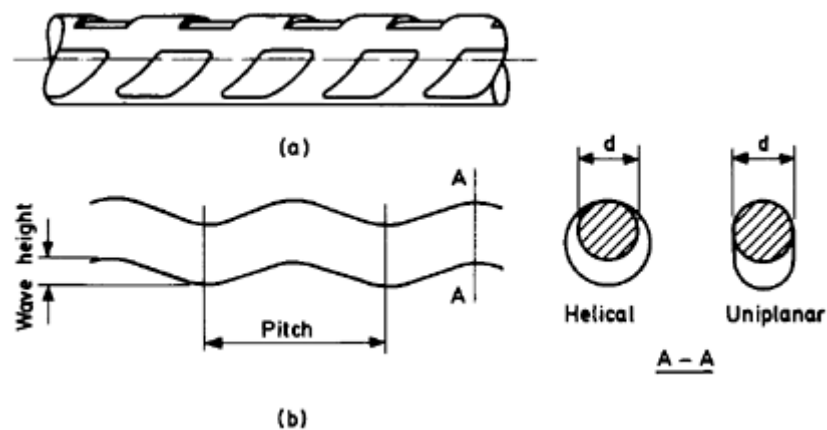
Figure 2.5 Wire for prestressing: (a) indentations; (b) crimps.
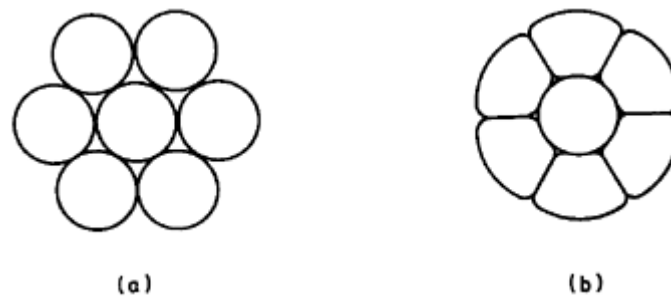
Figure 2.6 Prestressing strands: (a) wound; (b) drawn.

standard or *super* and can also be drawn through a die to compact them, when they are known as *'drawn'* strands; the cross-section is then as shown in Fig. 2.6(b). All three types of strand can be produced with either normal- or low-relaxation properties.

Hot-rolled alloy-steel bars vary in diameter from 20 to 40 mm, and are stretched once they have cooled in order to improve their mechanical properties. They may be ribbed, to provide a continuous thread, or smooth with threads at the ends of the bars. In both cases the threads are used to anchor the bars or to provide a coupling between adjacent bars.

The properties of the various types of wire, strand and bar are summarized in Table 2.5. Each manufacturer will have its own range of products, and reference should be made to trade literature before deciding on the choice of prestressing steel.

An important point to consider with all the types of steel described above is that their high strength is produced by essentially a cold-working process. Thus, during storage and construction care must be taken not to expose the steel to heat, from causes such as welding. Further information on the manufacture and properties of prestressing steel may be found in Bannister (1968).

2.7 RELAXATION OF STEEL

Relaxation of steel stress is similar to creep in concrete in that it is time-dependent deformation under constant load. The amount of relaxation depends on time, temperature and level of stress. The standard test for relaxation determines the value after 1000 hours at 20 °C and it is these values which are shown in Table 2.5. Values of 1000-hour relaxation may be taken from manufacturers' test certificates or, alternatively, from Fig. 2.7.

Two classes of relaxation are specified in BS5896, Class 1 corresponding to stress-relieved, or normal-relaxation, wires, and Class 2 corresponding to stabilized, or low-relaxation, wires.
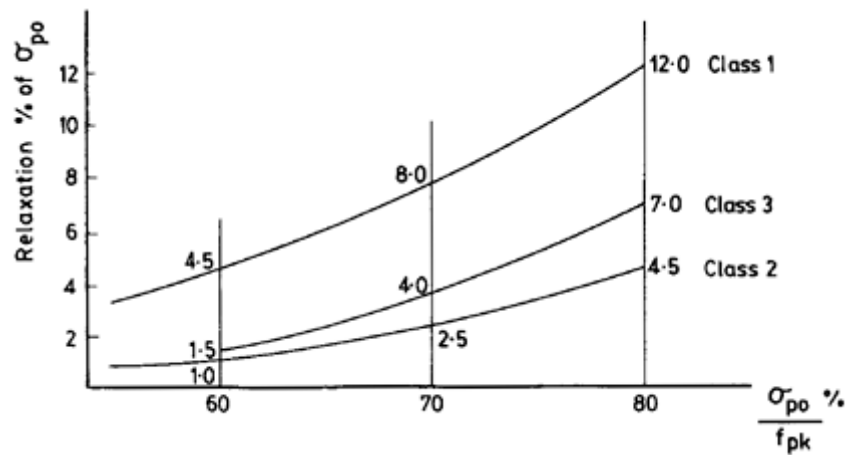
Figure 2.7 Relaxation of steel at 20 °C after 1000 h.
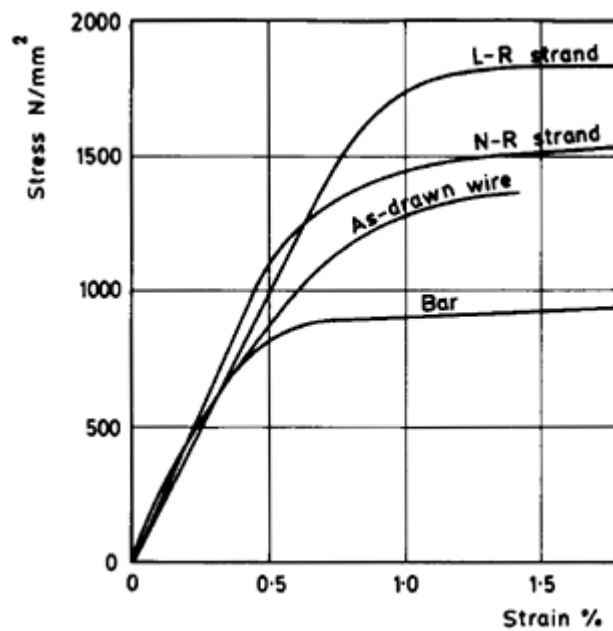
Figure 2.8 Stress-strain curves for prestressing steel.

2.8 STRESS-STRAIN CURVES FOR STEEL

Typical stress-strain curves for prestressing steel are shown in Fig. 2.8. These high-strength steels do not possess the same well-defined yield point as mild steel, and so the *proof* stress is defined as the stress at which, when the load is removed, there is a given permanent deformation. The deformation specified in British Standards for prestressing steel is 0.1% elongation, and so in Table 2.5 the 0.1% proof

Table 2.5 Properties of prestressing steel

BS	Type of tendon	Nominal diameter (mm) (and steel area (mm²))		Nominal tensile strength f_{pk} (N/mm²)	Specified characteristic load (kN)		Maximum relaxation (%) after 1000 h	
					Breaking load (A)	0.1% proof load or load at 1% elongation	at 70% of A	at 80% of A
						0.1% proof load	Class 1	
5896	Cold-drawn steel wire (Pre-straightened)	7	(38.5)	1670	64.3	53.4	8	12
		7		1570	60.4	50.1	Class 2	
		6	(28.3)	1770	50.1	41.6	2.5	4.5
		6		1670	47.3	39.3		
		5	(19.6)	1770	34.7	28.8		
		5		1670	32.7	27.2		
		4.5	(15.9)	1620	25.8	21.4		
		4	(12.6)	1770	22.3	18.5		
		4		1670	21.0	17.5		
						Load at 1% elongation		
	Wire in mill coils (As-drawn wire)	5	(19.6)	1770	34.7	27.8	For all wires	
		5		1670	32.7	26.2		
		5		1570	30.8	24.6		
		4.5	(15.9)	1620	25.8	20.6	10	
		4	(12.6)	1770	22.3	17.8		
		4		1720	21.7	17.4		
		4		1670	21.0	16.8		
		3	(7.1)	1860	13.1	10.5		
		3		1770	12.5	10.0		

						0.1% proof load		
5896	*7-wire steel strand*	15.2	(139)	1670	232	197	Class 1	
	Standard	12.5	(93)	1770	164	139	8	12
		11	(71)	1770	125	106	Class 2	
		9.3	(52)	1770	92	78	2.5	4.5
	Super	15.7	(150)	1770	265	225		
		12.9	(100)	1860	186	158		
		11.3	(75)	1860	139	118		
		9.6	(55)	1860	102	87		
		8	(38)	1860	70	59		
	Drawn	18	(223)	1700	380	323		
		15.2	(165)	1820	300	255		
		12.7	(112)	1860	209	178		
4486	*Hot-rolled or hot-rolled and processed alloy steel bars*							
	Hot rolled	40	(1257)	1030	1300	1050	3.5	6
		32	(804)		830	670		
		25	(491)		505	410		
		20	(314)		325	260		
	Hot rolled and processed	32	(804)	1230	990	870	3.5	6
		25	(491)		600	530		
		20	(314)		385	340		

loads are given. Alternatively, the load to cause 1% elongation may be specified. Also specified in Table 2.5 is the characteristic strength of the steel. This term will be explained in more detail in Chapter 3, but for the present it can be regarded as the breaking load of the wire or strand.

The heat-treating processes applied to the as-drawn wire not only decrease the relaxation of the steel, but also increase the proof stress, thus extending the linear elastic range.

Although the modulus of elasticity for various types of prestressing steel varies, for design purposes it is given in EC2 as 200×10^3 N/mm^2 for all types of steel.

2.9 CORROSION OF STEEL

As with steel reinforcing bars, prestressing steel must be protected from attack by moisture permeating the surrounding concrete. In pretensioned members this is prevented by having adequate cover to the tendons and also by using concrete with a sufficiently low water/cement ratio, which is usually the case for the high-strength concretes used for prestressed concrete.

The ducts in post-tensioned members were, for many years, grouted after tensioning. However, it has recently been considered that, following several failures which have been attributed to corrosion of partly-grouted tendons, all post-tensioned tendons should be left unbonded. A combination of greasing and coating with plastic has been used successfully as an alternative protection to the tendons. Measures such as pressure-testing of ducts before grouting may well lead to acceptance of grouted ducts once again. For bridges it is now considered essential to inspect the tendons at regular intervals during the design life of the structure, and this must be taken into account at the design stage. The technique of external prestressing, described in Chapter 1, allows regular monitoring to take place.

Another form of corrosion which can affect wires and strands is known as *stress corrosion,* and arises from a breakdown of the structure of the steel itself. Small cracks appear and the steel becomes brittle. Little is known about stress corrosion, except that it occurs at high levels of stress, to which prestressing steels are continually subjected.

Further information on corrosion and its prevention may be found in Libby (1971).

REFERENCES

Abeles, P.W. and Bardhan-Roy, B.K. (1981) *Prestressed Concrete Designer's Handbook,* Viewpoint, Slough.

Bannister, J.L. (1968) *Concrete,* August, pp. 333–342.

Department of the Environment (1975) *Design of Normal Concrete Mixes,* Her Majesty's Stationery Office, London.

Libby, J.A. (1971) *Modern Prestressed Concrete,* Van Nostrand Reinhold, New York.

Neville, A.M. (1996) *Properties of Concrete,* Pitman, London.

3

Limit state design

3.1 INTRODUCTION

The early codes of practice for reinforced concrete and steelwork design were based on the concept of working stresses. That is, the maximum elastic stresses in the materials under the design, or working, loads were compared to allowable values, based on the stresses at failure of the material divided by a suitable factor of safety. It was soon realized that concrete is an inelastic material, although elastic methods are still suitable for design load conditions for prestressed concrete members. This was reflected in the first code of practice for prestressed concrete, British Standard CP115, which adopted separate approaches for the design load and ultimate load behaviour of members. This was an early example of *limit state design*—identifying all the possible loading conditions for a member and choosing the most critical as the basis of design, while checking the other load conditions afterwards. A general approach based on limit state principles, which also identifies factors affecting the performance of structures other than loading, was incorporated into British Standards CP110 and BS8110, covering both reinforced and prestressed concrete, and has been retained in EC2.

3.2 LIMIT STATES

The limit state concept involves identification of the various factors that affect the suitability of a structure to fulfil the purpose for which it is designed. Each of these factors is termed a *limit state,* and if any of them is not satisfied, then the structure is deemed to have 'failed'. The consequences of failure, however, vary considerably between the limit states, and this may be accounted for by using different factors of safety for each. The two principal limit states for most structures are: ultimate limit state and serviceability limit state.

For any given structure, the limit states relevant to the loads acting upon, and the environment surrounding, the structure must be identified and the most critical defined.

For most prestressed concrete structures the design process entails initially considering the serviceability limit state of cracking, and then checking the ultimate strength limit state. Reinforced concrete design, by contrast, is usually based on the ultimate strength limit state, with later checks on the serviceability limit states.

(a) Ultimate limit state

Ultimate limit states that must be considered are:

(i) Strength

This is the most important of the ultimate limit states. The structure must be able to withstand, with an acceptable factor of safety against collapse, the loads likely to act upon it. Collapse can occur in several ways, including fracture of an individual member, instability of the structure as a whole, or by buckling of part of the structure. An adequate factor of safety against collapse under accidental overloading must also be provided, although this is generally lower than that provided for the design loads.

(ii) Fire resistance

The structure must stand for sufficient time to allow any occupants to escape. The fire resistance of a concrete structure is mainly determined by the concrete cover to the steel, since it is the steel strength which is greatly reduced with increasing temperature.

(iii) Fatigue

For structures subject to cyclic loading, this could be important, especially in the case of prestressed concrete structures, where the stress level in the prestressing steel is very high.

(b) Serviceability limit state

There are several serviceability limit states that need to be considered, the two most important of which are deflection and cracking.

(i) Deflection

The deflections of the structure under the design load must not be excessive, otherwise damage to finishes, partitions or cladding may result.

(ii) Cracking

Excessive cracking may not only be unsightly, but may lead to excessive ingress of water into the concrete, leading to corrosion of the steel.

(iii) Durability

If the concrete is too permeable then the risk of corrosion of the steel is increased. Possible attack by an aggressive environment, such as seawater, must also be considered. The main factors influencing the durability of prestressed concrete structures are the concrete mix proportions, the cover to the steel and protection to post-tensioning tendons.

(iv) Vibration

This is important in structures such as machine foundations.

3.3 CHARACTERISTIC LOADS AND STRENGTHS

An important concept in limit state design is that of a *characteristic* load, or material strength. This is a concept taken from the theory of probability and reflects the fact that, for instance, the concrete strength to be used in calculations should not be the mean strength determined from a series of cylinder tests, but rather a figure much lower than the mean, such that there is an acceptable probability that any given test result will be less than a specified value. This value is known as the *characteristic strength,* f_k.

The spread of cylinder test results from any mix of the same nominal proportions will generally follow a normal distribution curve, as shown in [Fig. 3.1](). The value of f_k is defined such that the shaded area corresponding to results below f_k is 5% of the total area under the curve. In terms of probability, this is equivalent to saying that there is a 1 in 20 chance of any test result falling below f_k, which is considered an acceptable probability.

From the mathematical properties of the normal distribution curve, it can be shown that

$$f_k = f_m - 1.64\sigma,$$

where σ is the standard deviation of the set of test results.

The distributions of strength of both prestressing and reinforcing steel also follow a normal curve, and in all subsequent work f_{ck} will be taken as the *characteristic concrete cylinder strength,* f_{yk} as the *characteristic yield strength* of untensioned steel and f_{pk} the *characteristic breaking strength* of prestressing steel.
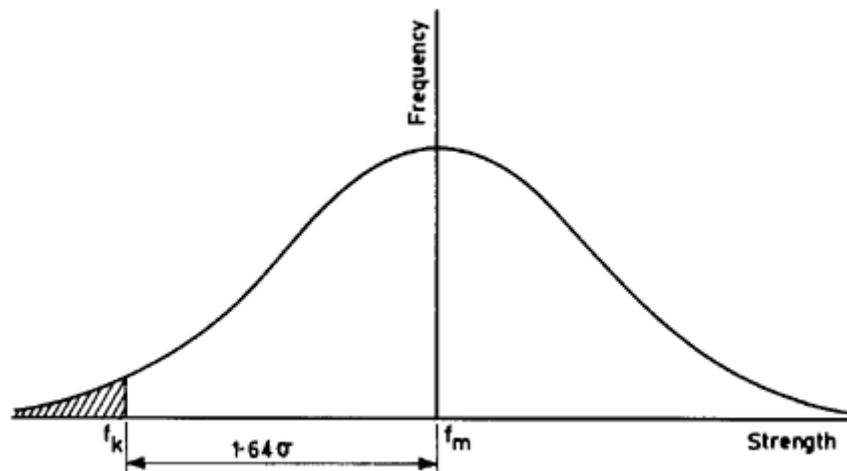
Figure 3.1 Concrete strength distribution.
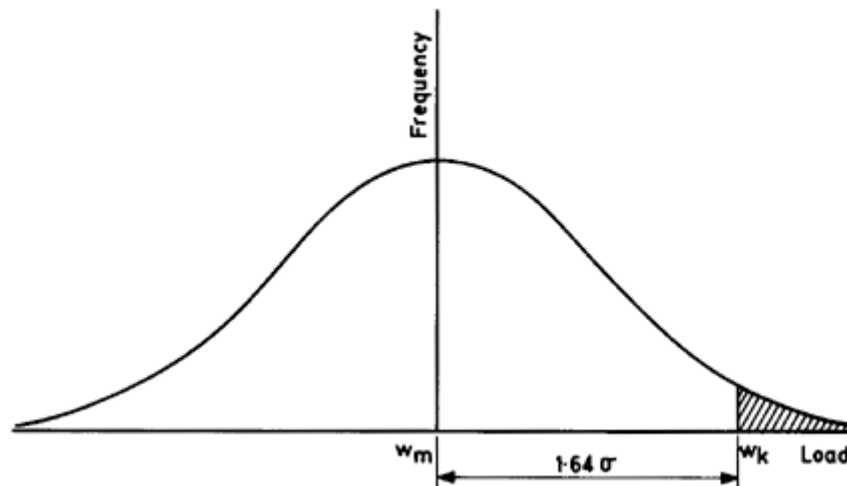
Figure 3.2 Load distribution.

In the case of loading on a structure, although there are at present insufficient data available fully to justify the use of probability methods, the limit state approach in EC2 assumes that the distribution of load on a structure also follows a normal curve, as shown in Fig. 3.2. The characteristic load on the structure, w_k, is defined as that load which has a 1 in 20 chance of being exceeded. In terms of the normal distribution curve this means that the shaded area is 5% of the total area under the curve, and the value of w_k is given by

$w_k = w_m + 1.64\sigma.$

3.4 PARTIAL FACTORS OF SAFETY

The characteristic values of strength and load are those which are used in calculations rather than average values, but for several reasons they are adjusted by the use of *partial factors of safety*.

For material properties, the characteristic strengths are divided by a partial factor of safety γ_m, so that the design strength is given by

design strength=f_k/γ_m

The use of γ_m is to account for various factors which are difficult to quantify individually; it is found that the use of an overall factor to cover them is satisfactory. The value of γ_m is chosen to take account of the variability of the strength properties of the material used, the difference between site and laboratory strengths, the accuracy of the methods used to determine the strength of sections, and variations in member geometry which affect this stength. The value of γ_m for concrete is higher than that for steel to allow for the lesser degree of control that can be exerted over the production of concrete compared with steel.

For loading, the characteristic load is multiplied by a partial factor of safety γ_f, so that the design load is given by

design load=$w_k \times \gamma_f$.

The values of γ_f accommodate the inherent uncertainties in the applied loading, the analytical methods used to obtain the bending moment and shear force distributions within a structure, and the effects on the design calculations of construction tolerances. The value of γ_f also reflects the importance of a given limit state and the consequences of its being exceeded. Thus the highest values of γ_f are assigned to the ultimate limit states.

An advantage of using partial factors of safety is that their values may be amended if more or less information is available. Thus if particularly good quality control of concrete production under factory conditions can be demonstrated, then a lower value of γ_m may be used. Conversely, if concrete production is known to be in the hands of unsupervised, unskilled labour, then γ_m may be increased. Some loads can be predicted more accurately than others, such as dead loads, or loads due to soils and liquids, and so a lower value of γ_f may be justified than when the loading is more difficult to predict.

The values of γ_f for the ultimate limit state recommended in EC2 for building structures are given in Table 3.1 and are suitable for most design purposes. Those for the serviceability limit state are generally taken as 1.0 for both dead and imposed loads. For the case of dead, wind and imposed loads acting together at the serviceability limit state, γ_f is 1.0 for the first and 0.9 for the latter two loads.

Table 3.1 Partial factors of safety for loads

	Dead		Imposed			
	Adverse	Beneficial	Adverse	Beneficial	Earth and water pressure	Wind
1. Dead and imposed (and earth and water pressure)	1.35	1.0	1.5	0	1.35	–
2. Dead and wind (and earth and water pressure)	1.35	1.0	–	–	1.35	1.5
3. Dead and wind and imposed (and earth and water pressure)	1.35	1.0	1.35	0	1.35	1.35

The values of γ_m are to be taken as 1.5 and 1.15 for concrete and steel, respectively. Although not stated specifically in EC2 the values of γ_m at the serviceability limit state are generally taken as 1.0 for both materials.

The value of the partial factor of safety for prestress force, γ_p, is 1.0 for most situations, although in some limit state calculations it is taken as the more onerous of 0.9 or 1.2, while for some serviceability limit state calculations the more onerous of 0.9 or 1.1.

For the load combinations in Table 3.1 the adverse γ_f is applied to any loads producing a critical condition for a given section, while the beneficial γ_f is applied to any load which lessens this condition.

Consideration should be given to the effects of large accidental overloads caused, for instance, by an explosion. In this case the loading should be as specified in Eurocode 1: *Basis of Design and Actions on Structures* (EC1), with γ_f taken as 1.0.

3.5 STRESS-STRAIN CURVES

The short-term stress-strain curves for concrete and prestressing steel in Chapter 2 are idealized in EC2 for design purposes, and these are shown in Figs 3.3 and 3.4 respectively, where the stresses have been divided by the appropriate γ_m. Note that the factor of 0.85 in Fig. 3.3 relates the cylinder strength of concrete and the flexural strength in an actual member.

These curves are suitable for determining the strength and short-term deformations of members, but for long-term deformations the modulus of elasticity of concrete should be modified, as described in Chapter 6.
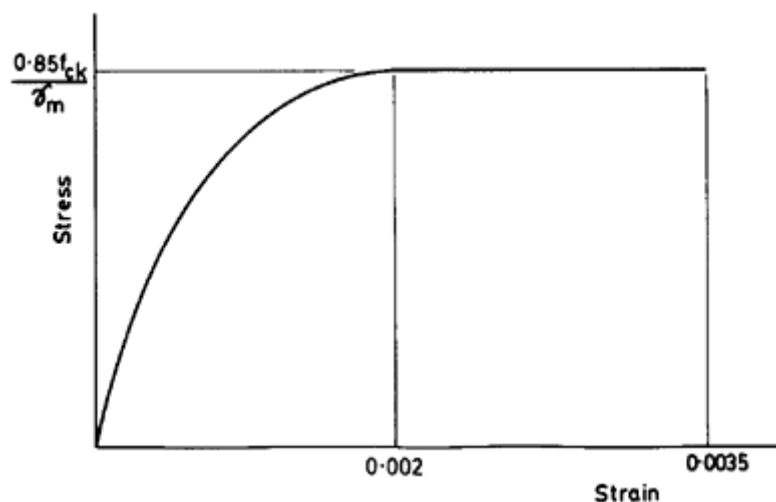
Figure 3.3 Design stress-strain curve for concrete.
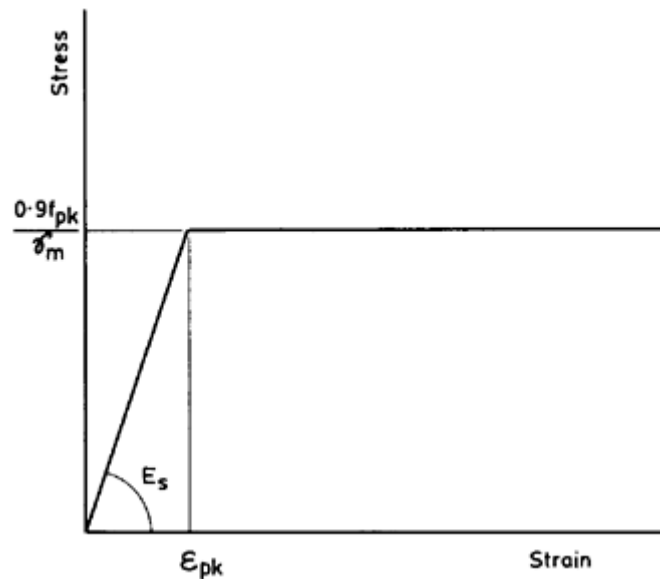
Figure 3.4 Design stress-strain curve for prestressing steel.

3.6 LOADING CASES

It was noted in Chapter 1 that, unlike reinforced concrete, for prestressed concrete members the minimum load condition is always an important one. Most prestressed concrete members are simply supported beams, and so the minimum bending moment at any section is that which occurs immediately after transfer of the prestress force. This is usually due to the self weight of the member, although in some cases additional dead load due to finishes may be present. Prestressed concrete members are often moved from their formwork soon after transfer and it can be assumed that the prestress force is a maximum, since only the short-term losses have occurred. The concrete is usually weaker than it is under the total load and so the allowable stresses at transfer are less than for that case.

An important consideration in composite construction, where a precast beam acts together with an *in situ* slab is the bending moment, M_d, due to the dead load, that is the weight of the beam and slab. In this case most of the losses have usually occurred and so the prestress force should be taken as a minimum.

The maximum bending moment occurs under the total design load and at this stage most of the long-term losses have occurred and the prestress force is a minimum.

For continuous beams, consideration must also be given to pattern loading, with the adverse and beneficial values of γ_f given in Table 3.1 applied to the various spans to give the maximum and minimum

bending moments for each span. Thus a third combination must be considered, that of minimum bending moment and minimum prestress force.

The principal loading cases for a simply supported member are summarized in Fig. 3.5, where P_o is the initial prestress force and αP_o and βP_o are the effective prestress forces for the respective loading cases (see Chapter 4).

The *design load* to which a structural member is subjected at the serviceability limit state is categorized in EC2 as one of the following:

(i) quasi-permanent

This represents the sustained load on the member, such as self weight and finishes, and is used for checking maximum concrete stresses and deflections of prestressed concrete members;

(ii) frequent

This represents a combination of sustained and variable imposed load which has a high probability of being achieved and is used to check the limit state of cracking in prestressed concrete members;

(iii) rare

This represents the total value of sustained and variable imposed loads that can occur and is used to check maximum concrete stresses.

The various characteristic imposed loads to be applied to any given structure are given in BS6399, Parts 1 and 3, and CP3: Chapter V: Part 2.
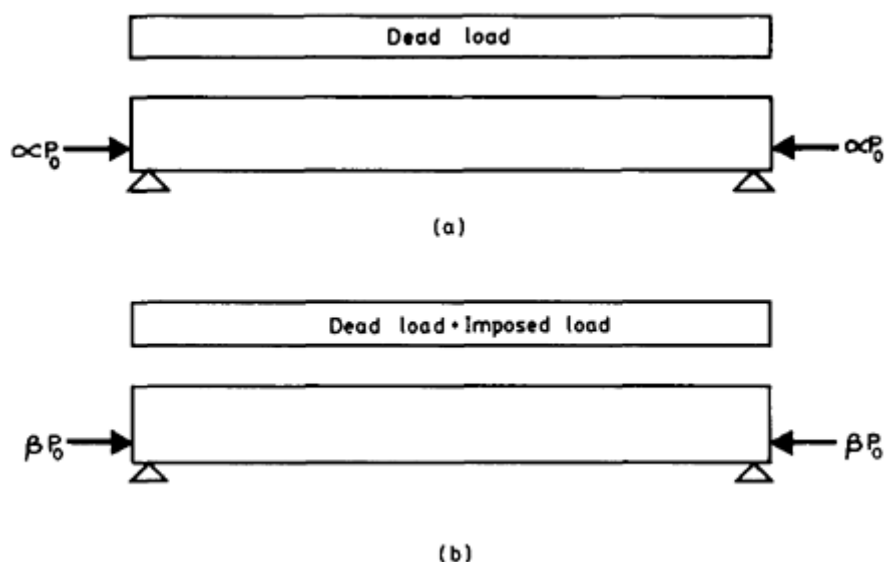
Figure 3.5

The partial factors of safety to be applied to the different types of characteristic load to give the quasi-permanent or frequent loads are shown in Table 3.2. The factors in Table 3.2 are for single independent load cases. If there are two or more such load cases acting together then separate partial factors of safety apply to the additional loads, given in EC2.

An important loading case for many prestressed concrete members is that which occurs when a slender member is being lifted, either for storage in a casting yard or factory, or into its final position on site. Lateral bending may occur in slender members, and a realistic estimate of the imperfections induced during the casting of the member must be made. Some guidance on estimation of the lateral bending moments induced is given in Rowe *et al*. (1987).

3.7 ALLOWABLE STRESSES

The allowable compressive stress in prestressed concrete is $0.6\,f_{ck}$ under the rare load combination, or $0.45\,f_{ck}$ under the quasi-permanent loads. The latter requirement is made in order to limit the creep deformations to those predicted by other parts of EC2. The maximum compressive stress at transfer, in most cases, can be taken as $0.6\,f_{ck}$.

The allowable tensile stresses in the various grades of concrete are shown in Table 2.1. At transfer, the concrete grade achieved at that time should be used. The allowable stresses apply to members with both bonded and unbonded tendons.

There is a requirement in EC2 that the stress in tendons should not exceed $0.75\,f_{pk}$, after all losses have been taken into account. However, this is rarely likely to be critical.

3.8 FIRE RESISTANCE

The fire resistance period for a structure, or a portion of a structure, is defined as that period for which the structure must remain intact during a fire, in order that all occupants may escape. The requirements for a

Table 3.2 Factors γ_f for quasi-permanent and frequent load combinations

Loading type	Quasi-permanent	Frequent
Dwellings	0.2	0.4
Offices and stores	0.3	0.6
Parking areas	0.6	0.7
Snow and wind	0	0.2

given structure are contained in the regulations, applicable to that structure.

The fire resistance of prestressed concrete members, as with reinforced concrete members, is governed by the loss of strength of the steel with increase in temperature, rather than by loss of concrete strength. Generally, failure of prestressed concrete members is only likely at temperatures above 400 °C. The high-strength prestressing steels lose a greater proportion of their strength at a given temperature than do reinforcing steels, being approximately one-half of the characteristic strength at 400 °C for strands. Thus greater fire resistance, in the form of cover to the steel, is required in prestressed concrete members than in reinforced concrete members. The cover required is usually greater than that required for protection against corrosion, and so should be considered at an early stage in the design process. For good fire resistance of all concrete members, attention must be paid to detailing, since reinforcement is required near the member faces to prevent spalling. Cracked members can withstand very high temperatures better than uncracked members, since their greater proportion of lower-strength steel is less affected by high temperatures. Lightweight aggregate concretes exhibit better fire resistance than normal-density concretes, since less spalling occurs and better insulation is afforded to the steel.

Fire resistance requirements will be given in Part 10 of EC2. In the meantime the provisions of BS8110 should be followed. The nominal covers specified in BS8110 for varying periods of fire resistance and type of structural elements are shown in Table 3.3. The lower cover values given for continuous members in all types of prestressed concrete, compared with the simply supported condition, are due to the fact that continuous members have the ability to redistribute the load if one region loses strength in a fire.

Table 3.3 Concrete cover for fire resistance (mm)

Fire resistance (h)	Beams		Floors		Ribs	
	Simply supported	Continuous	Simply supported	Continuous	Simply supported	Continuous
0.5	20	20	20	20	20	20
1	20	20	25	20	35	20
1.5	35	20	30	25	45	35
2	60	35	40	35	55	45
3	70	60	55	45	65	55
4	80	70	65	55	75	65

Detailed information is given in Part 2 of BS8110 on determining the fire resistance period of given structural elements, and also specified in the code are minimum overall dimensions of concrete members to provide given fire resistance periods. Further information on fire resistance of prestressed concrete members may be found in Abeles and Bardhan-Roy (1981).

3.9 FATIGUE

For prestressed concrete members subjected to repeated loading, the fatigue strength must be considered. The major areas where fatigue failure could occur are in the concrete in compression, the bond between the steel and concrete, and the prestressing steel.

The compressive stress level in concrete above which failure could occur is approximately $0.6\,f_{ck}$ and in the life of most prestressed concrete members this ensures that failure due to fatigue in the concrete is unlikely. Bond failures have been observed in tests on short members such as railway sleepers, but for most applications this does not present a problem.

Although the stress levels in prestressing tendons are high, the range of stress in the tendons is usually small. Fatigue failure of tendons has been observed in tests, generally associated with high concentrations of stress in the vicinity of cracks in the concrete. If the concrete remains uncracked, the range of stress in the steel is small. Uncracked members thus exhibit much better fatigue resistance than cracked members.

The fatigue strength of prestressing tendons may be taken to be between 65% and 75% of the characteristic strength for two million load cycles, and this is usually much greater than the maximum stress in the steel under total design load.

One area which has been identified as potentially troublesome is in pretensioned members where the tendons have been deflected. There are stress concentrations at the deflection points and deflected tendons should be avoided if the members are to be subjected to cyclic loading.

The stress variations in unbonded tendons are transferred to the anchorages rather than distributed to the surrounding concrete as with bonded tendons. Unbonded tendons should thus generally be avoided if fatigue is a consideration.

A method of determining the fatigue resistance of prestressed concrete members may be found in Warner and Faulkes (1979), and general information on fatigue found in Abeles and Bardhan-Roy (1981).

3.10 DURABILITY

There have been many failures of structures in recent years which can be attributed to poor durability of concrete. These failures have generally not resulted in actual collapse of a structure but serious corrosion of reinforcement has sometimes occurred, significantly weakening the structure.

Five degrees of exposure of concrete members are identified in EC2 and these are shown in Table 3.4. The minimum cover requirements for all types of steel in prestressed concrete members are given in Table 3.5. For members in exposure class 5c extra measures should be applied, such as ensuring that all sections remain in compression under all possible load combinations or providing a protective barrier to all steel in the section. The figures in Table 3.5 include a minimum construction tolerance of 5 mm. However, in a practical design other considerations, such as those outlined in the previous section and also in Chapter 9, also affect the final choice of cover.

Durability is further achieved by ensuring that the requirements of

Table 3.4 Classes of exposure

Exposure class	*Examples of environmental conditions*
1. Dry environment	Interior of buildings for normal habitation or offices
2. Humid environment	*a*Interior of buildings with high humidity Exterior components Components in non-aggressive soil
	*b*As *a* above but with exposure to frost
3. Humid environment with frost and de-icing salts	Interior and exterior components exposed to frost
4. Seawater environment	*a*Components completely or partially submerged in seawater or in the splash zone Components in saturated salt air
	*b*As *a* above but with frost
5. Aggressive chemical environment (in conjunction with classes 1–4)	*a*Slightly aggressive chemical environment Aggressive industrial atmosphere
	*b*Moderately aggressive chemical environment
	*c*Highly aggressive chemical environment

Table 3.5 Concrete cover for durability (mm)

Exposure class	Prestressing	Reinforcement
1	25	20
2a	40	35
2b	40	35
3	45	40
4a	45	40
4b	45	40
5a	40	35
5b	40	35
5c	50	45

Table 3.6 Criteria for limit state of crack width

	Design crack width under frequent load combination	
Exposure class	Post-tensioned	Pretensioned
1	0.2 mm	0.2 mm
2	0.2 mm	Decompression
3 & 4	Decompression or coating of the tendons and w_k=0.2 mm	Decompression

Table 3.6 are met. These apply to members with bonded tendons only; those with unbonded tendons should be treated as reinforced concrete members with regard to cracking (see Section 5.11). In Table 3.6 the term *'decompression'* is taken to mean that *all* of the tendons lie at least 25 mm within the compression zone. In theory, decompression can be achieved in both cracked and uncracked sections but, in practice, the 0.2 mm crack width limit applies to cracked sections and the decompression criterion applies only to uncracked sections.

3.11 VIBRATION

The fact that thinner members are used in prestressed concrete construction than in comparable reinforced concrete construction leads to the natural frequency of prestressed structures being near enough to the frequency of the applied loading to cause problems of resonance in some cases. Examples of structures where vibrations should be considered include foundations for reciprocating machinery, bridge beams (especially those in footbridges), long-span floors and structures subjected to wind-excited oscillations, such as chimneys.

A method is given in Warner and Faulkes (1979) for finding the natural frequency of most types of prestressed concrete members. Information is given in Concrete Society (1994) on the vibration of post-tensioned concrete floors.

REFERENCES

Abeles, P.W. and Bardhan-Roy, B.K. (1981) *Prestressed Concrete Designer's Handbook,* Viewpoint, Slough.

Concrete Society (1994) *Post-Tensioned Concrete Floors—Design Handbook,* Technical Report No. 43, London.

Rowe, R.E. *et al.* (1987) *Handbook to British Standard BS8110:1985 Structural Use of Concrete.* Viewpoint, London.

Warner, R.F. and Faulkes, K.A. (1979) *Prestressed Concrete,* Pitman, Sydney.

4

Loss of prestress force

4.1 INTRODUCTION

In Chapter 3 it was shown that one of the design conditions is that of maximum bending moment and minimum prestress force at any section. It is important, therefore, to obtain an estimate of the minimum prestress force throughout the structure.

There are several factors which cause the force in the prestressing tendons to fall from the initial force imparted by the jacking system. Some of these losses are immediate, affecting the prestress force as soon as it is transferred to the concrete member. Other losses occur gradually with time. These short- and long-term losses are summarized in Table 4.1.

Friction losses only affect post-tensioned members, and vary along their length. Thus the resulting prestress force anywhere in a post-tensioned member not only varies with time but with the position considered.

Experience with the production of prestressed concrete members will allow good estimates of the loss of prestress force to be made, but in the absence of such information estimates may be based on the recommendations given in the following sections. This information is, of necessity, general and approximate, and any given structure should be examined carefully to determine whether these recommendations are valid. Many successful highway bridges have been constructed in the USA using lump-sum estimates of the loss of prestress force, rather than by determining the contribution of each of the effects listed in Table 4.1.

High accuracy is rarely justified in determining the loss of prestress force and an accuracy of ±10% is sufficient for most purposes. The ultimate strength of prestressed concrete members is very little affected by the initial prestress force. Also, there is a low probability of the member being subjected to the full dead and imposed load, and there are partial factors of safety incorporated in the allowable concrete

Table 4.1 Prestress losses

Short-term	*Long-term*
Elastic shortening	Concrete shrinkage
Anchorage draw-in	Concrete creep
Friction	Steel relaxation
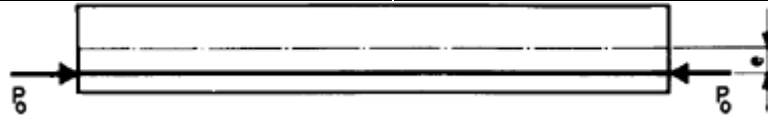
Figure 4.1

stresses. All these factors indicate that a prestressed concrete member is able to tolerate a small variation of prestress force.

4.2 ELASTIC SHORTENING

Consider a pretensioned member with an eccentric prestress force P_o transferred to it as shown in Fig. 4.1. At the level of the prestressing tendons, the strain in the concrete must equal the change in the strain of the steel.

Thus:

$$\sigma_{cg}/E_{cm} = \Delta\sigma_p/E_s;$$
$$\therefore \Delta\sigma_p = m\sigma_{cg},$$

(4.1)

where $m = E_s/E_{cm}$, the modular ratio, σ_{cg} is the stress in the concrete at the level of the tendons, $\Delta\sigma_p$ is the reduction in stress in the tendons due to elastic shortening of the concrete to which they are bonded, and E_s and E_{cm} are the moduli of elasticity of the steel and concrete respectively. The stress in the concrete is given by

$$\sigma_{cg} = \frac{P_e}{A_c} + \frac{(P_e e)e}{I_c}$$

$$= \frac{P_e}{A_c}\left(1 + \frac{e^2}{r^2}\right),$$

(4.2)

where P_e is the effective prestress force after elastic shortening, A_c and I_c are the cross-sectional area and second moment of area of the concrete

section respectively, and r is the radius of gyration, given by $r^2=I_c/A_c$.

Also,
$P_e=A_p(\sigma_{po}-\Delta\sigma_p)$,
(4.3)

where σ_{po} is the initial stress in the tendons and A_p is their cross-sectional area. Although, strictly speaking, the right-hand side of Equation 4.3 is the force in the tendon, for no applied axial force on the section this must equal the force in the concrete. Combining Equations 4.1, 4.2 and 4.3 gives

$$\sigma_{cg} = \frac{\sigma_{po}}{\left[m + \dfrac{A_c}{A_p\,(1 + e^2/r^2)} \right]}$$

(4.4)

If the tendons are closely grouped in the tensile zone, the loss due to elastic shortening may be found with sufficient accuracy by taking σ_{cg} as the stress in the concrete at the level of the centroid of the tendons. If the tendons are widely distributed throughout the section, then the above approximation is no longer valid. In this case the influences of the tendons, or groups of tendons, should be determined separately and then superimposed to give the total effective prestress force.

For a post-tensioned member the change in strain in the tendons just after transfer can be assumed to be equal to the strain in the concrete at the same level, even though the ducts have not been grouted and there is no bond between the steel and concrete. The loss of stress in the tendon is therefore still given by Equation 4.1. In practice, the force in post-tensioned members at transfer is not constant owing to friction. However, it is sufficiently accurate to base the elastic shortening loss on the initial prestress force P_o, assumed constant along the member.

The value of σ_{cg} in Equation 4.4 should reflect the fact that, in general, a member deflects away from its formwork during tensioning and the stress at any section is modified by the self weight of the member. The additional tensile stress at the level of the tendon is equal to $M_o e/I_c$, so that the total value of σ_{cg} is given by

$$\sigma_{cg} = \frac{\sigma_{po}}{\left[m + \dfrac{A_c}{A_p\,(1 + e^2/r^2)} \right]} - \frac{M_o e}{I_c}$$

(4.5)

The value of σ_{cg} will vary along a member, since generally both e and M_o will vary. In this case an average value of σ_{cg} should be assumed.

For a post-tensioned member with a single tendon, or with several

tendons tensioned simultaneously, there is no elastic shortening loss, since jacking will proceed until the desired prestress force is reached. In the more usual, and more economical, case where the tendons are tensioned sequentially, after the first tendon the tensioning of any subsequent tendon will reduce the force in those already anchored, with the exception of the last tendon, which will suffer no loss.

While it is possible to determine the resulting forces in a group of tendons for a given sequence of tensioning, the amount of work involved may be large. An acceptable approximation is to assume that the loss in each tendon is equal to the average loss in all the tendons. The loss for the first tendon is approximately equal to $m\sigma_{cg}$ (in practice it is always less but approaches this value as the number of tendons increases), and the loss for the last tendon is zero, so that the average loss is $m\sigma_{cg}/2$.

In the case of pretensioned tendons, it is usually assumed that the total force is transferred to the member at one time and that the elastic shortening loss is $m\sigma_{cg}$.

Example 4.1 ■■

Determine the loss of prestress force due to elastic shortening of the beam shown in Fig. 4.2. Assume that σ_{po}=1239 N/mm², A_p=2850 mm² and m=7.5 for the concrete at transfer.

Section properties:

w_o=9.97 kN/m; A_c=4.23×10⁵ mm²; I_c=9.36×10¹⁰ mm⁴; r=471 mm.

At midspan:

$$M_o = 9.97 \times 20^2/8 = 498.5 \text{ kNm}$$

$$\sigma_{cg} = \cfrac{1239}{\left[7.5 + \cfrac{4.23 \times 10^5}{2850(1 + 560^2/471^2)} \right]} - \cfrac{498.5 \times 10^6 \times 560}{9.36 \times 10^{10}} = 14.97 \text{ N/mm}^2$$

At the supports:

$$\sigma_{cg} = \frac{1239}{(7.5 + 4.23 \times 10^5/2850)} = 7.95 \text{ N/mm}^2.$$

Thus, in Equation 4.1:

$\Delta\sigma_p$=1/2×7.5×(14.97+7.95)/2=43 N/mm2,

which represents a loss of 3.5% of the initial stress.
    ■■
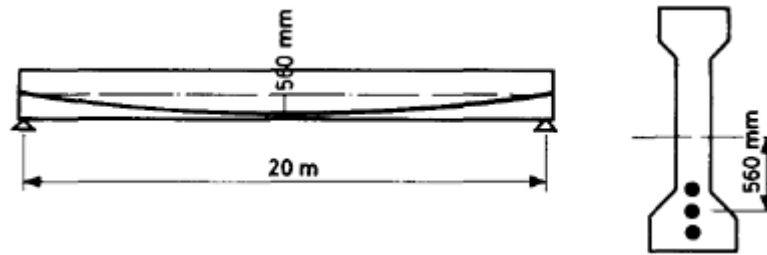
Figure 4.2

For pretensioned members, and for post-tensioned members once the ducts have been grouted, the short-term prestress force is effectively held constant. Any bending moment at a section will induce extra stresses in the steel and concrete due to composite action between the two materials (see Section 5.3), but the prestress force, as measured by the actual force transmitted to the ends of the member *via* the tendons, remains unaltered. For unbonded members, the prestress force will vary with the loading on the member, but in practice this effect is ignored.

4.3 FRICTION

In post-tensioned members there is friction between the prestressing tendons and the inside of the ducts during tensioning. The magnitude of this friction depends on the type of duct-former used and the type of tendon. There are two basic mechanisms which produce friction. One is the curvature of the tendons to achieve a desired profile, and the other is the inevitable, and unintentional, deviation between the centrelines of the tendons and the ducts.

A small, but finite, portion of a steel cable partly wrapped around a pulley is shown in Fig. 4.3(a). Since there is friction between the cable and the pulley, the forces in the cable at the two ends of the section are not equal. The frictional force is equal to μN, where μ is the coefficient of friction between cable and pulley. The triangle of forces for the short length of cable Δs is shown in Fig. 4.3(b); for the small angle $\Delta\alpha$, $N = T\Delta\alpha$. Thus, considering the equilibrium of the length of cable Δs:

$$T\cos(\Delta\alpha/2) + F = (T - \Delta T)\cos(\Delta\alpha/2).$$

For the small angle $\Delta\alpha$, $\cos(\Delta\alpha/2) \approx 1$.

$$\therefore T + F = T - \Delta T;$$
$$\therefore \mu T\,\Delta\alpha = -\Delta T.$$

Thus, in the limit as $\Delta s \to 0$:

$$dT/d\alpha = -\mu T.$$
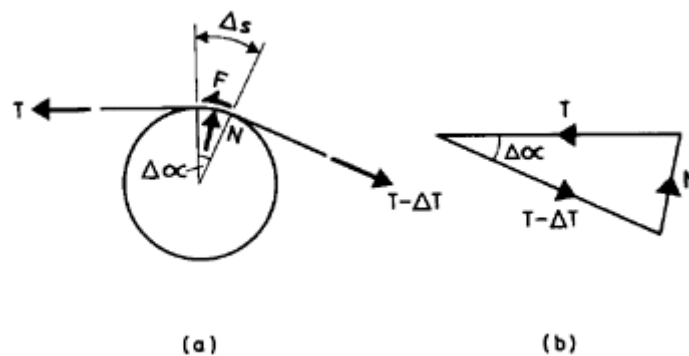
Figure 4.3 Friction in a cable.

The solution of this is

$$T(\alpha)=e^{-\mu\alpha} \equiv \exp{(-\mu\alpha)}$$

or

$$T_f=T_o \exp{(-\mu\alpha_o)},$$

(4.6)

where T_o and T_f represent the initial and final cable tensions respectively for a length of cable undergoing an angle change α_o.

The variation in tension in a tendon inside a duct undergoing several changes of curvature, as shown in Fig. 4.4, may be described using Equation 4.6. For the first portion of the curve, with radius of curvature r_{ps1}, the force in the tendon at point 2 is given by

$$P_2=P_1 \exp{(-\mu\alpha_1)}$$
$$=P_1 \exp{(-\mu s_1/r_{ps1})},$$

where s_1 is the length of the tendon to point 2. The force in the tendon has been denoted by P since it is the force in the concrete that is used in design. As noted previously, for no applied axial load the forces in the tendon and concrete must be equal. For most tendon profiles, s may be taken as the horizontal projection of the tendon, so that

$$P_2=P_1 \exp{(-\mu L_1/r_{ps1})}.$$

For the portion of the tendon 2–3, the initial force is P_2, and the final force P_3 is given by

$$P_3=P_2 \exp{[-\mu(L_2/r_{ps2})]}$$
$$=P_1 \exp{[-\mu(L_1/r_{ps1}+L_2/r_{ps2})]}.$$

This process can be repeated for all the changes in curvature along the length of the tendon. The force $P(x)$ in a curved tendon at an intermediate point along the curved length is given by

$$P(x)=P_o \exp{(-\mu x/r_{ps})},$$

(4.7)

where x is the distance from the start of the curve and P_o is the tendon force at the beginning of the curve.

Only variations of curvature in the vertical plane have so far been considered, but in many large bridge decks tendons curve in the horizontal plane as well, and the friction losses for these curvatures must also be taken into account.

The variation between the actual centrelines of the tendon and duct is known as the 'wobble' effect (Fig. 4.5). This is generally treated by considering it as additional angular friction, so that the expression for the force in a tendon due to both angular friction and wobble is given by

$$P(x)=P_o \exp \left[-\mu(x/r_{ps}+kx)\right],$$
(4.8)

where k is a profile coefficient with units of rad./m. The value of k depends on the type of duct used, the roughness of its inside surface and how securely it is held in position during concreting.

If $\mu (x/r_{ps}+kx) < 0.2$ then Equation 4.8 may be simplified to

$$P(x)=P_o \left[1-\mu (x/r_{ps}+kx)\right].$$

Values of k should be taken from technical literature relating to the particular duct being used and are generally in the range 50–100×10^{-4} rad/m. For greased strands wrapped in plastic sleeves, as used in slabs, k may be taken as 600×10^{-4} rad/m.
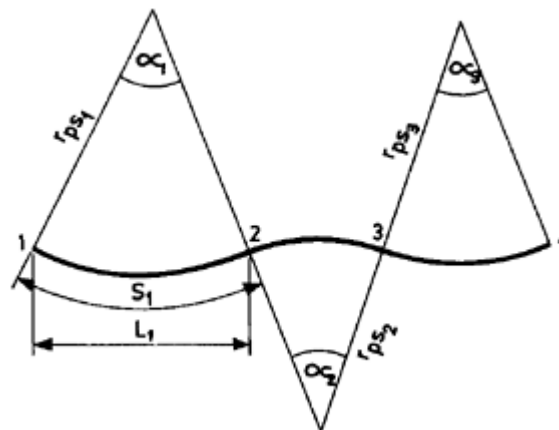
Figure 4.4 Tendon with several curvature changes.

Figure 4.5 The 'wobble' effect.

Typical values of μ for wires and strands against different surfaces for tendons which fill approximately 50% of the duct are shown in Table 4.2.

Example 4.2 ∎∎

For the beam in Example 4.1 determine the prestress loss due to friction at the centre and the right-hand end if the prestress force is applied at the left-hand end. Assume $\mu=0.19$ and $k=50\times10^{-4}$ rad./m.

The total angular deviation in a parabolic curve may be conveniently determined using the properties of the parabola shown in Fig. 4.6.

Thus, for the tendon profile in Fig. 4.2:

$\alpha=2\tan^{-1}(4d_r/L)$
$=2\tan^{-1}(4\times560/20000)$
$=0.223$ rad.

The radius of curvature is given by

$r_{ps}=(d^2y/dx^2)^{-1}=L^2/8d_r$
$=20^2/(8\times0.560)$
$=89.29$m.

Table 4.2 Coefficients of friction for different tendon types

Type of wire/strand	Bonded Grouted duct	Unbonded Steel tube	Unbonded HDPE tube
Lubricated:			
Cold drawn wire		0.16	0.10
Strand		0.18	0.12
Non-lubricated:			
Cold drawn wire	0.17	0.24	0.12
Strand	0.19	0.25	0.14
Greased strand			0.05
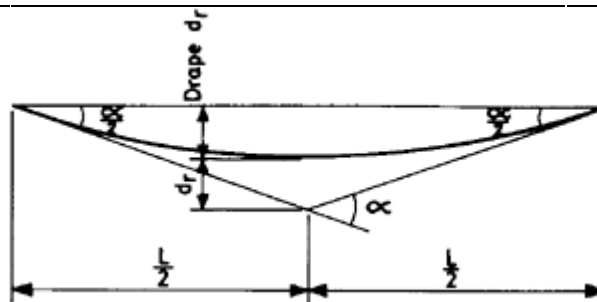
Figure 4.6 Properties of parabolic profiles.

$P_o = 2850 \times 1239 \times 10^{-3}$
$= 3531.2$ kN.

Thus, using Equation 4.8:

$P(x) = 3531.2 \exp [-0.19(x/89.29 + 50 \times 10^{-4}x)]$.

At midspan:

$P(x=10) = 3531.2 \exp [-0.19(10/89.29 + 50 \times 10^{-4} \times 10)]$
$= 3424.4$ kN.

Thus the loss is 106.8 kN, which is 3.0% of the initial force.
At the right hand end:

$P(x=20) = 3531.2 \exp [-0.19(0.223 + 50 \times 10^{-4} \times 20)]$
$= 3321.6$ kN.

The loss is now 209.6 kN, that is 5.9% of the initial force.
■■

The friction losses in the relatively shallow tendon in Example 4.2 are small, but in members with tendons of large curvature the losses may be so large that the member must be tensioned from both ends to achieve an acceptable value of prestress force at the centre. In members with many tendons, it is the usual practice to tension half the number of tendons from one end and the remainder from the opposite end, resulting in the same net prestress force at midspan but a more even distribution of prestress force along the member than if all the tendons had been tensioned from the same end.

Example 4.3 ■■
For the beam in Figure 4.7, determine the minimum effective prestress force if an initial prestress force of 3000 kN is applied (i) at the left-hand end only; (ii) at both ends. Assume the same values of μ and k as in Example 4.2.
   (i)   The total angular change for the full length of the tendon is given by

$$\sum \frac{x}{r_{ps}} = \frac{18.75}{121.93} + \frac{12.5}{77.39} + \frac{18.75}{121.93}$$
$$= 0.469 \text{ rad.}$$

The minimum prestress force occurs at the right-hand end of the beam:

$P(x=50) = 3000 \exp [-0.19(0.469 + 50 \times 10^{-4} \times 50)]$
$= 2616.9$ kN.

① r_{ps} = 121·93m   ② r_{ps} = 77·39m
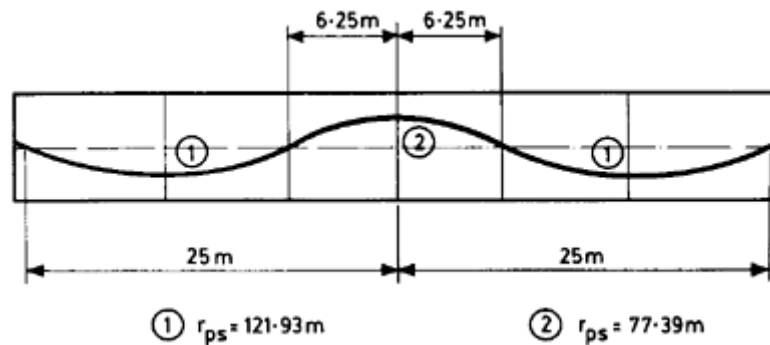
Figure 4.7

Thus the loss is 383.1 kN, which is 12.8% of the initial force.

(ii) If the beam is tensioned from both ends, the minimum prestress force is at the centre of the beam. Then:

$$\Sigma \frac{x}{r_{ps}} = \frac{18.75}{121.93} + \frac{6.25}{77.39}$$
$$= 0.235 \text{ rad.}$$

$$\therefore P(x = 25) = 3000 \exp\left[-0.19(0.235 + 50 \times 10^{-4} \times 25)\right]$$
$$= 2801.7 \text{ kN}$$

The loss is now 198.3 kN, i.e. 6.6% of the initial force.

The frictional losses in the right-hand span have been greatly reduced by tensioning from both ends, although the prestress force at the centre support is the same in both cases.

■■

There are two additional frictional effects which occur. The first takes place as the tendons pass through the anchorages. This effect is small, however, of the order of 2%, and is usually covered by the calculated duct friction losses, which tend to be conservative. There is also a small amount of friction within the jack itself, between the piston and the jack casing, which causes the load applied to the tendon to be smaller than indicated by the hydraulic pressure within the jack. This is usually determined by the jack manufacturer and compensation made in the pressure gauge readings.

Although friction is a cause of loss of prestress force principally in post-tensioned members, in pretensioned members there is some loss if the tendons are tensioned against deflectors, caused by friction between

the tendon and the deflector. The magnitude of this loss will depend upon the details of the deflector, and will usually be determined from tests on the particular deflection system being used.

Many modern bridges now employ external post-tensioned tendons. Where these pass over deflectors or through diaphragms there is some loss of prestress. However, mid-length friction losses using such tendons are small.

Further information on friction during tensioning may be found in a report of the Construction Industry Research and Information Association (1978).

4.4 ANCHORAGE DRAW-IN

A prestressing tendon may undergo a small contraction during the process of transferring the tensioning force from the jack to the anchorage; this is known as anchorage 'draw-in'. The exact amount of this contraction depends on the type of anchorage used and is usually specified by the manufacturer of the anchorage. In the case of pretensioning it can be compensated easily by initially over-extending the tendons by the calculated amount of the anchorage draw-in.

Many anchorage systems use wedges to grip the tendon and transfer the tendon force to a solid steel anchorage set in the concrete. There is some deformation of the solid anchorage itself, but this is very small, and most of the contraction in the length of the tendon takes place as a result of slip between the tendon and the wedges. A typical value would be 5 mm. The slip of wedges can be reduced by ensuring that they are pushed forward as far as possible to grip the tendons before releasing the jack. Those anchorages which transfer the prestress force through a bar with a threaded nut or a wire with a shaped end suffer negligible draw-in.

Since the anchorage draw-in is a fixed amount which is dependent only on the type of anchorage used, the effect is much greater on a short prestressed concrete member than on a long one. However, the effect is greatly reduced in post-tensioned members by the friction that exists between the tendons and the ducts as the tendons move back due to the draw-in. The length of tendon used to determine this loss of prestress is not the total length of the tendon, but a smaller effective length, as shown in the next section.

4.5 VARIATION OF INITIAL PRESTRESS FORCE ALONG A MEMBER

It is now possible to look at how the prestress force varies along the length of a post-tensioned member immediately after transfer of the prestress force (ignoring elastic shortening). The line *ABC* in Fig. 4.8

represents the variation in prestress force away from the anchorage, based on Equation 4.8.

The vertical ordinate AD represents the loss of prestress force due to draw-in, ΔP_A. Over the length AB, the tendons are being relaxed, so that they tend to move in the opposite direction to the original direction moved during tensioning. On the assumption that Equation 4.8 applies regardless of which way the tendons are actually moving, the variation of prestress force follows the curve DB, which is the reflection of the curve AB. Beyond point B the force in the tendon is unaffected by the draw-in. For most shapes of tendon profile used, the total deviated angle is small, and the two curves AB and DB in Fig 4.8 may be approximated by straight lines, as shown in Fig. 4.9.

If the friction loss per metre is p, then from Fig. 4.9 it can be seen that

$$\Delta P_A/2 = p x_A.$$
(4.9)

If the anchorage draw-in is δ_{ad}, then the reduction in stress is based on an effective length of the tendons x_A, since beyond this length the tendon is unaffected by the draw-in.

Thus, the loss of stress in the steel is given by

$$\Delta\sigma_p = \varepsilon_s E_s$$
$$= (\delta_{ad}/x_A) E_s.$$

Since $\Delta\sigma_p A_p = \Delta P_A/2$, then:

$$\Delta P_A/2 = (\delta_{ad}/x_A) E_s A_p$$
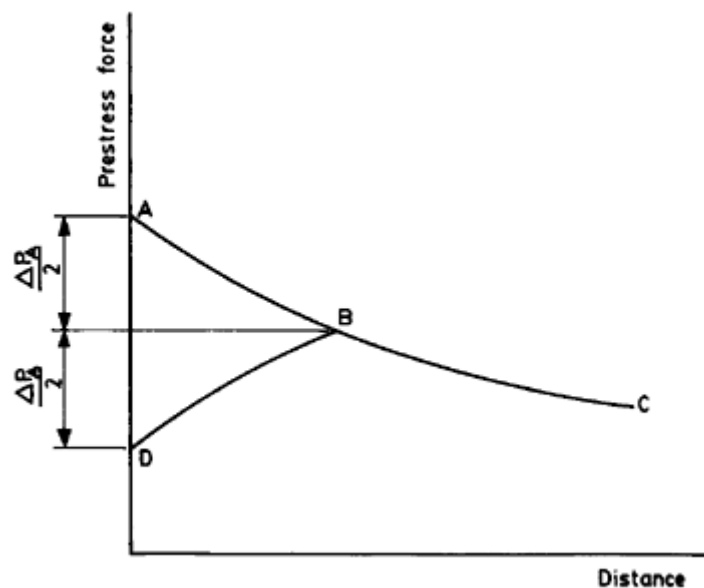
Figure 4.8 Anchorage draw-in.
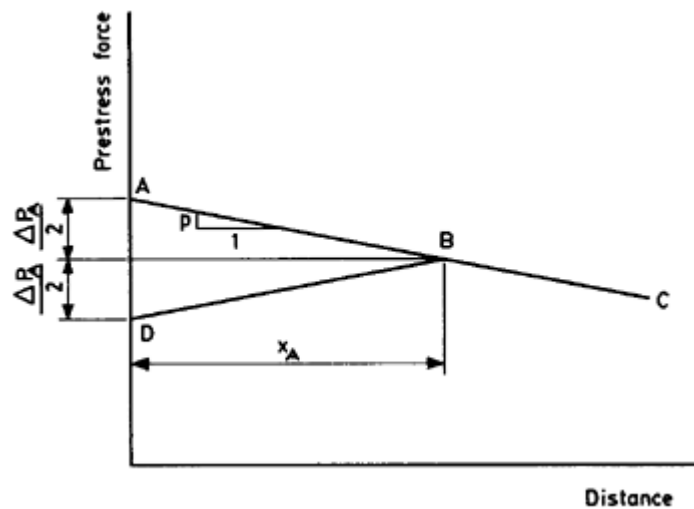
Figure 4.9 Idealized prestress force distribution.

Thus, in Equation 4.9:

$$px_A=(\delta_{ad}/x_A)E_sA_p;$$
$$\therefore\ x_A=(\delta_{ad}E_sA_p/p)^{1/2}.$$
(4.10)

Example 4.4 ∎∎
   For the beam in Example 4.1 determine the initial prestress force distribution along the beam if the anchorage draw-in is 5 mm.
   The friction loss per unit length near the anchorages is given by

$$p=P_o\{1-\exp[-\mu(1/r_{ps}+k)]\}$$
$$=3531.2(1-\exp[-0.19(1/89.29+50\times10^{-4})]\}$$
$$=10.83\ \text{kN/m}.$$

Thus, in Equation 4.10:

$$x_A=(5\times200\times10^3\times2850/10.83)^{1/2}\times10^{-3}$$
$$=16.22\ \text{m}.$$

The loss of prestress force at the left-hand end is given by

$$\Delta P_A=2\times10.83\times16.22$$
$$=351.3\ \text{kN}.$$

The total force variation due to friction in the tendon at transfer is as shown in . From this must be deducted the elastic shortening loss.
   The prestress force at midspan is 3288.2 kN, representing a loss of

9.3%. In this example there would be no benefit from tensioning from the right-hand end as well, since in this case the prestress force distribution (shown by broken lines in Fig. 4.10) would result in a prestress force at the right-hand end which is less than that obtained if tensioning were carried out from the left-hand end only.

■■

4.6 LONG-TERM LOSSES

Shrinkage of concrete was discussed in Chapter 2, and one of its effects in prestressed concrete members is that, since the prestressing steel is connected by bond or anchorage to the concrete, the steel also contracts, and the prestress force is reduced.

Shrinkage is dependent on many factors, and approximate long-term values for shrinkage strain to be used in design are given in EC2 and Table 2.4.

The phenomenon of creep in concrete was also discussed in Chapter 2, and its principal effect in prestressed concrete members is the same as that due to shrinkage, namely a reduction in prestress force caused by shortening of the member with time. As with shrinkage, there are many factors which affect the creep of concrete, and approximate values of the creep coefficient, to be used in estimating prestress losses due to creep, are given in EC2 and Table 2.3.
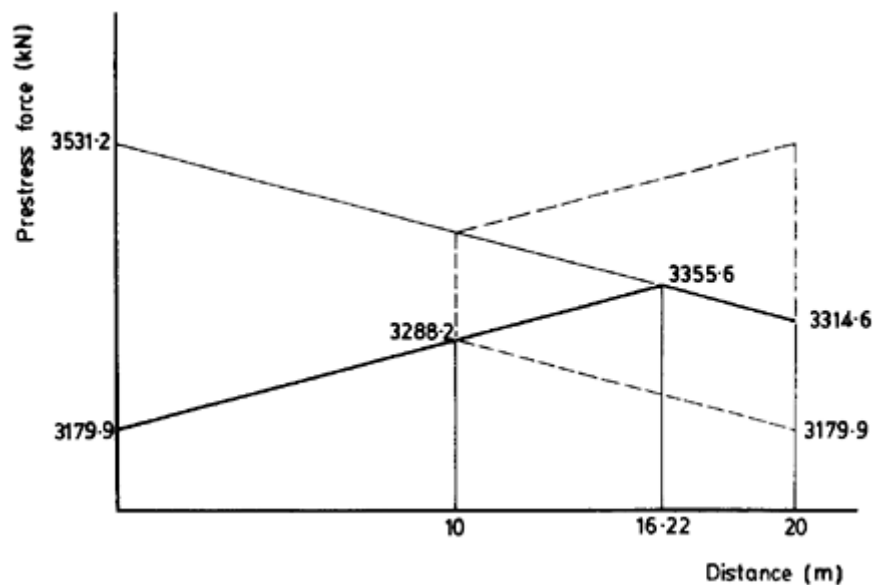
Figure 4.10 Prestress force distribution for beam in Example 4.1.

Creep and shrinkage losses are very little affected by the grade of steel used. It is thus advantageous to use as high a grade of steel as possible, since the percentage losses of prestress force due to creep and shrinkage will be minimized.

For lightweight aggregate concretes, the creep and shrinkage effects are greater than, and the modulus of elasticity less than, those of normal-density concretes. Thus the loss of prestress force to be expected will be greater.

Steel relaxation is described in Chapter 2, along with the manufacturing processes used to minimize relaxation. The long-term relaxation loss is specified in EC2 as the 1000-hour relaxation test value given by the tendon manufacturer or, in the absence of this, the value given in Table 2.5 multiplied by the factors in Table 4.3. These factors include allowances for the effects of creep and shrinkage and in the case of pretensioned members, the effects of elastic shortening. In cases where the tendons are subjected to high temperature, due allowances for the increase in relaxation should be made.

The long-term losses due to concrete shrinkage and creep, and to steel relaxation, can be determined separately and then summed. Alternatively, the following expression is given in EC2 for the long-term losses due to concrete shrinkage and creep, and to steel relaxation:

$$\Delta\sigma_{p,c+s+r} = \frac{\varepsilon_{sh}E_s + \Delta\sigma_{pr} + m\,\phi(\sigma_{cg} + \sigma_{cpo})}{1 + mA_p/A_c\,[(1 + A_c\,e^2/I_c)\,(1 + 0.8\phi)]}\,,$$

(4.11)

where ε_{sh} is the estimated shrinkage strain from Table 2.4; m is the modular ratio E_s/E_{cm} (where E_{cm} is based on the long-term value of concrete strength); φ is the creep coefficient from Table 2.3; $\Delta\sigma_{pr}$ is the variation of stress in the tendons due to steel relaxation (from Fig. 2.7); σ_{cg} is the stress in the concrete adjacent to the tendons, due to self weight and any other permanent loads; σ_{cpo} is the initial stress in the concrete adjacent to the tendons due to prestress; and e is the eccentricity of the tendons.

Strictly speaking, Equation 4.11 is iterative, since the expression for $\Delta\sigma_{pr}$ depends on the final value of prestress. However, examination of

Table 4.3 Relaxation factors

	Class 1 (wire and strand)	Class 2 (wire and strand)	Class 3 (bars)
Pretensioning	1.5	1.2	–
Post-tensioning	2.0	1.5	2.0

Fig. 2.7 shows that, with the usual initial stress in tendons of 0.7 f_{pk}, for long-term losses of more than 15%, the relaxation losses are sensibly constant.

Example 4.5 ■■

For the beam in Example 4.1, determine the total prestress losses due to shrinkage, creep and steel relaxation, if the quasi-permanent load is 40 kN/m.

From Table 2.4, assuming indoor conditions of exposure and that $2A_c/u$ is approximately 200, ε_{sh} is 590×10^{-6}. From Table 2.3, with transfer at 7 days, φ is 2.93. For long-term concrete strength, m=6.25.

Assuming that the prestressing tendons are of low-relaxation steel (BS5896, Class 2), from Fig 2.7 for long-term steel stress of 0.6 f_{pk} and from Table 4.3:

$\Delta\sigma_{pr}$=0.01×1239×1.5
=18.6 N/mm^2.

At midspan:

M_{qp}=49.97×20^2/8
=2498.5 kNm.

From Fig. 4.10 and Example 4.1, at the left-hand support:

$$\sigma_{cg} = \sigma_{cpo} \quad = \frac{3057.3 \times 10^3}{4.23 \times 10^5} = 7.23 \text{ N/mm}^2.$$

At midspan:

$$\sigma_{cg} = \frac{3165.6 \times 10^3}{4.23 \times 10^5} + \frac{3165.6 \times 10^3 \times 560^2}{9.36 \times 10^0} - \frac{2498.5 \times 10^6 \times 560}{9.36 \times 10^0}$$
$$= 7.48 + 10.61 - 14.95$$
$$= 3.14 \text{ N/mm}^2.$$

$$\sigma_{cpo} = 7.48 + 10.61$$
$$= 18.09 \text{ N/mm}^2.$$

At the right-hand support:

$$\sigma_{cg} = \sigma_{cpo} \quad = \frac{3192 \times 10^3}{4.23 \times 10^5} = 7.55 \text{ N/mm}^2.$$

The total long-term prestress losses due to shrinkage, creep and steel relaxation are thus:

At the left-hand support:

$$\Delta\sigma_{p,c+s+r} = \frac{590 \times 10^{-6} \times 200 \times 10^3 + 18.6 + 6.25 \times 2.93 \times 7.23}{1 + 6.25 \times 2850/4.23 \times 10^5[(1 + 4.23 \times 10^5/9.36 \times 10^{10})(1 + 0.8 \times 2.93)]}$$
$$= 236 \text{ N/mm}^2.$$

At midspan:

$$\Delta\sigma_{p,c+s+r} = \frac{590 \times 10^{-6} \times 200 \times 10^3 + 18.6 + 6.25 \times 2.93(3.14 + 18.09)}{1 + 6.25 \times 2850/4.23 \times 10^5[(1 + 4.23 \times 10^5 \times 560^2/9.36 \times 10^{10})(1 + 0.8 \times 2.93)]}$$
$$= 392 \text{ N/mm}^2.$$

At the right-hand support:

$$\Delta\sigma_{p,c+s+r} = \frac{590 \times 10^{-6} \times 200 \times 10^3 + 18.6 + 6.25 \times 2.93 \times 7.55}{1 + 6.25 \times 2850/4.23 \times 10^5[(1 + 4.23 \times 10^5/9.36 \times 10^{10})(1 + 0.8 \times 2.93)]}$$
$$= 241 \text{ N/mm}^2.$$

The average long-term loss is thus 290 N/mm^2; this represents 23.4% of the initial prestress.

∎∎

4.7 TOTAL PRESTRESS LOSSES

If the initial prestress force applied to a member is P_o, then the effective prestress force at transfer is αP_o, and at design load βP_o. The value of α reflects the short-term losses due to elastic shortening, anchorage draw-in and friction, while the value of β accounts for the long-term losses due to concrete creep and shrinkage and steel relaxation.

Although there are many factors which affect the total loss of prestress force, as described in the preceding sections, it is very useful at the initial design stage to have an approximate figure for the prestress loss. This can be refined later in the design process, when more details of the prestressing steel are available.

For both pretensioned and post-tensioned members, the approximate values of α and β may be taken as 0.9 and 0.75 respectively. For the beam in Example 4.1, the corresponding values are 0.9 and 0.66.

Lump-sum estimates for losses are given in the American specification for bridges, AASHTO (1975). For losses other than those due to friction and anchorage draw-in, these are 310 N/mm^2 and 228 N/mm^2 for pretensioned and post-tensioned members respectively.

4.8 MEASUREMENT OF PRESTRESS FORCE

The actual force transmitted to the prestressing steel by the jack in a post-tensioned member is measured by a combination of measurement of the hydraulic pressure in the jack and measurement of tendon extension during tensioning. Most jacks are compensated for the small

amount of friction between the pistol and the jack casing. They are calibrated by the manufacturers against load cells and are usually accurate to within a few percent.

Knowledge of the expected extension of the steel during tensioning serves as a check on the calculations for the loss of prestress force due to friction and elastic shortening. If the measured extension for a given jack hydraulic pressure deviates by more than 5% from the expected value, then corrective action should be taken.

If the measured extension is too low, then the friction effects have been underestimated and the prestress force along the member will be less than expected. Conversely, if the measured extension is too high, the friction effects have been overestimated and the actual prestress force along the member will be greater than expected. The first situation is potentially the more serious, and may be remedied by making a revised estimate of $\mu(1/r_{ps}+k)$ based on the actual extension achieved, recalculating the extension required to give the desired prestress force along the member and continuing the tensioning until this extension is reached. The initial tendon force must not exceed $0.8 f_{pk} A_p$ however, as described in the next section.

The measured extension may also indicate whether a blockage has occurred in the duct during tensioning. Thus, if only half the expected extension is achieved, even though the jack pressure indicates that the full force has been applied to the tendon, this could indicate that the tendon is not being tensioned uniformly along its length and that grout may have entered the duct during concreting, effectively holding a portion of the tendon rigid. This illustrates why prestress force measurement should not be based on tendon extension alone, since, in the example mentioned above, tensioning would have continued, possibly causing fracture of the tendon.

If a steel tendon with length L is tensioned gradually from zero tension up to the maximum force of $0.7 f_{pk} A_p$ the expected elongation, ignoring friction, is given by

$$\delta_e = 0.7 f_{pk} L / E_s.$$

There is always some initial slack in a tendon, and the usual procedure is to apply a small force P', of the order of 10% of the final prestress force, and to measure the total extension from the initial extension due to this force. The extra elongation expected δ_{ex}, when the tendon is tensioned to its full force, is then given by

$$\delta_{ex} = [(P_o - P')/P_o]\delta_e.$$

The elastic shortening of the concrete must be added to, and any anchorage draw-in at the untensioned, or dead-end, anchorage deducted from, the calculated elongation.
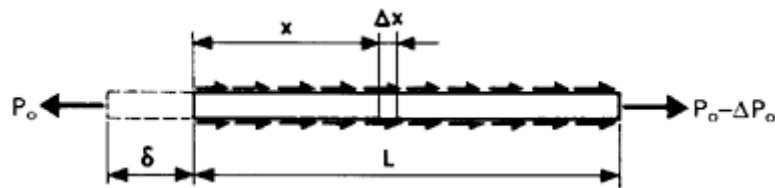
Figure 4.11 Tendon elongation.

In order to consider the effect of friction on the elastic elongation of the prestressing steel, consider a length L of steel tendon, subjected to a prestress force P_o, as shown in Fig. 4.11. The force in the tendon at a distance x from the tensioned end is given by Equation 4.8, that is

$$P(x) = P_o \exp\left[-\mu(x/r_{ps} + k)\right].$$

For a small length of tendon Δx, the extension is given by

$$\Delta\delta_e = \Delta x P(x)/(E_s A_p).$$

Thus, for the total length L, the extension is given by

$$\delta_e = \int_0^l \frac{P(x)}{E_s A_p}\, dx$$

$$= (P_o/E_s A_p) \int_0^l \exp\left[-\mu(1/r_{ps} + k)x\right] dx$$

$$= \frac{-P_o\{\exp\left[-\mu(1/r_{ps} + k)L\right] - 1\}}{E_s A_p \mu(1/r_{ps} + k)}.$$

(4.12)

Example 4.6 ■■
  Determine the measured elongation for the beam in Example 4.1.
  From Equation 4.12,

$$\delta_e = \frac{-3531.2\{\exp[-0.19(1/89.29 + 50 \times 10^{-4}) \times 20] - 1\}}{200 \times 10^6 \times 2850 \times 10^{-6} \times 0.19(1/89.29 + 50 \times 10^{-4})}$$
$$= 0.12 \text{ m, or } 120 \text{ mm.}$$

Ignoring the frictional resistance, $\delta_e = 124$ mm.
  ■■

4.9 INITIAL OVERTENSIONING

One way of overcoming the losses due to anchorage draw-in and friction is to tension the tendons initially to a stress greater than the usual $0.7 f_{pk}$. It is stipulated in EC2 that, for mature concrete, the maximum initial stress in the tendons is $0.8 f_{pk}$ and should not be greater than $0.75 f_{pk}$ once the immediate losses have occurred.

Example 4.7 ■■
   Determine the initial prestress force distribution for the beam in Example 4.1 if the tendons are initially tensioned to $0.8 f_{pk}$.

   Initial prestress force$=0.8 \times 1770 \times 2850 \times 10^{-3}$
   $=4035.6$ kN.

Thus the friction loss per metre p is given by

   $p=4035.6(1-\exp[-0.19(1/89.69+50 \times 10^{-4})]\}$
   $=12.37$ kN/m.

Thus, in Equation 4.10:

   $x_A=(5 \times 200 \times 10^3 \times 2850/12.37)^{1/2} \times 10^{-3}$
   $=15.18$ m.

The loss of prestress force at the anchorage is thus given by

   $\Delta P_A=2 \times 12.37 \times 15.18$
   $=375.6$ kN.

The prestress force distribution due to friction is as shown in Fig. 4.12. The effective prestress force at the tensioning end is 3660.0 kN, corresponding to $0.73 f_{pk}$, and the prestress force at midspan is 3783.7 kN, which is a 15.1% increase on the midspan value obtained if the tendons are initially tensioned to $0.7 f_{pk}$.
   ■■

   Further information on prestress losses in general may be found in Abeles and Bardhan-Roy (1981) and Rowe *et al.* (1987), and on the behaviour of tendons during tensioning in FIP (1986).

PROBLEMS

4.1 A minor source of loss of prestress force, which is usually ignored, arises from the change in profile of internal tendons resulting from the deflection of the concrete members through which they pass. A

Figure 4.12 Initial overtensioning for beam in Example 4.1.

Figure 4.13

Figure 4.14

prestressed concrete beam, of section size 800 mm×400 mm and length 15 m, is shown in Fig. 4.13. The initial stress in the tendons is 1239 N/mm^2, giving an initial prestress force of 1800 kN, with the centre of the beam initially fixed in position vertically. If the restraint is subsequently released, determine the percentage loss of prestress force in the tendons ignoring all other sources of loss. It may be assumed that E_s and E_{cm} are 200×10^3 and 32×10^3 N/mm^2, respectively.

4.2 Determine the radii of curvature of the two portions of the tendon profile shown in Fig. 4.14 and the eccentricity at the inflexion point.

4.3 For the beam in Example 4.1 determine the average elastic shortening loss if the tendons are each tensioned one by one from the lowest one upwards to their full design value, as measured according to the jack hydraulic pressure gauge. It may be assumed that the vertical spacing of the tendons is 75 mm and that the beam lifts from its soffit shutter on tensioning of the first tendon.

4.4 For the beam in Example 4.4 what is the maximum value of anchorage draw-in such that tensioning from both ends of the beam would be beneficial?

REFERENCES

Abeles, P.W. and Bardhan-Roy, B.K. (1981) *Prestressed Concrete Designer's Handbook,* Viewpoint, Slough.

American Association of Highway and Transportation Officials (1975) *AASHTO Interim Specifications—Bridges,* Subcommittee on Bridges and Structures, Washington.

Construction Industry Research and Information Association (1978) *Prestressed Concrete—Friction Losses During Stressing.* Report No. 74 CIRIA, London.

Fédération Internationale de la Précontrainte (1986) *Tensioning of Tendons: Force Elongation Relationship.*

Rowe, R.E. *et al.* (1987) *Handbook to British Standard BS8110:1985 Structural use of Concrete,* Viewpoint, London.

5

Analysis of sections

5.1 INTRODUCTION

The design of a prestressed concrete structure involves many considerations, the most important of which is the determination of the stress distributions in the individual members of the structure. In most types of structure it is usually sufficient to consider certain critical sections where the stresses are greatest. In prestressed concrete structures, however, since high stresses are introduced by the prestress force, all sections must be considered as critical and the stress distributions checked for all stages of loading. The practical means of carrying this out will be discussed in Chapter 9.

This chapter is concerned with the distribution of flexural stresses at the serviceability and ultimate limit states. These two distributions are different, but in determining them the three basic principles employed are the same. These are: (a) strain distribution, (b) material stress-strain curves and (c) equilibrium. The basic difference between the analysis of sections at the serviceability and ultimate limit states is that in principle (b) different regions of the stress-strain curves are used in each case.

(a) Strain distribution

This is assumed to be linear in elastic bending theory, and this assumption is also found to be sufficiently true for concrete members even up to the point of failure. The strain in the steel in pretensioned and bonded post-tensioned members is assumed to be the same as that in the concrete at the same level.

(b) Material stress-strain curves

These have been described in detail in Chapter 2 for both steel and concrete.

(c) Equilibrium

At any section in a prestressed concrete member there must be equilibrium between the stress resultants in the steel and concrete and the applied bending moment and axial load (if any) at that section.

5.2 SERVICEABILITY LIMIT STATE

The analysis of sections in uncracked members at the serviceability limit state is carried out by treating the section as linearly elastic and using ordinary bending theory. (The analysis for cracked members will be considered in Section 5.11.) This is justified by the fact that, at the design load, the stress-strain curve for steel is linear, and for concrete it is approximately linear.

In Section 1.3 it was shown that, in an unloaded prestressed concrete member, at any cross-section the concrete behaves as if it were subjected to an axial force P and a bending moment Pe, where e is the eccentricity of the prestress force at that section (Fig. 5.1). Thus the stress distribution due to an eccentric prestress force can be written as:

$$\sigma_t = (P/Ac) - (Pe/Z_t)$$
$$\sigma_b = (P/Ac) + (Pe/Z_b),$$

where e is taken as positive if it is below the member centroidal axis, A_c is the cross-sectional area, σ_t and σ_b are the stresses, and Z_t and Z_b the section moduli for the top and bottom fibres of the member respectively. The sign convention used is that compressive stresses and sagging bending moments are positive. If an external sagging bending moment M is now applied to the section, an additional distribution of stresses is introduced and the resultant stress distribution due to prestress force and applied bending moment may be found by superposition.

$$\sigma_t = (P/A_c) - (Pe/Z_t) + (M/Z_t)$$
(5.1a)

$$\sigma_b = (P/A_c) + (Pe/Z_b) - (M/Z_b).$$
(5.1b)
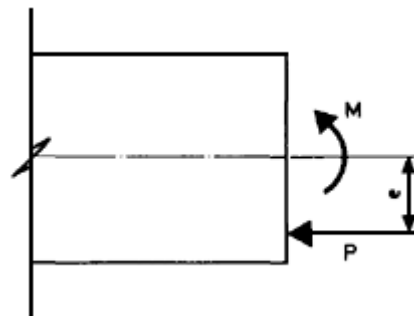
Figure 5.1 Prestress moment and applied moment at a section.
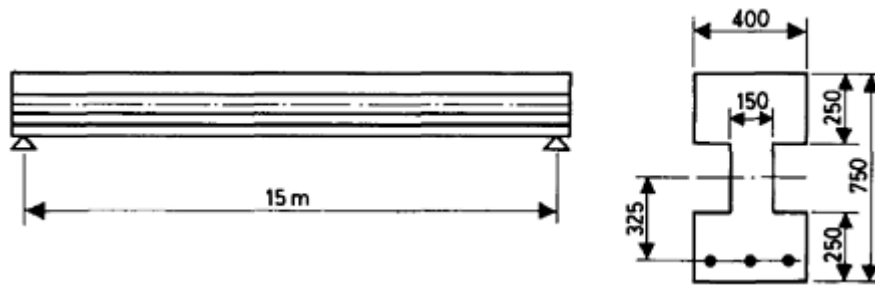
Figure 5.2

If in addition to the applied bending moment at the section there is also an applied axial load, then the force P in the first term on the right-hand side of Equations 5.1(a) and (b) is the sum of the prestress force and the applied axial load.

Example 5.1 ■■

A simply supported pretensioned concrete beam has dimensions as shown in Fig. 5.2 and spans 15 m. It has an initial prestress force of 1100 kN applied to it and it carries a uniformly distributed imposed load of 12 kN/m. Determine the extreme fibre stresses at midspan (i) under the self weight of the beam, if the short-term losses are 6% and the eccentricity is 325 mm below the beam centroid; (ii) under the total design load, when the prestress force has been reduced by a further 14%.

$A_c = 2.38 \times 10^5$ mm^2
$Z_b = Z_t = 36.63 \times 10^6$ mm^3
$w_o = 5.7$ kN/m
$M_o = 5.7 \times 15^2/8 = 160.3$ kNm
$M_{des} = 17.7 \times 15^2/8 = 497.8$ kNm
$\alpha P_o = 0.94 \times 1100 = 1034$ kN
$\beta P_o = 0.8 \times 1100 = 880$ kN.

(i)

$$\sigma_t = \frac{1034 \times 10^3}{2.38 \times 10^5} - \frac{1034 \times 10^3 \times 325}{36.63 \times 10^6} + \frac{160.3 \times 10^6}{36.63 \times 10^6}$$
$$= 4.34 - 9.17 + 4.38$$
$$= -0.45 \text{ N/mm}^2.$$

$$\sigma_b = 4.34 + 9.17 - 4.38$$
$$= 9.13 \text{ N/mm}^2.$$

(ii)
$$\begin{aligned}
\sigma_t &= \frac{880 \times 10^3}{2.38 \times 10^5} - \frac{880 \times 10^3 \times 325}{36.63 \times 10^6} + \frac{497.8 \times 10^6}{36.63 \times 10^6} \\
&= 3.70 - 7.81 + 13.59 \\
&= 9.48 \text{ N/mm}^2.
\end{aligned}$$

$$\begin{aligned}
\sigma_b &= 3.70 + 7.81 - 13.59 \\
&= -2.08 \text{ N/mm}^2.
\end{aligned}$$

The two stress distributions, at transfer and under the total design load, are shown in Fig. 5.3(a) and (b) respectively. Figure 5.3(b) is valid only if $\sigma_b > f_{ctm}$.

■■

The stress distributions shown in Fig. 5.3 are typical of those in a prestressed concrete member under maximum and minimum loads, and illustrate the point made in Chapter 1 that an important difference between prestressed and reinforced concrete is that with prestressed concrete the minimum load condition is always an important one. These four stress conditions lead to a method of design for prestressed concrete sections which will be discussed in further detail in Chapter 9.

So far the prestress force in a prestressed concrete member has been provided by a single layer of tendons, so that the resultant prestress force coincides with the physical location of the layer of tendons at each section. However, there is usually more than one layer of tendons in prestressed concrete members. In this case the resultant prestress force coincides with the location of the resultant of all the individual prestressing tendons, even if it is not physically possible to locate a tendon at this position. For members with external prestressing, none of the tendons actually lie within the concrete section.
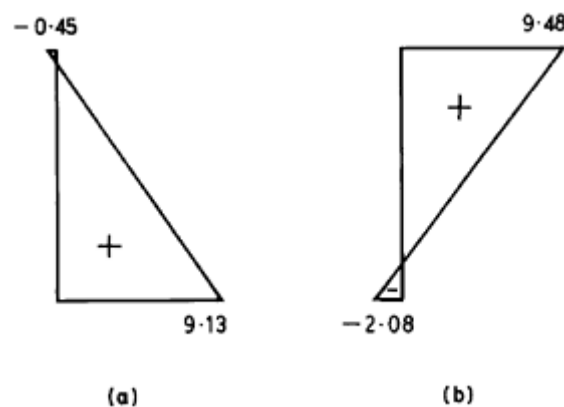
Figure 5.3 Stress distribution for beam in Example 5.1 (N/mm^2) (a) at transfer and (b) under the total design load.

For post-tensioned members where the duct diameter is not negligible in comparison with the section dimensions, due allowance for the duct must be made when determining the member section properties. For pretensioned members, the transformed cross-section should, strictly speaking, be used. However, in practice, the section properties are generally determined on the basis of the gross cross-section.

5.3 ADDITIONAL STEEL STRESS DUE TO BENDING

In the case of ungrouted post-tensioned members there is no bond between the prestressing steel and the surrounding concrete, but with pretensioned and grouted post-tensioned members a bond is present, and bending of the member induces stress in the steel, as in a reinforced concrete member. It is the bond between the steel and concrete which makes the ultimate load behaviour of pretensioned and grouted post-tensioned members very similar to that of reinforced concrete members, and different from that of ungrouted post-tensioned members. The bond enables composite behaviour between the steel and concrete to take place, and the extra stresses induced in the steel at the serviceability limit state may be determined by using the transformed cross-section properties.

Example 5.2 ■■
   The beam in Example 5.1 is pretensioned with tendons having a total cross-sectional area of 845 mm^2. Determine the stress in the tendons under the total design load based on a composite section.
   All of the loads acting on the beam are resisted by the transformed concrete section, as shown in Fig. 5.4. The transformed area of the prestressing steel is mA_p, where m is the modular ratio, E_s/E_{cm}. For values of E_s and E_{cm} of 200×10^3 and 32×10^3 N/mm^2 respectively, m is 6.25.
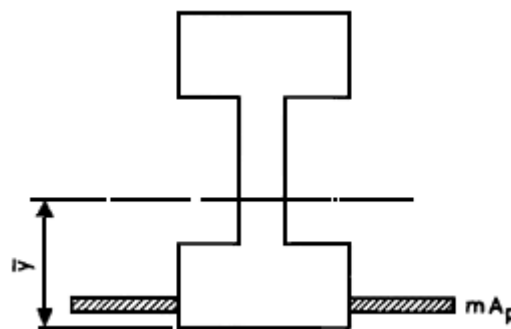
Figure 5.4 Transformed section.

Assuming a linear distribution of concrete stress it can be shown that y=368 mm and that the second moment of area of the transformed section is 1.43×10^{10} mm^4. The eccentricity of the prestress force about the centroid of the transformed section is 318 mm.

The steel stress induced by the applied load is given by

$\Delta\sigma_{pb}=m(M_{des}-M_o)y/I_{comp}$
$=6.25 (497.8-160.3)\times10^6\times318/(1.43\times1010)$
$=47$ N/mm^2.

The effective steel prestress after all losses have occurred is given by

$\sigma_{pe}=880\times10^3/845$
$=1041$ N/mm^2,

and the total steel stress σ_p is now 1041+47=1088 N/mm^2. The extra stress induced by bending in this, and most other cases, is thus small and is usually ignored.

5.4 POST-CRACKING BEHAVIOUR

If the imposed load on the beam is increased, then the tensile stress at the soffit of the beam will increase proportionately, until the tensile strength of the concrete is reached. If this is, say 2.9 N/mm^2 for the concrete in the beam in Example 5.1, then the bending moment M_{cr} which will cause this stress to be reached is given by

$$-2.9 = \frac{880 \times 10^3}{2.38 \times 10^5} + \frac{880 \times 10^3 \times 325}{36.63 \times 10^6} - \frac{M_{cr} \times 10^6}{36.63 \times 10^6}$$

$$\therefore M_{cr} = 527.7 \text{ kNm.}$$

(5.4)

If the imposed load is increased beyond this value then the concrete in the tensile zone must be assumed to have cracked. In EC2 it is stated that once this happens under a rare load combination then stresses under all load combinations should be determined using a cracked-section analysis. In this, the contribution of all concrete below the neutral axis is neglected. It is assumed that there is still a bond between the concrete and steel, even though the concrete surrounding the steel is cracked. This is the same assumption that is made in reinforced concrete section analysis.

The usual procedure for determining the neutral axis of a cracked reinforced concrete section is no longer applicable since the prestrain in
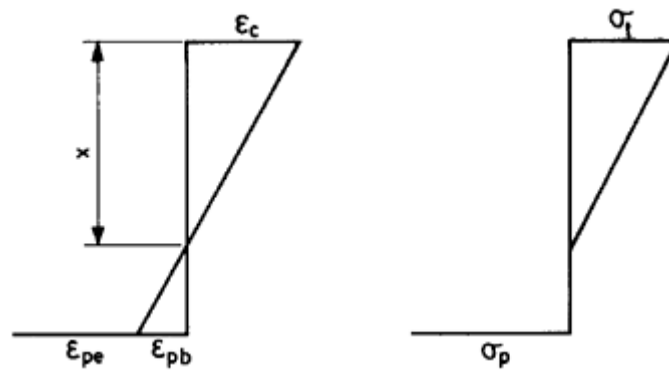
Figure 5.5 Strain and stress distributions for cracked section.

the tendons must be taken into account. A numerical solution is often the simplest.

The strain and stress diagrams for a cracked section are shown in Fig. 5.5, and the procedure for a cracked-section analysis is as follows:

(a) Choose a strain in the concrete extreme fibres, ε_c;
(b) Choose a neutral axis depth, x;
(c) Determine the concrete and steel stresses from the relevant stress-strain curves, neglecting the concrete in tension below the neutral axis;
(d) Check whether total compression equals total tension within the section (for no applied axial load). If it does, determine the moment of resistance of the section. If not, go back to steps (a) and (b) and repeat steps (c) and (d);
(e) Repeat steps (a)–(d) until the moment of resistance equals the applied bending moment.

Note that when determining the force in the prestressing steel, the total strain ε_p comprises two components, that due to the bending action of the beam, ε_{pb} and that due to the effective prestrain in the tendon, ε_{pe}.

A cracked-section analysis is extremely laborious, since there are two unknowns, ε_c and x, and is best carried out using a computer spreadsheet program. An example is given in Chapter 13. The procedure is exactly the same as that which will be used in the next section to analyse a member at the ultimate load. There, the value of ε_c is fixed, leaving x as the only unknown, which simplifies the calculations considerably.

Cracked-section analyses are necessary for checking that the crack widths are not excessive (see Section 5.11) and also for checking deflections (see Section 6.4).

Example 5.3 ■■

For the beam in Example 5.1 use a cracked-section analysis for an applied bending moment of 527.7 kNm to determine the stress in the steel.

$$\varepsilon_{pe} = \frac{880 \times 10^3}{845 \times 200 \times 10^3} = 0.00521$$

The stress and strain distributions which give equal tension and compression and also balance the applied bending moment are found using the trial and error approach outlined above, taking into account the varying beam width, and are shown in Fig. 5.6.

From Fig. 5.6, the moment of resistance is given by

M_r=933.3×0.565
=527.3 kNm;
σ_p=(0.00521+0.000311)×200×10^3
=1104 N/mm^2.

■■

It has been assumed in the foregoing that the concrete stress-strain curve is linear. Although this is a reasonable approximation for the initial region of the stress-strain curve, for the analysis of a cracked section at much higher loads the full non-linear curves for both steel and concrete must be considered.

5.5 ULTIMATE LOAD BEHAVIOUR

As the imposed load is increased still further, both the concrete and steel stresses will increase, following the respective stress-strain curves.
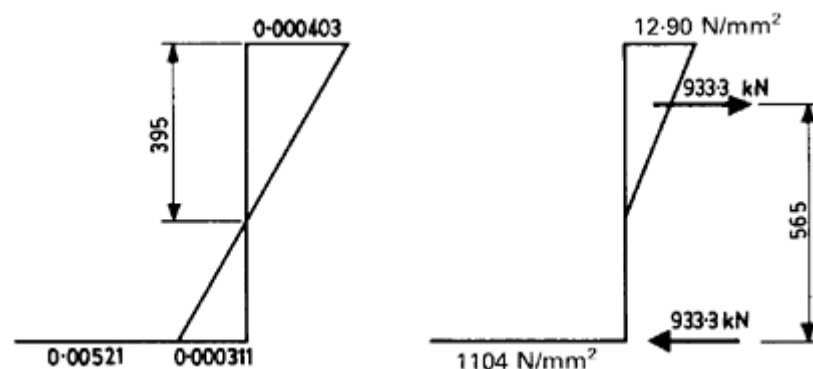
Figure 5.6 Strain and stress distributions for Example 5.3.
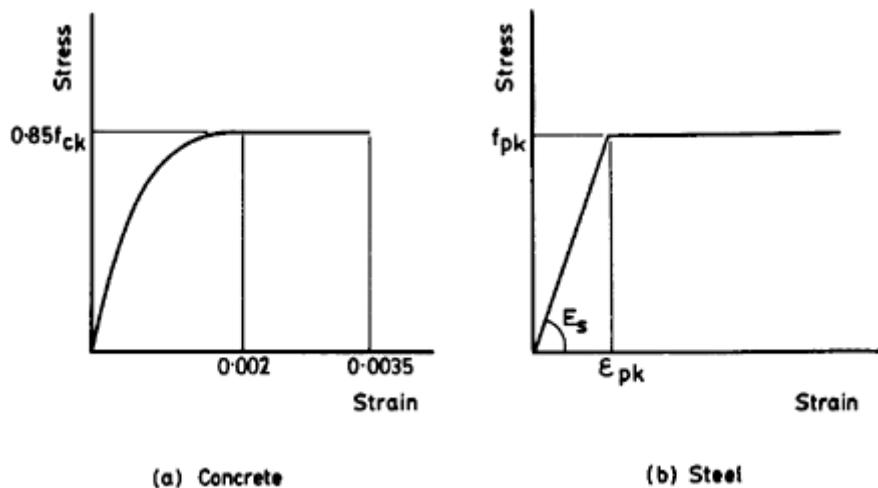
Figure 5.7 Stress-strain curves for (a) concrete and (b) steel.

These are shown in Fig. 5.7, and show the actual values that occur in the materials. These curves differ from those shown in Figs 3.3 and 3.4, where the *design* stress-strain curves are given. At present, the *actual* behaviour of the beam is being considered, with γ_m for both concrete and steel taken as 1.0. The design, or allowable, ultimate load on the beam, which incorporates partial factors of safety, will be considered later.

As the load is increased, the strain and stress distributions across the section change, the strain distribution remaining linear as described in Section 5.1. The stress in the extreme fibres of the section follows the stress-strain curve in Fig. 5.7(a), and will eventually reach the limiting value of 0.85 f_{ck}, although the extreme-fibre concrete strain continues to increase, until it reaches its maximum value, ε_{cu}, of 0.0035. This strain has been found to be the average maximum that concrete of all grades can withstand before crushing of the material. At all times the total compression in the concrete and the tension in the steel are equal (for no applied axial load) and the moment of resistance is always given by *Cz* or *Tz* (Fig. 5.8).

By the time the limiting concrete strain has been reached, the total strain in the prestressing steel, ε_p, can either be (a) *greater* than ε_{pk}, in which case the steel will have yielded before the concrete finally crushes—a *ductile* failure (such a section is termed *under-reinforced*); or (b) *less* than ε_{pk}, in which case the steel will not have yielded before the concrete finally crushes—a *brittle* failure (such a section is termed *over-reinforced*). If the steel strain equals ε_{pk}, then the section is said to be *balanced*. In order to ensure ductile failure, a limit is placed by EC2 on the depth of the neutral axis. For concrete grades less than C35/45, *x/d*
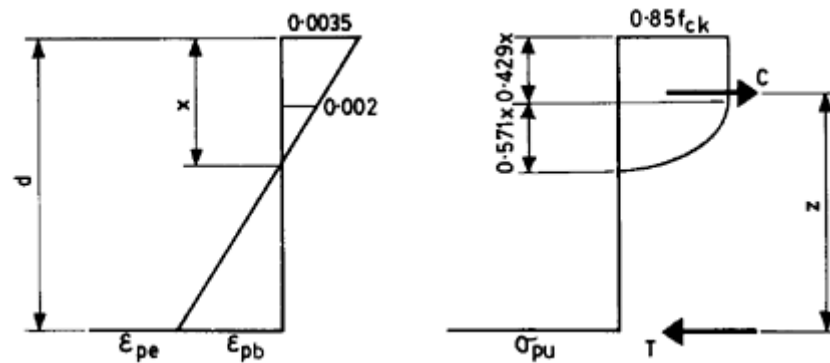
Figure 5.8 Strain and stress distributions from Fig. 5.7.

should be less than 0.45, while for concrete grades greater than C40/50, *x/d* should be less than 0.35. However, there are further restrictions on the depth of the neutral axis when moment redistribution takes place at a section, as described in Section 11.4.

This situation is analogous to that in reinforced concrete members at the ultimate limit state, the only difference being that the initial strain ε_{pe} in the steel must be considered. As with reinforced concrete members it is the ductile failure which is desirable, since it is gradual and gives ample warning. The load-deflection curves for typical under-reinforced and over-reinforced members are shown in Fig. 6.10.

Example 5.4 ■■

Determine the ultimate load that the beam in Example 5.1 can support if the concrete is grade C30/37 and f_{pk}=1860 N/mm^2.

The procedure is similar to that used in the cracked-section analysis of Example 5.3, except that now the extreme-fibre concrete strain is fixed at ε_{cu}=0.0035. The stress and strain distributions determined from Figs 5.7(a) and (b) are shown in Fig. 5.8.

$$\varepsilon_p=0.00521+[(d-x)/x]0.0035,$$

where *d* is the effective depth of the tendon.

With the value of ε_c fixed at ε_c=0.0035, *x* is determined by considering internal equilibrium. With irregular sections it may be easier to determine *x* numerically rather than to find it directly. Note that the concrete stress block is made up of two portions, corresponding to the two portions of the concrete stress-strain curve, one rectangular and one parabolic. The dimensions of the stress block are shown in Fig. 5.8.

The resulting strain and stress distributions are shown in Fig. 5.9. The ultimate moment of resistance of the section is then given by
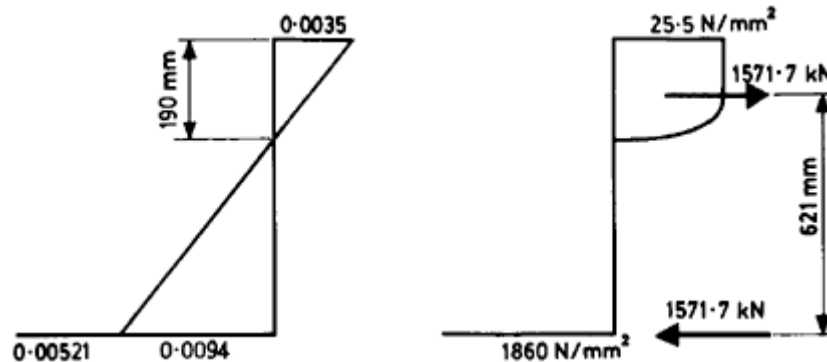
Figure 5.9 Strain and stress distributions for Example 5.4.

M_u=1571.7×0.621
=976 kNm.

This corresponds to a uniformly distributed load of 34.7 kN/m. The total steel strain for this neutral axis depth is greater than ε_{pk}, so this is an example of a ductile, under-reinforced section.

∎∎

It should be noted here that the load of 34.7 kN/m is that which would cause *actual* failure of the beam. What is usually required is the maximum safe load that can be supported. This will be considered in Section 5.7. The full analysis of the behaviour of a prestressed concrete beam from transfer of prestress force to ultimate load has been shown in Examples 5.1–5.4 to illustrate the basic approaches to the analysis. For uncracked sections, an analysis by elastic bending theory can be used. Once the concrete has cracked, this theory is still applicable, except that the cracked-section properties must be considered. Once the concrete stress in the extreme-fibres approaches the non-linear portion of the concrete stress-strain curve, then elastic bending theory is no longer valid, and the analysis must be carried out using the three basic principles stated in Section 5.1. Throughout, however, the equilibrium conditions between internal stress resultants and applied loads have been shown in order to emphasize the same basic behaviour of the beam at all levels of load.

5.6 VARIATION OF STEEL STRESS

In order to obtain an overall view of the behaviour of the beam in Examples 5.1–5.4, it is useful to consider the variation of stress in the

prestressing steel at the centre of the beam as the load on the beam is increased. This is shown in Fig. 5.10.

Assuming that the tendons are initially stressed to 0.7 f_{pk}, that is 1302 N/mm², and that the immediate loss due to elastic shortening is 6%, then the initial stress in the steel at midspan is 1224 N/mm², point *A*. On removal of the falsework, or lifting of the beam from its casting bed, there is a slight increase in the steel stress as the beam begins to support its own weight, point *B*.

When the beam is in position and subjected to its total design load of 17.7 kN/m, the prestress force is assumed to have been reduced by a further 14% due to long-term losses, but the bending moment at the section has increased, leading to a net steel stress of 1088 N/mm², point *C,* as determined in Example 5.2.

As the load is increased, the stress increases slightly until point *D,* at which point the concrete in the extreme bottom fibres of the beam cracks, causing a sudden increase in steel stress to 1104 N/mm², point *E,* as shown in Example 5.3. From this point onwards, the stress increases more rapidly as the neutral axis rises and the extreme-fibre concrete stress increases. Finally, the steel stress reaches the yield value of 1860 N/mm², point *F,* after which it remains constant until point *G,* when failure occurs by crushing of the concrete.

A useful way of looking at the various stages in the behaviour of a prestressed concrete member is to look at its load-deflection curve. A typical such curve is shown in Fig. 5.11, along with the stress distributions in the member at each stage.
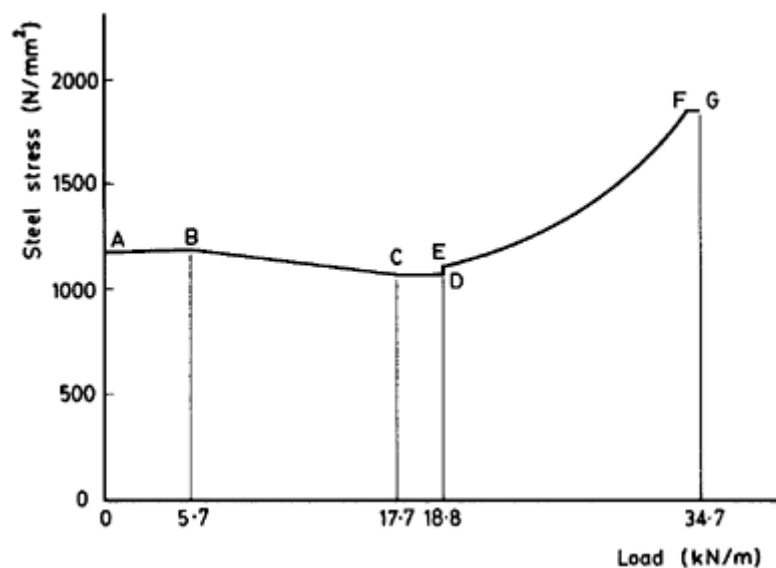
Figure 5.10 Variation of steel stress for beam in Examples 5.1–5.4.
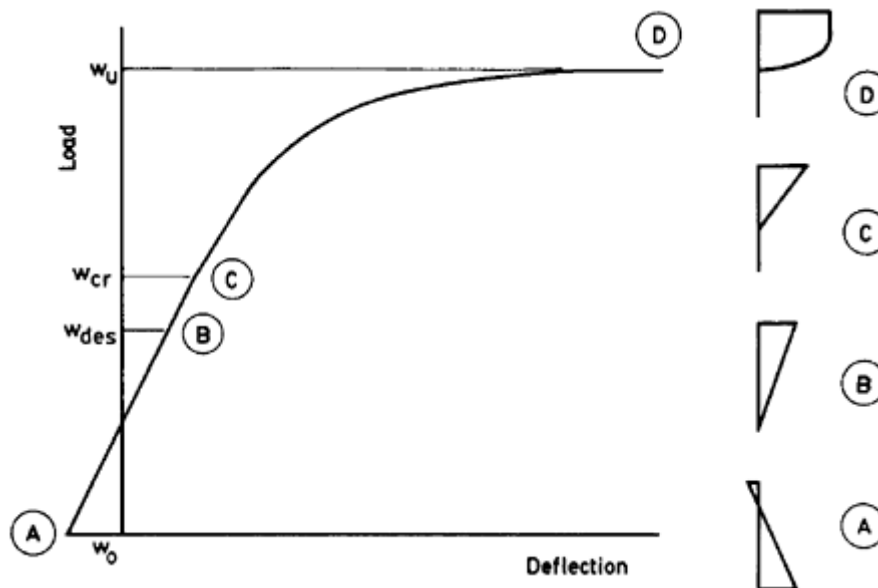
Figure 5.11 A typical load-deflection curve for a prestressed concrete member.

5.7 DESIGN ULTIMATE STRENGTH

The uniform load of 34.7 kN/m determined in Example 5.4 is that which would cause physical collapse of the beam. What is more usually required is the *safe* or *design* ultimate load that the beam can support, that is the load that gives an adequate factor of safety against failure of the materials. This is found by introducing the partial factors of safety for the steel and concrete material properties described in Chapter 3. The stress-strain curves shown in Fig. 5.7 are now modified to those shown in Fig. 5.12 with γ_m for concrete and steel taken as 1.5 and 1.15 respectively.

The stress-strain curve for concrete leads to the strain and stress distributions within the section shown in Fig. 5.13.

For prestressed concrete sections at the ultimate limit state the partial factor of safety for prestress force, γ_p, should be taken as 1.0, provided that not more than 25% of the tendons are located within the compression zone and that the stress in the tendons closest to the tension face is not less than $0.78 f_{pk}$. If either of these conditions is not met then γ_p should be taken as 0.9.

Example 5.5 ■■
Determine the design ultimate moment of resistance of the beam in Example 5.1, using the stress-strain curves in Fig. 5.12.
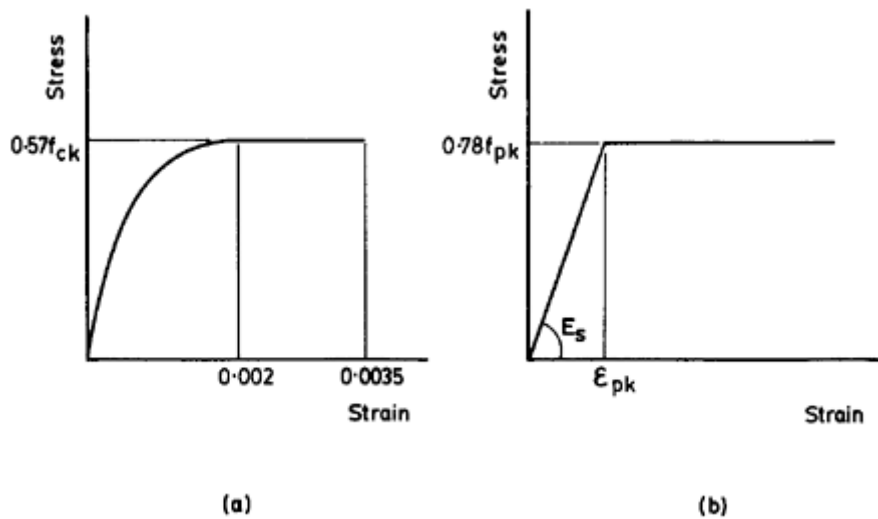
Figure 5.12 Design stress-strain curves for (a) concrete and (b) steel.
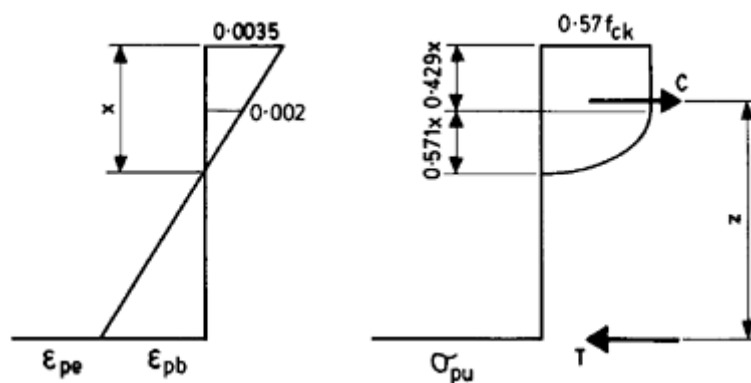
Figure 5.13 Strain and stress distributions from Fig. 5.12.

As in Example 5.4, *x* may be found by equating the total compression and tension forces. For this example, the stress and strain distributions which satisfy this requirement are shown in Fig. 5.14. It can be seen that the steel stress at failure of the beam is equal to the yield stress and that therefore the mode of failure is ductile.
   The ultimate moment of resistance is given by

M_u=1225.9×0.608
=745.3 kNm.

For an applied bending moment of this amount, the total ultimate uniformly distributed load is 26.5 kN/m. The allowable imposed load *w* is given by
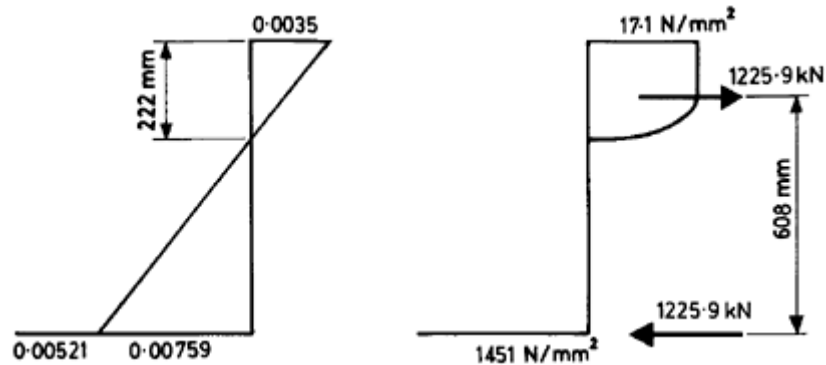
Figure 5.14 Strain and stress distributions for Example 5.5.

$\qquad$ 1.35×5.7+1.50 w=26.5
$\qquad$ ∴w=12.5 kN/m;

and the total design load is thus 18.2 kN/m.

■■

In order to illustrate the different approaches using the serviceability and ultimate limit states, consider the beam designed with zero tension under the total design load. For the same prestress force and eccentricity used in these examples, this load can be shown to be 15 kN/m. For the ultimate limit state approach, the total design load is 18.2 kN/m. Thus, for this type of beam design is usually based on the serviceability limit state.

5.8 SIMPLIFIED CONCRETE STRESS BLOCK

In order to simplify the calculations involved using the concrete stress block shown in Fig. 5.13, a simplified rectangular stress block is given in EC2 shown in Fig. 5.15. This stress block gives the same total concrete force in compression as that in Fig. 5.13, and enables ultimate strength calculations to be performed quickly by hand.

Example 5.6 ■■
Determine the design ultimate moment of resistance of the beam in Example 5.1, using the EC2 simplified stress block.
By equating tension and compression within the section, the neutral axis depth is found to be 224 mm, and the steel stress, from Fig. 5.12(b),
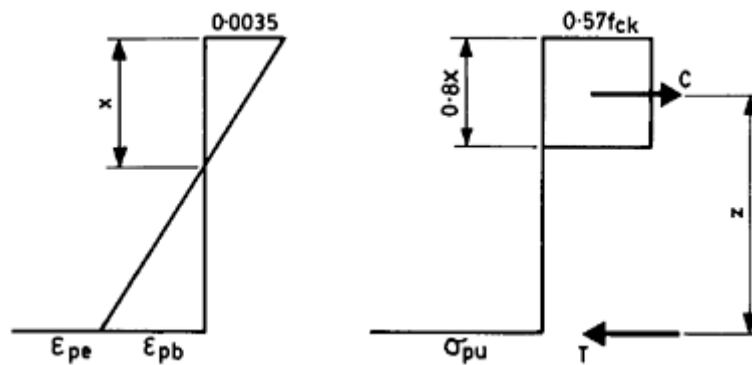
Figure 5.15 Simplified stress block.

is equal to the yield stress. The ultimate moment of resistance is then given by

$M_u = 0.78 \times 1860 \times 845(700 - 0.8 \times 224/2) \times 10^{-6}$
$= 748.3$ kNm.

The agreement between this value and that in Example 5.5 is very close.
∎∎

5.9 DESIGN CHARTS

As an alternative to the two methods described previously, design charts may be used for rectangular sections and for T-beams where the neutral axis lies within the flange. A typical design chart is shown in Fig. 5.16. This has been constructed using a spreadsheet software program, based on the design stress-strain curves shown in Fig. 5.12. Successive values of x are chosen and the corresponding moment of resistance calculated based on the principles stated in Section 5.1. The chart is valid for values of β greater than or equal to 0.6.

Example 5.7 ∎∎
    Determine the design ultimate moment of resistance of the beam in Example 5.1 using the design chart in Fig. 5.16.

$(A_p f_{pk})/(b d f_{ck}) = (845 \times 1860)/(400 \times 700 \times 30)$
$= 0.187$.

Thus, from the design chart;

$M_u = 0.127 \times 400 \times 700^2 \times 30 \times 10^{-6}$
$= 746.8$ kNm.
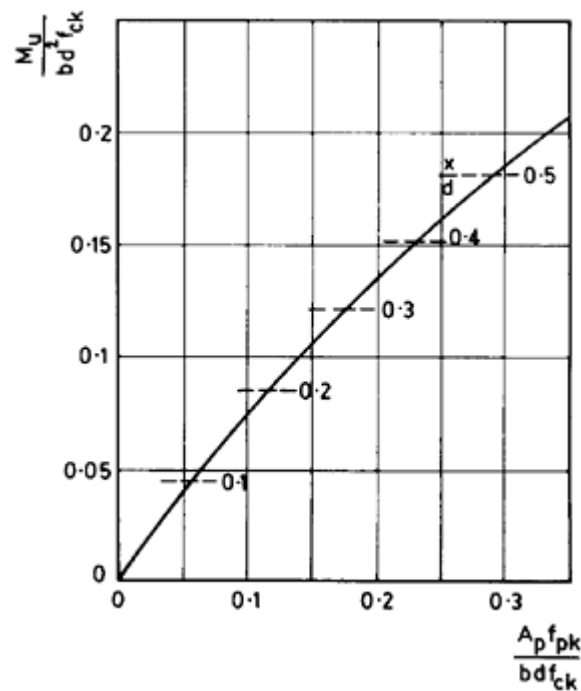
Figure 5.16 Variation of design stress in tendons (from Table 5.1).

Also, *x/d* is approximately equal to 0.32, so that the neutral axis depth is 224 mm, lying within the flange as assumed.

■■

5.10 UNTENSIONED REINFORCEMENT

It is usually found that the ultimate strength of uncracked members is satisfactory, but with some cracked members it is often found that the ultimate moment of resistance based on the prestressing steel alone is insufficient.

In this case, either the section size should be increased, or untensioned reinforcement added. In order to find the moment of resistance of a section with both tensioned and untensioned steel, the basic principles stated in Section 5.1 are still used, except that the relevant stress-strain curve for the untensioned reinforcement must also now be considered. This is similar to that shown in Fig. 5.12(b), except that the yield stress is now 0.87 f_{yk}, where f_{yk} is the characteristic yield strength of the reinforcement.

Example 5.8 ■■

Determine the design ultimate moment of resistance of the beam section in Example 5.1, if four T10 bars are added at the same level as the prestressing steel. Assume that f_{yk}=460 N/mm^2.

The same basic stress block used in Example 5.6 will be used here, except that the stress in the untensioned reinforcement must now be added. The resulting strain and stress diagrams are shown in Fig. 5.17. The neutral axis depth has been found initially assuming that both the tensioned and untensioned steel have yielded. As shown in Fig. 5.17, this assumption is justified.

The ultimate moment of resistance is given by

M_u=1351.7×0.601
=812.4 kNm.

The ultimate moment of resistance has been increased from the value of 748.3 kNm found in Example 5.6.

■■

The full analysis of sections with untensioned reinforcement has been shown in the above example in order to illustrate the basic principles. However, in most practical cases, it is sufficiently accurate to replace the cross-sectional area of this reinforcement by an equivalent area $A_s f_{yk}/f_{pk}$ and then to analyse the section using any of the methods described previously.

The presence of steel, either tensioned or untensioned, in the compression zone can be treated in a similar manner to the strain compatibility method described above for steel in the tension zone.

Untensioned reinforcement really becomes useful only after the concrete in a section has cracked, and particularly at the ultimate limit
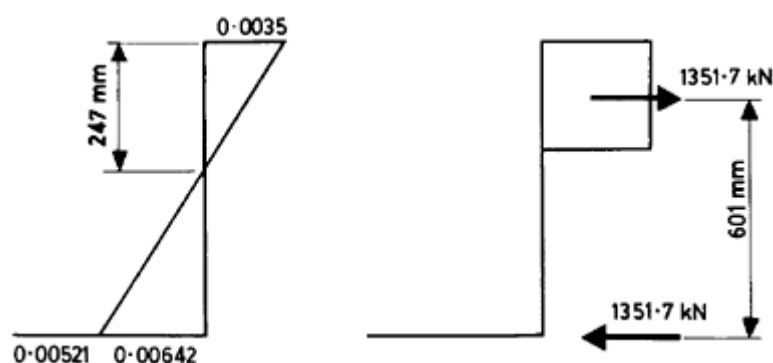
Figure 5.17 Strain and stress distributions for beam in Example 5.8.

state. At design loads, the stress in this steel is small and may even be compressive, depending on its location within the section. The addition of untensioned reinforcement is very useful in limiting cracking and providing sufficient ultimate strength capacity soon after transfer, when the concrete is still immature. It is good practice to provide untensioned reinforcement in any region of a member where tension is likely to occur. It is of particular use at the supports of members with straight tendons, where the allowable tensile stresses, particularly at transfer, may be exceeded. This reinforcement will also resist any cracking that may occur due to accidental mishandling of structural members. This may be caused, for instance, by a simply supported beam being lifted at its centre.

5.11 CRACKED MEMBERS

The analysis for the serviceability limit state outlined in Section 5.2 is suitable for members which are uncracked in tension. However, for members which are cracked in tension, depending on the class of exposure it may be necessary to check that the crack widths are acceptable according to the criteria given in Table 3.7. This can be achieved either by determining the crack width directly, as outlined below, or, for sections with bonded reinforcement or tendons, by following the rules for bar size and spacing given in Tables 5.1 and 5.2, respectively.

The formula given in EC2 for the flexural crack width in a concrete member is

$$w_k = 1.7 \, \varepsilon_{sm} \, s_{rm},$$
(5.2)

where w_k is the design crack width; ε_{sm} is the average concrete strain at the level of the steel; s_{rm} is the average crack spacing.

Table 5.1 Bar size limits (mm)

Steel stress N/mm^2	Reinforced concrete sections	Prestressed concrete sections
160	32	25
200	25	16
240	20	12
280	16	8
320	12	6
360	10	5
400	8	4
450	6	–

Table 5.2 Bar spacing limits (mm)

Steel stress N/mm^2	Reinforced concrete sections	Prestressed concrete sections
160	300	200
200	250	150
240	200	100
280	150	50
320	100	–
360	50	–

The average concrete strain at the level of the steel is given by

$$\varepsilon_{sm} = \sigma_s[1 - \beta_1\,\beta_2(\sigma_{sr}/\sigma s)^2]/E_s,$$
(5.3)

where β_1 is a coefficient which for plain bars or prestressing tendons should be taken as 0.5 and for high-bond bars as 1.0; β_2 is a coefficient which should be taken as 1.0 for single short-term loading and 0.5 for repeated or sustained loading; σ_{sr} is the steel stress induced by bending, based on a cracked section, for the loading which just causes cracking; and σ_s is the steel stress induced by bending, based on a cracked section, under the frequent loading combination. In the determination of both σ_s and σ_{sr}, $\gamma_p = 0.9$.

The average crack spacing in mm is given by:

$$s_{rm} = 50 + 0.25\,k_1\,k_2\,\varphi/\varrho_r,$$
(5.4)

where k_1 is a coefficient which takes account of the bond properties of the steel in the section (for high-bond bars, $k_1 = 0.8$, while for prestressing tendons k_1 should be taken as 2.0, in the absence of better information), k_2 is a coefficient which takes account of the form of the strain distribution across the section (for bending, k_2 should be taken as 0.5), φ is the average size of the tendons and reinforcement, ϱ_r is the effective reinforcement ratio, $(A_p + A_S)/A_{c.eff}$, where $A_{c.eff}$ is the area of concrete surrounding the steel to a depth equal to 2.5 times the distance from the tension face of the section to the centroid of the steel. In the determination of ϱ_r any unbonded tendons should be ignored.

An upper bound to the crack spacing for sections with no bonded reinforcement may be determined from:

$$s_{rm} = (h - x),$$

where h is the overall depth of the section, and x is the depth of the neutral axis under the action of the prestress force and the frequent load combination.

As an alternative to the calculation of crack width described above, for sections with bonded reinforcement the limit state of cracking is deemed to be satisfied if *either* the bar size *or* bar spacing requirements of Tables 5.1 and 5.2, are complied with, provided the minimum amount of reinforcement shown in Section 9.11 is provided. When using Tables 5.1 and 5.2 sections with unbonded tendons should be considered as reinforced concrete sections. The values given in Table 5.1 are for high-bond bars. The bond strength properties of prestressing tendons are lower than those for this type of bar. The reduction in bond strength is given in EC2 as approximately 40%; the bar diameters in Table 5.1 should be reduced accordingly.

A derivation of the EC2 provisions for crack width assessment may be found in Beeby and Narayanan (1995).

Example 5.9 ■■

For the beam in Example 5.1 determine the design crack width under a frequent load of 17.7 kN/m, assuming that the section is cracked under the rare load combination.

$M_{\mathrm{fr}}=17.7\times15^2/8$
$=497.8$ kNm.

For $\gamma_{\mathrm{p}}=0.9$, $M_{\mathrm{cr}}=485.5$ kNm.

Using the cracked-section analysis procedure outlined in Section 5.4, the neutral axis depths and the strain and stress distributions are as shown in Fig. 5.18(a) and (b) for the cracking and frequent loads, respectively.

For no untensioned reinforcement in the section, with β_1 and β_2 taken as 0.5 and 1.0, respectively, the crack width is given by

$w_{\mathrm{k}}=1.7(750–334)\times93[1–0.5\times(75/93)2]/(200\times103)$
$=0.22$ mm.

This is more than the allowable value of 0.2 mm for exposure class 1 and thus a small amount of additional untensioned reinforcement is required. An example of the design of such a section is given in Section 9.8, while an example of the calculation of crack width in a section with both prestressing tendons and reinforcement is given in Chapter 13.
■■

(a) Cracking load
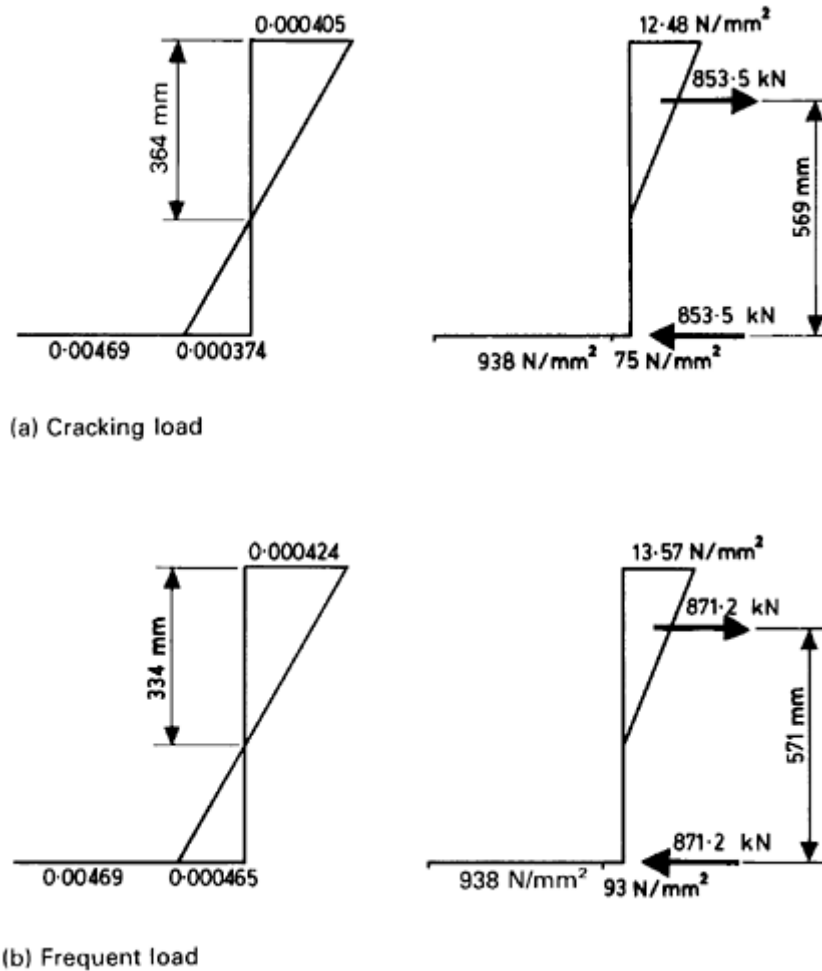
(b) Frequent load

Figure 5.18 Cracked section strain and stress distributions for (a) cracking and (b) frequent loads.

5.12 MEMBERS WITH UNBONDED TENDONS

As mentioned in Chapter 1, the current trend is towards the use of unbonded tendons. The effect of this at the serviceability limit state is very small, since in Section 5.3 it was shown that the extra stresses induced in the prestressing steel by the composite behaviour of the bonded steel and concrete are usually small.

However, the behaviour at the ultimate limit state is markedly different, and the ultimate moment of resistance of an unbonded section is generally smaller than that of a similar bonded section. As the applied bending moment at a given section in such a member increases, the steel stress increases less rapidly than in a bonded section, as the increase in

strain in the steel is uniform along the entire length of the member, rather than gradual along the member in line with the bending moment diagram. When the concrete crushes, therefore, the available tensile force to form the internal resisting moment is smaller than in a similar, bonded, member.

The analysis of unbonded sections at the ultimate limit state cannot be carried out based on the three basic principles stated in Section 5.1, since assumption (a) is no longer valid, that is the strain in the steel is no longer equal to the strain in the concrete at the same level, since there is no bond between the two materials.

It is stated in Part 1–5 of EC2 that the increase in stress in an unbonded tendon at the ultimate limit state should be taken as 100 N/mm^2, where the length of the tendon does not exceed that of a single span. For longer tendons this increase should be reduced taking account of the number of spans and the loads acting.

Example 5.10 ■■

The cross-section of an unbonded post-tensioned slab is shown in Fig. 5.19. Determine the ultimate moment of resistance if the concrete is grade C30/37 and f_{pk}=1820 N/mm^2. Assume that the total prestress losses are 25%.

For unit width of slab

A_p=165/0.2=825 mm2/m.
σ_{pe}=0.7×0.75×1820
=956 N/mm^2.

Thus the stress in the tendons at the ultimate limit state=1056 N/mm^2.

The depth of the neutral axis is given by

0.57×30×10^3×0.8x=825×1056
∴ x=64 mm,

and

M_u=825×1056×(225–0.4×64)×10^{-6}
=173.7 kNm/m.

■■

Cracking in unbonded members at the ultimate limit state tends to be concentrated in a few large cracks rather than spread among many smaller cracks, as in bonded members. The addition of untensioned reinforcement will limit the width of the cracks and will also add to the ultimate strength of the member. The ultimate moment of resistance in

15·2mm dia.
drawn strands
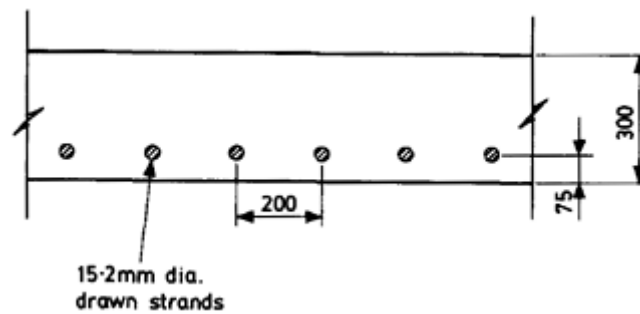
Figure 5.19

this case may be found by replacing the area of additional steel A_s by an equivalent area of prestressing steel $A_s f_{yk}/f_{pk}$.

A disadvantage of using unbonded tendons is that complete reliance is placed on the anchorages, so that in the event of failure of the tendons the anchorages must withstand the effect of the sudden release of strain energy stored in the tendons. With bonded tendons, the release of strain energy is also absorbed by the concrete surrounding the tendons. The lack of bond will be an advantage, however, if ever the tendons need to be re- or de-tensioned. As mentioned in Chapter 1, increasing concern is being expressed over the demolition of prestressed concrete structures that have reached the end of their useful life. If the tendons are unbonded, the force in the tendons may be transferred to a jack, depending on the type of anchorage, and then gradually reduced to zero by releasing the jack hydraulic pressure. With bonded tendons, a considerable force will still be locked in the tendons due to the bond between the steel and concrete. However this may be advantageous during demolition, since the tendons can be cut into small lengths, with each section now behaving as a pretensioned tendon.

Much of the application of prestressing to slab construction is carried out using unbonded tendons, since the large number of tendons in slabs makes grouting an expensive operation. These are often greased, wrapped in tape and cast, untensioned, into the concrete slab. The grease not only serves to destroy any bond between steel and concrete, but it also helps to reduce friction when the tendons are tensioned. Information on the protection of unbonded tendons may be found in FIP (1986).

PROBLEMS

5.1 The beam in Fig. 5.20 has a constant width of 300 mm and a long-term prestress force of 1000 kN. If it supports a uniform imposed load of

Figure 5.20

Figure 5.21

8 kN/m determine the maximum compressive and tensile stresses in the beam.

5.2 The precast grandstand seating unit shown in Fig. 5.21 has a total long-term prestress force of 100 kN, and supports an imposed load of 5 kN/m over a span of 5 m. Using the general form of the expression for elastic stresses in an asymmetrical section determine the stresses at points A and B at midspan, assuming that the section remains uncracked.

5.3 The beam in Example 5.1 can be modelled by the plane framework shown in Fig. 5.22. The upper chord members are given the section properties of the concrete beam; the vertical members are given the same properties. The lower chord members are given the section properties of the pretensioning tendons and an initial strain of 0.00651 (see Problem 1.6). Using this model, determine the elastic shortening loss of prestress in the tendons and the stresses in the concrete at midspan under the action of the prestress force and self weight. What

Figure 5.22

Figure 5.23

modification to the model would be necessary in order to simulate post-tensioning tendons?

5.4 The pretensioned double-tee section shown in Fig. 5.23 supports a dead load, including self weight, of 16 kN/m and an imposed load of 12 kN/m over a 16 m span, with a 2 m cantilever. A permanent transverse load of 30 kN is supported at the end of the cantilever. The initial prestress force in each of the strands is 130 kN, with long-term losses of 20%. The lowest four strands in each rib are debonded over the cantilever support. The properties of the double-tee section are: $A_c = 3.33 \times 10^5$ mm^2, $I_c = 1.81 \times 10^{10}$ mm^4. Determine the stresses in the concrete at the upper and lower faces for the cantilever support and at midspan, assuming that the section remains uncracked.

5.5 The precast floor unit shown in Fig. 5.24 supports a quasi-permanent imposed load of 10 kN/m^2 over a span of 15 m. The long-term losses are 20%, the area of the wires is 896 mm^2, $f_{pk} = 1860$ N/mm^2 and $E_{cm} = 32$ kN/mm^2. Determine the stresses in the concrete and the steel at midspan, assuming that the section has cracked.

5.6 Determine the design ultimate moment of resistance, using the simplified concrete stress block, of the section shown in Fig. 5.25. Each
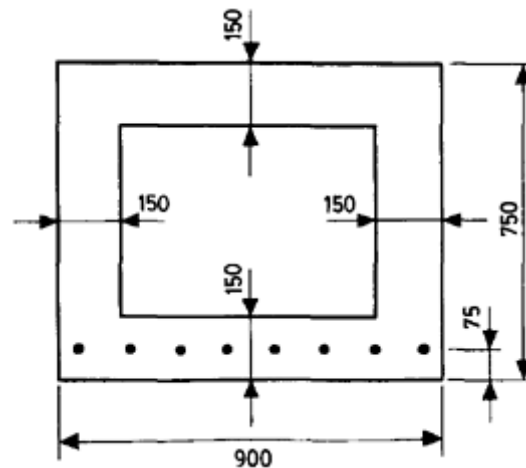
Figure 5.24
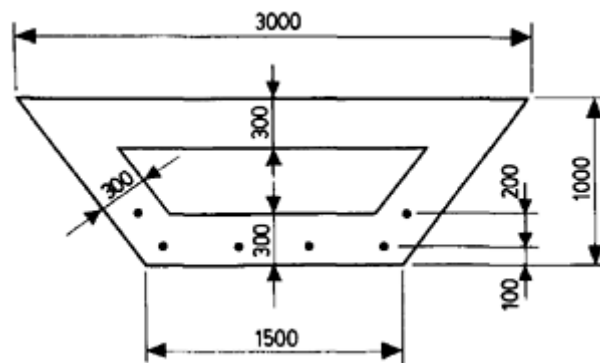
Figure 5.25

tendon has A_p=2700 mm^2 and f_{pk}=1770 N/mm$_2$. The concrete is grade C40/50 and long-term losses are 25%.

5.7 Determine the formula relating the two variables in Fig. 5.16.

REFERENCES

Beeby, A.W. and Narayau, R.S. (1995) *Designer's Handbook to Eurocode 2, Part 1.1: Design of Concrete Structures,* Thomas Telford, London,

Fédération Internationale de la Précontrainte (1986) *Corrosion Protection of Unbonded Tendons,* London.

Rowe, R.E. *et al.* (1987) *Handbook to British Standard BS8110; 1985 Structural Use of Concrete,* Viewpoint, London.

6

Deflections

6.1 LIMITS TO DEFLECTIONS

In prestressed concrete members, unlike reinforced concrete ones, deflections under a given load can be eliminated entirely. This is achieved by the use of a suitable arrangement of prestressing. The deflection in prestressed concrete members usually occurs with no applied load; this is known as *camber* and is generally an upward deflection.

The importance of the serviceability limit state of deflection was described in general terms in Chapter 3. The effect of deflections in particular structures varies according to the use of the structure. For bridges, excessive deflections may lead to the creation of pools of water on road surfaces, a problem which can also occur where deflections of roof beams in buildings are large. If this ponding becomes too severe, an unacceptable extra dead load may be placed on the beams. Large deflections of floors in buildings may cause the cracking of partitions and windows.

It is recommended in EC2 that, for structures where the sag of a member would be noticeable, the deflection under quasi-permanent load be limited to $L/250$, where L is the span of a beam or the length of a cantilever. For structures where partitions, cladding and finishes have not been specifically designed to allow for movement of the surrounding structure, it is recommended that deflections after construction do not exceed $L/500$. The limit of $L/250$ may also be taken to apply to the initial upwards camber for prestressed concrete members.

The deflections of concrete structures cannot be predicted with a high degree of accuracy, since there are many non-linear factors involved. Concrete itself does not have a linear stress-strain curve, and the load-deflection characteristics of concrete beams, reinforced or prestressed, are non-linear in general, since the stiffness changes sharply once the concrete has cracked. The methods of calculation outlined in the

following sections should be regarded as giving only estimates of the deflections. For most structures, the best that can be said is that the deflections lie within certain bounds. If it is very important to know the exact deflection of a particular structure, the only reliable method is to carry out tests on a model of the structure, using similar materials.

The use of prestress to control deflections makes it difficult to specify span/depth ratios for initial estimation of member size, which is the practice for reinforced concrete members. Nevertheless, some rough guidelines may be given for simply supported beams. For beams carrying heavy loads, such as bridge beams, a span/depth ratio in the range 20–26 for uncracked members would be suitable, while for cracked floor or roof beams, a span/depth ratio in the range 26–30 would give a good initial estimate of section size. Span/depth ratios for prestressed concrete flat slabs are discussed in Chapter 12.

As described in Chapter 2, under load concrete deforms instantaneously and also with time, due to shrinkage and creep. Thus the deflections of concrete structures should be assessed under both short-and long-term conditions.

6.2 SHORT-TERM DEFLECTIONS OF UNCRACKED MEMBERS

The prediction of deflections is more straightforward for uncracked prestressed concrete members than for reinforced concrete members, since the ordinary strength-of-materials methods for finding deflections are applicable. There are several such methods, but the one which is used here is based on the principle of virtual work.

The principle is best illustrated by means of a simple example. The beam in Fig. 6.1(a) is simply supported and is in equilibrium under a point load W. Some arbitrary deflected shape of the beam is shown in Fig. 6.1(b). This need have no relation to the true deflected shape of the beam under the load W; all that is required is that the displacements at every point are small and geometrically compatible with the curvature along the beam.

The principle of virtual work states that the work done by the external applied load W moving through the displacement given by the arbitrary deflected shape is equal to the internal work done along the beam during that displacement. This work is usually considered as that due to bending only. Thus:

$$W\delta = \int_0^L M(x)\mathrm{d}\theta,$$

where $M(x)$ is the bending moment at a section x induced by the applied load, and θ is the rotation of the member at that section due to the arbitrary displacement. The way in which this principle is used to find the deflection of a structure is to apply a unit load at the point where the
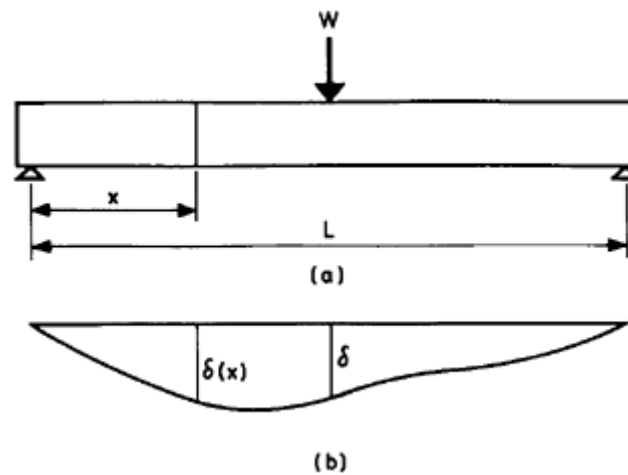
Figure 6.1 The virtual work principle.

deflection is required, and in the same direction as the required displacement. The arbitrary deflected shape is then taken as the true deflected shape of the structure. The virtual work equation can now be written as

$$1 \times \delta = \int_0^L M'(x)d\theta,$$

(6.1)

where $M'(x)$ is the bending moment at a section x under the action of the unit point load.

The rotation $\Delta\theta$ over any small length of the beam Δx under the applied load W is given by

$\Delta\theta = [M(x)/EI]\Delta x,$

where EI is the flexural stiffness of the beam. Thus Equation 6.1 becomes

$$\delta = \int_0^L [M'(x)M(x)/EI]dx.$$

The integration of the two bending moment diagrams is best carried out numerically, using Simpson's rule.

In order to determine the deflections of simply supported members under prestress force only, use is made of the fact that the moment in the member at any section x is equal to $Pe(x)$ where $e(x)$ is the eccentricity at that section. The prestress moment diagram is thus proportional to the area between the member centroid and the location of the resultant prestressing force, as shown in (b) for the beam shown in (a).

With statically indeterminate prestressed concrete members, the location of the resultant prestress force is not necessarily coincident with the centroid of the tendons and the prestress moment diagram cannot

(a)

(b)
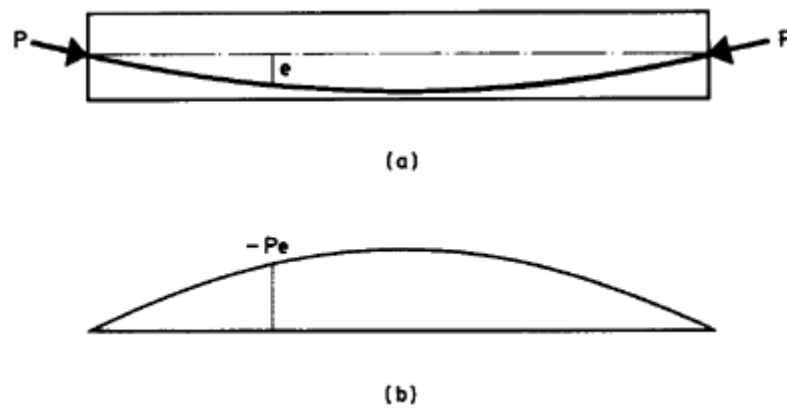
Figure 6.2 Relationship between (a) tendon eccentricity and (b) prestress moment diagram.
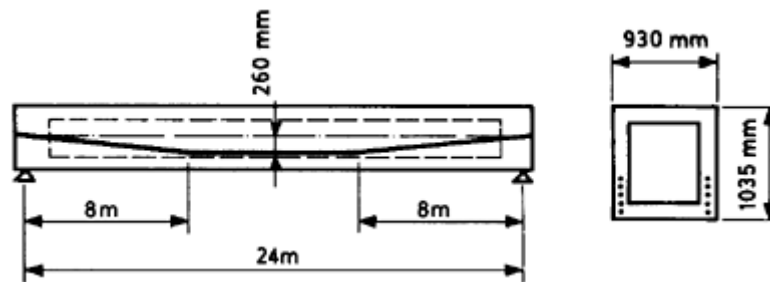
Figure 6.3

be determined as described above. Nevertheless, once the moment diagram due to the prestressing force has been determined (using the methods described in Chapter 11), the virtual work principles as outlined above can still be used to find the deflection at any point.

Example 6.1 ■■

Determine the midspan deflections of the beam shown in Fig. 6.3: (i) at transfer with an initial prestress force of 6800 kN; (ii) under a quasi-permanent imposed load of 30 kN/m when the prestress force has been reduced to 4500 kN.

Beam self weight=11.26 kN/m,
Total quasi-permanent load=11.26+30
=41.26 kN/m.

The bending moment distributions due to self-weight, M_0, and quasi-permanent load, M_{qp}, are shown in Fig. 6.4(a) and (b) respectively.
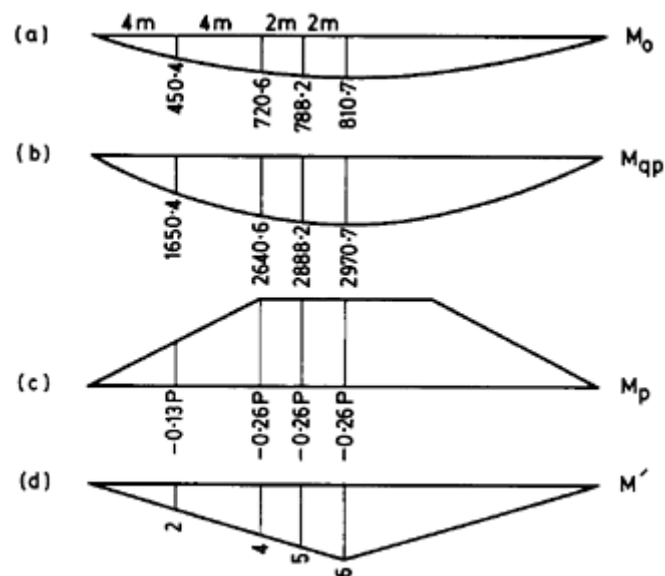
Figure 6.4 Bending moments for beam in Example 6.1 (kNm).

Figure 6.4(c) shows that due to the prestress force alone, M_p, and Fig. 6.4(d) that due to a unit vertical load at the centre of the beam, M'.
   (i) At transfer, the midspan deflection is given by

$$\delta_0 = \int_0^L [M'(M_0 + M_p)/EI]\, dx.$$

Thus:

$\delta_0 = (2 \times 8/6EI)[4(450.4 - 0.13P)(2) + (720.6 - 0.26P)(4)]$
$+ (2 \times 4/6EI)[(720.6 - 0.26P)(4) + 4(788.2 - 0.26P)(5)$
$+ (810.7 - 0.26P)(6)].$

With

$P = 6800$ kN,
$\delta_0 = -59795/EI.$

For the section used, $I_c = 0.06396$ m^4, and the short-term value of E_{cm} can be taken as 28×10^3 N/mm^2.

$\therefore \delta_0 = -59795/(28 \times 106 \times 0.06396)$
$= -0.0334$ m.

That is, the deflection is 33.4 mm upwards, representing a camber of 1 in 719, which is satisfactory.
   (ii) Under the quasi-permanent load, the maximum deflection is given by

$$\delta_{qp} = \int_0^L [M'(M_{qp} + M_p)/EI]\, dx.$$

Thus,

$$\delta_{qp}=(2\times8/6EI)[4(1650.4-0.13P)(2)+(2640.6-0.26P)(4)]$$
$$+(2\times4/6EI)[(2640.6-0.26P)(4)+4(2888.2-0.26P)(5)$$
$$+(2970.7-0.26P)(6)].$$

With

$$P = 4500 \text{ kN},$$
$$\delta_{qp} = 106\,482/EI.$$
$$\therefore \delta_{qp} = \frac{106\,482}{28 \times 10^6 \times 0.06396}$$
$$= 0.0595 \text{ m}.$$

That is, the maximum quasi-permanent load deflection is 59.5 mm, or 1 in 404. This is less than the maximum deflection of 1 in 250 for partitions made of non-brittle materials and is thus satisfactory. If the beam in Example 6.1 were treated simply as an elastic beam under a uniformly distributed load, then the maximum deflection would be given by

$$\delta_{qp} = \frac{5}{384} \times \frac{41.26 \times 24^4}{28 \times 10^6 \times 0.06396}$$
$$= 0.0995 \text{ m}.$$

The maximum deflection would thus be 99.5 mm, or 1 in 241, just above the maximum allowable deflection for partitions of non-brittle material. The action of the prestressing force has been to reduce this deflection to within acceptable limits.

∎∎

6.3 LONG-TERM DEFLECTIONS

The deflections of prestressed concrete members determined so far have been short-term deflections caused by elastic deformation of the concrete in response to loading. However, long-term shrinkage and creep movements will cause the deflections of concrete members to increase with time.

The effects of creep may be estimated by using a method given in EC2 whereby an effective modulus of elasticity, $E_{c.eff}$, is given by

$$E_{c.eff}=E_{cm}/(1+\varphi),$$
(6.2)

where E_{cm} is the instantaneous modulus of elasticity at the age of loading and φ is the creep coefficient defined in Chapter 2. The increase in long-term values of E_{cm} may be taken as approximately 15%.

When a concrete beam shrinks it does not usually do so uniformly across the section since it is restrained by any steel present, the concentration of which is usually greater on the tension face than on the compression face. This gives rise to an extra component of deflection. A method is given in EC2 for determining this additional deflection in reinforced concrete beams but it is not readily adaptable to prestressed concrete members. However, shrinkage effects can be taken into account, if necessary, by increasing the long-term deflections caused by loading and creep by approximately 20%.

6.4 DEFLECTIONS OF CRACKED MEMBERS

The ordinary strength-of-materials approach to the calculation of deflections may be used for members uncracked in tension, but for cracked members account must be taken of the loss in stiffness of the section after cracking has occurred.

The general relationship between the curvature $1/r$ at a point x along a member and the corresponding deflection y is given by

$$1/r = d^2y/dx^2.$$
(6.3)

In order to find the deflection at any point in a member, Equation 6.2 must be integrated twice, and this is best carried out numerically.

The following expression is given in EC2 for the average curvature, $1/r_m$, of a section cracked in flexure:

$$1/r_m = (1-\zeta(1/r_1) + \zeta(1/r2),$$
(6.4)

where $1/r_1$ and $1/r_2$ are the radii of curvature for the uncracked and cracked sections, respectively. The factor ζ describes the proportion of the concrete in tension which is assumed to be fully cracked, the remainder of the concrete between the actual cracks remaining uncracked. The value assigned to ζ takes into account the bond properties of the reinforcement and the effect of sustained or repeated loading. The following expression for ζ is given in EC2:

$$\zeta = 1 - \beta_1\,\beta_2\,(\sigma_{sr}/\sigma_s)^2,$$
(6.5)

where β_1, β_0, σ_{sr} and σ_s are as defined in Section 5.11, with σ_s, determined for the quasi-permanent load. The value of σ_{sr}/σ_s can be approximated by M_{qp}/M_{cr}. A derivation of Equations 6.4 and 6.5 is given in Beeby and Narayanan (1995).

The cracked radius of curvature may be found using the analysis procedure outlined in Section 5.4, while that of the uncracked section may be determined from the expression:

$$1/r_1 = M_{qp}/EI.$$
(6.6)

A simplified method of finding the maximum deflection of concrete members, which takes into account shrinkage movements, was outlined in BS8110 and assumes that the distribution of curvature, cracked or uncracked, is similar to the shape of the bending moment diagram. In this case the maximum deflection, y_{max}, is given by

$$y_{max} = KL^2/r_b,$$
(6.7)

where L is the effective span, $1/r_b$ is the curvature at midspan, or at the support for a cantilever, and K is a constant which depends on the shape of the bending moment diagram. The values of K for some common bending moment diagrams are shown in Table 6.1. However, the deflections for complex loading cases should not be obtained by superposition of values of K for simpler loading cases. In this case, a value of K appropriate to the actual load should be used. The values of deflection should be determined separately on the basis of both uncracked and cracked sections and then combined using a relationship similar to Equation 6.4.

Example 6.2 ■■
    The beam shown in Fig 6.5 has a prestress force after losses of 100 kN and supports a uniform quasi-permanent load of 32 kN/m, including its own weight. Determine the maximum long-term deflection, (i) using Equation 6.3 and (ii) using Equation 6.7.

Table 6.1 Coefficient K for use in Equation 6.7

Type of loading	Bending moment diagram	K
		0.104
		$\dfrac{3 - 4a^2}{48(1 - a)}$
		0.25
		0.125
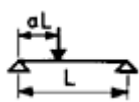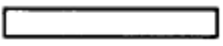
Beam section properties:

A_c=3.75×10⁵ mm²; Z_b=46.88×10⁶ mm³.
(i) σ_{pe}=100×10³/100
=1000 N/mm²
ε_{pe}=1000/(200×10³)
=0.005.

The cracking moment of the section, M_{cr}, for grade C30/37 concrete is given by

$$-2.9 = \frac{100 \times 10^3}{3.75 \times 10^5} + \frac{100 \times 10^3 \times 325}{46.88 \times 10^6} - \frac{M_{cr} \times 10^6}{46.88 \times 10^6}$$
$$\therefore M_{cr} = 181 \text{ kNm.}$$

This bending moment is reached at points 2.09 m from the supports.

The radius of curvature of the cracked section is found by considering equilibrium within the section, as outlined in Section 5.4, using the long-term value for concrete modulus of elasticity and γ_p=1.0.
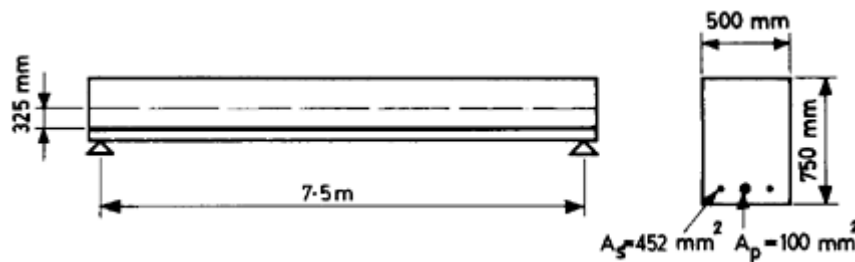
Figure 6.5

Table 6.2 Curvatures and slopes for beam in Example 6.2

Distance (m)	1.045	2.09	2.92	3.75	4.58	5.41	6.455	7.5
M_{qp} (kNm)	107.9	181	214	225	214	181	107.9	0
x (mm)	–	136	135	135	135	136	–	–
ε_c (×10⁻⁴)	–	4.25	5.38	5.77	5.38	4.25	–	–
σ_s (N/mm²)	–	352	450	482	450	352	–	–
ζ (1/mm)	–	0	0.39	0.47	0.39	0	–	–
$1/r_1$(1/mm×10⁻⁷)	5.34	8.95	10.59	11.13	10.59	8.95	5.34	0
$1/r_2$(1/mm×10⁻⁷)	–	31.25	39.85	42.74	39.85	31.25	–	0
$1/r_m$(1/mm×10⁻⁷)	5.34	8.95	22	25.99	22	8.95	5.34	–
dy/dx (×10⁻⁴)	3.05	10.94	24.65	45.27	65.71	79.59	87.49	90.53

From Table 2.1, long-term E_{cm}=1.15×32=36.8×10^3 N/mm^2.

From Table 2.3, with $2A_c/u$=300 mm, outdoor exposure and age at transfer of 7 days, φ=2.2. Thus:

$E_{c.eff}$=36.8/(1+2.2)=11.5×10^3 N/mm2.

The resulting curvatures, and slopes relative to the left-hand support, along the beam are shown in Table 6.2 with both β_1 and β_2 taken as 1.0 for the cracked sections. The slopes have been determined by numerical integration of $1/r_m$ along the beam.

The difference in displacement between the left-hand support and the midspan section is then given by

$$\left[y\right]_0^{3.75} = (2090/6)(4 \times 3.05 + 10.94) \times 10^{-4}$$
$$+ (1660/6)(10.94 + 4 \times 24.65 + 45.27) \times 10^{-4}$$
$$= 5.09 \text{ mm}$$

$$\left[y\right]_0^{7.5} = (2090/6)(4 \times 3.05 + 10.94) \times 10^{-4}$$
$$+ (3320/6)(10.94 + 4 \times 45.27 + 79.59) \times 10^{-4}$$
$$+ (2090/6)(79.59 + 4 \times 87.49 + 90.53) \times 10^{-4}$$
$$= 33.95 \text{ mm}$$

With deflection upwards as positive this represents an upward deflection of the right-hand end of the beam relative to the left-hand end. However, a double integration process has been carried out and, so far, only one boundary condition has been imposed, namely that of zero deflection at the left-hand support. In order to satisfy the other boundary condition of zero deflection at the right-hand support, a linear transformation of the deflected shape as calculated above must be performed.

Thus at midspan the long-term deflection, allowing for shrinkage effects, is given by

y_{max}=1.2×(5.09–33.95/2)
=−14.26 mm.

This represents a downward deflection of L/526, which is satisfactory.

(ii) From Table 6.1, K=0.104. From Table 6.2 the uncracked curvature at midspan is 11.13×10^{-7} mm.

Thus:

$[y_{max}]_{uncr}$=0.104×7500^2×11.13×10^{-7}
=6.51 mm.

Similarly,

$[y_{max}]_{cr}$=0.104×7500^2×42.74×10^{-7}
=25 mm.

The maximum long-term deflection is thus given by

y_{max}=1.2×[(1–0.47)×6.51+0.47×25]
=18.24 mm.

It can thus be seen that using Equation 6.7 gives a conservative result and will be sufficient for most purposes. The full derivation using Equation 6.3 has been shown to illustrate the calculation process, but such accuracy will rarely be required.

■■

6.5 LOAD BALANCING

The fact that an eccentric prestress force gives rise to vertical deflections in a prestressed concrete member leads to a method of design known as *load balancing*. By suitable adjustment of the prestress force and eccentricity, the deflection of a member can be made to be zero under all, or some proportion, of the total load. In this case the stresses in the member are purely axial. The extra deflections under any unbalanced load may be determined using any of the usual strength-of-materials methods.

There is much room for judgement on the part of the designer as to what proportion of the total load should be balanced. If the total load is balanced, then an unacceptable camber may result at transfer. If only the dead load is balanced, then routine load deflections may be excessive. One common criterion used in design is to balance the quasi-permanent load on the structure.

Theoretically, a uniform applied load can only be balanced by a continuously draped tendon, while a concentrated load can only be balanced by a sharp change of curvature. In practice, however, any given load can be balanced approximately by either type of tendon, or a combination of both.

Example 6.3 ■■
For the beam shown in Fig. 6.6, determine the prestress force required to balance a total applied load of 20 kN/m. Determine, also, the stress distribution at midspan.
From Chapter 1, the uniform lateral load from a parabolic tendon is given by

$w = 8Pe/L^2$
$\therefore P = wL^2/8e.$
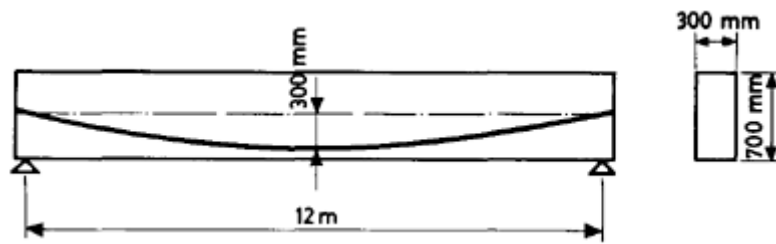
Figure 6.6

Thus the prestress force required to balance a uniform load of 20 kN/m is given by

$P=(20\times12^2)/(8\times0.3)$
$=1200$ kN.

Section properties:

$A_c=2.1\times10^5\text{mm}^2$
$Z_b=Z_t=24.5\times10^6$ mm^3

At midspan,

$$M = (20 \times 12^2)/8$$
$$= 360 \text{ kNm}$$
$$\sigma_t = \frac{1200 \times 10^3}{2.1 \times 10^5} - \frac{1200 \times 10^3 \times 300}{24.5 \times 10^6} + \frac{360 \times 10^6}{24.5 \times 10^6}$$
$$= 5.71 - 14.69 + 14.69$$
$$= 5.71 \text{ N/mm}^2$$

$$\sigma_b = 5.71 + 14.69 - 14.69$$
$$= 5.71 \text{ N/mm}^2.$$

That is, the section is in a state of uniform compression, as expected.
■■

6.6 LOAD-DEFLECTION CURVES

Typical load-deflection curves for a beam with varying degrees of prestress are shown in Fig. 6.7, based on Abeles (1971). In each case, the ultimate strength is made the same by addition of untensioned reinforcement where necessary. Curve (a) represents a beam that is over-prestressed, and shows that failure occurs suddenly with little warning given. Curve (b) represents a beam with zero tension under total design load and curve (c) an uncracked beam with tension. The much better warning given of imminent failure by these beams is
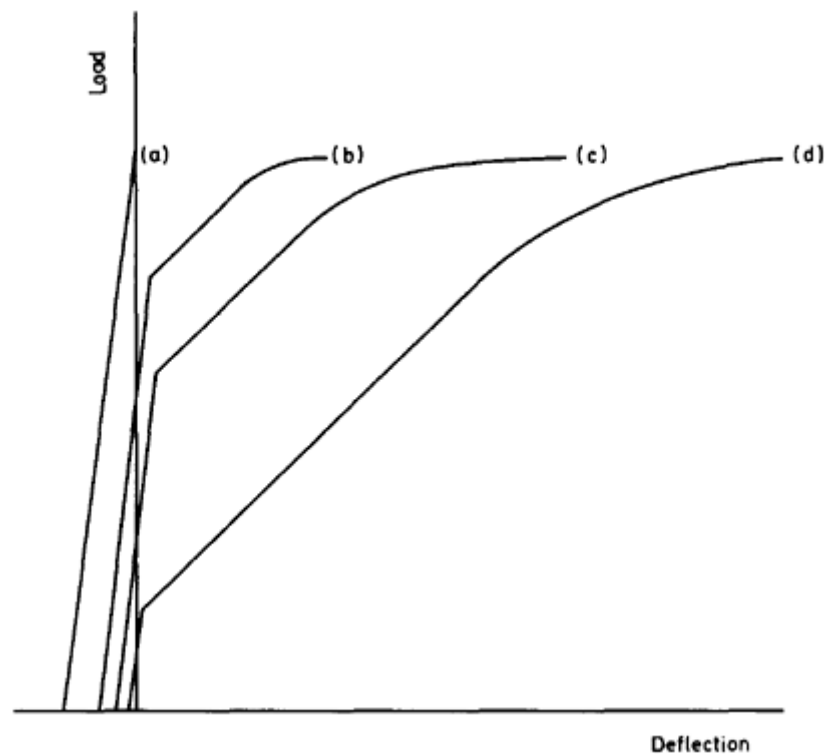
Figure 6.7 Load-deflection curves for beam with varying prestress.
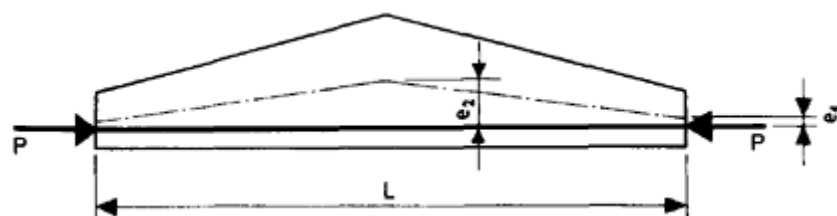
Figure 6.8 Load-deflection curves for beam with varying prestress.

evident from the larger deflections prior to collapse. Curve (d) represents a cracked beam, and this curve is similar to that for a reinforced concrete beam with a small percentage of steel.

In curves (b), (c) and (d), the sharp change in stiffness of the beam is clearly seen, corresponding to the point where the beam is cracked. Also shown are the different initial cambers associated with each degree of prestress.

The much smaller deflections of the uncracked beams at failure compared with cracked prestressed and reinforced concrete members

are due to the fact that a large proportion of the strain required to achieve the large stress in the tendons at failure is locked into the member at transfer. The extra flexural strain induced is thus relatively small.

PROBLEMS

6.1 The beam in Fig. 6.8 has constant width b and depth varying linearly from h to $2h$ at midspan. If the prestress force is constant along the span determine the upward camber at midspan.

6.2 For the beam in Example 4.1, determine the camber at midspan due to prestress only based on the distribution of prestress force resulting from elastic shortening losses, and friction losses as shown in Fig. 4.10. Assume that the concrete is grade C25/30 at transfer.

REFERENCES

Abeles, P.W. (1971) *The Structural Engineer,* **49,** No. 2, pp. 67–86.

Beeby, A.W. and Narayanan, R.S. (1995) *Designers' Handbook to Eurocode 2,* Thomas Telford, London.

7

Shear

7.1 INTRODUCTION

The approach in EC2 to the determination of the shear resistance of prestressed concrete members is similar to those adopted in the earlier CP110 and BS8110, namely consideration of the ultimate limit state.

The shear resistance of prestressed concrete members at the ultimate limit state is dependent on whether or not the section in the region of greatest shear force has cracked. The actual mode of failure is different for the two cases. If the section is uncracked in flexure, then failure in shear is initiated by cracks which form in the webs of I- or T-sections once the principal tensile strength has been exceeded (Fig. 7.1(a)). If the section is cracked in flexure then failure is initiated by cracks on the tension face of the member extending into the compression zone, in a similar manner to the shear failure mode for reinforced concrete members (Fig. 7.1(b)).

In EC2 consideration is only given to the cracked shear resistance of prestressed concrete members. This comprises the dowel action of any longitudinal reinforcement crossing the shear crack, aggregate interlock across the two faces of the crack and the contribution of any vertical or inclined shear reinforcement crossing the crack.

Since there is enhanced shear resistance of members close to a support, it is usually only necessary, for beams with distributed loading, to determine the shear resistance at a distance from the face of a support equal to d, the effective depth of the reinforcement or prestressing tendons. In the determination of d, the effect of any inclined tendons is ignored.

7.2 DESIGN SHEAR RESISTANCE

The shear resistance, V_{Rd1}, of a given section of a prestressed concrete member with no shear reinforcement is given in EC2 by:

$$V_{Rd1} = [\tau_{Rd} k (1.2 + 40 \varrho_1) + 0.15 \sigma_{cp}] b_w d,$$
(7.1)
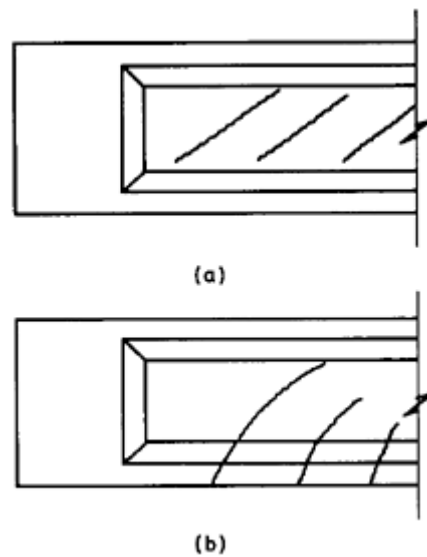
Figure 7.1 Types of shear cracking.

Table 7.1 Basic concrete shear strength τ_{Rd} (N/mm^2)

Concrete grade					
C25/30	C30/37	C35/45	C40/50	C45/55	C50/60
0.30	0.34	0.37	0.41	0.44	0.48

where τ_{Rd} is the basic shear strength taken from Table 7.1; k is a factor allowing for the section depth, given by $k=(1.6-d)$, where d is not greater than 0.6 m; b_w is the minimum width of the section; ϱ_l is the tension reinforcement ratio, with a maximum value of 0.02, defined as $(A_p+A_s)/b_w d,$ where A_s is the area of untensioned reinforcement; A_p is the area of any non-inclined prestressing tendons at the section considered (all reinforcement and pretensioned tendons must extend a distance past the section equal to the sum of the effective depth and the anchorage length of the bars or tendons), and σ_{cp} is the axial stress arising from the prestressing force and any applied axial load.

If the applied shear force at a section, V_{sd}, taking into account the effect of any inclined tendons (as described in Chapter 1), with γ_p taken as 0.9, exceeds V_{Rd1} then shear reinforcement must be provided. The shear resistance is calculated on the basis of a truss analogy, whereby the compression elements of the truss are formed by the concrete and the tension elements by the reinforcement, as shown in Fig. 7.2.

There are two alternative methods given in EC2 for determining the shear resistance of a section with a given amount of reinforcement, but
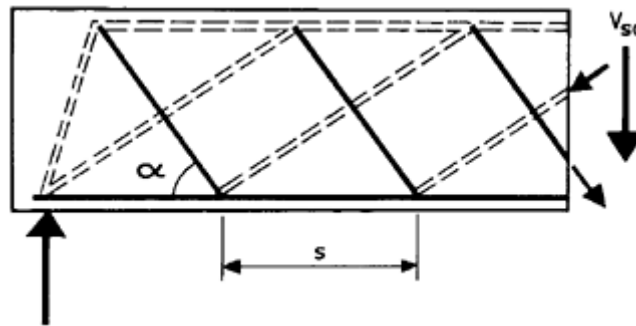
Figure 7.2 Truss analogy.

only the requirements of what is termed the 'standard' method are given here.

The shear reinforcement must be such that

$$A_{sw}/s = (V_{sd} - V_{Rd1})/[0.78\ d f_{yk}(1 + \cot \alpha)\sin \alpha],$$
(7.2)

where A_{sw} is the area of shear reinforcement over a length s, f_{yk} is its characteristic strength and α is the angle between the shear reinforcement and the longitudinal axis of the beam. This reinforcement can be a combination of links and inclined bars, but at least 50% should be in the form of links.

The maximum shear resistance of a section, V_{Rd2}, is given by

$$V_{Rd2} = 0.3\ v f_{ck} b_w d(1 + \cot \alpha),$$
(7.3)

where $v = 0.7 - f_{ck}/200$ ($v > 0.5$). In order to allow for the effect of axial compression in the section, where $\sigma_{cp} > 0.27 f_{ck}$, the value of V_{Rd2} should be further reduced to

$$1.67\ (1 - 1.5\ \sigma_{cp}/f_{ck}) V_{Rd2}.$$
(7.4)

If the applied shear force exceeds V_{Rd2} then the section size must be increased.

If a web contains grouted ducts with diameters greater than $b_w/8$ then the web thickness should be reduced by 0.5 (sum of duct perimeters), determined at the most unfavourable level, in the calculation of V_{Rd2}.

The force in the longitudinal reinforcement of the truss shown in Fig. 7.2 must also be determined. This is given by

$$T_d = M_{sd}/z + V_{sd}(1 - \cot \alpha)/2,$$
(7.5)

where M_{sd} is the ultimate bending moment at the section and z is the lever arm, which can be taken as 0.9d. It is generally only necessary to check the force in the longitudinal steel near supports, since at midspan it is sufficient to check that the ultimate limit state of collapse is satisfied.

If V_{sd} is less than V_{Rd1} then a minimum amount of shear reinforcement must be provided, given by

$$A_{sw}/s = \varrho_w b_w \sin \alpha$$
(7.6)

where ϱ_w is found from Table 7.2. The maximum size of links should be 12 mm for mild steel and the maximum spacing should not exceed the smaller of:

  (i) 0.8 d, or 300 mm, if $V_{sd} < V_{Rd2}/5$;
 (ii) 0.6 d, or 300 mm, if $V_{Rd2}/5 < V_{sd} < 2V_{Rd2}/3$;
(iii) 0.3 d, or 200 mm, if $V_{sd} > 2V_{Rd2}/3$.

Example 7.1 ■■
   The beam in Fig. 7.3 supports an ultimate load, including self weight, of 85 kN/m over a span of 15 m and has a final prestress force of 2000 kN. Determine the shear reinforcement required. Assume that the concrete is grade C30/37 and that $A_p = 2010$ mm².

$A_c = 2.9 \times 10^5$ mm²
$\sigma_{cp} = 2000 \times 10^3/(2.9 \times 10^5)$
$= 6.90$ N/mm² $(= 0.23 f_{ck})$
$v = 0.7 - 30/200$
$= 0.55$.

Table 7.2 Minimum values for ϱ_w

	Steel type	
Concrete grade	Mild	High tensile
C25/30–C35/45	0.0024	0.0013
C40/50–C50/60	0.0030	0.0016
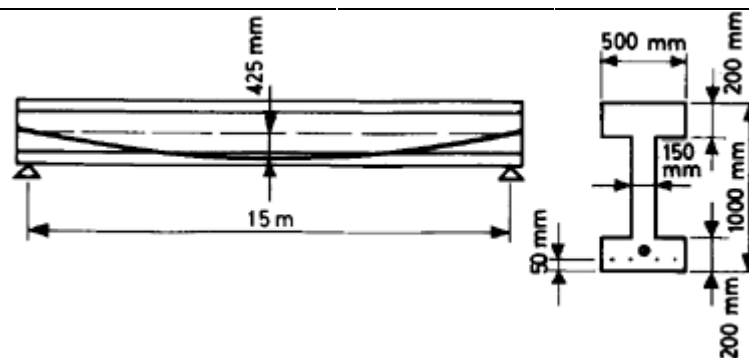
Figure 7.3

At 0.95 m from the support, the inclination of the tendons is given by:

$\theta = \tan^{-1} [4 \times 0.425(1 - 2 \times 0.95/15)/15]$
$= 5.65°$.

Also,

$e = 4 \times 0.425 \times 0.95(15 - 0.95)/15^2$
$= 0.101$ m
$\therefore d = 601$ mm.

The ultimate bending moment and shear force diagrams are shown in Fig. 7.4(a) and (b), respectively. The vertical component of the tendon force at the support is $0.9 \times 2000 \sin \theta$, or 177.2 kN, and thus V_{sd} at the section is 379.6 kN.

$V_{Rd2} = 0.3 \times 0.55 \times 30 \times 150 \times 601 \times 10^{-3}$
$= 446.2$ kN

$\varrho_1 = 2010/(150 \times 601) = 0.022 > 0.02$
$\therefore \varrho_1 = 0.02$.

The value of k is 1.0 at this section.
   For the section with no shear reinforcement:

$V_{Rd1} = [0.34 \times 1.0(1.2 + 40 \times 0.02) + 0.15 \times 6.90] \times 150 \times 601 \times 10^{-3}$
$= 154.6$ kN.

Thus shear reinforcement is required. For vertical links $\cot \alpha = 0$.
   Thus:

$A_{sw}/s = (379.6 - 154.6) \times 10^3/(0.78 \times 601 \times 250)$
$= 1.92$.

For R12 links at 100 mm centres, $A_{sw}/s = 2.26$.
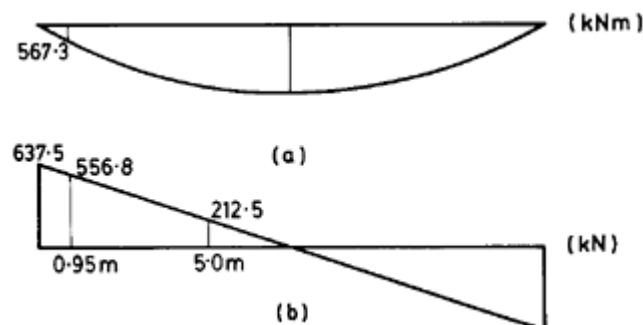
Figure 7.4 Ultimate (a) bending moments and (b) shear forces for beam in Example 7.1.
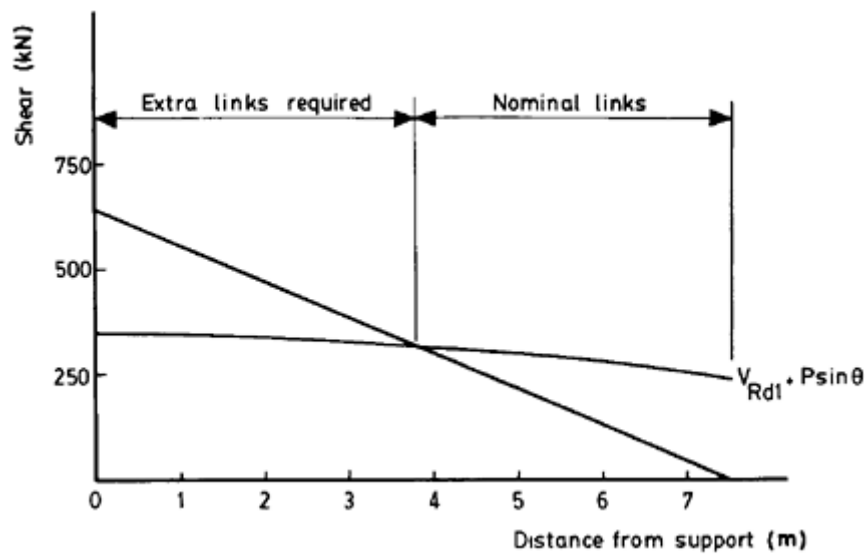
Figure 7.5 Shear resistance of beam in Example 7.1.

For the longitudinal steel, from Fig. 7.4,

$$T_d = \frac{567.3}{0.9 \times 0.601} + \frac{556.8}{2}$$
$$= 1327.2 \text{ kN}$$
$$A_s = \frac{1327.2 \times 10^3}{0.87 \times 460} = 3316 \text{ mm}^2.$$

At 5 m from the support, $\theta=2.16°$ and the vertical component of the tendon force is 75.5 kN. The design shear force is thus 137 kN, which is less than the value of V_{Rd1}, and thus only nominal shear reinforcement is required. From Table 7.2, this is given by

$A_{sw}/s=0.0024\times150=0.36$.

At the point where only nominal links are required, $V_{sd}=380$ kN. Since this is between 1/5 and 2/3 V_{Rd2} the maximum link spacing is 0.6 d, or 570 mm. For R12 links at 500 mm centres, $A_{sw}/s=0.45$.

The shear resistance along the beam is shown in Fig. 7.5. It can be seen that nominal links are adequate in the middle region of the beam, with increased spacing required near the supports, as for a reinforced concrete beam.

■■

8

Prestressing systems and anchorages

8.1 PRETENSIONING SYSTEMS

The essential features of the pretensioning of concrete members were described in Chapter 1. The anchorages used to maintain the tendons in tension until the concrete has hardened sufficiently must be reusable and the commonest system is a single barrel-and-wedge arrangement, shown in Fig. 8.1. Once the tendons have been tensioned to the required level, the jack is released and the wedges lock against the sides of the tendon and the barrel as the tendon contracts. The barrels bear directly against an anchor block which transmits the tensioning force *via* the prestressing bed to the other end of the tendon.

Once the concrete in the member has reached sufficient strength for transfer to take place, a prefabricated 'stool' is inserted between the anchor block and the jack. The barrel-and-wedge anchorage is relieved of its pressure by jacking the tendon to its original force, and then the loosened anchorage assembly may be removed. The jack pressure is released and the prestressing force is transferred to the concrete members along the prestressing bed.

Where deflected tendons are required in pretensioned members, the strands are initially tensioned in their original straight profiles and then deflected up (or down) at the desired locations by hydraulic jacks. They are then locked in this deflected position by a holding-down device, securely fixed to the prestressing bed. The jack used to deflect the tendons may then be removed.

An alternative method is to tension the tendons in their deflected shape, with the holding-down device in place and secured to the prestressing bed before tensioning begins. With this system, the friction between the tendons and the holding-down device must be taken into account when determining the expected extension of the tendons at the anchor block.
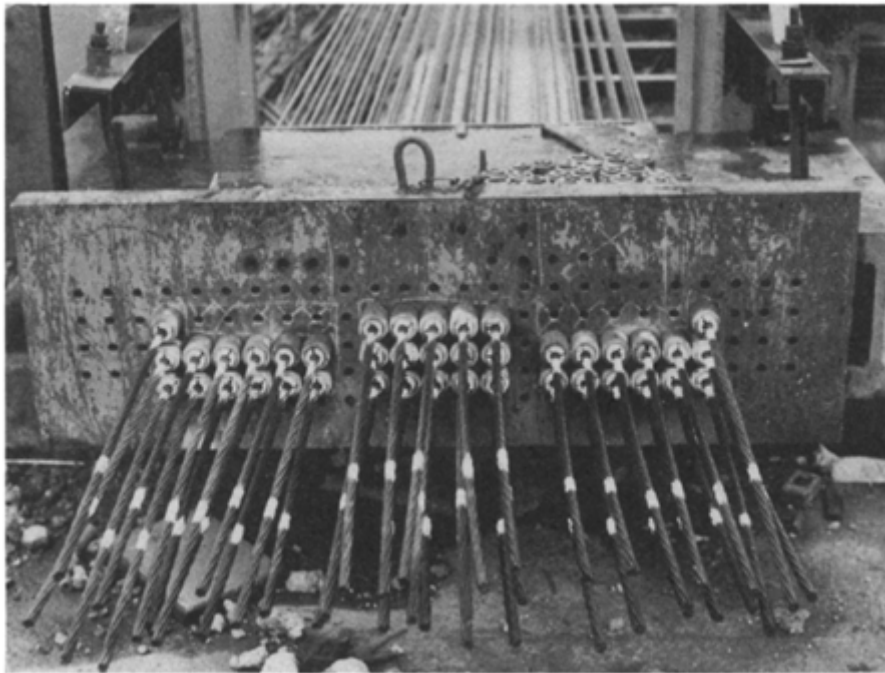
Figure 8.1 Pretensioning anchorage.

8.2 POST-TENSIONING SYSTEMS

The main difference between the anchorages used in post-tensioning and pretensioning is that, in the latter, the anchorages should be reusable, but in the former the anchorages must be cast into the member and can only be used once.

There are many proprietary systems of post-tensioning anchorage available, but they fall into three main categories.

(a) Wedge anchorages

These are similar to the usual type of anchorage used in pretensioning work and may be used for tendons comprising either wires or strands. The restraining force on the tendon is provided by friction between the tendon and wedges bearing against the sides of a tapered hole in a steel plate or block. However, unlike most pretensioning applications, where each tendon is composed of a single wire or strand, in post-tensioned concrete members the tendons usually consist of many strands or wires running through the same duct. These wires or strands are usually all anchored within the same anchorage, which is more economical than providing separate anchorages for each component of the tendon.

One such barrel-and-wedge anchorage is shown in , both as a
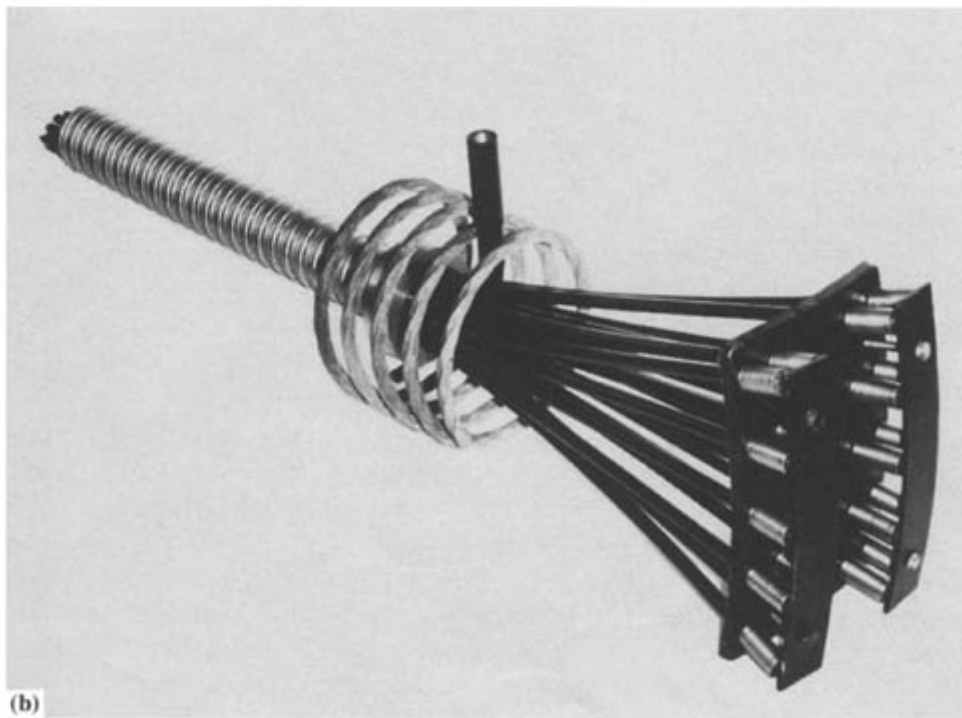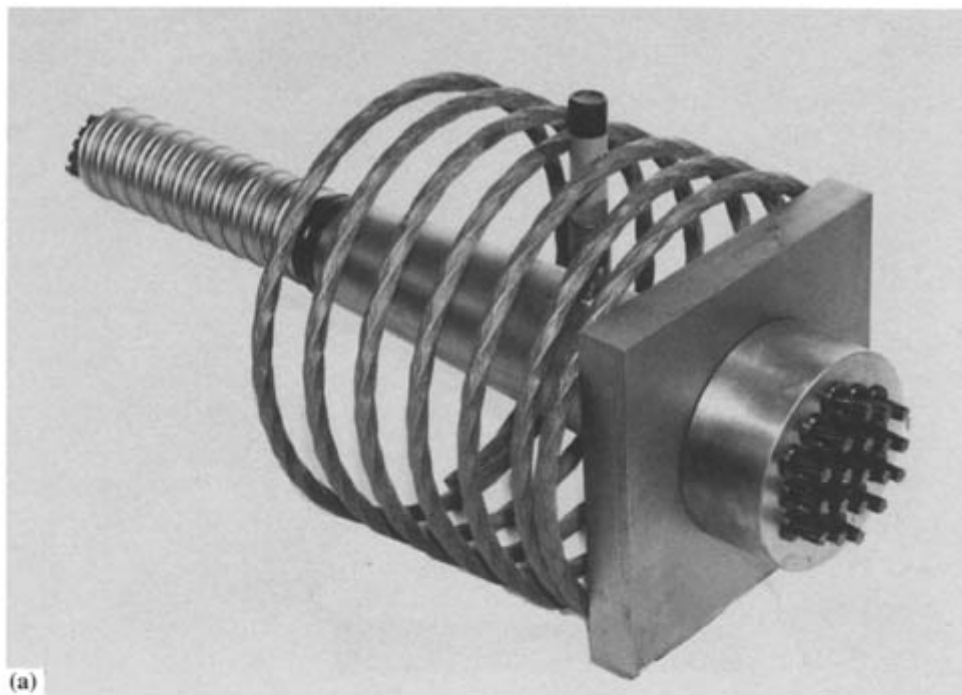
Figure 8.2 Post-tensioning wedge anchorages: (a) tensioning anchorage (b) dead-end anchorage *(courtesy VSL International)*.

tensioning and as a non-tensioned or 'dead-end' anchorage. Note that both types incorporate helical reinforcement around the main body of the anchorage. This is to counter the tensile forces which are set up within the concrete by the large concentrated force applied to it through the anchorage; this will be dicussed in more detail in Section 8.3. Each individual strand in the tensioning anchorage has its own set of wedges within an anchor block and the force in each strand is transmitted to the concrete through a steel bearing plate.

Tensioning is carried out using a single hydraulic jack for each tendon. All the strands in the tendon are gripped simultaneously by the jack and pulled until the desired extension and pressure are reached. The jack pressure is then released and the slight draw-in of the strands locks the wedges firmly in their seating in the anchor block. For large tendon forces, the jacks required are very heavy and must be positioned using a crane or a hoist. Some systems which also use the wedge principle allow each strand in the tendon to be tensioned individually, so that a much smaller and more easily handled jack may be used. A 1000 tonne jack used in the tensioning of a bridge deck is shown in Fig. 8.3.

Also shown in Fig. 8.2 are the duct former leading from the anchorage, and also a grout inlet so that the duct may be injected with grout after the tendon has been tensioned. This is in order to provide
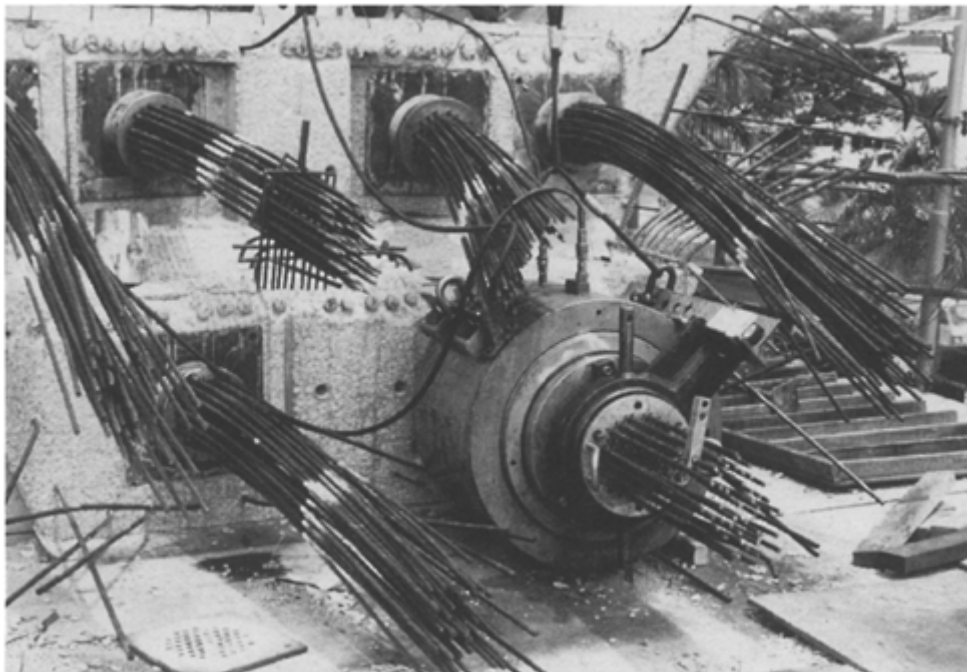
Figure 8.3 Post-tensioning using 1000 tonne jack.

protection to the tendon and to bond it to the surrounding concrete *via* the duct former. For most applications the duct formers are corrugated and made from thin galvanized steel strip and are flexible enough to enable them to be fixed in the curved profiles usually adopted. They are also rigid enough not to distort during concreting. In special applications, such as in nuclear reactor pressure vessels or offshore platforms, the tendons may be housed in steel tubes. Where contact with chemical products is likely, plastic ducts may be used for greater protection. Once the tensioning and grouting are complete, the exposed portion of the anchorage is usually encased in concrete for protection.

(b) Buttonhead anchorages

For tendons comprising wires, an alternative to locking them through friction is to form a 'buttonhead' at the end of the wire and to have this shaped end bear against a plate. A typical anchorage for such a system is shown in Fig. 8.4, both as a tensioning and as a dead-end anchorage. The wires in the tensioning anchorage bear against an anchor block which is threaded to fit inside the jack, so that all the wires may be tensioned simultaneously. After tensioning, steel shims are inserted between the anchor block and the bearing plate, and these may be seen in Fig. 8.4(a).

There is negligible anchorage draw-in with this system and thus it is particularly suitable for short members. It also offers the possibility of easily adjusting or releasing the tension in the tendons at a later stage, since no protruding wires are required for gripping by the jack. One disadvantage of this system compared with a system using wedges is that the initial length of the wires must be known accurately, since the buttonheads at either end of the wire must fit snugly on the anchor block.

(c) Threaded bar anchorages

The third main category of anchorage uses a simple threaded bar, with a nut bearing against a steel plate to maintain the force in the bar. An example is shown in Fig. 8.5. If the thread is continuous, this allows greater tolerance on the length of the bar and also gives better bond with the surrounding grout inside the duct former. The grout is injected through the hole in the bearing plate after tensioning.

A ring spanner is placed over the nut and then covered by a tensioning stool which allows the nut to be tightened continuously during tensioning. The hydraulic jack bears against the stool and pulls the bar until the desired extension and pressure are achieved. By tightening the nut firmly at this stage, anchorage draw-in is virtually eliminated on release of the jack pressure.
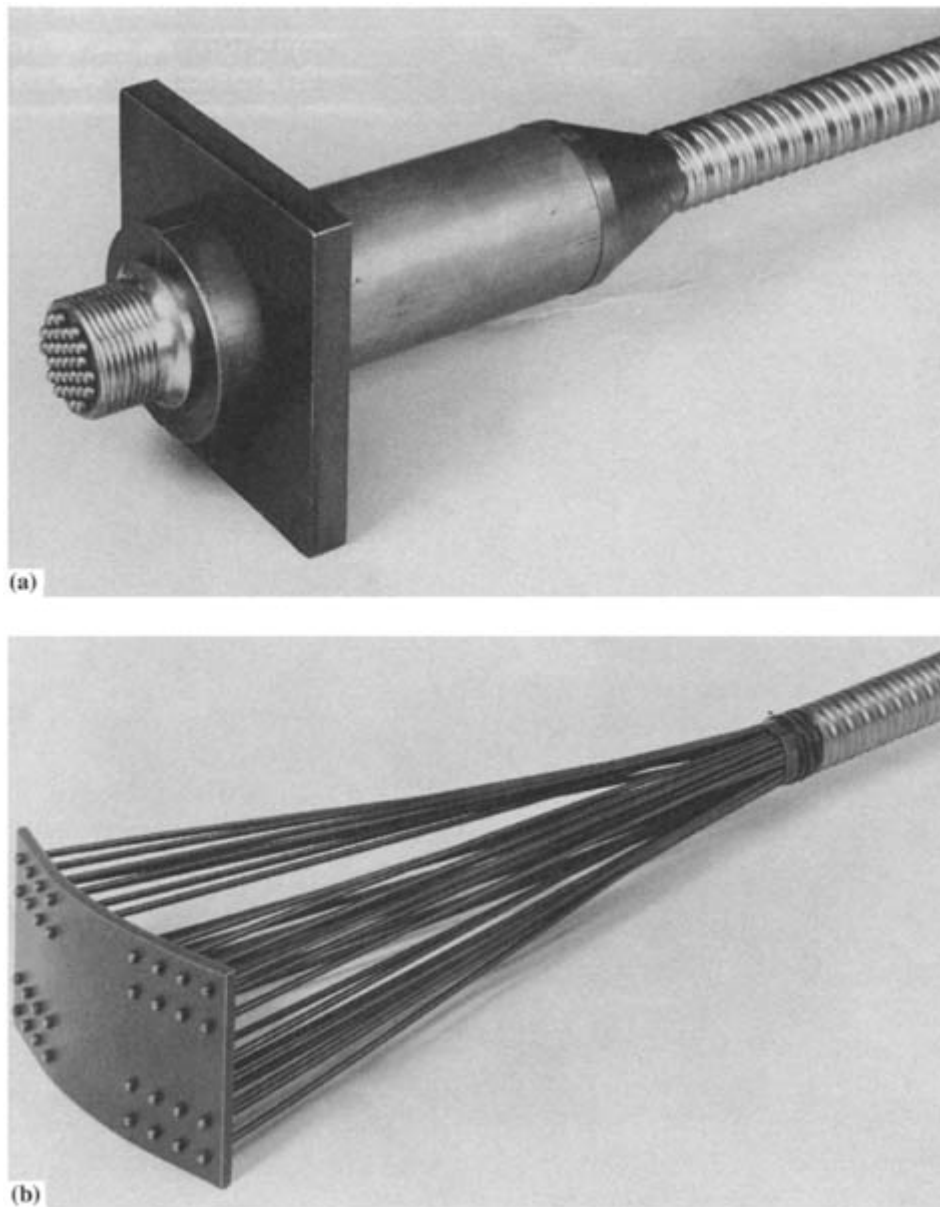
Figure 8.4 Buttonhead anchorages: (a) tensioning anchorage; (b) dead-end anchorage *(courtesy Bureau BBR Ltd).*

A sequence of construction often used for multi-span bridges involves attaching tendons to the ends of those which have already been tensioned. A coupler for the buttonhead system is shown in Fig. 8.6; each system has similar arrangements.

A type of anchorage which should be mentioned briefly is that which
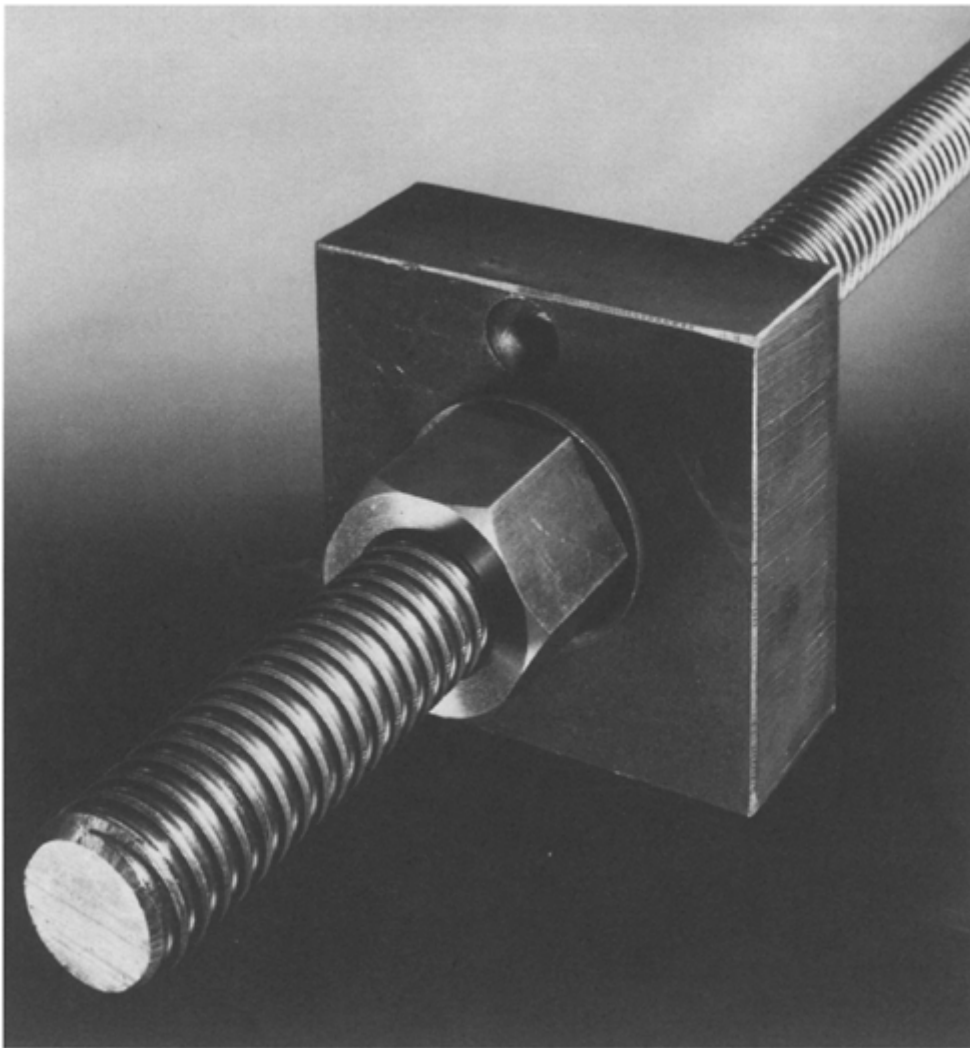
Figure 8.5 Bar anchorage *(courtesy McCalls Special Products)*.

is used for the circumferential prestressing of tanks and silos. One such anchorage is shown in (see also). The strands pass through an anchor block from both directions and are tensioned in groups alternately. The anchor block moves back and forth within a recess in the tank wall during tensioning. Once this is complete, the anchorage is encased in concrete to give a flush surface. An alternative to this system is to have both ends of the tendon overlapping and ending in conventional anchorages. However, these anchorages would be proud of the tank surface and encased in a block-out.

Two types of anchorage commonly employed in slab construction are
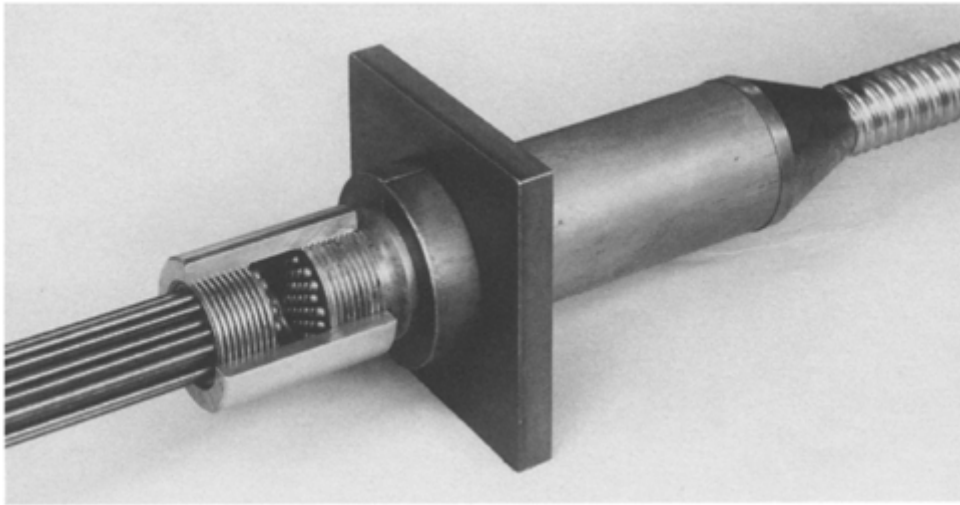
Figure 8.6 Coupler *(courtesy Bureau BBR Ltd)*.
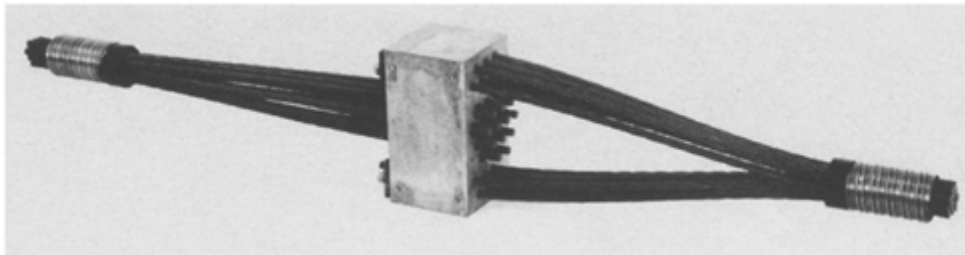
Figure 8.7 Anchorage for circumferential prestressing *(courtesy VSL International)*

shown in Fig. 8.8. An anchorage for a single unbonded strand is shown in Fig. 8.8(a), whilst Fig. 8.8(b) shows an anchorage for a group of four bonded strands.

The anchorage details of the post-tensioning system to be used must be considered at an early stage in the design process, since the spacing of the anchorages is not only governed by the type of jack to be used but also by the bursting forces set up within the anchorage zone.

8.3 BURSTING FORCES IN ANCHORAGE ZONES

For post-tensioned members, the prestressing force in a tendon is applied through the anchorages as a concentrated force. By St Venant's principle, the stress distribution in a member is reasonably uniform
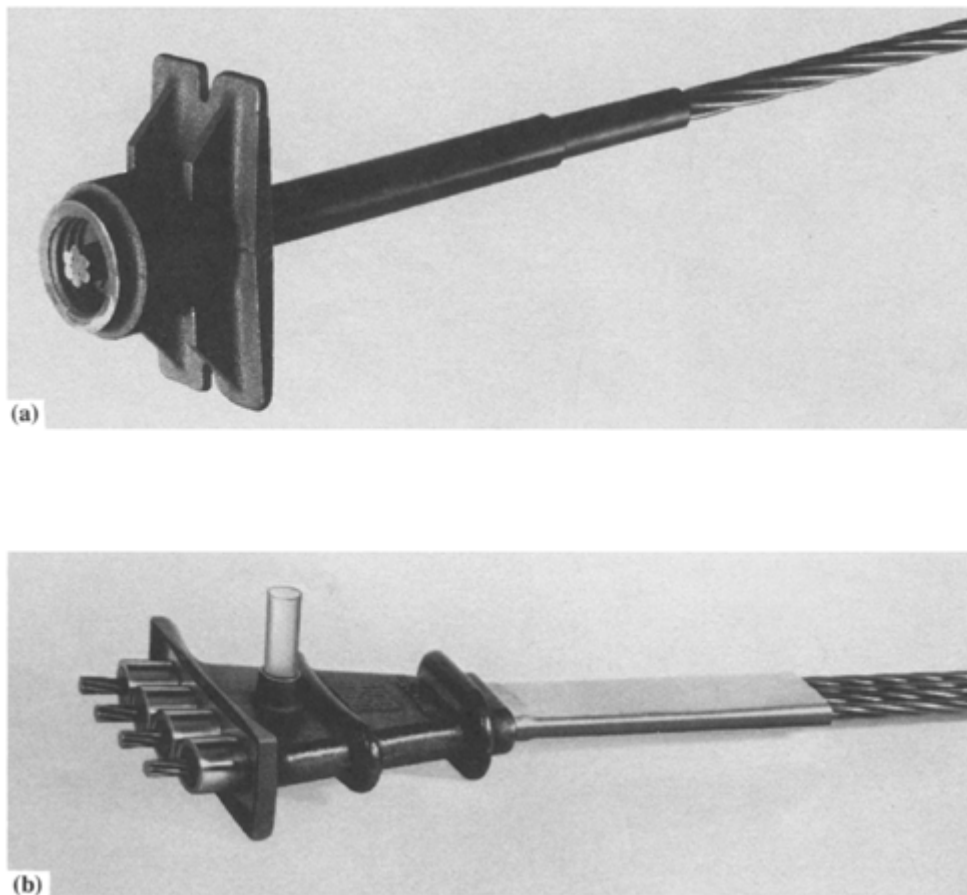
Figure 8.8 Anchorages for slabs: (a) unbonded; (b) bonded *(courtesy Bureau BBR Ltd)*.

away from the anchorage, but in the region of the anchorage itself the stress distribution within the concrete is complex. The most significant effect for design, however, is that tensile stresses are set up transverse to the axis of the member, tending to split the concrete apart, rather like a nail being driven into the end of a timber joist. Reinforcement must be provided to contain these tensile stresses.

Various theoretical and experimental studies have been carried out into the anchorage zone stresses, and the recommendations in EC2 give results which are a reasonable approximation to the experimental ones.

The end-block of a concentrically-loaded post-tensioned member of rectangular cross-section is shown in Fig. 8.9(a), which also shows the distributions of principal tensile and compressive stresses within this zone. This stress distribution is for a flat plate anchorage but a similar
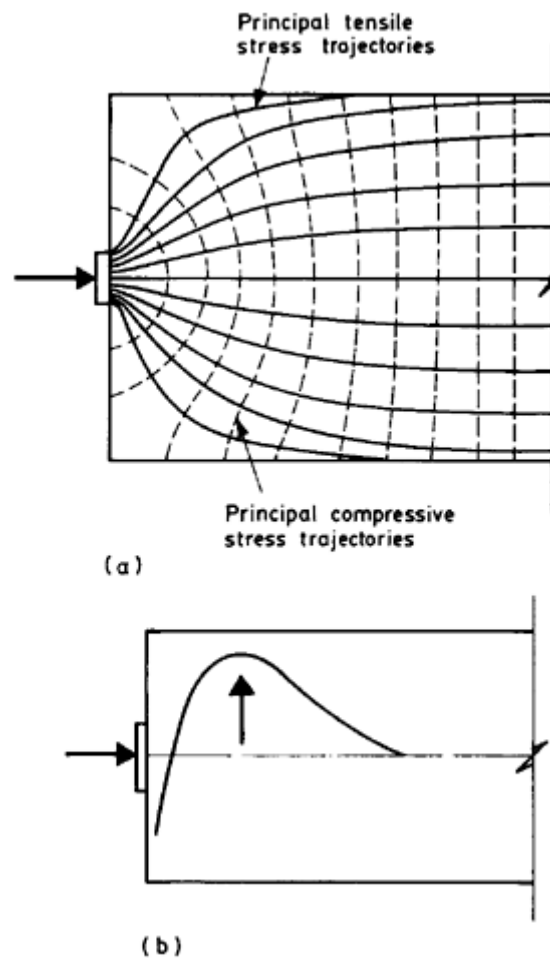
Figure 8.9 End-block (a) stress distribution and (b) bursting forces.

stress distribution is obtained with a conical anchorage. The actual distribution of the bursting forces is not uniform but varies approximately as shown in Fig. 8.9(b).

It is recommended in EC2 that a strut-and-tie model be used to determine the reinforcement in the anchorage zone necessary to resist the bursting forces. A representation of this model is given in Fig. 8.10. The reinforcement should be designed on the assumption that the stress in it is 0.87 f_{yk}, and the stress in the concrete 'struts' should not exceed 0.4 f_{ck}. The force in the tendon is the characteristic value, $f_{yk}A_p$.

In addition, the bearing stress under the anchorage plates should be less than

$$0.67 f_{ck}(A_{c1}/A_{co})^{1/2} \leq 2.2 f_{ck},$$
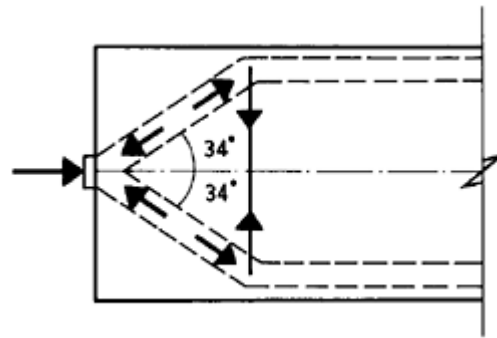
Figure 8.10 Strut-and-tie model of end-block.
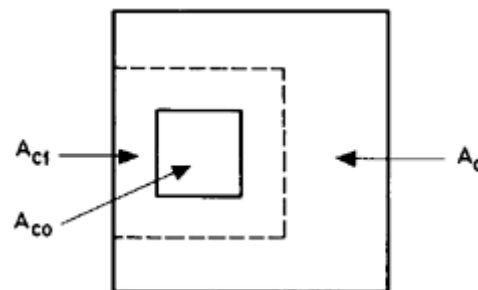
Figure 8.11

where A_{co} is the loaded area and A_{c1} is the maximum area corresponding geometrically to A_{co}, with the same centroid, which it is possible to inscribe in the total cross-sectional area, A_c (Fig. 8.11).

Reinforcement should be in the form of links spread over a length approximately equal to the greatest lateral dimension of the end-block. At any part of the zone the reinforcement ratio on either side of the block should be a minimum of 0.15% in both directions.

Where an end-block contains several anchorages, it should be divided into a series of symmetrically loaded end-blocks and then each one treated separately, as described above. Additional reinforcement should be provided around the whole group of anchorages to maintain overall equilibrium. More information on the treatment of end-block design may be found in Abeles and Bardhan-Roy (1981) and in the guide of the Construction Industry Research and Information Association (1976).

Example 8.1 ■■

The beam end shown in Fig. 8.12 has six anchorages, each with conical anchors of 100 mm diameter, and a characteristic force of 400 kN
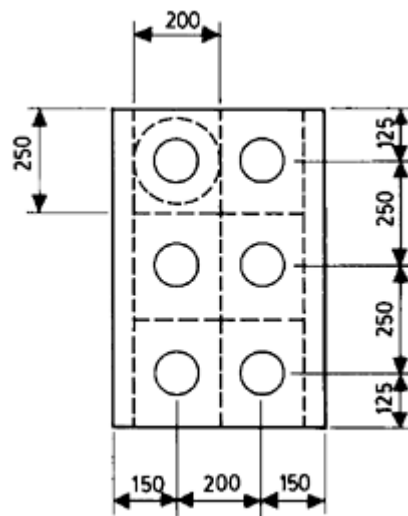
Figure 8.12

applied to the tendon. Determine the bearing stresses under the anchorages, the reinforcement required to resist bursting forces and the local stresses in the concrete end-block. Assume that the concrete is grade C40/C50 and f_{yk}=460 N/mm2.

The overall end-block can be divided into separate effective end-blocks, each with dimensions 200×250 mm.

The bearing stress under the anchor plate

$$= \frac{400 \times 10^3}{100^2 \times \pi/4} = 50.9 \text{ N/mm}^2.$$

The allowable bearing stress

$=0.67 \times 40 \times (200^2/100^2)^{1/2}$
$=53.6 \text{ N/mm}^2.$

For an individual anchorage, the stress in the concrete 'struts' of Fig. 8.10

$$= \frac{400 \times 10^3}{2 \times 200 \times 100 \times \cos^2 34°}$$
$$= 14.6 \text{ N/mm}^2.$$

The allowable concrete stress

$=0.4 \times 40=16 \text{ N/mm}^2.$

The area of reinforcement required to resist bursting stresses

$$= \frac{400 \times 10^3 \times \tan 34°}{2 \times 0.87 \times 460}$$
$$= 337 \text{ mm}^2.$$

Thus three T10 closed links are adequate around each anchorage, giving a total cross-sectional area of 471 mm^2. These should be placed uniformly over a length equal to the greatest lateral dimension of the end-block, that is 250 mm.

For the anchorage as a whole, the effective end-block has dimensions of 750×400 mm. The area of reinforcement required

$$= \frac{6 \times 400 \times 10^3 \times \tan 34°}{2 \times 0.87 \times 460}$$
$$= 2023 \text{ mm}^2.$$

Thus five T16 closed links are sufficient, encompassing the six individual anchorages and giving a total cross-sectional area of 2010 mm^2. These should be placed uniformly over a length of 750 mm. The practical detailing of the end-block is shown in Fig. 8.13.
■■

8.4 TRANSMISSION LENGTHS IN PRETENSIONED MEMBERS

Once the tendons in a pretensioned member have been cut, the force in them, which was initially maintained by the anchorages at the ends of the pretensioning bed, is transferred suddenly to the ends of the
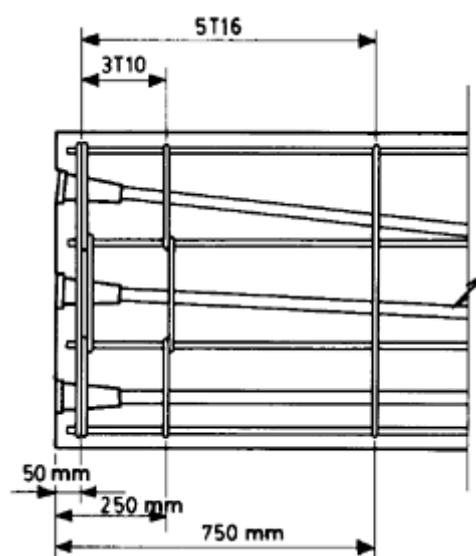
Figure 8.13 Detailing for beam in Example 8.1.
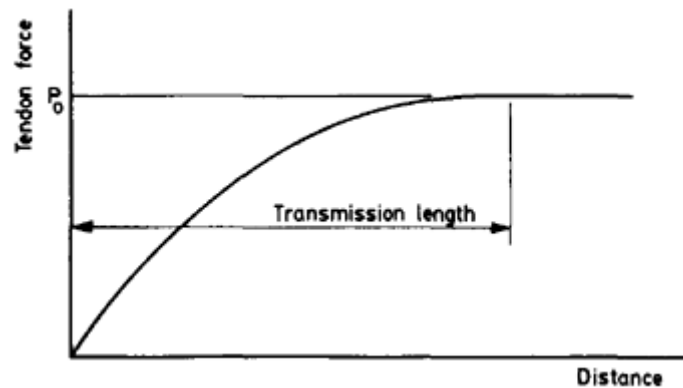
Figure 8.14 Transmission length.

concrete member. However, since there is no anchorage at the end of the member, as in the case of post-tensioning, there can be no force in the tendon there. Further along the tendon, the bond between the steel and the concrete enables the force in the tendons to build up, until at some distance from the end of the member a point is reached where the force in the tendons equals the initial prestress force. This distance is known as the *transmission length*. A typical variation of prestress force along a pretensioned member is shown in Fig. 8.14. There are many factors which affect the transmission length; the transmission lengths for wires have been found to vary between 50 and 160 diameters. An investigation into these various factors is described in Base (1958).

At the end of the member, the bond between steel and concrete tends to break down and the tendons slip relative to the concrete, thus setting up a friction force between the two materials. The force in the tendons near the ends of the member decreases after their release, and their diameters increase slightly due to the Poisson's ratio effect, thus increasing the frictional resistance. If the tendons are wires which have been mechanically crimped, this will provide better frictional resistance and thus reduce the transmission length; this is important in short members such as railway sleepers. Strands have been found to give better frictional resistance than smooth wires of equivalent area.

Further away from the free end of the member, the Poisson's ratio effect is reduced, since the reduction in tendon force is smaller, and the force in the tendons is built up primarily by bond between the steel and concrete. The bond forces developed are dependent on the concrete strength, being larger for high strengths, and also on the degree of compaction of the concrete. This is often better at the bottom of horizontally-cast members than at the top. Also, for a given area of cross-section, several small tendons have larger surface area than one larger tendon, and thus the bond forces developed will be greater, the

same consideration which applies to local bond stresses in a reinforced concrete member.

Transmission lengths should be determined as far as possible from factory or site conditions. However, in the absence of such data the following formula for the transmission length, l_{bp}, is given in EC2:

$$l_{bp} = \beta_b \varphi,$$
(8.1)

where β_b is a coefficient taken from Table 8.1 for strands with cross-sectional area less than 100 mm^2 and for indented wires with diameter, φ of 8 mm or less. The design value of transmission length, l_{bpd}, is to be taken as 0.8 l_{bp} or 1.2 l_{bp}, whichever is less favourable.

In addition to the development of prestress force at transfer, it must also be checked whether the required force at the critical section for the ultimate limit state can be developed through anchorage bond. This is similar to the anchorage requirements for reinforcement in reinforced concrete members and thus anchorage bond will generally only be important in short members.

Since the bond between the steel and concrete is so important in developing the prestress force in a pretensioned member, it is important to limit the cracking which may occur near the ends of these members, both at the serviceability and ultimate limit states. This cracking would cause very high increases in bond stress adjacent to the cracks and could lead to bond slip of the steel. Provision of additional untensioned reinforcement should limit the cracking to acceptable levels.

The reduced prestress force near the ends of pretensioned members must be allowed for in the checking of stresses at various sections along the member. It is usually desirable to have a reduced eccentricity near the ends of simply supported beams, since the bending moments are lower in these regions. In post-tensioned members this is easily achieved, but in pretensioned members, although the eccentricity near the ends may be reduced by deflecting the tendons, this is an expensive procedure and an alternative would be to eliminate the bond between the steel and concrete over a given length deliberately by greasing the

Table 8.1 Transmission length factor β_b

	Concrete grade at transfer					
	C25/30	C30/37	C35/45	C40/50	C45/55	C50/60
Strands and smooth or indented wires	75	70	65	60	55	50
Ribbed wires	55	50	45	40	35	30
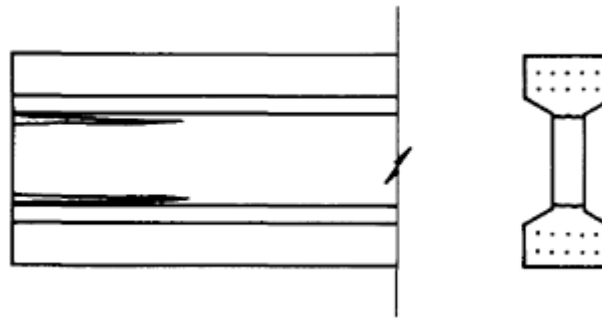
Figure 8.15 Cracking in a pretensioned member.

tendons or providing them with sleeves which allow the tendons to move freely within them. In this case, debonding can only begin at a point that is at a distance of 1.2 l_{bp} nearer the support than the point where the prestress force can theoretically be reduced.

The prestressing force in pretensioned members is applied gradually along the transmission length, and the bursting forces associated with post-tensioned members do not usually arise. However, where the pretensioning tendons are placed in two widely separated groups, as shown in Fig. 8.15, horizontal cracks may develop and these should be restrained by the provision of link reinforcement placed around both groups of tendons.

REFERENCES

Abeles, P.W. and Bardhan-Roy, B.K. (1981) *Prestressed Concrete Designer's Handbook,* Viewpoint, Slough.

Base, G.D. (1958) *An Investigation of the Transmission Length in Pretensioned Concrete.* Cement and Concrete Association Publication 41.005, London.

Construction Industry Research and Information Association (1976) *A Guide to the Design of Anchor Blocks for Post-Tensioned Prestressed Concrete Members.* Guide No. 1, London.

9

Design of members

9.1 INTRODUCTION

In Chapter 5 the analysis of sections under given prestress force and applied loading was considered. The general problem, however, is that of design: given a structure with overall geometry and applied loading, what size of member is required and what are the details of the prestressing force and tendon profile? A trial-and-error approach could be used, the test being whether the serviceability and ultimate limit state requirements are met at all sections under all possible load combinations. This might prove to be a very lengthy process, however, and a more systematic approach would clearly be advantageous.

The design of a post-tensioned concrete beam, with exposure class 3, will be illustrated in the following sections. From Table 3.6, durability is to be achieved by designing the beam for decompression. In the following examples, the tensile stresses in the concrete will be limited to those in Table 2.1, that is the section will be assumed to be uncracked. Once the prestress force and tendon profile have been determined, based on the allowable concrete stresses, the limit state of decompression will be checked and the prestress force and tendon profile adjusted if necessary. This approach will be adequate in most design cases.

The design of a beam cracked in tension will be considered in Section 9.8.

9.2 BASIC INEQUALITIES

As a starting point in the design process, consider a simply supported beam carrying a uniform load, as shown in Fig. 9.1

If the initial prestress force and eccentricity at midspan are P_o and e, respectively, then the midspan stresses at the top and bottom fibres of the beam at transfer and under the quasi-permanent, and rare load combinations may be described by the five equations given below.
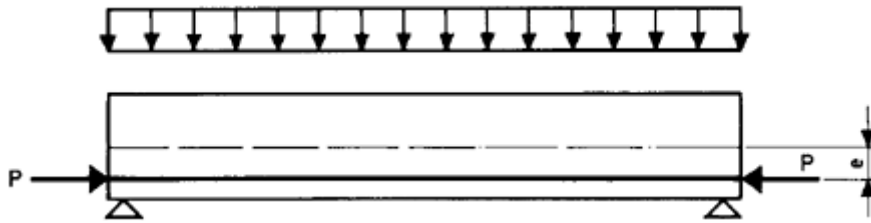
Figure 9.1

Transfer:

$$\sigma_t = \frac{\alpha P_o}{A_c} - \frac{\alpha P_o e}{Z_t} + \frac{M_o}{Z_t}$$

(9.1 (a))

$$\sigma_b = \frac{\alpha P_o}{A_c} + \frac{\alpha P_o e}{Z_b} - \frac{M_o}{Z_b};$$

(9.1(b))

Quasi-permanent and rare load combinations:

$$\sigma_{tqp} = \frac{\beta P_o}{A_c} - \frac{\beta P_o e}{Z_t} + \frac{M_{qp}}{Z_t}$$

(9.1(c))

$$\sigma_{tra} = \frac{\beta P_o}{A_c} - \frac{\beta P_o e}{Z_t} + \frac{M_{ra}}{Z_t}$$

(9.1(d))

$$\sigma_b = \frac{\beta P_o}{A_c} + \frac{\beta P_o e}{Z_b} - \frac{M_{ra}}{Z_b};$$

(9.1(e))

where Z_t and Z_b are the elastic section moduli for the top and bottom fibres, respectively, A_c is the concrete cross-sectional area, and α and β are the short- and long-term prestress loss factors, respectively. It is assumed in Equations 9.1(a)–(e) that the transfer, quasi-permanent, and rare load bending moments, M_o, M_{qp} and M_{ra}, respectively, are sagging moments. In sections of members where any of these are hogging moments the signs of M_o, M_{qp}, and M_{ra} in Equations 9.1(a)–(e) must be reversed.

If the maximum allowable compressive stresses in the concrete are f'_{max}, $(f_{max})_{qp}$ and $(f_{max})_{ra}$ at transfer, quasi-permanent and rare load, respectively, and the minimum stresses at transfer and rare load are f'_{min} and f_{min}, respectively (note that if f_{min} is negative it would indicate an allowable tensile stress), then Equations 9.1(a)–(e) may now be written as inequalities:

$$\frac{\alpha P_o}{A_c} - \frac{\alpha P_o e}{Z_t} + \frac{M_o}{Z_t} \geq f'_{min}$$

(9.2(a))

$$\frac{\alpha P_o}{A_c} + \frac{\alpha P_o e}{Z_b} - \frac{M_o}{Z_b} \leqslant f'_{max}$$

(9.2(b))

$$\frac{\beta P_o}{A_c} - \frac{\beta P_o e}{Z_t} + \frac{M_{qp}}{Z_t} \leqslant (f_{max})_{qp}$$

(9.2(c))

$$\frac{\beta P_o}{A_c} - \frac{\beta P_o e}{Z_t} + \frac{M_{ra}}{Z_t} \leqslant (f_{max})_{ra}$$

(9.2(d))

$$\frac{\beta P_o}{A_c} + \frac{\beta P_o e}{Z_b} - \frac{M_{ra}}{Z_b} \geqslant f_{min}.$$

(9.2(e))

The full set of inequalities have been given for the sake of completeness. In practice it is generally found that Inequalities 9.2(a) and (e), and the inequalities derived from them in the following sections, are the most critical cases, that is for minimum stress at transfer and under the rare load combination. However, for certain members, such as double-tee sections with narrow ribs, Inequality 9.2(b) can sometimes be critical. Inequalities 9.2(a)–(e) are shown graphically in Fig. 9.2 for an uncracked section. Also shown are the stresses for the limit state of decompression. For some sections this may be the criterion for determining the prestress force and eccentricity, which are described in the following sections.

By combining Inequalities 9.2(a) and (c), and 9.2(a) and (d), expressions for Z_t may be derived:

$$Z_t \geqslant \frac{(\alpha M_{qp} - \beta M_o)}{[\alpha(f_{max})_{qp} - \beta f'_{min}]}$$

(9.3(a))

$$Z_t \geqslant \frac{(\alpha M_{ra} - \beta M_o)}{[\alpha(f_{max})_{ra} - \beta f'_{min}]}$$

(9.3(b))

Similarly, Inequalities 9.2(b) and (e) may be combined to give an expression for Z_b:

$$Z_b \geqslant \frac{(\alpha M_{ra} - \beta M_o)}{(\beta f'_{max} - \alpha f_{min})}$$

(9.3(c))

Note that the two expressions for the minimum values of Z_t and Z_b depend only on the *difference* between the maximum and minimum bending moments and allowable stresses, and not on their absolute values. These minima, however, take no account of practical values of prestress force and eccentricity. In practice, values for Z_t and Z_b larger than those given by Inequality 9.3(a), (b) and (c) are usually chosen.
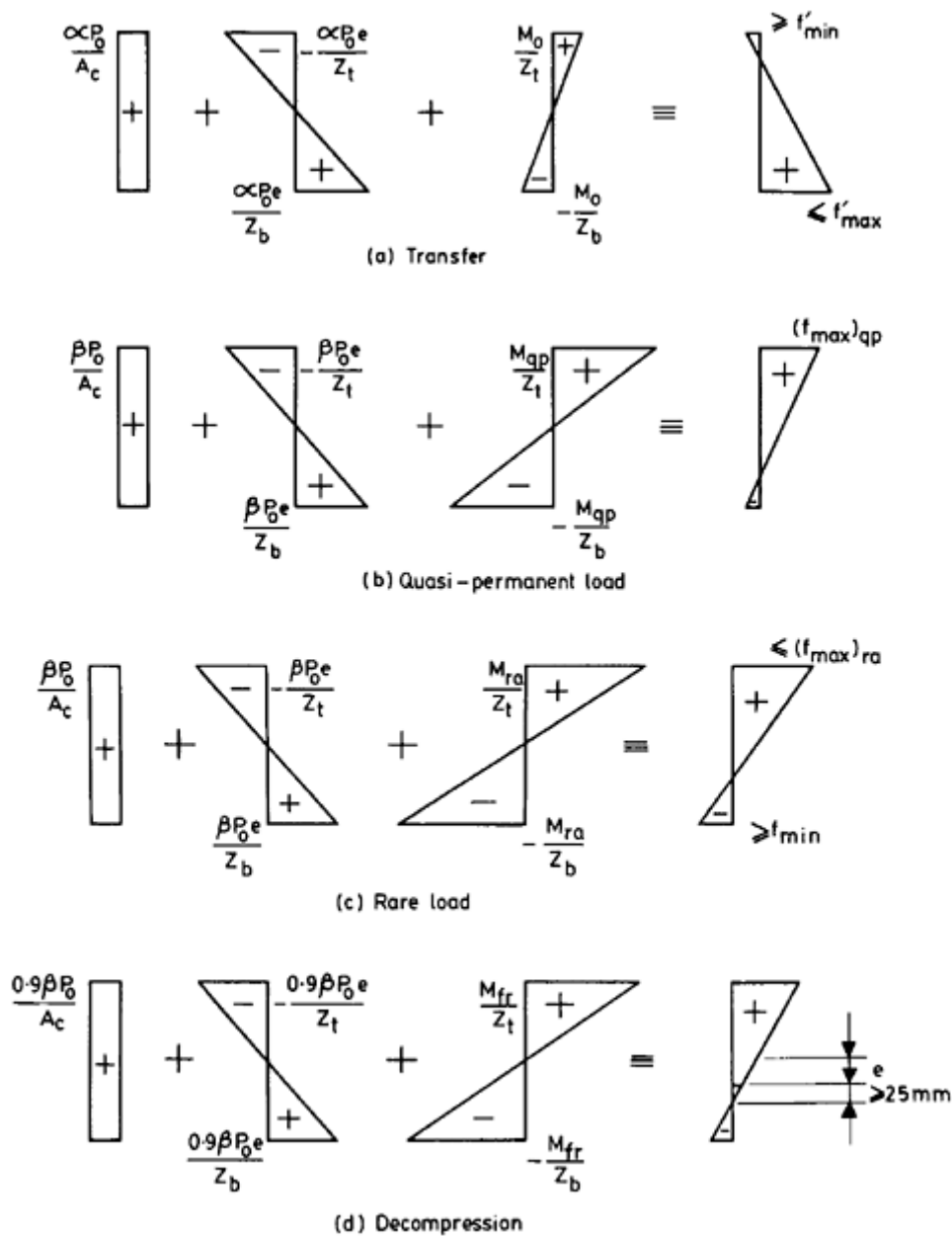
Figure 9.2 Design inequalities at (a) transfer (b) under quasi-permanent load (c) under rare load and (d) for decompression.

Example 9.1 ■■

A rectangular beam is simply supported over a span of 20 m. It carries an imposed load of 6 kN/m, of which 3.6 kN/m may be considered as quasi-permanent load and 4.2 kN/m as frequent load. The allowable

stresses are as given below. If the total short-term and long-term losses are 10% and 25%, respectively, and the concrete is grade C40/50 with grade C30/37 at transfer, determine the minimum concrete section required.

f'_{max}=18 N/mm^2 f'_{min}=−2.9 N/mm2
$(f_{max})_{qp}$=18 N/mm^2 $(f_{max})_{ra}$=24 N/mm2
f_{min}=−3.5 N/mm^2.

Making an allowance of 8 kN/m for the beam self weight,

w_{qp}=11.6 kN/m w_{fr}=12.2 kN/m
w_{ra}=14 kN/m.

At midspan,

M_o=400 kNm M_{qp}=580 kNm
M_{fr}=610 kNm M_{ra}=700 kNm.

Thus, from Inequalities 9.3(a), (b) and (c)

$$Z_t \geqslant \frac{(0.9 \times 580 - 0.75 \times 400) \times 10^6}{[0.9 \times 18 - 0.75 \times (-2.9)]} = 12.08 \times 10^6 \text{ mm}^3$$

$$Z_t \geqslant \frac{(0.9 \times 700 - 0.75 \times 400) \times 10^6}{[0.9 \times 24 - 0.75 \times (-2.9)]} = 13.88 \times 10^6 \text{ mm}^3$$

$$Z_b \geqslant \frac{(0.9 \times 700 - 0.75 \times 400) \times 10^6}{[0.75 \times 18 - 0.9 \times (-3.5)]} = 19.82 \times 10^6 \text{ mm}^3.$$

For an 850 mm deep by 400 mm wide section, $Z_{t=Zb}$=48.17× 10^6 mm^3.
■■

9.3 DESIGN OF PRESTRESS FORCE

The next stage in the design process is to find the prestress force, based on a maximum eccentricity determined from the section properties.
   Rearranging Inequalities 9.2(a)–(e) will yield inequalities for the required prestress force, for a given eccentricity:

$$P_o \geqslant \frac{(Z_t f'_{min} - M_o)}{\alpha(Z_t/A_c - e)}$$

(9.4(a))

$$P_o \leqslant \frac{(Z_b f'_{max} + M_o)}{\alpha(Z_b/A_c + e)}$$

(9.4(b))

$$P_o \leqslant \frac{[Z_t(f_{max})_{qp} - M_{qp}]}{\beta(Z_t/A_c - e)}$$

(9.4(c))

$$P_o \leqslant \frac{[Z_t(f_{max})_{ra} - M_{ra}]}{\beta(Z_t/A_c - e)}$$

(9.4(d))

$$P_o \geqslant \frac{(Z_b f_{min} + M_{ra})}{\beta(Z_b/A_c + e)}$$

(9.4(e))

There are thus three upper and two lower bounds to the value of the prestress force. Generally the minimum value within these bounds is required since the cost of the prestressing steel is a significant proportion of the total cost of prestressed concrete structures. As before, the full set of inequalities has been shown for completeness. However, Inequality (9.4c) is often more critical than Inequality (9.4d).

Example 9.2 ■■
For the beam in Example 9.1, if the maximum eccentricity of the tendons at midspan is 75 mm above the soffit, find the minimum value of prestress force required. Check that the stresses in the beam satisfy the various serviceability requirements.

$A_c = 3.40 \times 10^5$ mm^2 $e = 850/2 - 75 = 350$ mm
$I_c = 2.05 \times 10^{10}$ mm^4
$w_o = 8.2$ kN/m $M_o = 410$ kNm
$w_{qp} = 11.8$ kN/m $M_{qp} = 590$ kNm
$w_{fr} = 12.4$ kN/m $M_{fr} = 620$ kNm
$w_{ra} = 14.2$ kN/m $M_{ra} = 710$ kNm.

Inequalities 9.4(a)–(e) give the following values for P_o:

$P_o \leq 2931.8$ kN
$P_o \leq 2886.0$ kN
$P_o \geq -1773.3$ kN
$P_o \geq -2855.0$ kN
$P_o \geq 1468.2$ kN.

The range of values for P_o which lies within these limits is thus 1468.2 to 2886.0 kN. Note that for this example the denominator in Inequalities 9.4(a), (c) and (d) is negative. Multiplying both sides of an inequality by a negative number has the effect of reversing the sense of the inequality.
If seven 18 mm dia. drawn strands are used, with $f_{pk} = 1700$ N/mm2, the initial prestress force is given by

$P_o = 7 \times 0.7 \times 223 \times 1700 \times 10^{-3} = 1857.6$ kN.

If the allowable range of prestress force given by Inequalities 9.4(a)–(e) is small then it may be difficult to provide a practical arrangement of tendons which falls within this range. Unlike reinforced concrete, where the over-provision of reinforcement only adds to the strength of a member, with prestressed concrete too high a prestress force can lead to allowable stresses being exceeded at transfer.

The stresses at the various loading conditions are:

Transfer:

$$\sigma_t = \frac{0.9 \times 1857.6 \times 10^3}{3.40 \times 10^5} - \frac{0.9 \times 1857.6 \times 10^3 \times 350}{48.17 \times 10^6} + \frac{410 \times 10^6}{48.17 \times 10^6}$$

$$= 4.92 - 12.15 + 8.51$$
$$= 1.28 \text{ N/mm}^2 \quad (> f'_{min})$$

$$\sigma_b = 4.92 + 12.15 - 8.51$$
$$= 8.56 \text{ N/mm}^2 \quad (< f'_{max}).$$

Quasi-permanent load:

$\sigma_t=(0.75/0.9)\times4.92-(0.75/0.9)\times12.15+590\times10^6/(48.17\times10^6)$
$=4.10-10.13+12.25$
$=6.22\text{N/mm}^2 \ (<(f_{max})_{qp})$
$\sigma_b=4.10+10.13-12.25$
$=1.98\text{N/mm}^2 \ (>f_{min}).$

Rare load:

$\sigma_t=4.10-10.13+710\times10^6/(48.17\times10^6)$
$=-6.03+14.74$
$=8.71\text{N/mm}^2 \ (<(f_{max})_{ra})$
$\sigma_b=4.10+10.13-14.74$
$=-0.51\text{N/mm}^2 \ (>f_{min}).$

The stresses at the compression and tension faces of the beam are thus within the prescribed limits and the section is uncracked, as assumed. If it is found that either of the allowable tensile stresses are exceeded then a cracked-section analysis, as described in Section 5.4, must be carried out in order to determine the compressive stresses.

It is now necessary to check whether the tendons lie at least 25 mm within the compression zone. This is carried out by determining whether or not the concrete stress at 25 mm below the tendons is compressive under the frequent load combination. The value of the partial factor of safety for prestress force is taken as 0.9 in this instance, since this has an adverse effect on the minimum stress in the lower section of the beam.

$$\sigma_{b25} = 0.9 \times 4.10 + \frac{0.9 \times 0.75 \times 1857.6 \times 10^3 \times 350 \times 375}{2.05 \times 10^{10}}$$

$$-\frac{620 \times 10^6 \times 375}{2.05 \times 10^{10}} = 0.38 \text{ N/mm}^2,$$

which is a compressive stress, as required. It is also necessary to check that the section is uncracked at the soffit under the rare load combination, as assumed:

$$\sigma_b = 0.9 \times 4.10 + \frac{0.9 \times 0.75 \times 1857.6 \times 10^3 \times 350}{48.17 \times 10^6} - \frac{710 \times 10^6}{48.17 \times 10^6}$$

$$= -1.94 \text{ N/mm}^2 \quad (> f_{min}).$$

The tendons thus lie within the compression zone by at least the specified amount and the durability requirement is satisfied. If this were found not to be the case then the values of the prestress force and eccentricity would have to be adjusted accordingly.

■■

9.4 MAGNEL DIAGRAM

The five inequalities for the prestress force in Example 9.1 yielded a range of possible values for P_o. However, for a given value of e there may not be such a range, since the innermost of the bounds could overlap. In this case another value of e must be chosen and the limits for P_o found again, the process being repeated until a satisfactory combination of P_o and e is found. Clearly, a more direct way of arriving at such a combination would be very useful.

To this end Inequalities 9.4(a)–(e) may be written in the following form:

$$\frac{1}{P_o} \leqslant \frac{\alpha(Z_t/A_c - e)}{(Z_t f'_{min} - M_o)}$$

(9.5(a))

$$\frac{1}{P_o} \geqslant \frac{\alpha(Z_b/A_c + e)}{(Z_b f'_{max} + M_o)}$$

(9.5(b))

$$\frac{1}{P_o} \geqslant \frac{\beta(Z_t/A_c - e)}{[Z_t(f_{max})_{qp} - M_{qp}]}$$

(9.5(c))

$$\frac{1}{P_o} \geqslant \frac{\beta(Z_t/A_c - e)}{[Z_t(f_{max})_{ra} - M_{ra}]}$$

(9.5(d))

$$\frac{1}{P_o} \leqslant \frac{\beta(Z_b/A_c + e)}{(Z_b f_{min} + M_{ra})}.$$

(9.5(e))

As with the earlier inequalities, care must be taken with Inequalities 9.5(a), (c) and (d). They are only valid if the denominators are positive. If any of the denominators are negative then the original Inequality 9.2(a), (c) or (d) has been multiplied by a negative number and the sense of the inequality must be reversed.

The relationships between $1/P_o$ and e are linear and, if plotted graphically, they provide a very useful means of determining appropriate values of P_o and e. These diagrams were first introduced by the Belgian engineer, Magnel, after whom they are named.

Example 9.3 ■■

Construct a Magnel diagram for the beam in Equation 9.1 and find the minimum prestress force for a tendon eccentricity of 350 mm. What would be the effect of increasing the eccentricity to 400 mm?

Inequalities 9.5(a)–(e) may be written as

$10^8/P_o \geq 0.1637\ e - 23.196$
$10^8/P_o \geq 0.0705\ e + 9.985$
$10^8/P_o \geq 38.352 - 0.2707\ e$
$10^8/P_o \geq 23.82 - 0.1681\ e$
$10^8/P_o \leq 0.1385\ e + 19.626.$

Note that the inequality sign in Inequality 9.5(a) has been reversed since the denominator is negative. If the above inequalities are plotted with axes as $1/P_o$ and e then each is a linear relationship defining a feasible region, shown in . This also shows, for each inequality, which stress limit is used. Thus for Inequality 9.5(a) the limiting stress is at the top fibre at transfer.

For any given eccentricity it is easy to see which pair of Inequalities 9.5(a)–(e) will give the limits to P_o. For $e=350$ mm, the range of allowable values for P_o is given by Equations 9.5(b) and (e):

$P_o \geq 1468.2$ kN
$P_o \leq 2886.0$ kN.

If the value of e is increased to 400 mm, the range of values for P_o is given by Inequalities Equations 9.5(a) and (e):

$P_o \geq 1332.9$ kN
$P_o \leq 2365.0$ kN.

The eccentricity could be increased further, resulting in a range for P_o with smaller absolute values, but eventually the tendon position would reach the soffit of the beam.
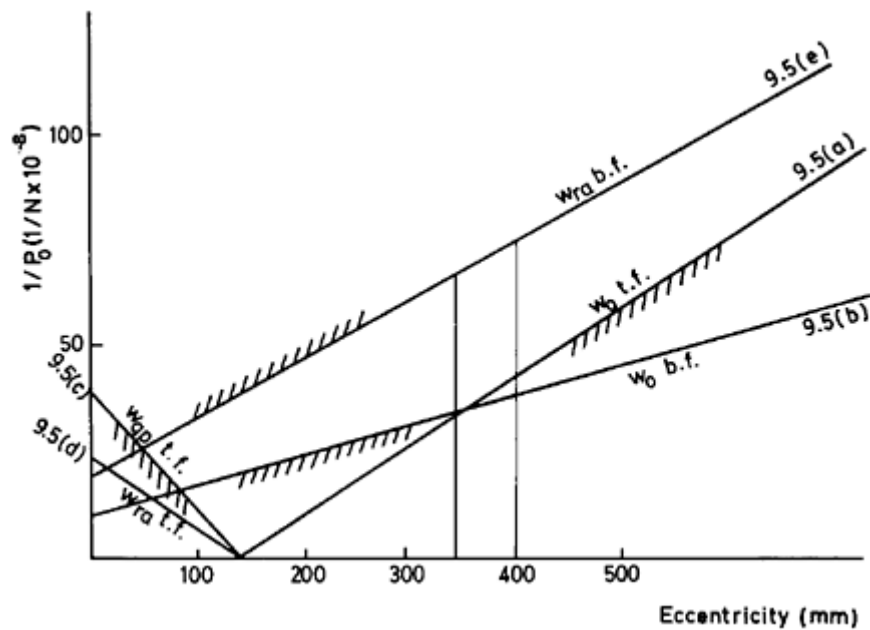
Figure 9.3 Magnel diagram.

These variations of P_o with e show a general trend, namely that increasing e reduces P_o and *vice versa*. For minimum prestress force, maximum eccentricity should be provided at the point of maximum applied bending moment. This will also ensure maximum ultimate strength.

■■

The Magnel diagram is a very useful tool for understanding the relationship between prestress force and eccentricity. Although many of the routine calculations involved in prestressed concrete design are nowadays carried out using computer programs, it is essential for a designer to understand the way in which the variables in the design process affect each other.

9.5 CABLE ZONE

Once the prestress force has been chosen, based on the most critical section, it is possible to find the limits of the eccentricity, *e,* at sections elsewhere along the member. Thus an allowable cable zone is produced, within which the profile may take any shape. Here, the term 'cable' is used to denote the resultant of all the individual tendons. As long as the cable lies within the zone the stresses at the different loading stages will

not exceed the allowable values, even though some of the tendons might physically lie outside the cable zone. It should always be remembered, however, that the limit state of decompression, if adopted, may be an additional limitation on the distribution of the tendons.

Inequalities 9.5(a)–(e) can be rearranged to give

(9.6(a))

$$e \leqslant \frac{Z_t}{A_c} + \frac{1}{\alpha P_o} (M_o - Z_t f'_{min})$$

(9.6(b))

$$e \leqslant \frac{1}{\alpha P_o} (M_o + Z_b f'_{max}) - \frac{Z_b}{A_c}$$

(9.6(c))

$$e \geqslant \frac{Z_t}{A_c} + \frac{1}{\beta P_o} [M_{qp} - Z_t (f_{max})_{qp}]$$

(9.6(d))

$$e \geqslant \frac{Z_t}{A_c} + \frac{1}{\beta P_o} [M_{ra} - Z_t (f_{max})_{ra}]$$

(9.6(e))

$$e \geqslant \frac{1}{\beta P_o} (M_{ra} + Z_b f_{min}) - \frac{Z_b}{A_c}.$$

Example 9.4 ■■

For the beam in Example 9.3, with prestress force of 1857.6 kN, determine the cable zone for the full length of the beam, and also a suitable cable profile.

The limits for the cable zone are given by Inequalities 9.6(a)–(e).

$e \leq 225.2 + 5.981 \times 10^{-7} M_o$
$e \leq 376.9 + 5.981 \times 10^{-7} M_o$
$e \geq 7.178 \times 10^{-7} M_{qp} - 480.7$
$e \geq 7.178 \times 10^{-7} M_{ra} - 688.1$
$e \geq 7.178 \times 10^{-7} M_{ra} - 262.7.$

The values of M_o, M_{qp}, M_{ra} and allowable values of e along the length of the beam are shown in Table 9.1; only one half of the beam is shown since the values are symmetrical about the centre line. In this example, Inequalities 9.6(a) and (e) will give the limits to the cable zone, which are shown in Fig. 9.4. This is often the case where the prestress force chosen is in the lower part of the feasible range, since Inequalities 9.6(a) and (e) relate to the minimum stresses under all load conditions.

The cable zone thus defined does not take into account the

Table 9.1 Limits to eccentricity for beam in Example 9.1

Position	M_o (kNm)	M_{qp} (kNm)	M_{ra} (kNm)	Equation 9.6(a)	9.6(b)	9.6(c)	9.6(d)	9.6(e)
0	0	0	0	≤225	≤377	≥−481	≥−688	≥−263
2.5	179.4	258.1	310.6	≤333	≤484	≥−295	≥−465	≥−40
5	307.5	442.5	532.5	≤409	≤561	≥−163	≥−306	≥120
7.5	384.4	553.1	665.6	≤455	≤607	≥−84	≥−210	≥215
10	410	590	710	≤471	≤622	≥−57	≥−179	≥247
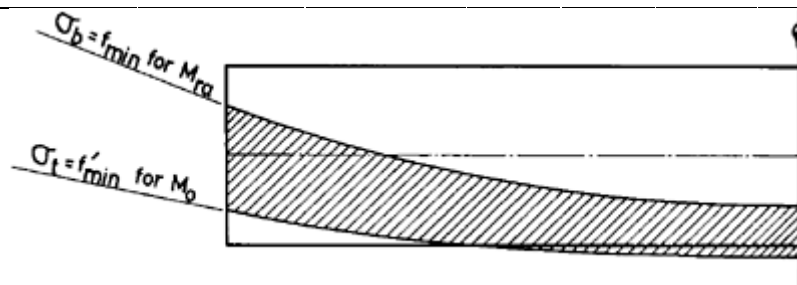
Figure 9.4 Cable zone.

decompression requirement, and if the cable profile were placed as low as possible in the section it would be possible that some of the tendons would be less than 25 mm within the compression zone. It is preferable, therefore, to allow some tolerance in the cable profile.

If the chosen shape of the cable profile is parabolic, then, if the eccentricity at midspan is 350 mm and at the support zero, the shape of the profile is defined by

$$y = 4 \times 0.350\, x\, (20-x)/20^2,$$

where y is a coordinate measured from the centroid of the section. The coordinates of the curve along the beam can be found from the above equation and these are used to fix the tendon ducts in position during construction (Fig. 9.5).

■■

One important factor in choosing a cable profile for a post-tensioned member is the detail of the end-blocks. Manufacturers of the various prestressing systems usually specify the clearances required for their
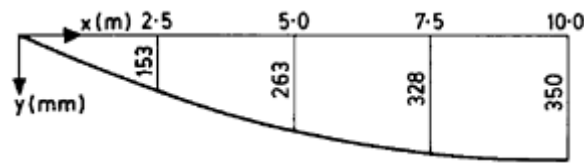
Figure 9.5 Cable profile.

anchorages, and these will influence the eccentricity of the tendons at the ends of the member. The design of end-blocks is described in Chapter 8.

In the above example the magnitude of the prestressing force was assumed to be constant; in real post-tensioned members the prestress force varies and the limits of the cable zone must be determined accordingly.

Once the prestress force and profile have been determined it should be checked that the assumed values for the prestress loss factors, α and β, are sufficiently accurate. If they are not, then the prestress force and profile must be adjusted accordingly.

9.6 MINIMUM PRESTRESS FORCE

As noted earlier, a significant proportion of the total cost of prestressed concrete members is in the prestressing steel. In any design, therefore, the aim should be to reduce the amount of prestressing steel to a minimum. Assuming that the steel is stressed to its limit this is equivalent to keeping the prestress force to a minimum.

It is useful to examine the prestress force required for a given section with a particular eccentricity but with varying transfer and total design load bending moments. For the beam in Example 9.1, Inequalities 9.4(a)–(e) can be rearranged as

$P_o \leq 745.1 + 5.334\, M_o$
$P_o \leq 1959.4 + 2.26\, M_o$
$P_o \geq -5549.4 + 6.4\, M_{qp}$
$P_o \geq -7399.3 + 6.4\, M_{ra}$
$P_o \geq -457.2 + 2.712\, M_{ra},$

where the forces and bending moments are in kN and kNm, respectively. These inequalities are shown graphically in Fig. 9.6, where it can be seen that the two limits for the prestress force are 1468.2 kN and 2886.0 kN, as determined previously. Figure 9.6 also shows that the minimum prestress force is governed by Inequality 9.4(e) up to the value of

3287.4 kN. After this point the prestress force is governed by Inequality 9.4(c) but, more importantly, the rate of increase in bending moment with prestress force is much reduced. The prestress force of 3287.4 kN may thus be regarded as an economic maximum force to provide. If a larger force is required for the given section, then it would be more economical to increase the section size.

It can also be seen from Fig. 9.6 that, for a given range of bending moment, there is a corresponding range of prestress force. If, in Example 9.1, M_o remains at 410 kNm but M_{ra} is increased to 1500 kNm then the limits to the prestress force are

$P_o \leq 2886.0$ kN
$P_o \geq 4050.6$ kN.

Clearly there is no feasible range for P_o and the depth of the section must be increased.

The ratio of M_{ra} to M_o (assuming that Inequality 9.4(e) is the critical one for minimum stress) will also affect the minimum prestress force. For a given section, if this ratio is low, as is usually the case with long-span beams, the prestress force may be placed at a greater eccentricity, and hence may be smaller in value, than in the same section where the ratio of M_{ra} to M_o is high, where minimum stresses at transfer usually govern.

For members which have a high ratio of M_{ra} to M_o, one solution is to apply the prestress force in stages. This is carried out either by initially
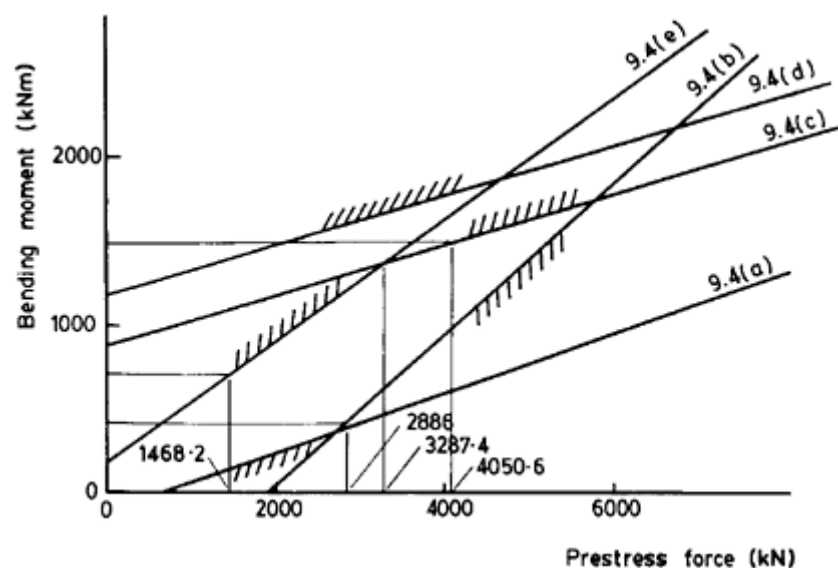
Figure 9.6 Limits to prestress force.

tensioning some, but not all, of the tendons to their full force, or by tensioning them all to a much lower initial force. In the latter case the anchorage system must allow the tendons to be tensioned again to their full force at a later stage. Another alternative is to have the initial prestress force provided by pretensioned tendons, and the remaining prestress force provided by post-tensioned tendons, tensioned at a later stage.

An example of where stage prestressing would be advantageous is in a building where a large clear span is required at ground floor level, and the columns from several upper floors are supported by a prestressed concrete beam at first floor level. If the beam were prestressed initially for the total design load then only a small eccentricity at midspan could be tolerated to cater for the minimum stress at transfer, leading to a large total prestress force. By tensioning the beam in stages, as each upper floor is added, the eccentricity at midspan could be increased, resulting in a smaller total prestress force.

9.7 ULTIMATE STRENGTH DESIGN

Once the details of the prestress force and cable profile have been determined the ultimate limit state must be satisfied. If the ultimate strength based on the tendons alone is insufficient then it will usually only be necessary to provide some extra untensioned reinforcement. The details of the analysis procedure in this case are given in Chapter 5.

The ultimate strength of a member at transfer is also important but, in practice, this will usually be satisfactory if the serviceability limit state at transfer is satisfied.

Example 9.5 ■■

For the beam in Example 9.1 determine the ultimate moment of resistance of the section at midspan, with e=350 mm. Assume that the tendon ducts have been grouted after tensioning of the tendons.

It is assumed initially that the prestressing steel has yielded. Thus, for equilibrium:

$0.57{\times}40{\times}400{\times}0.8\,x{=}0.78{\times}1700{\times}1561$

$\therefore x{=}284$ mm

$\therefore \varepsilon_{pe}{=}0.0035\,(775{-}284)/284$

$=0.00605$

$\varepsilon_{pb}{=}(0.75{\times}0.7{\times}1700)/(200{\times}10^3)$

$=0.00446$

$\therefore \varepsilon_p{=}0.00446{+}0.00605$

$=0.0105.$

For the prestressing steel,

$$\varepsilon_{yk} = \frac{0.78 \times 1700}{200 \times 10^3} = 0.00663.$$

Thus the steel has yielded as assumed.

M_r=0.78×1700×1561×(775−0.4×284)×10^{-6}
=1369.0 kNm
w_{ult}=1.35×8.2+1.5×6
=20.1 kN/m
M_{ult}=20.1×20^2/8
=1005.0 kNm,

and thus extra untensioned reinforcement is not required. If it is found that extra such reinforcement is required then the amount must be determined using the trial-and-error procedure outlined in section 5.10.
 ■■

9.8 CRACKED MEMBERS

While the critical limit state for many members is generally that of serviceability, for cracked members the most critical is often the ultimate limit state. Indeed one way of viewing cracked members is as reinforced concrete members with sufficient prestress force applied in order to restrict the cracking under frequent load.

An approach to the design of cracked members, therefore, is to find the total area of steel required to give the desired ultimate moment of resistance and then to proportion this area between the prestressing steel and untensioned reinforcement. There are several criteria for determining the proportions for each type of steel.

One method is to consider the member as having zero stress at the tensile face at the point of maximum bending moment under the quasi-permanent or frequent load. Alternatively, instead of considering the state of stress within a member at the critical sections, emphasis can be placed on the deflection of the member, since this can be controlled by prestressing. If draped tendons are used then the load balancing technique is very convenient in determining the prestress force required to give zero deflection under a given load. For members with straight tendons this method cannot be used and, in general, the deflections cannot be made to be zero everywhere along the member. However, by ensuring zero deflection at the critical section a reasonably level member will result.

In both approaches, depending on the class of exposure, the limit state of crack width must also be satisfied.

Example 9.6 ■■

The T-beam shown in Fig. 9.7 spans 15 m and supports an imposed load of 10 kN/m, 4 kN/m of which may be considered as quasi-permanent and 8 kN/m as frequent. Assume that the concrete is grade C40/50, f_{pk}=1770 N/mm^2, f_{yk}=460 N/mm2 and that the long-term losses are 20%. Determine the amounts of prestressing steel and untensioned reinforcement required based on the following criteria:

(a) zero tension at midspan under the quasi-permanent load;
(b) zero deflection under the quasi-permanent load.

In each case determine whether the limit state of cracking is satisfied, assuming exposure class 2.

The first step in each case is to determine the total area of steel required to achieve adequate ultimate strength.

w_o=7.2 kN/m
w_{ult}=1.35×7.2+1.5×10
=24.7 kN/m
M_{ult}=24.7×15^2/8
=694.7 kNm.

Initially, it may be assumed that only the prestressing steel contributes to the ultimate moment of resistance. If the neutral axis lies within the flange, two equations of equilibrium can be written:

0.57×40×700×0.8 x=0.78×1770×A_p
0.57×40×700×0.8 x (525−0.4 x)=694.7×10^6

Solving these two equations yields x=113 mm and A_p=1049 mm^2.
The steel strain must now be checked:

$$\varepsilon_{pb} = \frac{0.8 \times 0.7 \times 1770}{200 \times 10^3} + \frac{(525-113)}{113} \times 0.0035$$

$$= 0.0177.$$
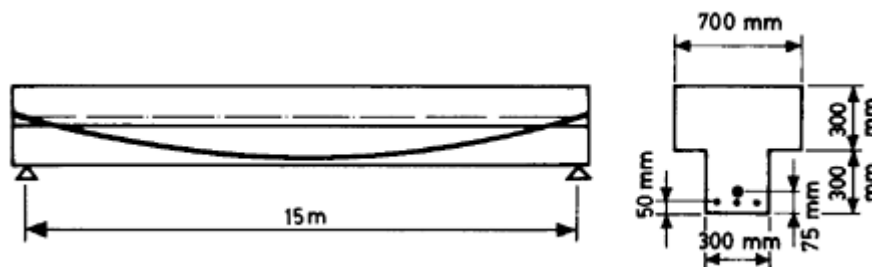
Figure 9.7

Since this is greater than ε_{yk} for the grade of steel used the steel has yielded, as assumed.

(a) For zero tension at the beam soffit at midspan under the quasi-permanent load,

w_{qp}=7.2+4
=11.2 kN/m
M_{qp}=11.2×15²/8
=315 kNm.

Section properties:

Z_b=22×10⁶ mm³
A_c=3×10⁵ mm²
e=285 mm.

The required prestress force is then given by

$$\frac{0.8\ P_o \times 10^3}{3 \times 10^5} + \frac{0.8\ P_o \times 10^3 \times 285}{22 \times 10^6} - \frac{315 \times 10^6}{22 \times 10^6} = 0$$

$$\therefore P_o = 1098.8 \text{ kN,}$$

and

$$A_p = \frac{1098.8 \times 10^3}{0.7 \times 1770} = 887 \text{ mm}^2.$$

Since this area of steel is less than the amount of prestressing steel required for the ultimate limit state, additional untensioned reinforcement is required. Again, two equilibrium equations can be formed, assuming that the neutral axis lies within the flange:

0.57×40×700×0.8 x=0.78×1770×887+0.87+460 A_s
0.78×1770×887 (525−0.4 x)+0.87×460×A_s (550−0.4 x)
=694.7×10⁶.

Solving these two equations yields x=113 mm and A_s=529 mm2. Checks on the steel strains show that both types of steel have yielded, as assumed.

(b) For zero deflection under the quasi-permanent load the required prestressing force may be found most conveniently using the load balancing technique.
If the tendon has zero eccentricity at the supports then the total drape is 285 mm. Thus:

0.8 P_o=(11.2×15²)/(8×0.285)
$\therefore P_o$=1381.6 kN,

and

$$A_\mathrm{p} = \frac{1381.6 \times 10^3}{0.7 \times 1770} = 1115 \text{ mm}^2.$$

In this case no extra reinforcement is required.

However, it now remains to determine whether the limit state of cracking is satisfied. For (a), a cracked section analysis under the frequent load combination shows that the bending stress in the reinforcement is 69 N/mm^2. From Tables 5.1 and 5.2, *either* the maximum bar size is 32 mm *or* the maximum bar spacing is 300 mm. Thus three T20 bars with spacing of 95 mm would be sufficient to satisfy both the serviceability and ultimate limit states.

For (b) it can be shown that, for P_o=1381.6 kN, the section is cracked under the rare load combination and that the reinforcement as for (a) is adequate.

Whichever method is used the design should be completed by checking the concrete compressive stresses at transfer and under the quasi-permanent and rare load combinations against the allowable stresses given in Section 3.7.

■■

The alternative designs in Example 9.6 illustrate the fact that, with cracked members, the designer has great freedom to choose the prestress force to suit any desired criterion, but careful attention must always be paid to the serviceability limit state.

It is interesting to note that if the beam in Example 9.6 had been designed as a member uncracked in tension under the rare load combination then the area of prestressing steel required, based on the bottom fibre concrete stress, would be 1144 mm^2 and no additional untensioned reinforcement would be required.

For a given structure, the choice of which type of member to use depends on the function of the structure and the nature of the loading. Where it is important to have a crack-free structure, such as in a liquid-retaining tank, or where the environment is particularly aggressive, members which are crack-free and remain in compression should be used. Cracked members are particularly suitable where the rare load is high in relation to the frequent load, since any cracks which open up under the higher load would close up again once the load is reduced. Cracked members are also particularly useful for structures subjected to impact loading. They deflect more, and therefore absorb more energy, than uncracked members. They also exhibit better elastic recovery after impact than reinforced concrete members.

A common concern has been that cracked members are less durable than uncracked ones. However, many such structures have been in service for more than 25 years and have performed satisfactorily.

9.9 CHOICE OF SECTION

In the previous examples the simplest shape of cross-section, namely rectangular, was used, chosen primarily to illustrate the basic principles of design. Where there is freedom to choose a more economical section the designer must decide which shape of section to use for a particular situation.

The solid rectangular section is one of the least economical sections, since the mid-depth regions are not usually highly stressed and the material is not used to its full extent. One way of overcoming this deficiency is to provide voids in the central region of the section; these provide a similar structural efficiency with less weight. A typical hollow-core slab is shown in Fig. 9.8(a). As with steel sections, an I-section is a very efficient shape, Fig. 9.8(b), providing maximum area of concrete at the furthest distance from the neutral axis. An alternative section, one with similar efficiency for bending but with far greater torsional stiffness, is the box-section, shown in Fig. 9.8(c).

The T-section shown in Fig. 9.8(b) is suitable for long-span beams, generally in bridges. For buildings, the T-section shown in Fig. 9.9(a) is
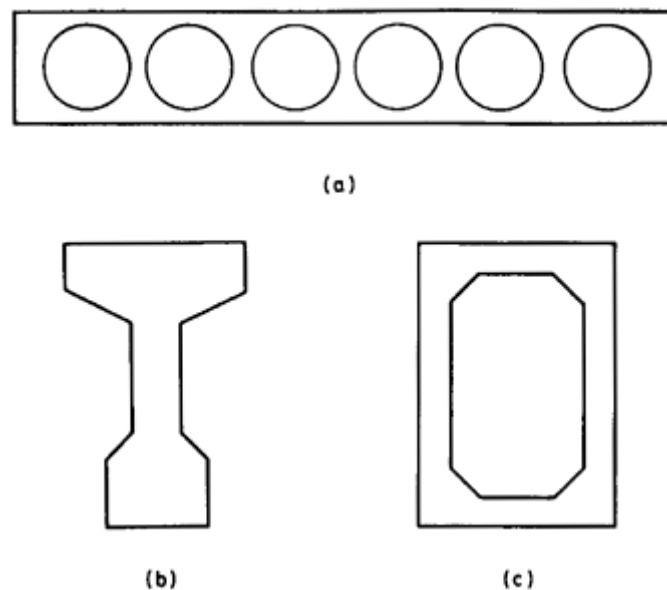
Figure 9.8 Sections: (a) hollow-core slab; (b) I-section; (c) box-section.
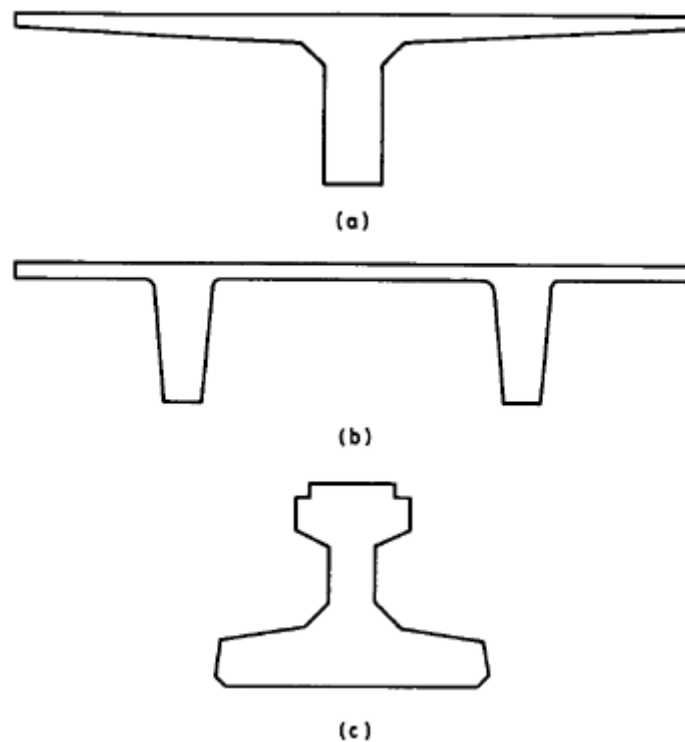
Figure 9.9 T-sections: (a) single; (b) double; (c) inverted.

often used. This has a large compression flange for the total design load but it is necessary to ensure that the compressive stresses in the rib at transfer are not excessive. If the rib is slender the possibility of buckling at transfer must also be considered. Single T-sections are not very stable during construction and a common solution is to use double T-sections, shown in Fig. 9.9(b). Both types of T-section are commonly used with a composite structural topping; the design of such members is dealt with in Chapter 10.

Another shape often used in composite construction is the inverted T-section, or 'top-hat' section shown in Fig. 9.9(c). The large flange at the soffit of the beam can accommodate a large bending moment due to the beam self weight and the weight of the *in situ* slab. Under total design load the compression flange is provided by the *in situ* slab, which acts compositely with the inverted T-section.

9.10 FLOW CHARTS FOR DESIGN

The methods of design for uncracked and cracked concrete members outlined in the preceding sections may be combined with the design elements considered in the previous chapters to give an overall view of

the design process. This is most conveniently summarized in the form of flow charts, and Figs 9.10 and 9.11 show these for uncracked and cracked members, respectively.

Many steps in the design process are common to both types of member and the main difference is the determination of the amount of prestressing steel. For uncracked members emphasis is usually placed on the stresses at the serviceability limit state, with checks for ultimate strength made afterwards. For cracked members the ultimate strength capacity is generally ensured first, and conditions at the serviceability limit state checked later.

The steps in Figs 9.10 and 9.11 are intended only as a guide, and with experience many of them may be combined or bypassed completely.

9.11 DETAILING

There are some practical details concerning the layout of tendons which may affect the design, and it is important to be aware of these when deciding on the number and shape of tendons to be provided.

Unless a prestressed concrete member remains in compression under the rare load combination a certain minimum percentage of steel is required to ensure that, when the concrete cracks, the additional force transferred to the steel does not cause immediate yield or rupture. The minimum amount of reinforcement stated in EC2 is given by

$$A_s \geq k_c k f_{ct} A_{ct}/f_{yk},$$

where A_s is the area of bonded reinforcement, both untensioned and bonded prestressed, in the tensile zone (unbonded tendons should be ignored); k_c is a coefficient which takes account of the form of the stress distribution within the section prior to cracking and varies between 0 and 0.4 (a method of determining which value of k_c to use is given in Beeby and Narayanan (1995)); k is a coefficient which allows for non-linear self-equilibrating stresses within the member (a value of 0.8 should normally be used, except in the case of externally applied deformations, such as foundation settlement, where the stress distribution remains linear and a value of 1.0 should be used); f_{ct} is the tensile strength of the concrete at the time when the cracks are first expected to form (the value of f_{ct} should not be less than 3 N/mm^2); A_{ct} is the area of concrete in tension just prior to the formation of the first crack; and f_{yk} is the tensile strength of the reinforcement (or prestressing steel).

A minimum number of tendons is required in members which are statically determinate and where no load redistribution can take place. The minimum numbers of different types of tendon are shown in Table 9.2, but it is also sufficient to provide one tendon comprising a seven-wire strand, with wires of diameter not less than 4 mm.
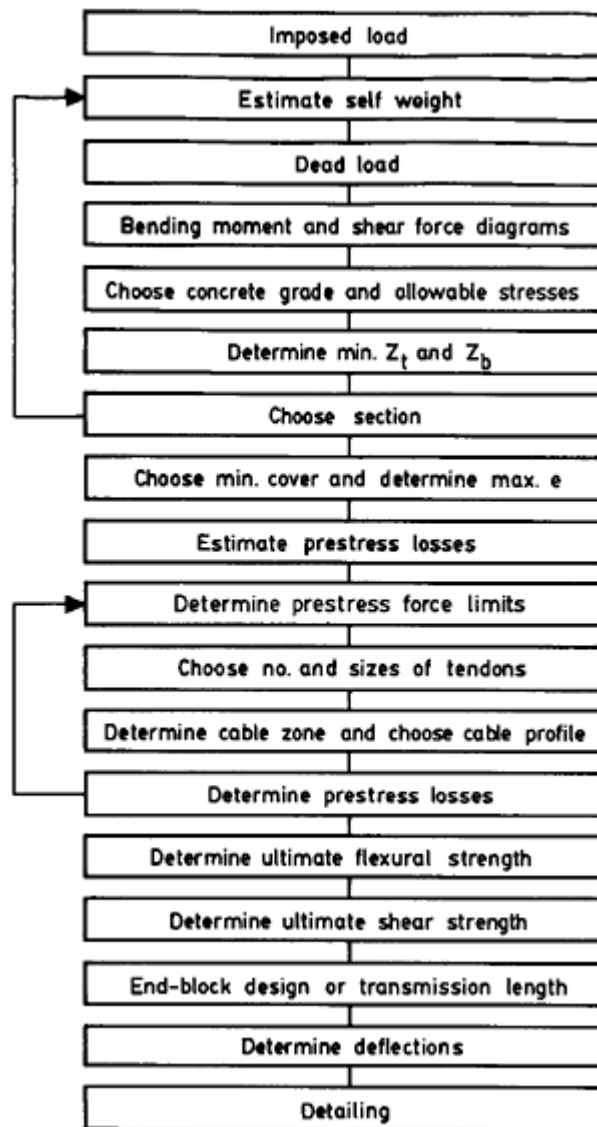
Figure 9.10 Flow chart for uncracked members.

Table 9.2 Minimum numbers of different types of prestressing steel

Individual bars or wires	Bars and wires forming a strand or tendon	Tendons (but see text)
3	7	3

Imposed load

Estimate self weight

Dead load

Bending moment and shear force diagrams

Choose concrete grade and allowable stresses

Choose section

Estimate prestress losses

Check ultimate flexural strength

Choose SLS criterion

Choose no. and sizes of tendons

Choose cable profile

Determine prestress losses

Determine additional untensioned steel

Check stresses and cracking at SLS

Determine ultimate shear strength

End-block design or transmission length

Determine deflections

Detailing

Figure 9.11 Flow chart for cracked members.

A factor which affects the choice of numbers and sizes of individual tendons is the clear space that must be provided between tendons in order to ensure proper placement and compaction of the surrounding concrete. These minimum distances are shown in Table 9.3, where d_g is the nominal aggregate size and φ is the diameter of the tendon or duct.

If a curved post-tensioned duct is placed near the surface of a concrete member, bursting of the concrete may occur in a direction perpendicular to the plane of curvature of the duct. In order to prevent this, a

Table 9.3 Minimum clear distances between prestressing tendons and ducts

Pretensioned		Post-tensioned	
Vertically	*Horizontally*	*Vertically*	*Horizontally*
$\geq d_g; \geq \varphi;$ ≥ 10 mm	$\geq d_g + 5$ mm; $\geq \varphi; \geq 20$ mm	$\geq \varphi; \geq 50$ mm	$\geq \varphi; \geq 40$ mm

minimum cover to the duct should be specified. No such cover is given in EC2, but the values recommended in the former BS8110 are given in <u>Table 9.4</u>. In order to prevent the crushing of the concrete between curved post-tensioning ducts which are in the same plane of curvature, the clear spacing between the ducts should be not less than the values given in <u>Table 9.5</u>.

The minimum cover to ducts and tendons is usually determined from durability and fire resistance considerations, and is described in <u>Chapter 3</u>. Manufacturers of prestressing systems usually also specify the minimum cover to be used with their products.

Most prestressed concrete members will contain untensioned reinforcement fabricated into a cage. This serves several purposes:

(a) to facilitate the placing of the post-tensioning ducts;
(b) to enhance the ultimate flexural and shear strength of the member;
(c) to resist any tensile stresses which may be set up by restraint of shrinkage of the member by the formwork before transfer; and
(d) to enable the member to withstand any sudden load applied to it (the reinforcement should preferably be mild steel).

The detailing of the untensioned reinforcement is covered in the relevant sections of EC2. An example of a reinforcement cage in a post-tensioned beam is shown in <u>Fig. 9.12</u>.

PROBLEMS

9.1 A post-tensioned I-section beam of overall depth 1220 mm spans 15 m and has the following section properties:

$w_o = 8.7$ kN/m $A_c = 3.694 \times 10^5$ mm^2
$Z_t = 80.75 \times 10^6$ mm^3 $Z_b = 119.32 \times 10^6$ mm^3
$e_{max} = 400$ mm $y_b = 490$ mm.

Short- and long-term loss factors are 10% and 25%, respectively. The dead load is 15 kN/m and the imposed load of 60 kN/m is applied in two

Table 9.4 Minimum cover (mm) to curved ducts

Radius of curvature of duct (m)	Duct internal diameter (mm)															
	19	30	40	50	60	70	80	90	100	110	120	130	140	150	160	170
	Tendon force (0.8 f_pk A_p)(kN)															
	296	387	960	1337	1920	2640	3360	4320	5183	6019	7200	8640	9424	10338	11248	13200
2	50	55	155	220	320	445								Radii not normally used		
4		50	70	100	145	205	265	350	420							
6			50	65	90	125	165	220	265	310	375	460				
8				55	75	95	115	150	185	220	270	330	360	395		
10				50	65	85	100	120	140	165	205	250	275	300	330	
12					60	75	90	110	125	145	165	200	215	240	260	315
14					55	70	85	100	115	130	150	170	185	200	215	260
16					55	65	80	95	110	125	140	160	175	190	205	225
18					50	65	75	90	105	115	135	150	165	180	190	215
20						60	70	85	100	110	125	145	155	170	180	205
22						55	70	80	95	105	120	140	150	160	175	195
24						55	65	80	90	100	115	130	145	155	165	185
26						50	65	75	85	100	110	125	135	150	160	180
28							60	75	85	95	105	120	130	145	155	170
30							60	70	80	90	105	120	130	140	150	165
32							55	70	80	90	100	115	125	135	145	160
34							55	65	75	85	100	110	120	130	140	155
36							55	65	75	85	95	100	115	125	140	150
38							50	60	70	80	90	105	115	125	135	150
40	50	50	50	50	50	50	50	60	70	80	90	100	110	120	130	145

Table 9.5 Minimum distance (mm) between ducts in plane of curvature

Duct internal diameter (mm)

Tendon force $(0.8\,f_{pk}\,A_p)$ (kN)

Radius of curvature of duct (m)	19	30	40	50	60	70	80	90	100	110	120	130	140	150	160	170
(Tendon force, kN)	296	387	960	1337	1920	2640	3360	4320	5183	6019	7200	8640	9424	10336	11248	13200
2	110	140	350	485	700	960		Radii not normally used								
4	55	70	175	245	350	480	610	785	940							
6	38	60	120	165	235	320	410	525	630	730	870	1045				
8			90	125	175	240	305	395	470	545	655	785	855	940		
10			80	100	140	195	245	315	375	440	525	630	685	750	815	
12						160	205	265	315	365	435	525	570	625	680	800
14						140	175	225	270	315	375	450	490	535	585	785
16							160	195	235	275	330	395	430	470	510	600
18								180	210	245	290	350	380	420	455	535
20									200	220	265	315	345	375	410	480
22											240	285	310	340	370	435
24												265	285	315	340	400
26												260	280	300	320	370
28																345
30																340
32																
34																
36																
38																
40	38	60	80	100	120	140	160	180	200	220	240	260	280	300	320	340
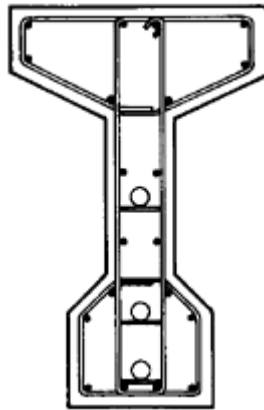
Figure 9.12 Reinforcement cage in a post-tensioned beam.

equal increments. Initially, only a limited number of the tendons required for the second loading stage are tensioned, the remainder being tensioned after the first stage imposed load has been applied. If each tendon has a value of P_o of 600 kN, determine the total number of tendons required, based on the stresses at midspan, and how many of them can be tensioned during the first stage. Assume grade C40/50 concrete with grade C30/37 achieved at transfer.

9.2 For the beam in Problem 9.1, determine the economical maximum total imposed load which can be applied in two stages, and the corresponding number of tendons to be used.

REFERENCE

Beeby, A.W. and Narayanan, R.S. (1995) *Designer's Handbook to Eurocode 2, Part 1.1: Design of Concrete Structures,* Thomas Telford, London.

10

Composite construction

10.1 INTRODUCTION

Many applications of prestressed concrete involve the combination of precast prestressed concrete beams and *in situ* reinforced concrete slabs. Some examples of such composite construction are shown in Fig. 10.1. An *in situ* infill between precast beams is shown in Fig. 10.1(a) while an *in situ* topping is shown in Fig. 10.1(b). The former type of construction is often used in bridges, while the latter is common in building construction. The beams are designed to act alone under their own weight plus the weight of the wet concrete of the slab. Once the concrete in the slab has hardened and provided that there is adequate horizontal shear connection between them, the slab and beam behave as a composite section under design load. The beams act as permanent formwork for the slab, which provides the compression flange of the composite section. The section size of the beam can thus be kept to a minimum, since a compression flange is only required at the soffit at transfer. This leads to the use of inverted T-, or 'top-hat', sections.

10.2 SERVICEABILITY LIMIT STATE

The stress distributions in the various regions of the composite member are shown in Fig. 10.2(a)–(d). The stress distribution in Fig. 10.2(a) is due to the self weight of the beam, with the maximum compressive stress at the lower extreme fibre. Once the slab is in place, the stress distribution in the beam is modified to that shown in Fig. 10.2(b), where the bending moment at the section, M_d is that due to the combined self weight of the beam and slab.

Once the concrete in the slab has hardened and the imposed load acts on the composite section, the additional stress distribution is shown in Fig. 10.2(c). This is determined by ordinary bending theory, but using the composite section properties. The final stress distribution is shown
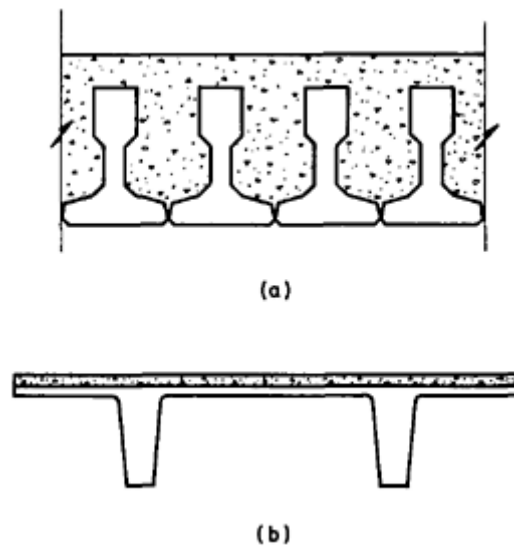
Figure 10.1 Examples of composite construction: (a) *in situ* infill; (b) *in situ* topping.
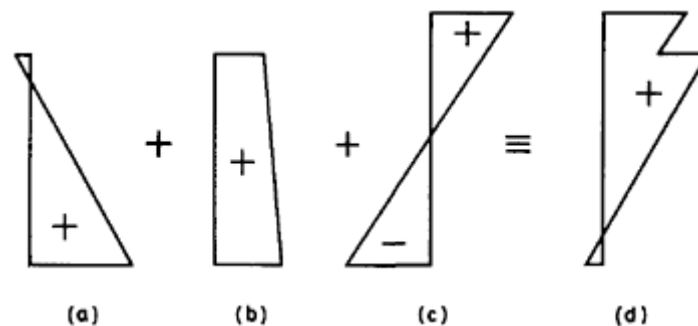
Figure 10.2 Stress distribution within a composite section.

in Fig. 10.2(d) and is a superposition of those shown in Fig. 10.2(b) and Fig. 10.2(c). The important feature to note is that there is a discontinuity in the final stress distribution under design load at the junction between the beam and slab. The beam has an initial stress distribution before it behaves as part of the composite section, whereas the slab only has stresses induced in it due to the composite action.

Example 10.1 ■■
   The floor slab shown in Fig. 10.3 comprises precast pretensioned beams and an *in situ* concrete slab. If the span of the beams is 5 m and the imposed load is 5 kN/m^2 (including finishes), determine the stress
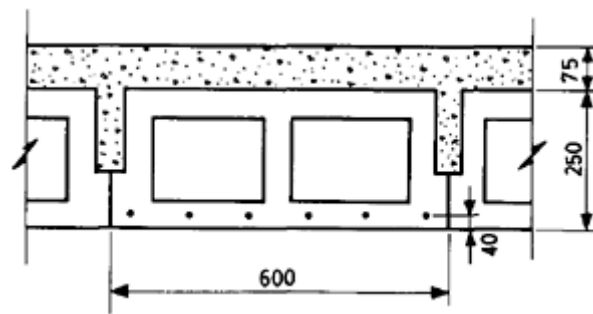
Figure 10.3

distributions at the various load stages. Assume all long-term losses have occurred before the beams are erected and that the net force in each wire is 19.4 kN.

Section properties of the beams:

$A_c = 1.13 \times 10^5$ mm^2
$I_c = 7.5 \times 10^8$ mm^4
$Z_t = Z_b = 6 \times 10^6$ mm^3.

Eccentricity of the wires = 125−40 = 85 mm.

(i) Self weight of the beams = 0.113×24
= 2.7 kN/m.
$M_o = (2.7 \times 5^2)/8$
= 8.4 kNm.

Total prestress force after all losses have occurred is given by

$\beta P_o = 6 \times 19.4$
= 116.4 kN.

The stress distribution in the beams is thus given by

$$\sigma_t = \frac{116.4 \times 10^3}{1.13 \times 10^5} - \frac{116.4 \times 85 \times 10^3}{6 \times 10^6} + \frac{8.4 \times 10^6}{6 \times 10^6}$$

$$= 1.03 - 1.65 + 1.40$$
$$= 0.78 \text{ N/mm}^2$$

$$\sigma_b = 1.03 + 1.65 - 1.40$$
$$= 1.28 \text{ N/mm}^2.$$

(ii) The weight of the slab is supported by the beams acting alone, so that

$M_d = 8.4 + 0.075 \times 0.6 \times 24 \times 5^2/8$
= 11.8 kNm.

The stress distribution within the beams is now given by

$$\sigma_t = 1.03 - 1.65 + \frac{11.8 \times 10^6}{6 \times 10^6}$$

$$= -0.62 + 1.97$$
$$= 1.35 \text{ N/mm}^2$$

$$\sigma_b = 1.03 + 1.65 - 1.97$$
$$= 0.71 \text{ N/mm}^2.$$

(iii) The imposed load of 5 kN/m^2 is supported by the composite section and the section properties of this are now required. To find the neutral axis of the composite section, taking moments about the soffit of the beams gives

$(1.13 \times 10^5 + 75 \times 600)y = (1.13 \times 10^5 \times 125 + 75 \times 600 \times 288)$
$\therefore y = 171$ mm.
$I_{comp} = 7.5 \times 10^8 + 1.13 \times 10^5 (171-125)^2$
$+(75^3 \times 600)/12 + (75 \times 600)/(288-171)^2$
$= 1.63 \times 10^9$ mm^4.

The imposed load bending moment, $(M_{des} - M_d) = 0.6 \times 5 \times 5^2/8$
$= 9.4$ kNm.

The stress distribution within the composite section under this extra bending moment is given by

$$\sigma_{t,slab} = \frac{9.4 \times 10^6}{1.63 \times 10^9} \times (325 - 171) = 0.89 \text{ N/mm}^2$$

$$\sigma_{t,beam} = \frac{9.4 \times 10^6}{1.63 \times 10^9} \times (250 - 171) = 0.46 \text{ N/mm}^2$$

$$\sigma_{b,beam} = \frac{-9.4 \times 10^6}{1.63 \times 10^9} \times 171 = -0.99 \text{ N/mm}^2.$$

The total stress distributions under the three load cases are shown in .
■■

The maximum compressive stress occurs at the upper fibres of the beams, but is significantly lower than the level of stress had the beam carried the total imposed load alone. This explains the advantage of inverted T-sections in composite construction, where only a small compression flange is required for bending moments M_o and M_d, the
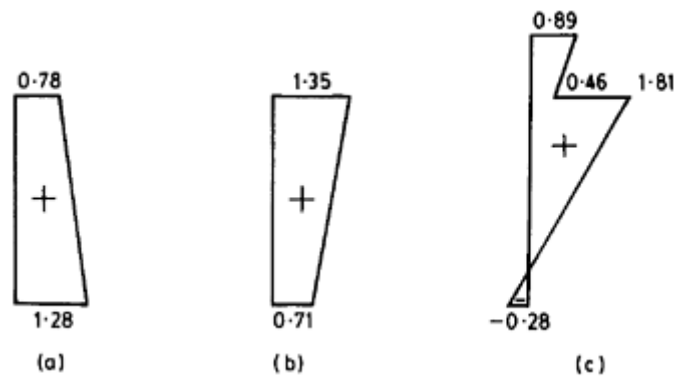
Figure 10.4 Stress distribution for composite section in Example 10.1 (N/mm^2): (a) beam; (b) beam and slab; (c) beam and slab and imposed load.

compression flange for bending moment M_{des} being provided by the slab.

The maximum compressive stress in the slab is much lower than in the beam and, for this reason, in many composite structures a lower grade of concrete is used for the *in situ* portion. The modulus of elasticity for this concrete is lower than that for the beam and this effect can be taken into account in finding the composite section properties by using an approximate modular ratio of 0.8.

The *in situ* slab in Example 10.1 lies above the composite section neutral axis and, therefore, the slab is in compression over its full depth under the total design load. However, for composite sections as shown in Fig. 10.1(a) the *in situ* portion of the section extends well below the neutral axis, so that the lower region is in tension. If the tensile strength of this concrete is exceeded then the composite section properties must be determined on the basis of the *in situ* section having cracked below the neutral axis.

10.3 ULTIMATE STRENGTH

The basic principles for the analysis of prestressed concrete sections at the ultimate limit state of flexural strength described in Chapter 5 are also applicable to composite sections. For the section shown in Fig. 10.5(a), it may be assumed initially that, at the ultimate limit state, the neutral axis lies within the slab and the section may then be treated effectively as a rectangular beam. The position of the neutral axis should later be checked to see whether it does, indeed, fall within the slab.

For the section shown in Fig. 10.5(b), the position of the neutral axis may be determined on the assumption that the section is rectangular,
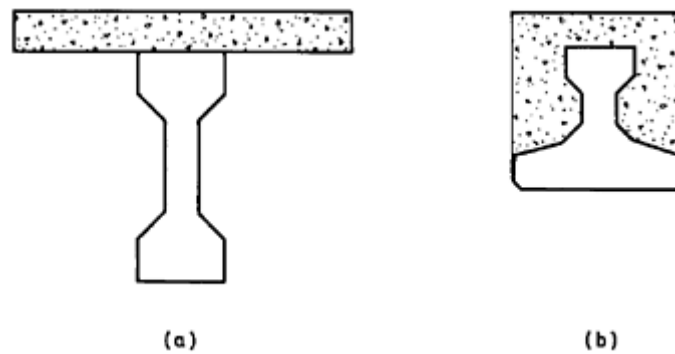
Figure 10.5
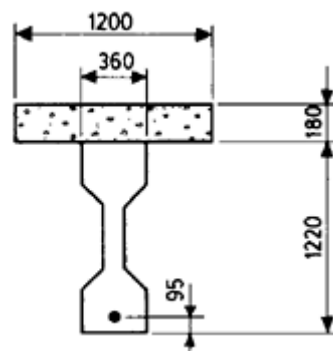
Figure 10.6 Composite section in Example 10.2.

but the different strengths of the concrete in the slab and beam regions of the compression zone should be taken into account.

Example 10.2 ■■
Determine the ultimate moment of resistance of the composite section shown in Fig. 10.6, if the concrete grades in the slab and beam are C25/ 30 and C50/60, respectively, f_{pk}=1820 N/mm², and A_p=2640 mm². Long-term losses are 25%.
The strain and stress distributions are shown in Fig. 10.7.
Initially it is assumed that the tendons have yielded and that the concrete stress block is a distance y below the top fibre of the beam.
For equilibrium:

0.78×1820×2640=0.57 (25×180×1200+50×360 y)
∴ y=65 mm.
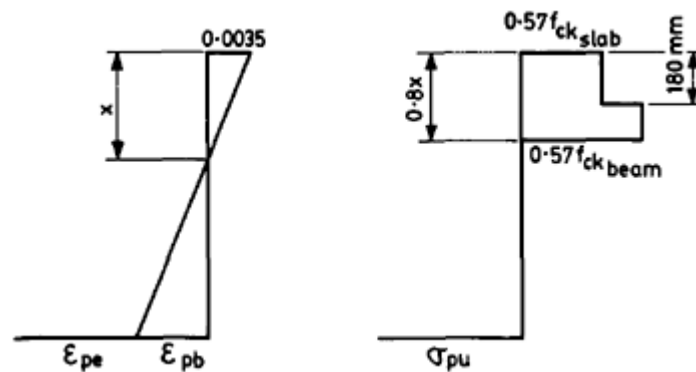
Figure 10.7 Ultimate strain and stress distributions for beam in Example 10.2.

The depth of the neutral axis is thus given by

$$0.8\,x = (180+65)$$
$$\therefore x = 306 \text{ mm.}$$

It must now be checked whether the steel has, indeed, yielded:

$$\varepsilon_{pe} = \frac{0.7 \times 0.75 \times 1820}{200 \times 10^3} = 0.00478.$$

Thus:

$$\varepsilon_p = 0.00478 + \frac{(1305 - 306)}{306} \times 0.0035$$

$$= 0.0162 \quad (\geqslant \varepsilon_{pk} = 0.0017).$$

The ultimate moment of resistance is then given by

$$M_u = [0.57\,(25 \times 1200 \times 180 \times 155 + 50 \times 360 \times 65^2/2)$$
$$+ 0.78 \times 1820 \times 2640\,(1305 - 245)] \times 10^{-6}$$
$$= 4471.4 \text{ kNm.}$$

If necessary, the effect of additional untensioned reinforcement can be taken into account, as described in Chapter 5. The ultimate strength of the precast beam supporting its own weight plus that of the slab should also be checked.

■■

10.4 HORIZONTAL SHEAR

The composite behaviour of the precast beam and *in situ* slab is only effective if the horizontal shear stresses at the interface between the two

regions can be resisted. For shallow members, such as that shown in Fig. 10.3, there is usually no mechanical key between the two types of concrete, and reliance is made on the friction developed between the contact surfaces. For deeper sections, mechanical shear connectors in the form of links projecting from the beam are used, which provide a much better shear connection.

The determination of the horizontal shear resistance is based on the ultimate limit state, and if this condition is satisfied it may be assumed that satisfactory horizontal shear resistance is provided at the serviceability limit state.

A simply supported composite section carrying a uniformly distributed load is shown in Fig. 10.8(a) and the free-body diagram for half the length of the *in situ* slab is shown in Fig. 10.8(b). At the simply supported end there must be zero force in the slab, while the maximum force occurs at the midspan. The distribution of shear forces on the underside of the slab is also shown in Fig. 10.8(b), being zero at midspan and reaching a maximum at the support. This behaviour is similar to that in an elastic beam, where the vertical and horizontal shear stresses increase towards the support for a uniformly distributed load.

The following expression is given in Part 1–3 of EC2 for the horizontal shear stress, τ_{sdj}:

$$\tau_{sdj}=\beta V_{sd}/(z\,b_j),$$

where β is the ratio of the longitudinal force in the slab to the total longitudinal force, given by M_{sd}/z, both calculated for a given section; V_{sd} is the transverse ultimate shear force; z is the lever arm; and b_j is the width of the interface.

The design shear resistance for horizontal joints with vertical shear reinforcement is given by

$$\tau_{Rdj}=k_T\tau_{Rd}+\mu\sigma_N+0.87\,f_{yk}\varrho\mu\leq0.33\,\nu f_{ck},$$

where k_T is a coefficient from Table 10.1, with $k_T=0$ if the joint is subjected to tension; τ_{Rd} is the basic design shear strength from Table

Figure 10.8 Horizontal shear: (a) composite section; (b) free-body diagram for *in situ* slab.

Table 10.1 Values for coefficients k_T and μ

Type of surface	k_T	μ
Rough	1.8	0.7
Smooth	1.4	0.6
Very smooth	0	0.5

7.1, based on the strength of the beam or slab, whichever is the lower; μ is the coefficient of shear friction from Table 10.1; σ_N is the stress per unit area arising from external normal forces across the joint, with a maximum value of 0.4 f_{ck}; v is an efficiency factor, defined in Section 7.2; and ϱ is the ratio of the shear reinforcement to the area of the joint, A_{sv}/A_j.

Thus the amount of vertical shear reinforcement required is given by

$$0.87 f_{yk}\varrho\mu = \tau_{sdj} - (k_T\tau_{Rd} + \mu\sigma_N).$$

Example 10.3 ∎∎

The composite section shown in Example 10.2 supports a uniformly distributed ultimate load of 60 kN/m over a span of 24 m. Determine the horizontal shear reinforcement required.

Maximum ultimate shear force and bending moments are given by

$V_{sd}=60\times24/2=720$ kN
$M_{sd}=60\times24^2/8=4320$ kNm.

From Example 10.2

$d=1400-95=1305$ mm
$z=1305-0.4\times306=1183$ mm
$M_{sd}/z=4320/1.183=3651.7$ kN.

The total force in the slab

$=0.57\times25\times1200\times180\times10^{-3}$
$=3078$ kN
$\therefore \beta=3078/3651.7=0.84$

and

$$\tau_{sdj} = \frac{0.84 \times 720.0 \times 10^3}{360 \times 1183} = 1.42 \text{ N/mm}^2.$$

From Table 10.1, for a rough surface, $k_T=1.8$ and $\mu=0.7$. From Table

7.1, τ_{Rd}=0.3 N/mm². The value of σ_N may conservatively be taken as zero.
Thus, for no shear reinforcement:

τ_{sdj}=1.8×0.3=0.54 N/mm²

and shear reinforcement is required. The amount is given by

0.87×460×0.7ϱ=(1.42–0.54)

∴ ϱ=0.00314

∴ A_{sv}=0.00314×360×10³=1130 mm²/m.

Thus the maximum shear reinforcement to be provided is T12 links at 200 mm centres, with A_{sv}=1130 mm²/m. This can be reduced away from the supports, in steps according to the shear force diagram.

Alternative arrangements for the anchorage of the links in the slab are shown in Fig. 10.9(a) and (b).

■■

For composite sections of the type shown in Fig. 10.1(a) the horizontal shear stress between the slab and the top of the beam may be determined using the method described above. However, it is not necessary to check the shear stresses down the sides of the beam and along its lower flange, since these will generally be satisfactory if adequate provision has been made for horizontal shear resistance at the top of the beam. Further information on horizontal shear resistance may be found in FIP (1982).

10.5 VERTICAL SHEAR

As with the flexural strength of composite sections, the vertical shear resistance must be checked at two stages: firstly for the beam carrying
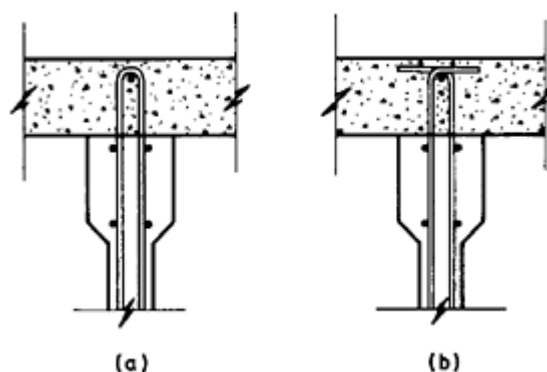
Figure 10.9 Horizontal shear connection alternatives.

the weight of the slab, and secondly for the composite section under the total design load. For the first stage, the shear resistance may be determined using the method described in Chapter 7. The same method may be used for the composite section, allowance being made for the increased effective depth.

10.6 DEFLECTIONS

The deflections of composite prestressed concrete members may be found using the methods described in Chapter 6, depending on whether the member is cracked or uncracked. However, as with the determination of stresses, account must be taken of the different types of section for each loading stage.

Example 10.4 ■■

For the composite section in Example 10.2 determine the maximum deflections at the various load stages. Assume that the tendon has a parabolic profile with eccentricity of 375 mm at midspan and zero at the supports. The self weight of the beam is 8.7 kN/m and the quasi-permanent imposed load is 18 kN/m.

(i) The bending moment distributions under the beam self weight, prestress force and under a central point load are shown in Fig. 10.10(a), (b) and (c), respectively. Using the method of virtual work described in Chapter 6:
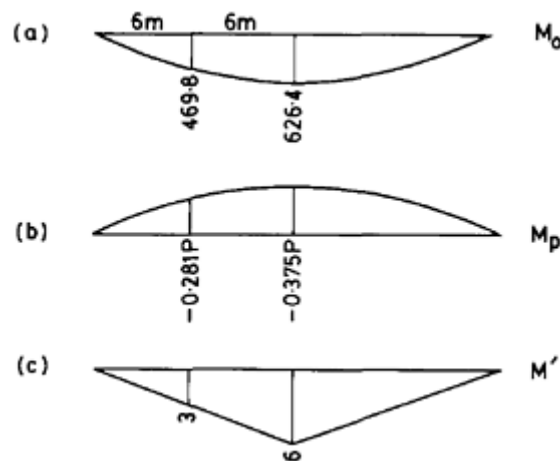
Figure 10.10 Bending moment diagrams for composite section in Example 10.4 (kNm): (a) beam self weight; (b) prestress force; (c) central point load.
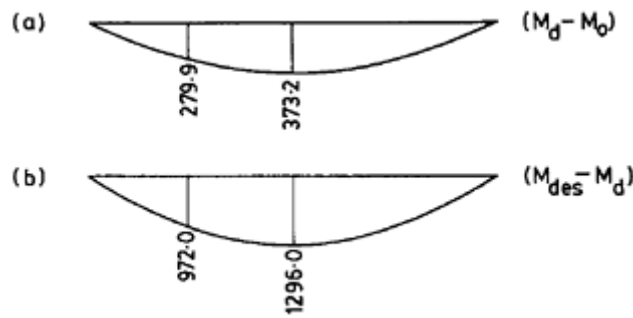
Figure 10.11 Bending moment diagrams for composite section in Example 10.4 (kNm): (a) weight of slab; (b) imposed load.

$$\delta_o = \int_0^L [M'(M_o + M_p)/EI]\mathrm{d}x$$

$$= (2 \times 12/6EI) [4(469.8 - 0.281P)(3) + (626.4 - 0.375P)(6)]$$

With $P=\alpha P_o=3000$ kN, $I_{beam}=0.059$ m^4 and E_{cm} at transfer$=33.5 \times 10^3$ N/mm^2, $\delta_o=-0.0151$ m.

(ii) The bending moment distribution for the weight of the slab is shown in Fig. 10.11(a):

$$\delta_d - \delta_o = \int_0^L [M'(M_d - M_o)/EI]\mathrm{d}x$$

$$= (2 \times 12/6EI) [4(279.9)(3) + (373.2)(6)]$$
$$= 0.0113 \text{ m.}$$
$$\therefore \delta_d = 0.0113 - 0.0152 = -0.0039 \text{ m.}$$

(iii) The bending moment distribution for the imposed load is shown in Fig. 10.11(b):

$$\delta_{qp} - \delta_d = \int_0^L [M'(M_{qp} - M_d)/EI]\mathrm{d}x$$

$$= (2 \times 12/6EI) [4(972)(3) + (1296)(6)].$$

For the composite section, $I_{comp}=0.151$ m^4 and the value of E_{cm} at the age of loading is 37×10^3 N/mm^2.

$$\therefore \delta_{qp} - \delta_d = 0.0139 \text{ m.}$$

Also, the prestress force has been reduced to $\beta P_o=2500$ kN and the above value of E_{cm} should now be used for the deflections under both self weight and weight of the slab. Thus,

$\delta_{qp}=0.0139-0.0086+0.0113\times33.5/37$
$=0.0155$ m, or 15.5 mm.

A load-deflection curve for the composite section is shown in Fig. 10.12. This clearly shows the stiffening effect produced by the composite action of the slab and beam. Long-term deflections can be determined using an effective value of E_{cm}, as described in Chapter 6.

■■

10.7 DIFFERENTIAL MOVEMENTS

The fact that the slab of a composite member is usually cast at a much later stage than the beam means that most of the time-dependent effects of shrinkage of the slab take place with the section acting compositely. Most of the shrinkage of the beam will already have occurred by the time the slab is in place, and the movement due to the shrinkage of the slab will induce stresses throughout the whole of the composite section. The water content of the slab concrete is often higher than that of the beam, since a lower strength is required, and this aggravates the problem of differential shrinkage. These extra stresses, which occur even under zero applied load, are not insignificant and should be considered in design.

Both the slab and beam undergo creep deformations under load and, although some of the creep deformations in the beam may have taken place before casting of the slab, the level of compressive stress is higher in the beam, and so the creep deformations are larger. The differential creep deformations between the slab and beam set up stresses in the
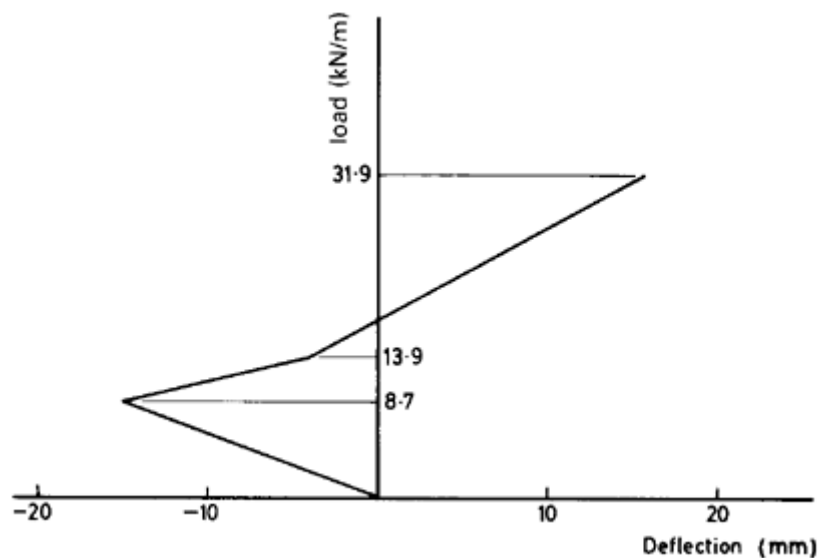
Figure 10.12 Load-deflection curve for composite section in Example 10.4.
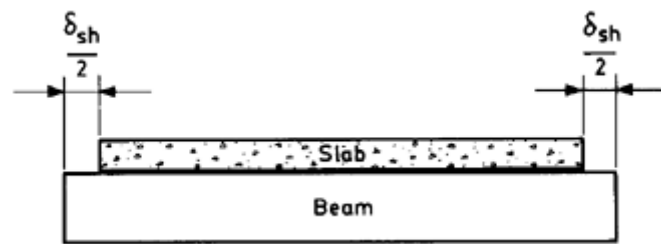
Figure 10.13 Differential movements.

composite section which tend to reduce those set up by differential shrinkage.

A problem which is encountered, particularly in connection with bridge decks, is that of varying temperature across a composite section, although this may still be a problem in composite members used as roof structures. The hotter upper surface tends to expand more than the cooler lower surface and stresses are induced throughout the composite section.

A method for determining the stresses due to differential shrinkage will now be outlined, and this can be adapted to find the stresses due to differential creep and temperature movements.

Consider a composite member as shown in Fig. 10.13, where the slab is shown to have a free shrinkage movement of δ_{sh} relative to the beam. In reality this movement is restrained by the shear forces which are set up between the slab and beam, putting the slab into tension and the beam into compression. The magnitude of the tensile force in the slab is given by

$$T = \varepsilon_{sh} A_{c,slab} E_{c,slab},$$

where $A_{c,slab}$ and $E_{c,slab}$ are the cross-sectional area and modulus of elasticity of the slab, respectively, and ε_{sh} is the free shrinkage strain of the slab concrete. The compressive force in the beam must be numerically equal to this tensile force.

In addition to the direct stresses described above, bending stresses are also introduced by restraint of the free differential shrinkage. In order to determine these stresses, the free bodies of the slab and beam are considered, as shown in Fig. 10.14. Initially, the slab can be regarded as having a force T applied through its centroid, so that its length is equal to that of the beam. There must be no net external force on the composite member due to differential shrinkage alone, so a pair of equal and opposite compressive forces must be applied to maintain equilibrium. However, these compressive forces act on the composite section and induce a bending moment at the ends of the member of
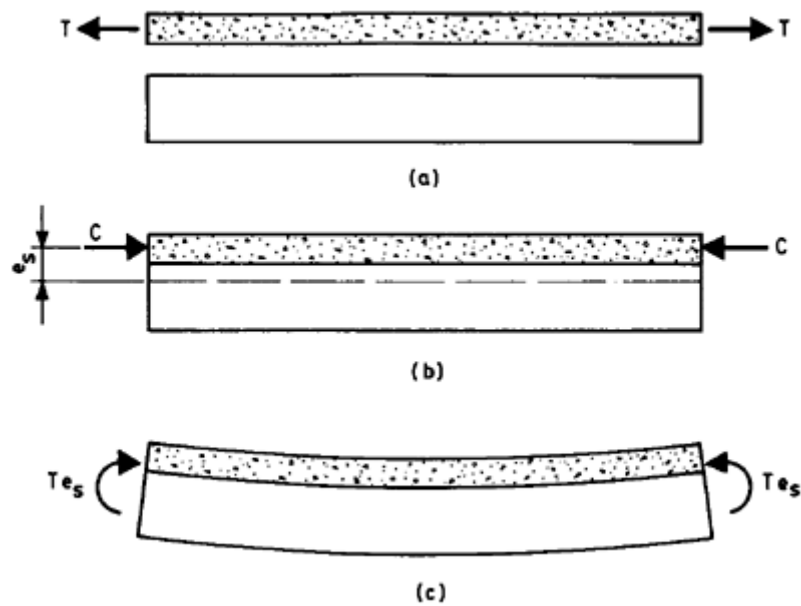
Figure 10.14 Internal stress resultants due to differential movements.
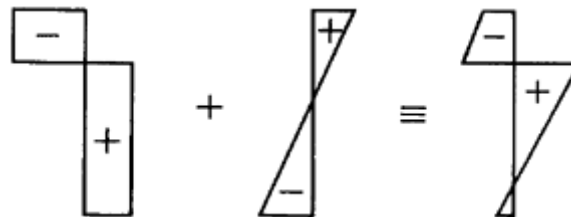
Figure 10.15 Stresses due to differential movements.

magnitude Te_s, where e_s is the distance between the centroids of the slab and composite sections. The total stress distribution across the section is shown in Fig. 10.15.

Example 10.5 ■■

For the composite section in Example 10.2 determine the stress distribution across the section if the slab undergoes a shrinkage strain of 100×10^{-6}. Assume $E_{c,slab} = 30.5 \times 10^3$ N/mm², $I_{comp} = 1.51 \times 10^{11}$ mm⁴ and $A_{c,beam} = 3.69 \times 10^5$ mm².

For the slab:

$A_{c,slab} = 1200 \times 180 = 2.16 \times 10^5$ mm²
$\therefore T = 100 \times 10^{-6} \times 30.5 \times 10^3 \times 2.16 \times 10^5 \times 10^{-3}$
$= 658.8$ kN.

$$\text{Thus the average stress in the slab} = -\frac{658.8 \times 10^3}{2.16 \times 10^5}$$

$$= -3.05 \text{ N/mm}^2.$$

$$\text{Thus the average stress in the beam} = \frac{658.8 \times 10^3}{5.85 \times 10^5}$$

$$= 1.13 \text{ N/mm}^2.$$

The centroid of the composite section can be shown to lie 606 mm from the top of the slab. Thus the eccentricity of the slab centroid about the centroid of the composite section is (606−90)=516 mm, and the moment about this centroid is

=658.8×0.516
=339.9 kNm.

Thus the bending stresses at the top of the slab, at the junction between slab and beam, and at the soffit of the beam are, respectively:

$$\sigma_{t,slab} = \frac{339.9 \times 10^6 \times 606}{1.51 \times 10^{11}}$$

$$= 1.36 \text{ N/mm}^2$$

$$\sigma_{b,slab} = \sigma_{t,beam} = \frac{339.9 \times 10^6 \times 426}{1.51 \times 10^{11}}$$

$$= 0.96 \text{ N/mm}^2;$$

$$\sigma_{b,beam} = -\frac{339.9 \times 10^6 \times 794}{1.51 \times 10^{11}}$$

$$= -1.79 \text{ N/mm}^2.$$

The resulting stress distribution is shown in Fig. 10.16. These stresses must be added to those due to the prestress force and applied load.
■■

The temperature distributions in real concrete structures are non-linear across the section. A full description of the analysis method for this case is given in Hambly (1991).
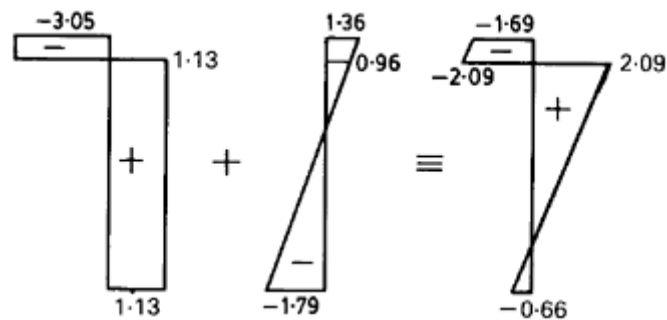
Figure 10.16 Stress distribution for composite section in Example 10.5 (N/mm^2).

10.8 PROPPING AND CONTINUITY

All the composite sections considered so far have comprised beams which are simply supported. This is particularly useful where continued access is required beneath the structure throughout construction, such as where a bridge passes over a busy road or railway. However, if it is possible to provide a temporary intermediate support to the beam during construction, a considerable saving may be made, since the loading condition for the beam carrying the weight of the slab concrete has a large influence on its design.

A beam with a temporary central support is shown in Fig. 10.17. Initially the beam supports its own weight, with distribution of bending moments as shown in Fig. 10.18(a). Once the temporary support is in place and the slab concrete poured, the extra bending moments are as in Fig. 10.18(b). The stresses in the beam in these two cases are found using the beam section alone. When the concrete has hardened sufficiently, the temporary support is removed and the beam stresses are found for the beam self weight and slab load acting on the simply supported composite section. Finally, the stresses induced by the imposed load bending moments, Fig. 10.18(c), acting on the composite section must be added. The final stresses in the beam will be less than if the beam had been unpropped, but the hogging bending moment induced in the beam when it is supporting the weight of the slab must be taken into consideration.

Clearly, the final stresses in the beam could be reduced further by introducing more temporary props at intermediate points in the span. The limiting case of this is to have the beam continuously propped. In this case, many of the advantages of using composite construction would be lost, but a good compromise may well be to have two or three intermediate supports, depending on the access required beneath the structure during construction.

Another extension of the basic form of composite construction is to
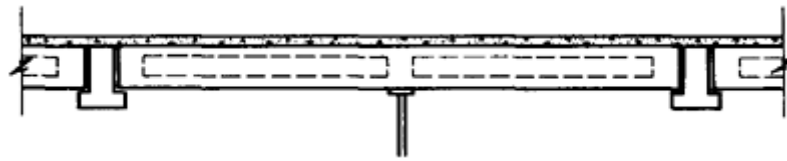
Figure 10.17 Propping.
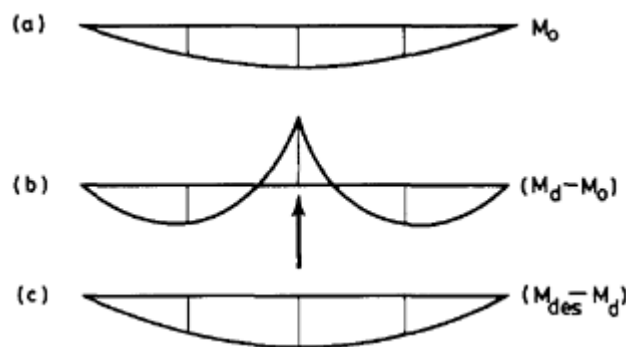
Figure 10.18 Effects of propping.
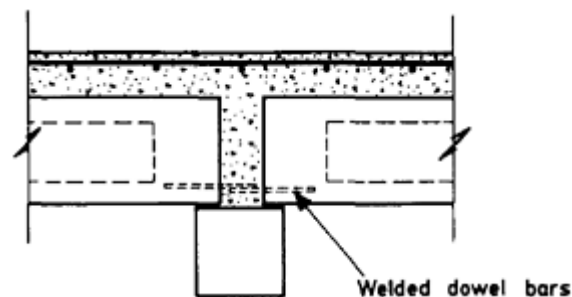
Figure 10.19 Continuity.

join adjacent simply supported spans so that, under imposed load, they behave as a continuous structure. Two such simply supported sections are shown in Fig. 10.19, which support their own weight and that of the slab concrete. The slab extends across the top of the supports and is reinforced so that it can resist the tensile stresses which are set up there once the whole structure behaves continuously under the imposed load. The design of this region of the continuous member should be carried out as for a reinforced concrete member.

The continuous behaviour of the composite structure shown in Fig. 10.19 under imposed load will induce tensile stresses in the top of the prestressed concrete beams adjacent to the supports. These stresses should be limited to those in Table 2.1. In determining the ultimate

strength of continuous members such as those shown in Fig. 10.19, the support sections should be considered as reinforced concrete sections. In the regions just beyond the bearing, the precompression in the concrete may be ignored over the transmission length of the tendons.

Another consideration in the use of continuous composite constructions is the secondary bending moments set up at the supports due to creep and shrinkage in the adjacent spans. Long-term creep effects due to prestressing cause an upward camber in the spans which induces a sagging bending moment at the support. Differential shrinkage and long-term creep effects due to the vertical load on the spans cause a downward deflection in the adjacent spans, inducing a hogging bending moment at the supports. The overall effect is usually a net sagging bending moment, requiring reinforcement at the bottom of the support section, as shown in Fig. 10.19. Further information on the assessment of these secondary bending moments may be found in Clark (1978).

10.9 DESIGN OF COMPOSITE MEMBERS

The same considerations that were applied to the design of a prestressed concrete member in Chapter 9 may be applied when the member acts compositely with an *in situ* slab. However, there are now, in general, eight inequalities, since the stresses due to the dead load of the beam and slab, and the stress in the *in situ* concrete must also be considered. The stress in the last case should be limited to $0.6 f_{ck}$. It is generally found that, of these eight stress conditions, the two most critical for determining the required prestress force and eccentricity are the upper fibre stress at transfer and the lower fibre stress under the total design load.

The minimum composite section size can be based on the stress conditions at the bottom fibre. When the beam is supporting its own weight, an inequality similar to 9.2(b) may be written:

$$\frac{\alpha P_o}{A_{c,beam}} + \frac{\alpha P_o}{Z_{b,beam}} - \frac{M_o}{Z_{b,beam}} \leqslant f'_{max},$$

where $A_{c,beam}$ and $Z_{b,beam}$ are the section properties of the beam. When the total design load is acting, the effect of the bending moment $(M_{ra} - M_d)$ is found by using the composite section properties:

$$\frac{\beta P_o}{A_{c,beam}} + \frac{\beta P_o}{Z_{b,beam}} - \frac{M_d}{Z_{b,beam}} - \frac{(M_{ra} - M_d)}{Z_{b,comp}} \geqslant f_{min},$$

where $Z_{b,comp}$ is the lower fibre section modulus for the composite section. Combining the above inequalities gives

$$Z_{b,comp} \geq \frac{\alpha(M_{ra} - M_d)}{(\beta f'_{max} - \alpha f_{min}) + (1/Z_{b,beam})(\beta M_o - \alpha M_d)}.$$

The range for the prestress force required may be found for a given eccentricity from

$$P_o \geq \frac{(Z_{t,beam} f'_{min} - M_o)}{\alpha[(Z_{t,beam}/A_{c,beam}) - e]}$$

$$P_o \geq Z_{b,beam} \frac{\{f_{min} + (M_{ra}/Z_{b,comp}) + M_d[(1/Z_{b,beam}) - (1/Z_{b,comp})]\}}{\beta[(Z_{b,beam}/A_{c,beam}) + e]}.$$

Note that if the denominator in the first expression is negative, the inequality is reversed. Once the prestress force has been chosen, the limits to the eccentricity may be found from

$$e \leq \frac{Z_{t,beam}}{A_{c,beam}} + \frac{1}{\alpha P_o}(M_o - Z_{t,beam} f'_{min})$$

$$e \geq \frac{1}{\beta P_o}\left[Z_{b,beam} f_{min} + M_d\left(1 - \frac{Z_{b,beam}}{Z_{b,comp}}\right) + \frac{Z_{b,beam}}{Z_{b,comp}}M_{ra}\right] - \frac{Z_{b,beam}}{A_{c,beam}}.$$

Further information on the design of composite structures may be found in Bate and Bennett (1976).

PROBLEMS

10.1 Beams similar to that in Problem 9.1 are placed at 1.2 m centres and, with a 180 mm deep reinforced concrete slab, form a composite bridge deck spanning 24 m. If the weight of finishes is 2 kN/m^2 and the total imposed load is 10 kN/m^2, determine the minimum prestress force required.

10.2 For the bridge deck in Problem 10.1 determine the ultimate moment of resistance if f_{pk}=1860 N/mm^2, A_p=1840 mm^2 and the slab is of grade C25/30 concrete.

10.3 A precast hollow-core floor slab, 1200 mm wide and 150 mm deep, with a 50 mm concrete topping, is to span 6 m. The section properties are: $Z_b=Z_t=4.38\times10^6$ mm^3, $A_c=1.53\times10^5$ mm^2. If the long-term prestress force is 115 kN, and the eccentricity is 40 mm, determine the stresses at the bottom of the precast slab at midspan for the following situations:

 (i) precast slab;
 (ii) precast slab and topping;
(iii) precast slab and topping, with slab propped at midspan;
(iv) propping removed and an imposed load of 3 kN/m^2 applied.

REFERENCES

Bate, S.S.C. and Bennett, E.W. (1976) *Design of Prestressed Concrete,* Wiley, New York.

Clark, L.A. (1978) *Concrete Bridge Design to BS5400,* Construction Press, London.

Fédération Internationale de la Précontrainte (1982) *Shear at the Interface of Precast and In Situ Concrete,* Slough.

Hambly, E.C. (1991) *Bridge Deck Behaviour,* Chapman & Hall, London.

11

Indeterminate structures

11.1 INTRODUCTION

All of the prestressed concrete members so far considered have been statically determinate. This reflects the major use of prestressed concrete in building structures, since the most common type of prestressed concrete construction is in the form of simply supported beams. However, there are important applications of prestressed concrete in statically indeterminate structures. Many of the features of the analysis and design of these structures are similar to those used for statically determinate structures, as outlined in previous chapters. There are two important differences, however: the introduction of secondary moments and the behaviour at the ultimate limit state. These will be discussed in the following sections.

The most important application of prestressed concrete indeterminate structures is in the field of multi-span bridges. This is a specialized area of design and construction and is well beyond the scope of this book, but many excellent reference books on the subject may be found in the Bibliography.

In the field of building structures, continuous prestressed concrete beams are sometimes employed, but a more widespread use is in prestressed concrete flat slabs. The design of these will be discussed in detail in Chapter 12.

11.2 SECONDARY MOMENTS

It was shown in Chapter 1 that for a statically determinate prestressed concrete member the line of pressure in the concrete is coincident with the resultant force due to the prestressing tendons, provided that there is no applied axial load on the member. For statically indeterminate prestressed concrete structures, this is not necessarily the case. The prestress moment in a statically determinate member at any section is

Pe, which is known as the *primary* prestress moment. In statically indeterminate structures, *secondary* or 'parasitic' prestress moments may be introduced into the structure due to prestressing. Support reactions and shear forces will also be present in this case, even though there is no applied load on the structure. The presence of these secondary moments involves extra work in the analysis and design of statically indeterminate prestressed concrete structures, although in nearly all other respects the design and analysis procedures outlined in the preceding chapters are applicable.

In order to understand how these secondary moments arise, consider a two-span continuous beam, as shown in Fig. 11.1(a), which has a constant prestressing force P acting at an eccentricity e.

If the central support were unable to restrain vertical upward movement of the beam, the deflected shape of the beam due to the prestressing force would be as shown in Fig. 11.1(b). The beam is now effectively statically determinate and the prestress moment at any section would be the primary moment Pe (Fig. 11.2(a)). However, in practice the beam would be restrained at the central support, and in order to maintain compatibility of displacements at this position, a downward reaction R must be applied at the support. The distribution of secondary moments induced in the beam by this reaction is shown in Fig. 11.2(b), whilst Fig. 11.2(c) shows the total distribution of the moments along the beam. Note that the secondary moment diagram varies linearly between supports, since it is produced only by the reactions at the supports induced by prestressing.

The resulting prestress moment at any section shown in Fig. 11.2(c) may be written as $Py,$ where y is some displacement. This may then be considered as the eccentricity of the resultant line of pressure in the concrete, and the locus of y along the beam may be considered as an effective tendon profile. The effective profile is obtained by raising or
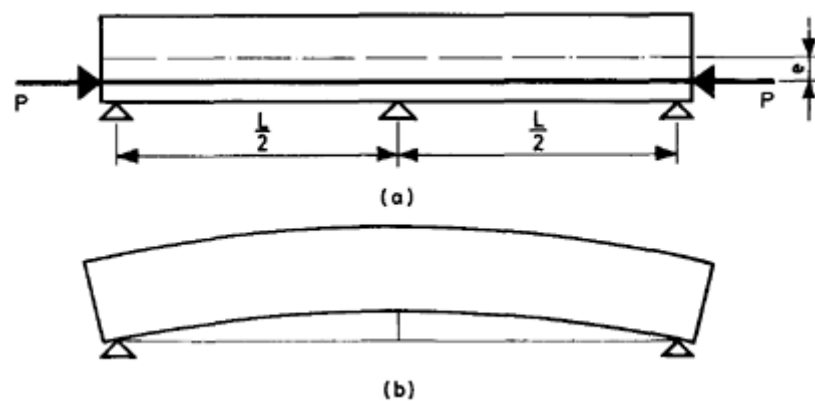
Figure 11.1 Continuous prestressed concrete beam.
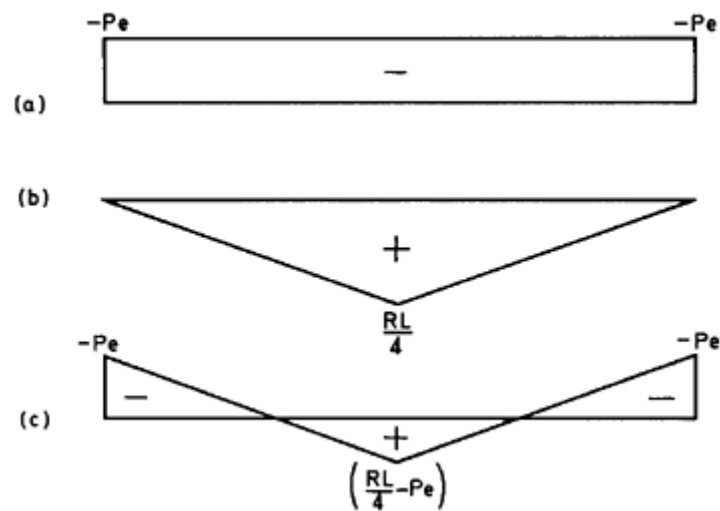
Figure 11.2 Secondary moments.
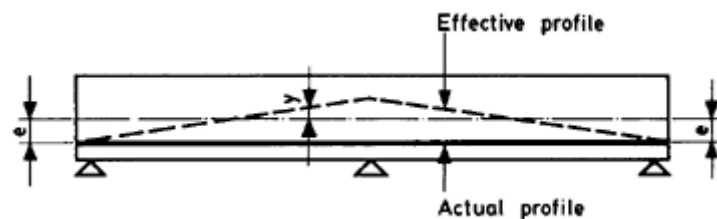
Figure 11.3 Effective tendon profile.

lowering the actual profile at interior supports, while keeping the basic shape of the profile constant, as shown in Fig. 11.3.

All the expressions given in Chapter 9 may be used for the design of statically indeterminate structures if, once the secondary moments have been determined, the actual eccentricity e is replaced by the effective eccentricity y. However, determination of the cable profile is generally then an iterative procedure.

Example 11.1 ■■

A two-span continuous beam ABC has spans of 10 m and a prestress force of 1500 kN acting at a constant eccentricity of 300 mm. Determine the distribution of prestress moments along the beam and the support reactions induced by prestressing.

On the assumption that there is no vertical restraint at the central support, the beam is subjected to a pair of end-moments equal to Pe,

that is 1500×0.3=450 kNm. The midspan upward deflection of a beam subjected to a pair of end-moments M is given by

$$\delta_M = ML2/8EI,$$

where EI is the constant flexural stiffness of the beam and L is the span.
  Thus, for this example,

$$\delta_M = 450 \times 20^2/8EI = 22\ 500/EI.$$

For a downward force R at the central support, the downward deflection at this point is given by

$$\delta_R = RL3/48EI$$
$$= R \times 20^3/48EI = 166.7\ R/EI.$$

For compatibility of displacements at the central support, these two deflections must be numerically equal. Thus:

$$22500/EI = 166.7R/EI$$
$$\therefore R = 135\ kN.$$

The end-support reactions are thus each 67.5 kN, upward.
  The primary, secondary and total distributions of prestress moments along the beam are shown in Fig. 11.4(a)–(c), respectively, whilst the effective tendon profile is shown in Fig. 11.5.
  An alternative method of analysis for the secondary moments is to consider the primary moment as a distributed applied moment on the structure and then to analyse it using any of the common methods of structural analysis. For the beam in this example, the method of moment distribution will be used. The fixed-end moments for each span may be
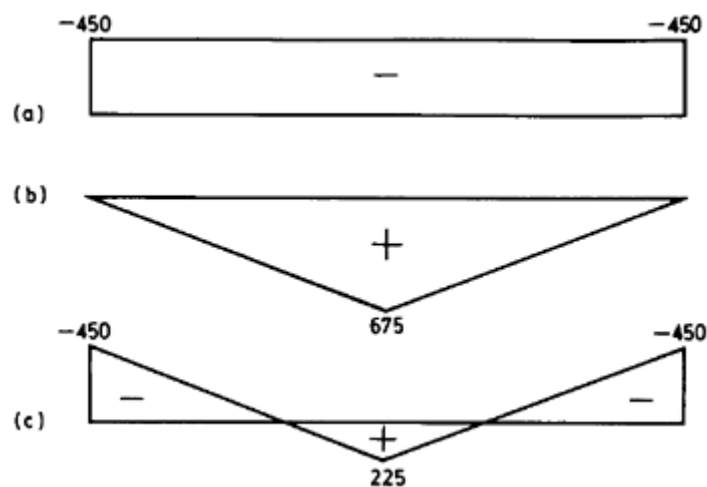
Figure 11.4 Prestress moments for beam in Example 11.1 (kNm).
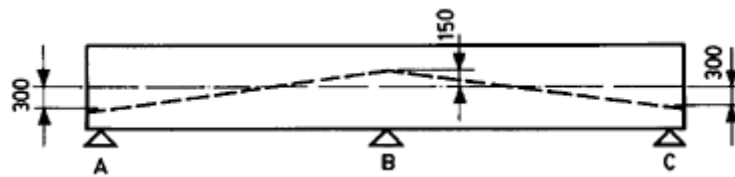
Figure 11.5 Effective tendon profile for beam in Example 11.1.
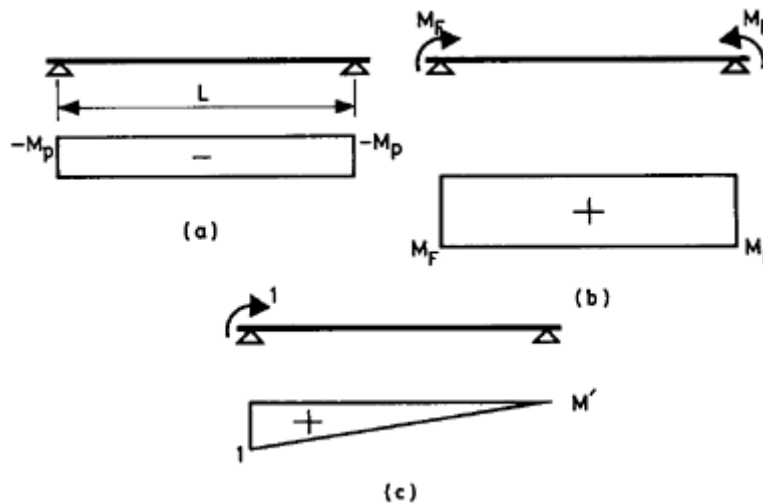
Figure 11.6 Primary moment as distributed applied moment.

found by considering the span as simply supported and with distributed moment, M_P, and end-moments, M_F, applied as shown in Fig. 11.6(a) and (b), respectively. From symmetry, the fixed-end moments M_F at each end of the span must be equal. The rotations at each end of the span due to the combination of M_P and M_F are zero for a fixed-end condition. This rotation may be found conveniently using the virtual work method. The same simply supported span is shown in Fig. 11.6(c), with a unit moment applied to the left-hand end. The rotation at this end due to the moments M_P and M_F is then given by

$$1 \times \theta_A = \int_0^L [M'(M_p + M_F)/EI] \mathrm{d}x.$$

From Simpson's rule:

$$\theta_A = (L/6EI)[(-M_P+M_F)(1)+4(-M_P+M_F)(1/2)]$$
$$= (-M_p+M_F)L/2EI.$$

Since this rotation must be zero, $M_p = M_F$. In this example, $M_p = 450$ kNm and so the fixed-end moments are 450 kNm. The moment distribution is shown in Fig. 11.7, showing that the secondary moment

	A		B			C
	AB		BA	BC		CB
D.F.			0.5	0.5		
F.E.M.	450		−450	450		−450
Balanace	−450					450
Carry-over			−225	225		
Total	0		−675	675		0

Figure 11.7 Moment distribution for beam in Example 11.1 (kNm).

at support B is 675 kNm, as found previously. The resulting total distribution of prestress moments throughout the structure is shown in Fig. 11.4(c).

■■

For less simple tendon profiles, the primary moment diagram shown in Fig. 11.6(a) is found by plotting the ordinates Pe along the span. The two fixed-end moments at either end of the span will, in general, be unequal, and the condition of zero end-slope must be applied to each end to enable solution of the unknowns.

The straight tendon profile shown in Fig. 11.1 was used only to illustrate how secondary moments arise. In practice the profile in continuous members is determined according to the same underlying principle that is used for simply supported members, namely that the prestressing tendons are so positioned as to counteract any tension induced by the applied load. In continuous members, hogging support bending moments produce tension at the top surface, and so the eccentricity of the tendons is usually above the centroid at the supports. A typical tendon profile is shown in Fig. 11.8(a) and an enlarged detail of the tendon geometry near the support is shown in Fig. 11.8(b). The inflexion point for the profile is commonly taken as one-tenth of the span.

A useful method of determining the *total* prestress moments in an indeterminate structure is to analyse the structure under the equivalent loading applied to the concrete by the prestressing tendons. For a smoothly draped, or a sharply deflected, tendon a vertical force is exerted on the concrete member and the total distribution of prestress moments may be determined by any of the usual methods of structural analysis. The equivalent loading for the tendon profile in Fig. 11.8(a) is shown in Fig. 11.9.
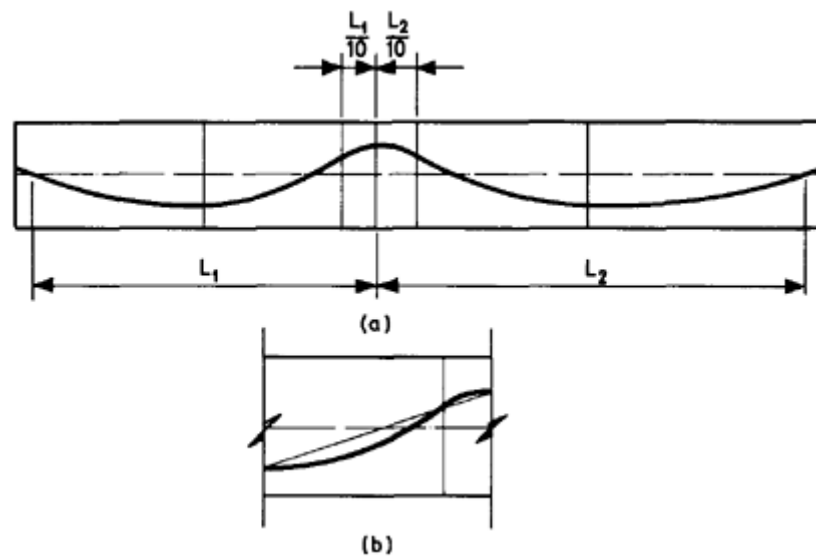
Figure 11.8 Practical tendon geometry: (a) typical profile; (b) enlarged detail near the support.
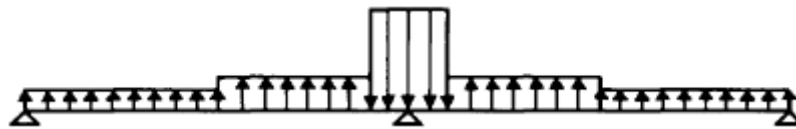
Figure 11.9 Equivalent loading from tendons.

For the straight tendon in Example 1.1, there is no vertical force exerted on the concrete, but there are end-moments as shown in Fig. 11.10. The moment distribution for the beam subjected to these end-moments is shown in Fig. 11.11 and the resulting distribution of total prestress moments is identical to that shown in Fig. 11.4(c). The secondary moments may be found by deducting the primary from the total prestressing moments, a procedure useful in analysis at the ultimate limit state, described in section 11.4.

Example 11.2 ■■

Determine the distribution of total prestress moments due to a prestress force of 1000 kN for the beam shown in Fig. 11.12. Also determine the support reactions induced by prestressing.

The equivalent uniform vertical load exerted on the concrete is given by

$w=P/r_{ps}$.
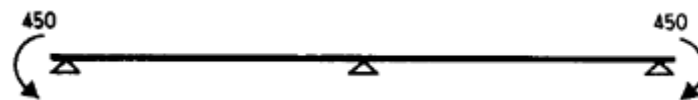
Figure 11.10 Applied moments for straight tendon profile (kNm).

	A		B	C
	AB	BA	BC	CB
D.F.		0.5	0.5	
F.E.M.	−450	−225	225	450
Total	−450	−225	225	450

Figure 11.11 Moment distribution for beam subjected to end-moments (kNm).

① r_{ps} = 93·74 m   ② r_{ps} = 37·45 m   ③ r_{ps} = 9·38 m
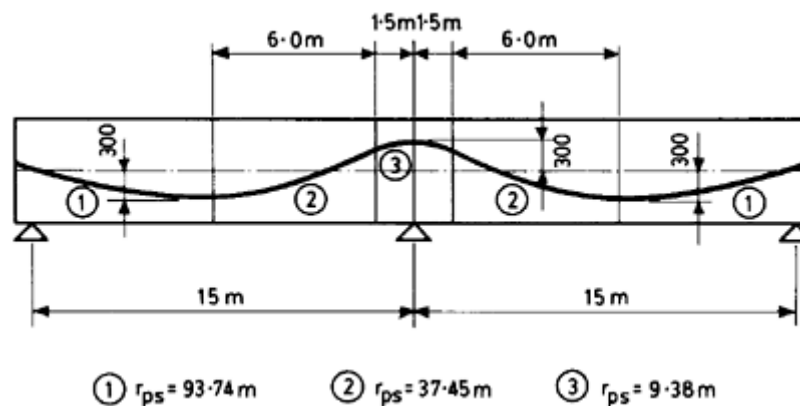
Figure 11.12

Thus:

w_1=1000/93.74=10.67 kN/m
w_2=1000/37.45=26.70 kN/m
w_3=1000/9.38=106.61 kN/m.

The beam can now be analysed under the loading shown in Fig. 11.13.

The resulting distributions of total and secondary prestress moments are shown in Fig. 11.14(a) and (b), respectively, the latter also showing the support reactions, and the effective tendon profile in Fig. 11.15. Note that, once again, the effective tendon profile has been obtained by raising or lowering the actual profile at the supports, keeping the shape constant between the supports.

■■
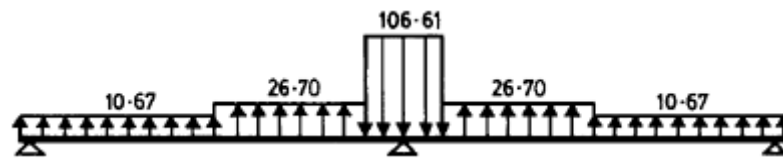
Figure 11.13 Equivalent loading for beam in Example 11.2 (kN/m).
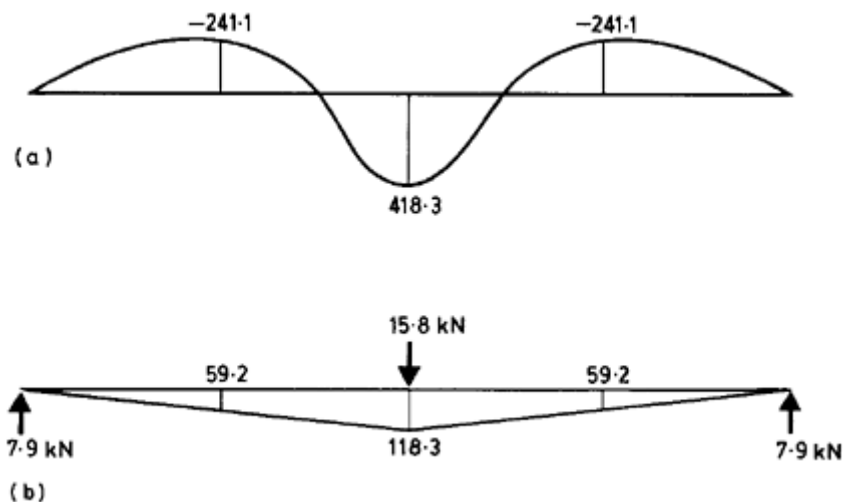
Figure 11.14 (a) Total and (b) secondary prestress moments for beam in Example 11.2 (kNm).
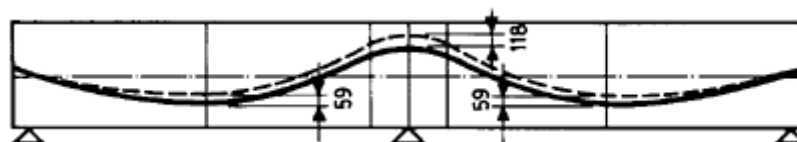
Figure 11.15 Effective tendon profile for beam in Example 11.2.

An alternative method of determining a tendon profile for the given eccentricities is shown in Concrete Society (1994). However, this will not always give maximum eccentricity at the desired points in the spans.

The profile shown in Example 11.2 gives rise to equivalent uniform loads. If there is a sharp change in curvature, then the equivalent force on the concrete member is concentrated, as described in Chapter 1.

In many long continuous prestressed concrete structures, such as bridge decks or floor slabs, some of the tendons are stopped off within a span. They may end there or be connected to other tendons some time later. At these points the effect of a concentrated vertical load and moment must be taken into account when applying equivalent loads to

the structure in order to determine the total prestress moment distribution.

Once the secondary moments have been determined, the total stresses at the serviceability limit state may be found by adding the total prestress moment to the applied load bending moment.

In assessing the elastic distribution of bending moments throughout the structure, the following load cases should be considered for beams in buildings without cantilevers and with predominantly uniform loads:

 (i) alternate spans loaded with dead load plus imposed load;
(ii) any two adjacent spans loaded with dead load plus imposed load and all other
       spans loaded with 1.0×dead load.

In the above, the imposed load is either the frequent or rare load combination, depending on whether crack widths or concrete stresses are to be determined, respectively.

For framed structures, the axial shortening in the beams caused by prestressing must also be considered in determining the secondary moments (see Problem 11.5).

11.3 LINEAR TRANSFORMATION AND CONCORDANCY

It was shown in the previous section that the line of pressure can be obtained from the actual tendon profile by raising or lowering the profile at an interior support while keeping the same basic shape in the spans either side of the support. This is an example of a *linear transformation* of a profile, since the amount by which the profile is raised or lowered at any point is directly proportional to the distance of that point from the support that is adjusted. Linear transformations of successive spans can be superimposed to produce a combined transformation.
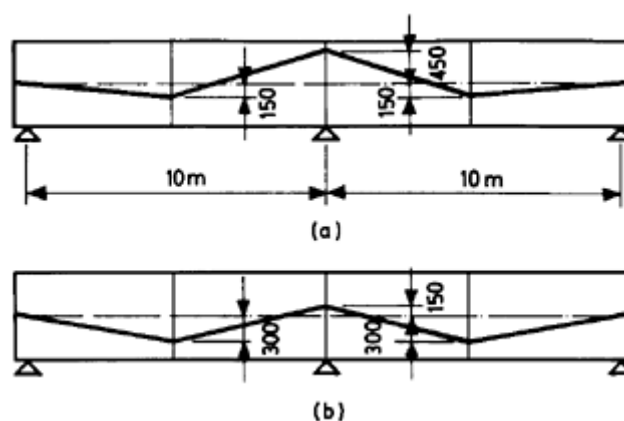
Figure 11.16 Linear transformation.
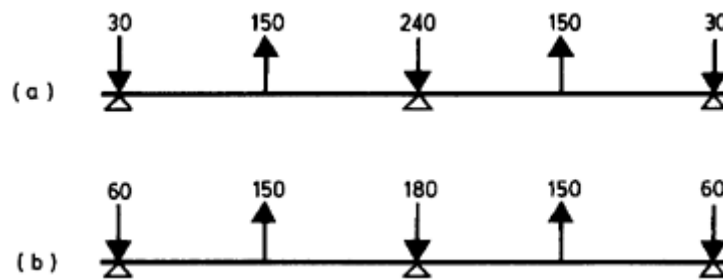
Figure 11.17 Equivalent loading for linear transformation (kN).

Consider the beams shown in Fig. 11.16(a) and (b). The profile in Fig. 11.16(b) is a linear transformation of that in Fig. 11.16(a). The equivalent loads on the concrete in the two cases are shown in Fig. 11.17(a) and (b). The equivalent loads within the spans in each case are the same, although the different inclinations of the tendons at the supports give rise to different vertical forces there. Since the loads within the spans are the same the distributions of total prestress moments must be the same. The lines of pressure in each case must thus be equal. However, the distributions of primary and secondary prestress moments, and the support reactions induced by prestressing, will be different in each case as shown in Fig. 11.18(a) and (b).

   In Fig. 11.16 the tendon profile is shown with a sharp change of curvature at the central support, for simplicity. In practice the profile would be more like that shown in Fig. 11.8. For this profile, a linear transformation would slightly alter the inflexion point between the two curved regions and similarly affect the equivalent loads within the span. A linear transformation of such a profile, in theory, would thus cause a change in the total distribution of moments due to the prestress force, but in practice this change is very small and is usually ignored.

   A general rule can now be stated, that if a tendon profile undergoes a linear transformation, the line of pressure in the concrete remains constant. This property is particularly useful in modifying tendon profiles when the limits to the cable zone, determined from Inequalities 9.6(a)–(e), do not permit a practical tendon profile. A profile can be chosen to lie within the theoretical cable zone, and a linear transformation performed to bring the actual profile into a more practical location.

   If the eccentricity of the straight tendon profile shown in Fig. 11.1 (a) is gradually reduced, the free upward movement of the member at the central support position also becomes smaller. The magnitude of the reaction required to maintain the beam in contact with the support is also lessened, and this implies that the secondary moments reduce. In the limiting case, the eccentricity becomes zero, and the beam is
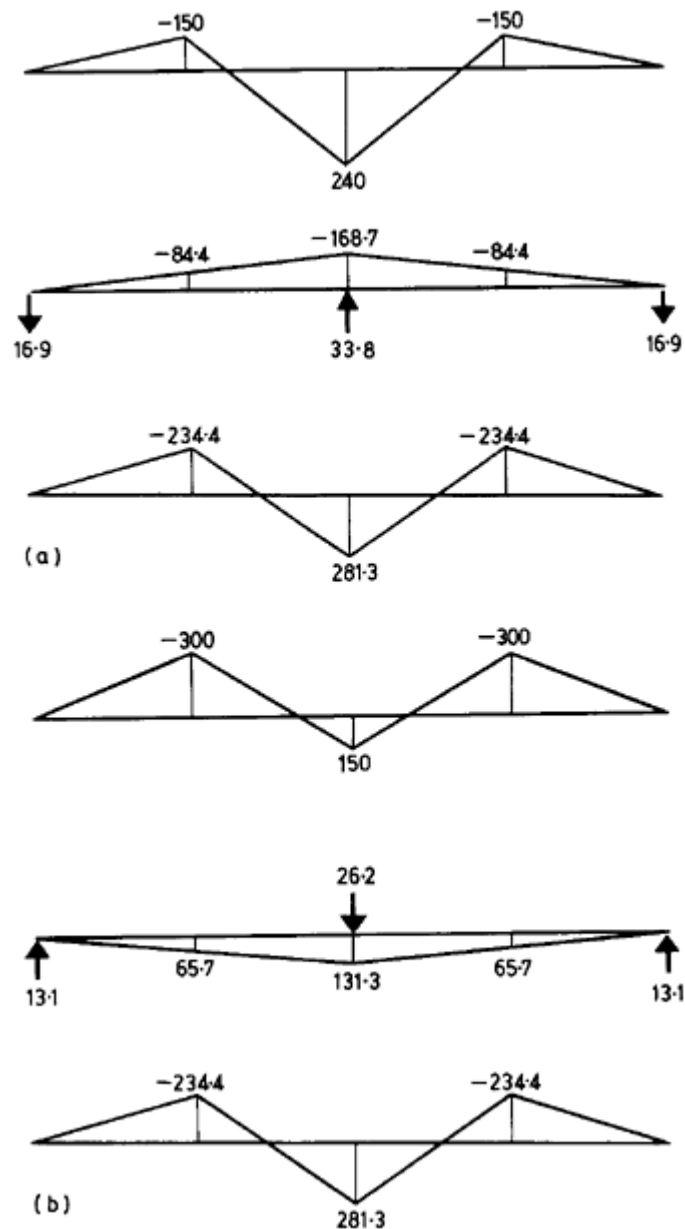
Figure 11.18 Primary, secondary and total prestress moments for beams (a) and (b) in Fig. 11.16 (kNm).

concentrically prestressed. The central support reaction and the secondary moments are then also zero. The total prestress moment in the beam at every section would be equal to the primary moment *Pe*, and the line of pressure would be everywhere coincident with the tendon profile.

Any tendon profile in a prestressed concrete member that has this property is known as a *concordant* profile. All profiles in statically

determinate members are thus concordant, but in statically indeterminate members most profiles are non-concordant. For any given member, there can be many different basic profiles that are concordant.

In the design of a statically indeterminate prestressed concrete member, it is not necessary to ensure that the chosen profile is concordant, although this simplifies the calculations. In practice it is found that concordant profiles are not the most economical, but in the design process it is quite useful to start with a concordant profile and then to modify it as necessary.

Consider now the continuous beam shown in Fig. 11.19(a) with a uniform load on each span. The distribution of bending moments is shown in Fig. 11.19(b). If tendons are fixed in the beam according to a profile determined from Fig. 11.19(b), then the equivalent load on the beam from the tendons must be of the form shown in Fig. 11.19(a), since any elastic bending moment distribution within a given structure can only correspond to one distribution of applied loads. The distribution of total prestress moments within the member must therefore be similar to that shown in Fig. 11.19(b). Since this distribution of moments is consistent with zero vertical deflection at the central support, this tendon profile must be concordant.

A general rule thus emerges for determining concordant profiles, that the bending moment diagram for any given loading on a structure yields a concordant profile.

Example 11.3 ■■

Determine a concordant profile for the beam shown in Fig. 11.20, using a prestress force of 500 kN.

A uniform load of 12 kN/m will be used to find a concordant profile. The bending moment diagram for this loading is shown in Fig. 11.21(a).
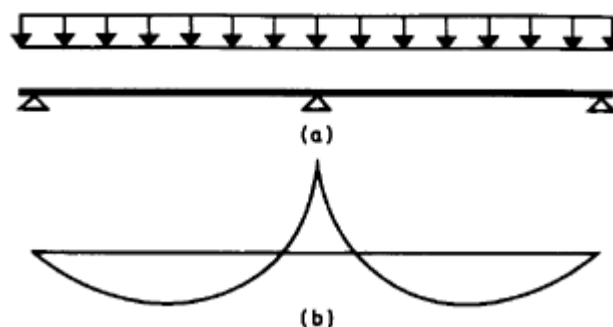
Figure 11.19 Continuous beam: (a) uniform load on each span; (b) bending moment distribution resulting from UDL.
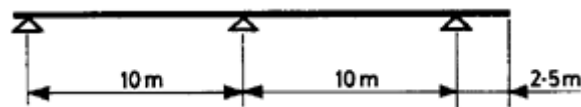
Figure 11.20

The concordant tendon profile is obtained by dividing the ordinates of the bending moment diagram in Fig. 11.21(a) by the prestress force. The resultant profile is shown in Fig. 11.21(b).
 ■■

This profile is just one such concordant profile, since any linear transformation of it will not alter the position of the pressure line in the concrete and thus the profile will remain concordant. The design could then proceed exactly as for a statically determinate structure, since, provided the chosen tendon profile is a linear transformation of that shown in Fig. 11.21(b), the secondary moments will be zero.

The above method of finding a concordant profile is strictly valid only if the prestress force is constant along the member. In practice the prestress force varies, and the concordant profile should be obtained by dividing the ordinate of the bending moment diagram in Fig. 11.21(a) at any section by the effective prestress force at that section.

11.4 ULTIMATE LOAD BEHAVIOUR

The analysis of prestressed concrete members at the ultimate limit state outlined in Chapter 5 is sufficient for statically determinate structures, since, for these structures, once the ultimate moment of resistance has been reached at any section, a mechanism is formed and the structure cannot support any more load.

The situation is different, however, for statically indeterminate structures. As the applied load is increased, the ultimate moment of resistance will be reached at some point in the structure, but in this case a mechanism will not form. Provided that the member at this point will allow rotation to take place at the *plastic hinge* which has formed, additional load can be carried by the structure, which effectively redistributes the load to less heavily loaded regions until sufficient plastic hinges have formed to produce a mechanism. This description of the plastic analysis of prestressed concrete structures is equally applicable to steel, timber or reinforced concrete structures, and the general background and details of the theory may be found in Coates, Coutie and Kong (1980). The full methods of plastic analysis may be used for prestressed concrete structures, but there are important
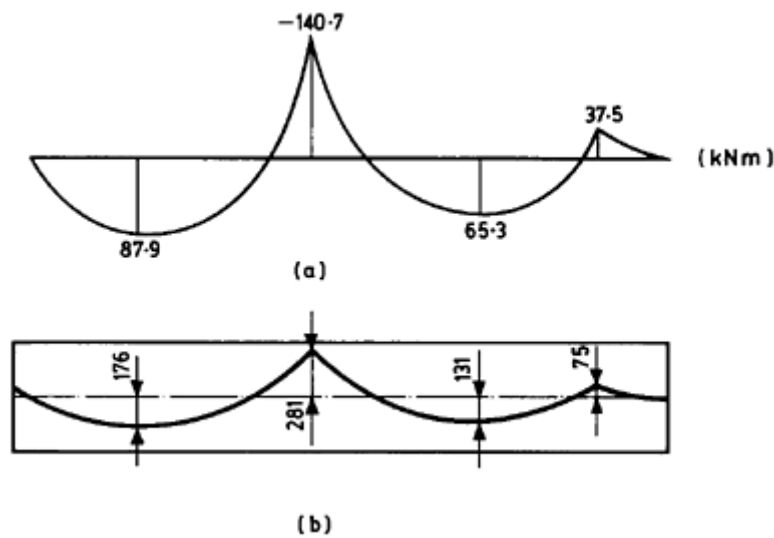
Figure 11.21 Concordant profile for beam in Example 11.3.
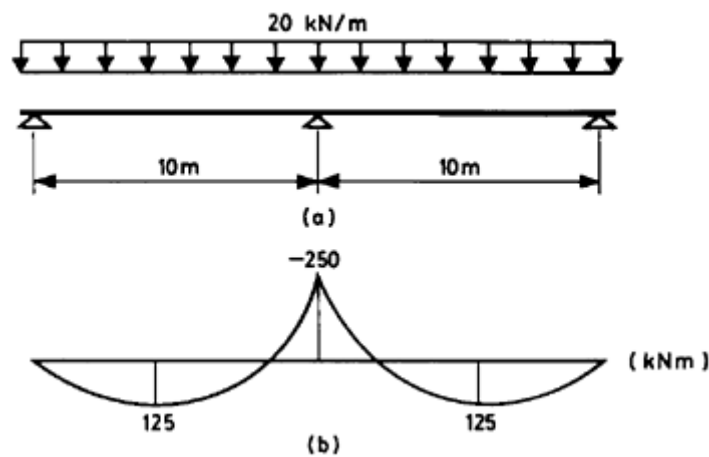
Figure 11.22

limitations imposed in EC2 on the amount of rotation that takes place at a given section once a plastic hinge has formed there.

Consider the two-span continuous beam shown in Fig. 11.22(a), which is subjected to a total ultimate uniform load of 20 kN/m. An elastic analysis of the structure would give the bending moment distribution shown in Fig. 11.22(b). If the ultimate moment of resistance of the beam at the central support is 175 kNm, then the bending moment distribution of Fig. 11.22(b) can never be achieved. At a load of 14 kN/m, the bending moment diagram would be as shown in Fig. 11.23(a). As the uniform load is increased from 14 kN/m to 20 kN/m, the
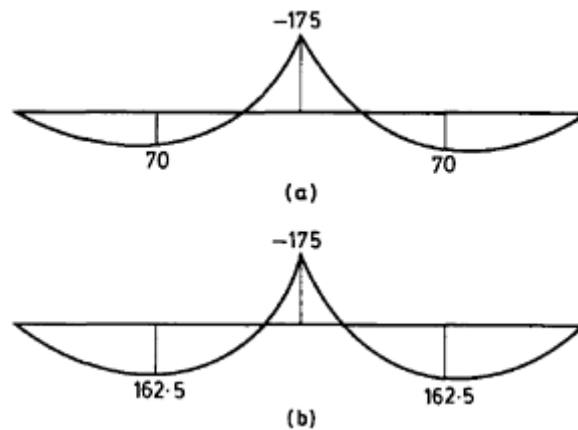
Figure 11.23 Moment redistribution (kNm).

bending moment at the central support is assumed to remain constant at 175 kNm, since a plastic hinge has formed there. In order to maintain equilibrium, the bending moment diagram becomes that shown in Fig. 11.23(b). Comparison of this with Fig. 11.22(b) shows that the elastic bending moment of 250 kNm at the support has been *redistributed* by 30% to give the value of 175 kNm in Fig. 11.23(b). However, the ultimate moment of resistance to be provided at the midspan sections has now increased to 162.5 kNm.

Moment redistribution may also be applied to the midspan sections. In this case it is the moment of resistance at the supports which must be increased to maintain equilibrium.

The 30% redistribution shown in the above example is the maximum permitted in EC2 for post-tensioned tendons. However, in practice the actual amount of redistribution permitted for a given section may be less than this figure. This is because for a statically indeterminate structure to resist an increase in load once the first plastic hinge has formed, rotation must take place at that hinge. The ability of a prestressed concrete member to undergo the required rotation once the ultimate moment of resistance has been reached is dependent on the position of the neutral axis within the section. Typical plots of moment-curvature for a given rectangular prestressed concrete section with varying amounts of prestressing steel are shown in Fig. 11.24. Each curve also corresponds to a different location of the neutral axis at the ultimate moment of resistance. For positions of the neutral axis high in the section, the amount of rotation that can take place after the plastic hinge has formed is much greater than for positions of the neutral axis lower in the section.

Strictly according to plastic theory, the ultimate strength of a prestressed concrete structure is independent of any secondary moments

induced by prestressing, in a similar way that it is also independent of such effects as settlement of supports; it depends solely on the mechanisms which can form. However, it is stated in EC2 that secondary moments and shear forces should be included in ultimate strength calculations, with a value of γ_p of 1.0. The inclusion of secondary moments generally increases span bending moments and decreases those at supports. For framed structures, such as prestressed flat slabs, described in Chapter 12, secondary moments will have an effect on the design moments for the columns.

The amount of redistribution allowed is linked directly in EC2 to the position of the neutral axis. The permitted values for prestressing tendons of δ, the ratio of the moment at a section after redistribution to that before redistribution, are shown in Table 11.1.

In assessing the elastic distribution of bending moments throughout the structure due to ultimate loads, the load combinations described in Section 11.2 should be used, in combination with the partial factors of safety given in Chapter 3.
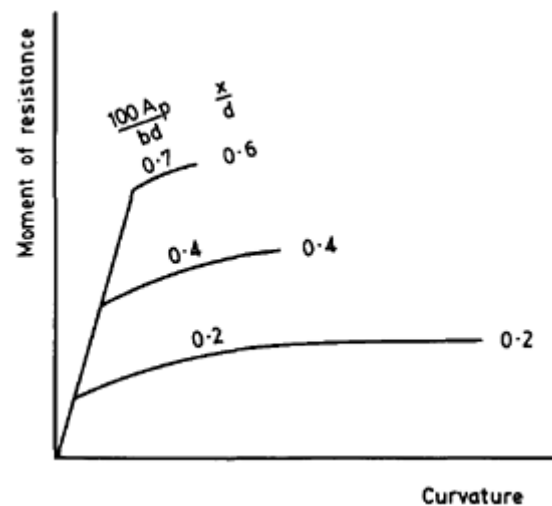
Figure 11.24 Moment-curvature relationships.

Table 11.1 Limits to redistribution

Concrete grade	Minimum value of δ		Maximum value of x/d
	Post-tensioning	Pretensioning	
≤C35/45	0.70	0.85	$0.8\,\delta-0.35 \leq 0.45$
>C35/45	0.70	0.85	$0.8\,\delta-0.45 \leq 0.35$

Example 11.4 ■■

Determine the maximum ultimate uniform load that can be supported by the beam in Example 11.2, if the beam dimensions are 750 mm deep by 400 mm wide and the area of prestressing steel is 1030 mm^2. Assume that the concrete is grade C40/50 and f_{pk}=1850 N/mm2.

At the central support:

$A_{p}f_{pk}/(bdf_{ck})$=(1030×1850)/(400×675×40)
=0.176.

From the design chart shown in Fig. 5.16,

M_u=0.121×400×675^2×40×10^{-6}
=882.1 kNm

Also from Fig. 5.16, x/d is 0.3. Thus from Table 11.1, δ=0.94 (>0.70).

For a uniform load, w, over the full length of the beam the maximum elastic support bending moment is wL^2/8, or 28.13 w. From Fig. 11.14 the secondary moment at the support is 18.3 kNm (with γ_p=1.0).

Thus:

0.94 (−28.13 w+118.3)=−882.1
∴ w_{ult}=37.6 kN/m

With no redistribution, w_{ult}=31.4 kN/m.

The secondary moment at midspan is 59.2 kNm. For a support bending moment of 882.1 kNm the corresponding midspan moment is

=37.6×15^2/16+59.2
=588.0 kNm.

Since this is less than the ultimate moment of resistance of the midspan section no additional untensioned reinforcement is required.

■■

PROBLEMS

11.1 For the beam in Example 11.1 determine the midspan deflection under the action of prestress force only.

11.2 For the beam shown in Fig. 11.25, determine the support reactions induced by prestressing:
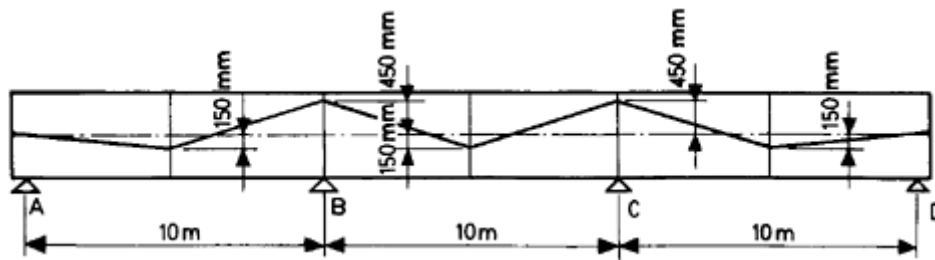
Figure 11.25
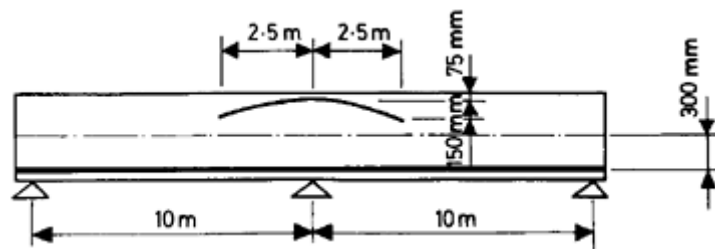
Figure 11.26
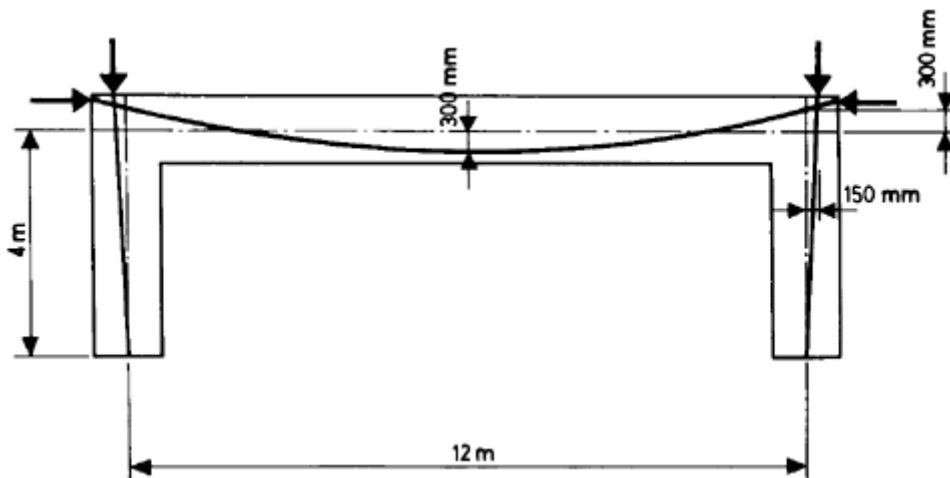
Figure 11.27

 (i) with the profile as shown;
(ii) with the profile at support B lowered by 300 mm, the basic shapes of the profiles in the adjacent spans remaining unaltered.

11.3 For the beam in Example 11.1, show that, if the tendon is placed along the original line of pressure, the new profile is concordant.

11.4 The beam in Example 11.1 is to have a circular cap cable over the central support, as shown in Fig. 11.26. The radius of the cable is 20.91 m and the prestress force is 900 kN. If the dimensions of the beam are 750 mm deep by 400 mm wide, determine the stresses in the top of the beam over the central support under the effect of prestress, self weight and an imposed load of 55 kN/m:

 (i) with no cap cable;
(ii) with cap cable.

For case (i), determine the maximum and minimum compressive stresses in the beam at midspan.

11.5 The pinned-base portal frame shown in Fig. 11.27 has a constant cross-section of 900×300 mm. It has a parabolic tendon profile in the beam with constant prestress force of 2000 kN, and straight tendons in the columns with prestress force of 500 kN. Determine the primary and secondary prestress moment diagrams and find the secondary support reactions. Assume $E_{cm}=35×103$ N/mm^2.

<div align="center">REFERENCES</div>

Coates, R.C., Coutie, M.G. and Kong, F.K. (1980) *Structural Analysis,* Nelson, Walton-on-Thames.

Concrete Society (1994), *Post-tensioned Concrete Floors—Design Handbook,* TR43, Slough.

12

Prestressed flat slabs

12.1 INTRODUCTION

The application of post-tensioned concrete to flat slab construction originated in the USA, and is now also widely used in Australia, Europe, the Far East and Southern Africa. Although its use in the UK has been uncommon until recently, the economic advantages of this form of construction are now more widely appreciated. Most examples utilize uniform-depth slabs with draped tendons, but an interesting development is the use of variable-depth slabs with straight tendons. Extra shear strength is often provided around the columns in the form of a thickening of the slab, or drop panel, or by increasing the column perimeter in a column 'head'.

No design guidance is given in EC2 regarding prestressed concrete slabs. Design should, therefore, be based on the recommendations given in the Concrete Society (1994) Technical Report TR43. Many of the clauses in TR43 are similar to those in BS8110.

Both bonded and unbonded tendons are employed in prestressed concrete flat slabs; the merits of each were discussed in Chapter 5. It is interesting to note that in the USA unbonded tendons are mainly used, whilst in Australia, Europe, the Far East and Southern Africa bonded construction is the norm. The choice would seem to depend on the local economics and design philosophy.

12.2 TWO-WAY LOAD BALANCING

A one-way spanning slab is essentially a very wide simply supported beam, the design of which is described in the preceding chapters. With a prestressed concrete slab simply supported on four edges, however, the situation is very different, since the structure is now highly indeterminate. A rectangular slab is shown in Fig. 12.1, supported on walls along each edge and prestressed with sets of uniformly spaced parabolic tendons in each direction.
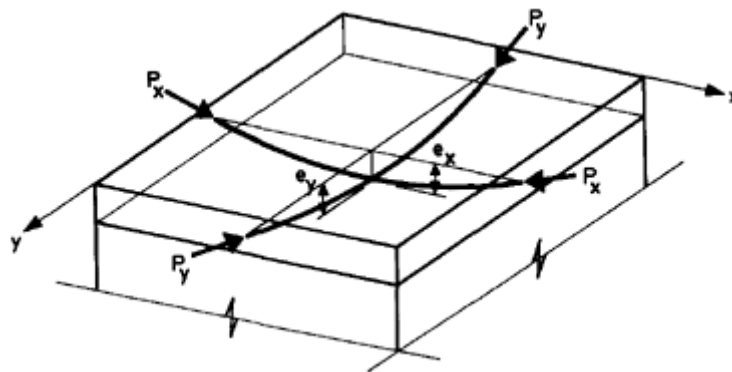
Figure 12.1 Two-way prestressed concrete slab.

For given tendon profiles and prestress forces in each direction, the slab could be analysed by theory of elasticity to give the distribution of stresses within the slab. This would be a complex problem, however, and an alternative method, based on the load balancing principle, is found to be very useful. The curved tendons exert an upwards force on the slab, and, by suitable choice of profile and prestress force, any given load can be balanced to give zero deflections at every point in the slab.

If the prestress forces in the x and y directions are, respectively, P_x and P_y per unit length, and the midspan eccentricities are e_x and e_y, respectively, then since the vertical forces due to the tendons in each direction are additive at any point in the slab, the total upward uniform load on the slab is given by

$$w = 8\, P_x e_x / L_x^2 + 8\, P_y e_y / L_y^2.$$

(12.1)

Since the tendons must have a minimum spacing between them, the stress distribution within the slab will not be exactly uniform, but in practice it would be reasonably so.

Prestressed concrete slabs such as that shown in Fig. 12.1 are rarely found in practice, and the more common form is the flat slab, supported only on columns, with no intermediate beams. A prestressed concrete flat slab with irregularly spaced columns is shown in Fig. 12.2. Consider the area of the slab bounded by gridlines A, B, 1 and 3. *Primary* parabolic tendons are placed evenly between gridlines A and B, and, by suitable adjustment of the profile and prestress force, the upward force from these tendons can be made to balance the applied load. Along gridlines A and B there will be a downward force exerted on the slab, due to the inclination of the primary tendons along these gridlines. For the slab shown in Fig. 12.1, these downward forces pass directly into the supporting walls, but in a flat slab there are no supporting beams or walls and some other means of resisting the forces is necessary.

P = Primary tendon   S = Secondary tendon
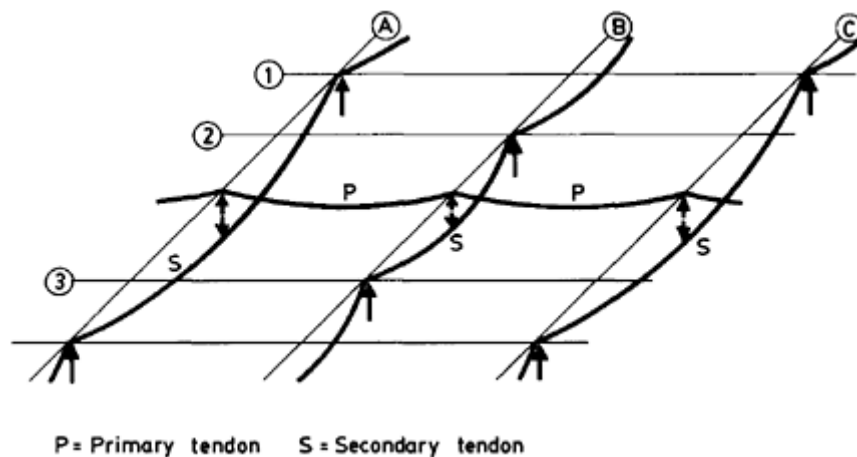
Figure 12.2 Transfer of load through tendons.

The downward forces are resisted by *secondary* parabolic tendons along gridlines A and B. The upward forces from these balance the downward forces from the primary tendons, and the downward forces from the secondary tendons pass directly into the columns. The uniform applied load on the slab has thus passed into the columns through the system of prestressing tendons, leaving the slab level and in a uniform state of compression. In practice, the forces in all the tendons are not constant and do not balance each other evenly, but the actual state of stress within the slab will be reasonably uniform.

The slab shown in Fig. 12.2 will resist any additional imposed load in much the same way as would a reinforced concrete flat slab, and the same analysis methods are applicable. Since this analysis need only be carried out for a small percentage, usually, of the total design load, any inherent inaccuracies in the method are not significant.

In practice, the sharp changes of curvature in the tendons shown in Fig. 12.2 are avoided by adopting smooth reverses in curvature, as shown in Chapter 11. A suitable layout of tendons within a flat slab with regularly spaced columns in each direction is shown in Fig. 12.3.

The distribution of bending moments in an interior panel of a flat slab, subjected to a uniform load, is shown in Fig. 12.4, and the distribution of prestress moments obtained from a layout of tendons similar to that shown in Fig. 12.3 is shown in Fig. 12.5 (Figs 12.4 and 12.5 are adapted from Birkenmaier, Welbergen and Winkler (1986)). The net bending moment distribution is thus very even, with small peaks along the column lines.

An alternative pattern of tendons which is often used is shown in Fig. 12.6, based on the distribution of primary and secondary tendons shown in Fig. 12.2. As noted above, this pattern is well suited to slabs
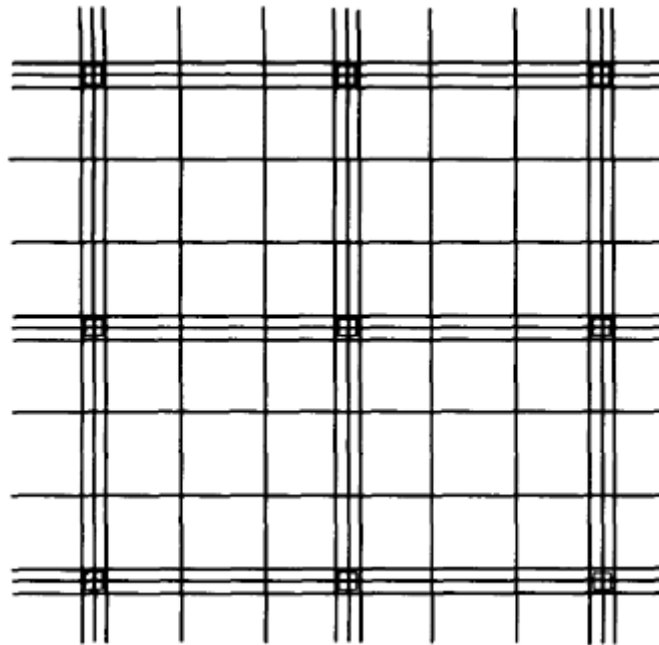
Figure 12.3 Tendon layout for square column grid.
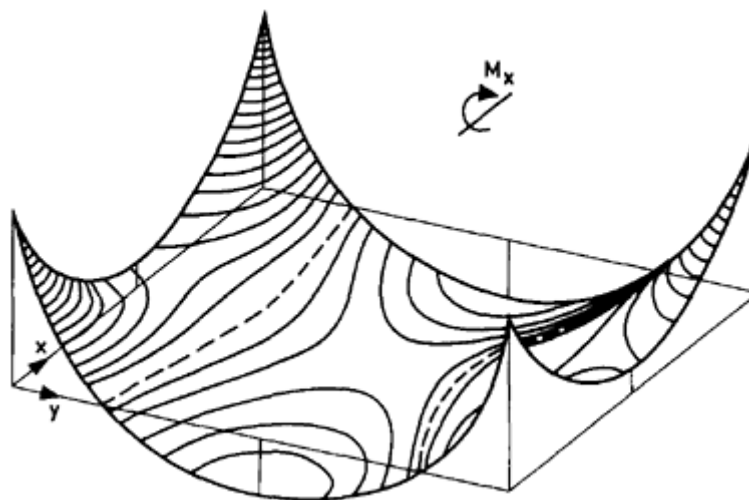
Figure 12.4 Bending moment distribution in flat slab panel due to applied loads.

with irregular column layouts, but shear strength will be reduced (see Section 12.6).

12.3 EQUIVALENT-FRAME ANALYSIS

The load balancing technique is very useful for estimating the prestress force required in each direction, but an analysis of the slab for the
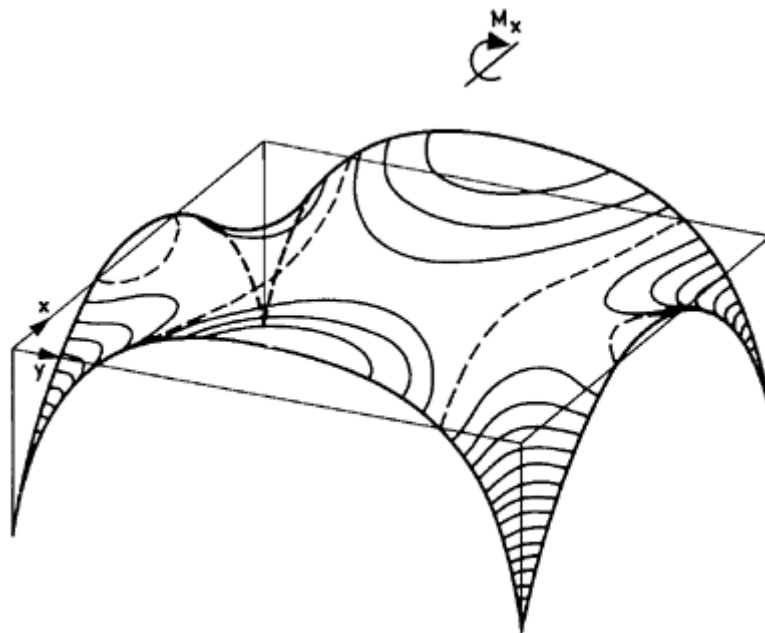
Figure 12.5 Prestress moment distribution in flat slab panel.
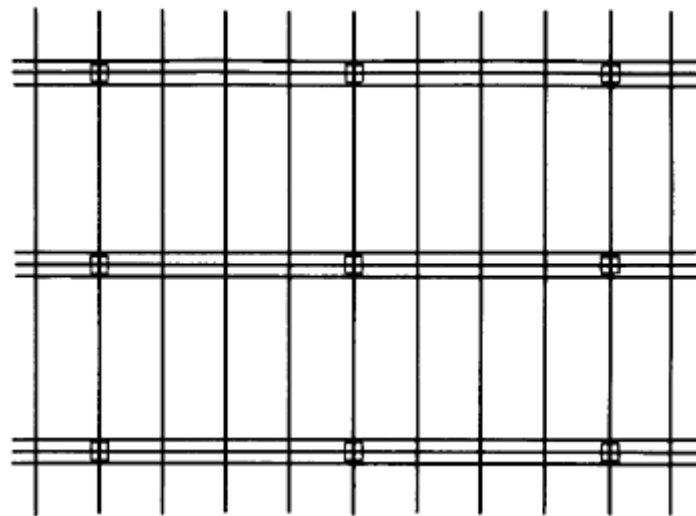
Figure 12.6 Tendon layout for rectangular column grid.

unbalanced loads must still be made. The analysis and design of reinforced concrete flat slabs with regularly spaced columns has for many years been based on a method which divides the slab and columns into a series of equivalent frames in each direction. The distributions of bending moment and shear force may be determined by any of the available methods of structural analysis. The equivalent-frame method has also been found to give acceptable results for prestressed concrete

flat slabs and is one of those recommended in TR43. It can be used to find the distribution of moments due to both the prestress force and the total design load, and not just the unbalanced loads.

Each equivalent frame comprises columns and strips of slab at each floor level. The width of slab to be used to determine the beam stiffness is generally equal to the full width of the panels for vertical loading, whilst for horizontal loading, where lateral stability is provided by the frame, one-half of the panel width should be used.

A multi-storey frame may be analysed as a whole, but, for vertical loads only, each strip of slab at a given floor level may be analysed as a separate frame, with columns above and below the slab assumed to be fixed in position and direction (Fig. 12.7). It should be noted that, for the effect of dead load and prestress only, the equivalent frame of Fig. 12.7 should only include columns below the slab, reflecting the normal construction sequence. However, this is often ignored in practice. Where drops are provided around the columns, an equivalent slab thickness may be found for the support section of the slab, with the same second moment of area as the true section, and the overall beam stiffness modified accordingly. Most slab layouts have a regular column spacing in both directions, but for layouts such as that shown in Fig. 12.2 the equivalent-frame method is not as suitable, and in order to analyse such slabs methods such as finite element or grillage analysis must be considered.

If the equivalent-frame method is used to determine the stresses under the design load, the analysis should be carried out for the following load cases:

 (i) All spans loaded with total design load;
(ii) Alternate spans loaded with total design load, all other spans loaded with dead load only.

If the frame provides lateral stability for the structure, the load cases considered must also include the wind load, with the respective partial factors of safety for dead, imposed and wind load described in Chapter 3 .
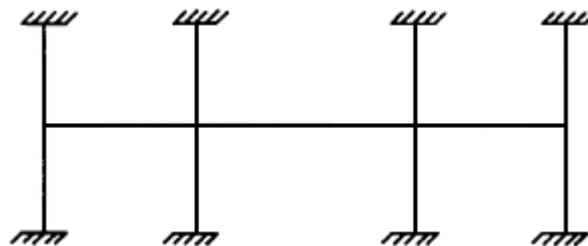
Figure 12.7 Equivalent frame.

As in the case of beams, if the load balancing technique is employed to estimate the prestress force required, it must be decided what proportion of the total design load is to be balanced, and, as described earlier, a common criterion is to balance the quasi-permanent load. The stresses should then be checked under the loading conditions stated above. Stresses at transfer should be checked assuming that only the dead load of the slab is acting, plus, perhaps, a small allowance for construction loads.

For a set of tendons which have been designed to balance a given applied load, Equation 12.1 indicates that the load is distributed to the supports by the tendons in each direction. However, in a flat slab, the 'supports' are themselves tendons, and in order to maintain equilibrium the total upward force in *each* direction provided by the total number of tendons in that direction must balance the *total* load on the panel. Thus, in using the load balancing technique to estimate the prestress force in each direction, prior to carrying out an equivalent-frame analysis, the tendons are determined using the total load to be balanced.

In determining the maximum allowable drape of the tendons in each direction, it is important to remember that the tendons have a finite diameter and, where they cross, one layer must be detailed to lie on top of the other, thus reducing the effective depth of the former. Account must also be taken, at an early stage, of any untensioned reinforcement over supports.

Consideration should be given to any restraint to the free movement of a prestressed concrete slab due to axial shortening, and creep and shrinkage effects. This restraint will have the effect of reducing the prestress in the slab and is caused by the columns and any walls connected to the slab, such as those from lift shafts, for instance. As a guide, if the axial stress in the slab is less than 2 N/mm^2, and there is not more than one stiff restraint between movement joints, then the restraint effect is usually ignored.

12.4 DESIGN AND DETAILING

Much of the design of prestressed concrete flat slabs is similar to that of beams outlined in the preceding chapters. Some of the differences from those methods are described here.

For preliminary estimation of the required slab depth, span/depth ratios in the range of 36–45 for floors and roofs, respectively, may be assumed. Waffle slabs are sometimes used, and the span/depth ratio for these should be taken as 25. Careful attention must be paid to the layout of tendons in these slabs, since they can only be placed in the ribs. Solid slabs with spans in excess of 10 m are likely to require drop panels in order to provide adequate shear resistance at the columns, and waffle

slabs with smaller spans than this will require at least a solid section near the column.

The allowable concrete stresses at the various locations are shown in Table 12.1), where bonded reinforcement may be either bonded tendons or untensioned reinforcement. These stresses are conservative, in order to allow for the fact that approximate analysis methods such as the equivalent-frame method assume uniform distribution of bending moments across any given section and thus underestimate the maximum negative bending moments at the supports. The stresses in Table 12.1 may be relaxed if a rigorous elastic analysis is performed. The allowable stresses given in Chapter 3 may then be used, provided that deflections and ultimate strength capacity are satisfied.

A commonly-used layout of tendons is to place 70% of the total number of tendons in a panel, determined from an equivalent-frame analysis, in a band of width equal to 40% of the bay width, centred on the columns. The remaining tendons are uniformly distributed across the panel, as shown in Fig. 12.3. Maximum spacing of tendons, or groups of tendons, should be six times the slab depth for unbonded tendons or eight times the slab depth for bonded tendons. The minimum spacing between ducts, or groups of ducts, should be 75 mm, or the width of the group of ducts. Cover requirements should be determined from Tables 3.3 and 3.5.

Untensioned reinforcement should be placed in the top of all slabs over the columns, equal in area to a minimum of 0.075% of the gross cross-section of the slab, placed in a width equal to that of the column plus one and a half times the slab depth on each side of the column. Bars should extend at least one-fifth of the span on either side of the column and have a maximum spacing of 300 mm. The combination of tendons and reinforcing bars in the region of the columns could lead to congestion and careful attention should be paid to the detailing in this area.

For unbonded tendon construction, if the midspan tensile stress exceeds $0.17\,f_{ck}^{1/2}$ then untensioned reinforcement is also required. The

Table 12.1 Allowable concrete stresses in slabs

	Compression	Tension	
		With bonded reinforcement	Without bonded reinforcement
At midspan	$0.41\,f_{ck}$	$0.50\,f_{ck}^{1/2}$	$0.17\,f_{ck}^{1/2}$
At columns	$0.30\,f_{ck}$	$0.50\,f_{ck}^{1/2}$	0
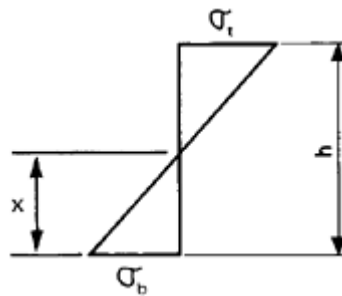
Figure 12.8 Stress distribution at serviceability limit state.

stress distribution within the section over a support at the serviceability limit state may be assumed to be that shown in Fig. 12.8. The untensioned reinforcement should be capable of resisting the total tensile force in the section, so that the area of steel required is given by

$A_s = F_t/(0.625 f_{yk})$
(12.2)

where

$F_t = -\sigma_t \, b(h-x)/2$

and

$(h-x) = -\sigma_t h/(\sigma_b - \sigma_t)$

Note that σ_t in the above expressions should be taken as negative.

Particular attention should be paid to the detailing of reinforcement around the anchorages, since the bursting forces may be high in the thin slab edge. Further information on the design and detailing of prestressed concrete flat slabs may be found in TR43.

Example 12.1 ■■

A prestressed concrete flat slab warehouse floor has the layout shown in Fig. 12.9. The imposed load is 10 kN/m². Determine a preliminary slab depth and layout of unbonded prestressing tendons.

Since the floor is heavily loaded, a span/depth ratio of 33 will be assumed initially. The slab depth required is then 7500/33=227 mm. However, an initial slab depth of 225 mm will be chosen, with drop panels of 100 mm depth.

Loading:

Slab self weight:	5.4 kN/m²
Finishes and services:	1.5 kN/m².
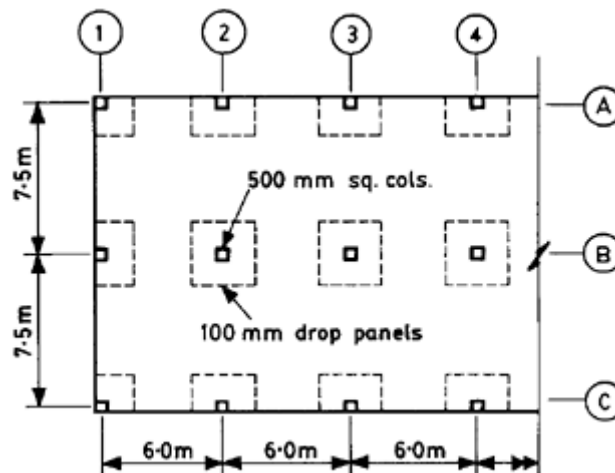
Figure 12.9

Material properties:

Concrete grade: C30/37
Tendons: f_{pk}=1770 N/mm2.

The load to be balanced will be taken as the quasi-permanent load, namely (6.9+0.3×10)=9.9 kN/m^2.

The preliminary design for the transverse tendons only will be presented here; the design for the longitudinal tendons is similar, however.

For exposure class 1, cover to the tendons is 25 mm, with tendon duct diameter of 19 mm. For the purposes of establishing a preliminary tendon profile the increased slab depth at the drop panel will be ignored. Assuming that the transverse tendons are in the outermost layers, and that there is additional untensioned reinforcement of 10 mm diameter over the supports, the maximum eccentricities of the tendons are thus:

Support: e=225/2–25–10−19/2=68 mm
Span: e=225/2−25−19/2=78 mm.

The idealized profile of the tendons is shown in Fig. 12.10. No allowance for the reverse curvature over the support is made at this stage; at detail design stage this refinement can be added. The drape of the tendons in each span is 112 mm, so that the required prestress force to balance the quasi-permanent load is given by

P_x=wL^2/8 d_r
=(9.9×7.5^2)/(8×0.112)
=621.5 kN/m.

Assuming $\beta=0.8$, the initial prestress force required is 776.9 kN/m. For a 15.7 mm dia. superstrand with $A_p=150$ mm^2, the initial prestress force is 185.9 kN, and thus the total number of tendons required per bay is 25.

The equivalent frame to be analysed is shown in Fig. 12.11. For the slab section at the drop, as shown in Fig. 12.12, $I=11.47\times10^9$ mm^4. This frame is most conveniently analysed using a linear elastic frame analysis computer program. The bending moment envelope from such an analysis for the load combinations specified in Section 12.3 is shown in Fig. 12.13.

In order to determine the total prestressing moments in the structure, the equivalent load per bay from the tendons is required:

$$w=8\times0.8\times25\times185.9\times0.112/7.5^2$$
$$=59.2 \text{ kN/m}.$$
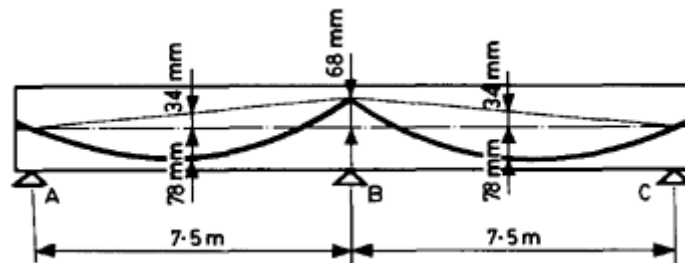
Figure 12.10 Idealized tendon profile.
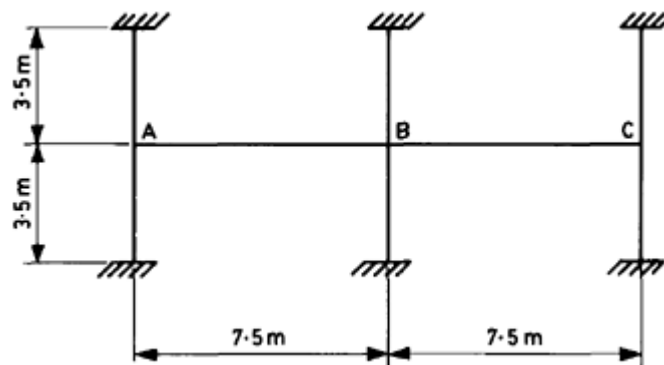
Figure 12.11 Equivalent frame.
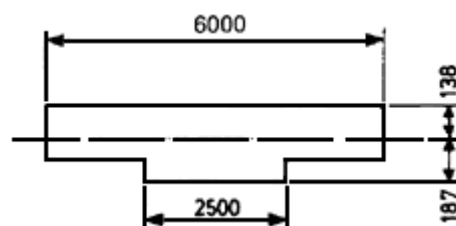
Figure 12.12 Equivalent slab section at drop panel.
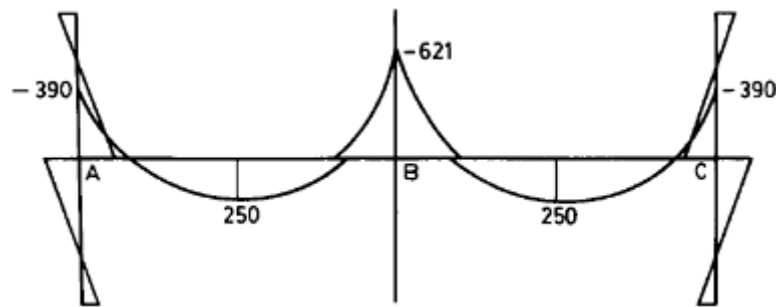
Figure 12.13 Serviceability limit state bending moment envelope (kNm).
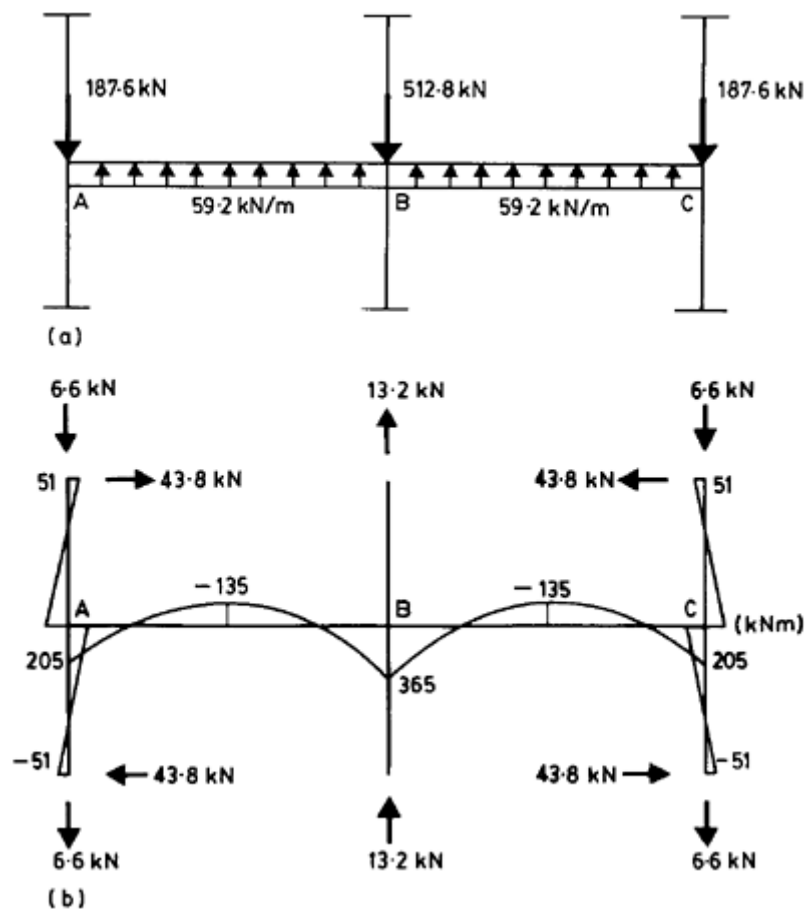
Figure 12.14 (a) Equivalent loads and (b) total prestress moments.

The equivalent loads on the frame from the prestressing tendons are shown in Fig. 12.14(a). The concentrated load at the centre column arises from the sharp change in curvature of the tendons assumed at this stage of the design process. The resulting total prestress moment diagram is shown in Fig. 12.14(b). The reactions on the frame have been shown for later use in finding the secondary moments.

In order to determine the stresses in the slab for support sections, the increase in depth at the drop panel should be considered. Thus:

$Z_t = 11.47 \times 10^9 / 13^8 = 83.12 \times 10^6$ mm^3
$Z_b = 11.47 \times 10^9 / 187 = 61.34 \times 10^6$ mm^3
$A_c = 6000 \times 225 + 2500 \times 100 = 1.6 \times 10^6$ mm^2.

For midspan sections:

$Z_t = Z_b = 6000 \times 225^2 / 6 = 50.63 \times 10^6$ mm^3
$A_c = 6000 \times 225 = 1.35 \times 10^6$ mm^2.

The resulting stresses at the critical sections are shown in Table 12.2, where M is the sum of the bending moments in Figs 12.13 and 12.14(b).

From Table 12.1, for C30/37 concrete the values of fm_{ax} are 12.3 N/mm^2 and 9 N/mm^2 for midspan and support sections, respectively, while the corresponding values of f_{min} are −2.74 N/mm^2 for both locations, assuming that there is sufficient untensioned reinforcement. At midspan, no additional untensioned steel is required since the stress in the concrete is greater than $-0.17 f_{ck}^{1\backslash 2}$.

The stresses in Table 12.2 for the column sections of the slab have been determined for the slab depth at the drop panel. The bending moments in the slab from Figs 12.13 and 12.14(b) are assumed to be distributed uniformly across the panel width, as noted earlier. The stresses in the slab at column sections away from the drop panel would thus be higher than those in Table 12.2. However, as shown in Fig. 12.4(b), the bending moments in flat slabs peak over the columns and the bending moments away from the drop panels would be much less than those indicated in Figs 12.13 and 12.14(b). This is one reason why the tendons are usually grouped close to the columns, as described above. The analysis of stresses described above is therefore only an approximation to the true state of stress in the slab, but it has been found to give satisfactory results.

Table 12.2 Design load stresses for slab in Example 12.1

		P/A_c (N/mm^2)	M (kNm)	M/Z (N/mm^2)	Total (N/mm^2)
Outer columns	Top	2.32	−185	−2.23	0.09
	Bottom	2.32		3.02	5.34
Midspan	Top	2.75	115	2.27	5.02
	Bottom	2.75		−2.27	0.48
Inner columns	Top	2.32	−256	−3.08	−0.76
	Bottom	2.32		4.17	6.49

The amount of untensioned reinforcement required per metre width of slab at the interior support is given by Equation 12.2:

$$A_s = \frac{0.76^2 \times 325 \times 10^3}{2(6.49 + 0.76) \times 0.625 \times 460}$$
$$= 45 \text{ mm}^2/\text{m}.$$

Thus, T10 bars at 300 mm centres, with $A_s = 262$ mm^2/m, would be sufficient.

In order to check the transfer stresses, assume $\alpha = 0.90$. The total bending moment distribution due to the prestress force and the dead load of the slab only is shown in , and the corresponding stresses are shown in . For $f_{ck} = 25$ N/mm^2 at transfer the values of f'_{max} are 10.25 N/mm^2 and 7.5 N/mm^2 for midspan and support sections, respectively. Again, no untensioned reinforcement is required at this location.

The design of the slab so far presented is only preliminary. The tendon profiles must be revised to give a smooth change of curvature over the columns and a detailed estimate made of the prestress losses. A
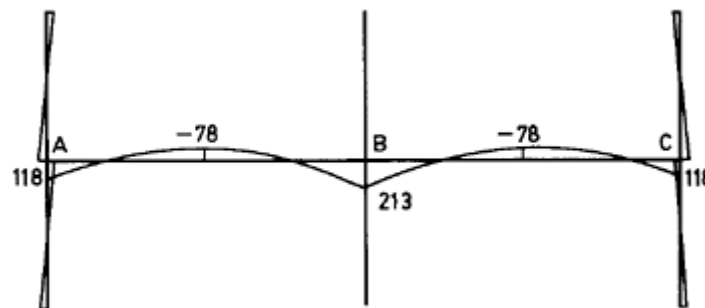
Figure 12.15 Bending and prestress moments at transfer (kNm).

Table 12.3 Transfer stresses for slab in Example 12.1

		P/A_c (N/mm^2)	M (kNm)	M/Z (N/mm^2)	Total (N/mm^2)
Outer columns	Top	2.61	118	1.42	4.03
	Bottom	2.61		−1.92	0.69
Midspan	Top	3.09	−78	−1.54	1.55
	Bottom	3.09		1.54	4.63
Inner columns	Top	2.61	213	2.56	5.17
	Bottom	2.61		−3.47	−0.86

revised analysis of the total prestress moments in the slab can then be carried out and the updated stresses checked against the allowable ones. With experience, the preliminary design should need very little amendment. Finally, the whole design process described above must be repeated for the longitudinal tendons.

■■

12.5 ULTIMATE STRENGTH

The equivalent-frame method described in Section 12.3 can be used to analyse a prestressed concrete flat slab at the ultimate limit state, using the load combinations described in Chapter 11. The method given in TR43 for the determination of the ultimate strength of a slab with unbonded tendons follows that given in BS8110 and is different from that given in Section 5.12. However, in the following the provisions of EC2 will be followed; in practice the differences will be small in most cases.

Most prestressed concrete flat slabs have small percentages of prestressing steel and are thus under-reinforced. Advantage can therefore be taken of moment redistribution, as outlined in Chapter 11, but the maximum amount of such redistribution permitted in BS8110 is 20%.

Example 12.2 ■■

Determine whether the ultimate strength capacity of the slab in Example 12.1 is adequate.

$w_{ult} = (1.4 \times 6.9 + 1.6 \times 10) \times 6$
$= 154$ kN/m.

(Note that the values of γ_f used here are those given in TR43, which follow BS8110.)

The envelope of bending moments for the load combinations specified in Chapter 11 is shown in Fig. 12.16. To this must be added the distribution of secondary moments, determined using $\gamma_p = 1.0$. This can be found either by deducting the primary prestressing moments Pe from the total prestressing moments shown in Fig. 12.14(b), or by analysing the equivalent frame under loading equivalent to the support reactions shown in Fig. 12.14(b), since these are due entirely to secondary effects. In either case, the resulting secondary moment and shear force diagrams are shown in Fig. 12.17(a) and (b), respectively.

The depth of the slab at the supports, and hence its ultimate strength, varies across the panel width due to the increase in slab depth at the drop. However, it is sufficient to check the ultimate strength of the
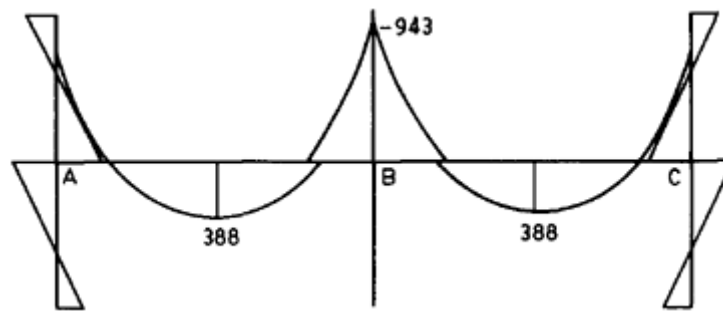
Figure 12.16 Ultimate bending moment envelope (kNm).
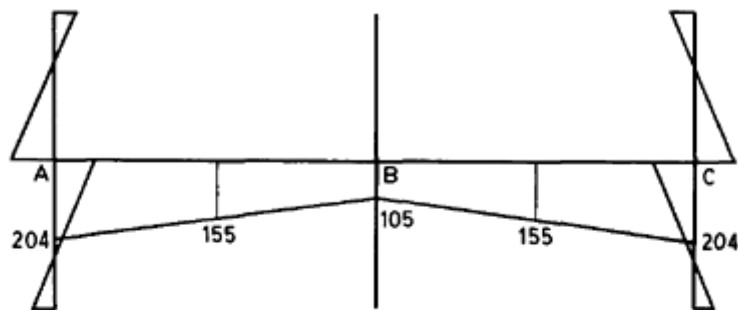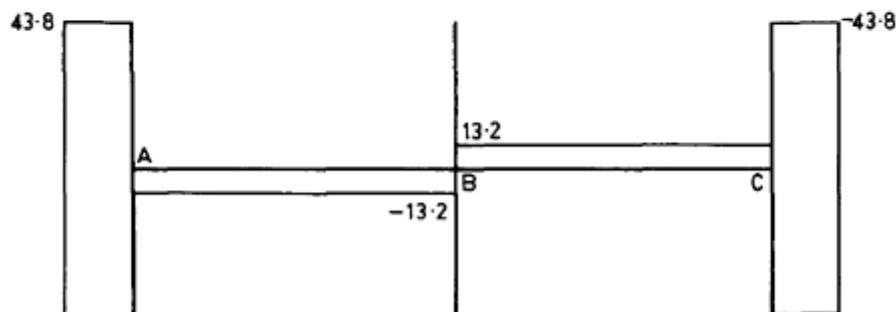
Figure 12.17 (a) Secondary moments (kNm) and (b) shear forces (kN).

support section based on the depth of the slab at the drop and the average ultimate bending moment and average area of prestressing tendons across the panel width. As with the serviceability limit state, the high concentration of actual ultimate bending moments over the columns will be compensated by the grouping of the tendons in the column regions.

For the support sections:

$d=325-25-10-19/2=281$ mm
$A_p=25\times150/6=625$ mm^2/m
$\sigma_{pe}=0.8\times0.7\times1770=991$ N/mm^2.

Thus the stress in the unbonded tendons at the ultimate limit state is 1091 N/mm^2.
The depth of the neutral axis is given by

$0.57\times30\times10^3\times0.8\ x=625\times1091$
$\therefore x=50$ mm.
$M_u=625\times1091\times(281-0.4\times50)\times10^{-6}$
$=178$ kNm/m.

At the central support:

$M_{ult}=(943-105)/6=139.7$ kNm/m.

For the midspan sections:

$d=225-25-19/2=191$ mm.

The depth of the neutral axis is the same as for the support sections and

$M_u=625\times1091\times(191-0.4\times50)\times10^{-6}$
$=116.6$ kNm/m.

At midspan:

$M_{ult}=(388+155)/6=90.5$ kNm/m.

The slab thus has adequate ultimate strength capacity and no additional untensioned reinforcement is required.
■■

12.6 SHEAR RESISTANCE

Wherever a concentrated force is applied to a slab the shear forces local to the force are high. In flat slabs, where the loads are predominately uniform, the areas where the shear resistance of the slab must be checked are around the columns, although if a heavy concentrated load is applied to the slab the shear resistance around this must also be checked.

The determination of the shear resistance of prestressed concrete slabs is carried out in much the same way as for reinforced concrete flat slabs. The clauses in TR43 are based on those in BS8110 for such slabs.

A section through a flat slab around a column is shown in
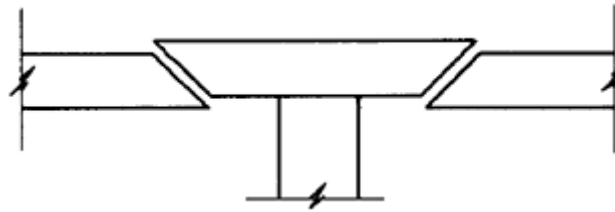
Figure 12.18 Punching shear.
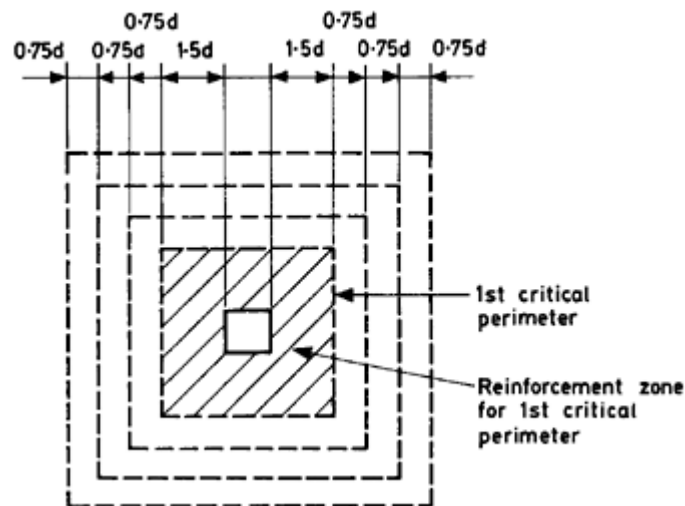
Figure 12.19 Failure zones.

and illustrates the typical *punching* mode of shear failure of such a slab. The actual failure is modelled by assuming a series of vertical failure zones around the column, shown in plan in Fig. 12.19. Each is defined by a *critical perimeter,* with side lengths increasing successively by 0.75 d in each direction, where d is the effective depth of the slab.

The maximum design ultimate shear stress in the slab at the face of the column should not exceed $0.89 f_{ck}^{1/2}$, or 5 N/mm^2, whichever is less.

The shear resistance, V_{cr}, along one side of a critical perimeter is given in TR43 as:

$$V_{cr} = v_c b_v d + M_z \, V/M,$$
(12.3)

where b_v is the length of one side of the critical perimeter, and v_c is taken from Equation 12.4, valid for $f_{ck} \leq 50$ N/mm^2

$$v_c = 0.79 \, (100 A_s / b_v d)^{1/3} \, (f_{ck}/31.25)^{1/3} \, (400/d)^{1/4}/1.25.$$
(12.4)

This value is dependent on the total tensile force along the side of the critical perimeter, and the value of A_s should take into account both

bonded prestressing steel and untensioned reinforcement crossing the critical perimeter. The contribution to shear resistance of unbonded tendons should be ignored. In Equation 12.3, V and M are the ultimate shear force and bending moment, respectively, at the section and M_z is the bending moment to produce zero stress at the extreme tension fibre of the slab, based on a prestress force with a partial factor of safety of 1.25 applied. Thus, for hogging moment regions:

$$M_z = 0.8\ P\ Z_t^*/A_c - 0.8\ P^*e^*,$$
(12.5)

where P is the average prestress force across a full panel width; P^* is the prestress force across the side of the critical perimeter being considered; e^* is the corresponding eccentricity (with positive direction downwards); Z_t^* is the section modulus over the length of the side of the critical perimeter; and A_c is the cross-sectional area of the slab across a full panel width.

Equation 12.3 is adapted from the expression given in BS8110 for the shear resistance of a cracked prestressed concrete section. It shows two components, one based on the tensile strength of the concrete and the other on the shear force in the slab at the section where the first cracking extends into an inclined shear crack (see Section 7.1).

The shear resistances along all sides of the critical perimeter are determined, allowing for the differing values for each side in Equation 12.3, and are summed to give the total shear resistance at the support.

In order to find the effective shear force applied at a column, the ultimate bending moments and shear forces should first be determined from an equivalent-frame analysis, based on the pattern loading described in the previous section. It is recognized that, where an appreciable bending moment is transferred to a column, the distribution of shear forces within the slab is not uniform around the column. An effective shear force, V_{eff}, is used in order to allow for this effect, given by

$$V_{eff} = V_t[1 + (1.5\ M_t/V_t b_v)],$$
(12.6)

where V_t and M_t are, respectively, the total shear force and bending moment transmitted to the column by the slab.

For approximately equal spans, and where the structure is braced against wind loads, V_{eff} may be taken as $1.15\ V_t$ for interior columns, where V_t is based on the case of maximum ultimate load applied to all adjacent panels. If the spans in each direction are substantially different, then Equation 12.6 should be applied independently for each direction and the design checked for the worst case. For corner columns, and for bending of edge columns about an axis perpendicular to the edge, V_{eff} may be taken as $1.4\ V_t$ for approximately equal spans.

The shear resistance at the first critical perimeter should be checked,

and, if V_{eff} is found to exceed the total value of V_{cr}, then either the slab thickness should be increased locally by providing a drop panel or shear reinforcement should be placed within the slab. The shear resistance along successive critical perimeters is then checked, until a point is reached where no reinforcement is required.

For slabs at least 200 mm thick, shear reinforcement in the form of links or bent-up bars may be provided. The area, A_{sv}, of this reinforcement is given by

$$A_{\text{sv}} > (V_{\text{eff}} - V_{\text{cr}})/(0.87\, f_{\text{yv}} \sin \alpha)$$
(12.7)

where f_{yv} is the characteristic strength of the shear reinforcement and α is the inclination of the shear reinforcement to the plane of the slab. In Equation 12.7, the value of $(V_{\text{eff}} - V_{\text{cr}}) > 0.4\ ud$, where $u = 4\ b_{\text{v}}$. The reinforcement should be distributed evenly around the zone, along at least two critical perimeters, and the spacing should not exceed $1.5\ d$. The total shear resistance, regardless of type of reinforcement used, should not exceed twice that of the slab with no reinforcement.

An alternative to links or bent-up bars is to use prefabricated steel shear-heads. The design of these is not covered by TR43 but a suitable method may be found in the American code ACI 318–77 (American Concrete Institute, 1977).

Further information on prestressed concrete flat slabs may be found in Cope and Clark (1984) (design) and Regan (1985) (shear resistance).

Example 12.3 ■■

For the slab in Example 12.1 determine the shear resistance at column B3.

The length of the side of the first critical perimeter is given by

$b_{\text{v}} = 500 + 2 \times 1.5 \times 281$
$= 1343$ mm.

The tendon profile shown in Fig. 12.10 was an approximate one for initial estimation of the prestress force. A more practical profile, showing a smooth change of curvature over the interior column, is shown in Fig. 12.20. The eccentricity at the edge of the critical perimeter can be shown to be −118 mm, allowing for the increase in depth within the drop panel.

The total prestress force across the panel width is given by

$P = 0.8 \times 25 \times 185.9$
$= 3718$ kN.
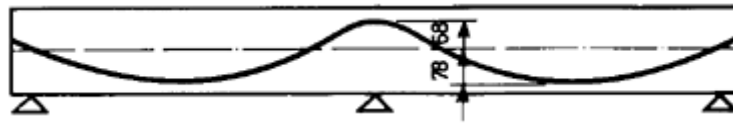
Figure 12.20 Actual tendon profile.

With 70% of the tendons grouped so that they cross the critical perimeter:

$P^*=0.7\times3178$
$=2602.6$ kN.

Also,

$A_c=1.60\times10^6$ mm^2
$Z_t^*=1343\times325^2/6$
$=23.64\times10^6$ mm^3.

The width of slab for placement of untensioned reinforcement

$=500+3\times325$
$=1475$ mm ($>b_v$).

Thus the effective area of reinforcement across the critical perimeter

$=(1.343/1.475)\times262$
$=239$ mm^2.

Ignoring the contribution of the unbonded tendons:

$100\ A_s/bd=100\times239/(1343\times281)$
$=0.063\%$.

Thus:

$v_c=0.79\times0.063^{1/3}(37/31.25)^{1/3}(400/281)^{1/4}/1.25$
$=0.29$N/mm^2.

From Equation 12.5,

$M_z=[0.8\times3718\times10^3\times23.64/1.60-0.8\times2602.6\times10^3\times(-118)]\times\ 10^{-6}=289.6$ kNm.

The ultimate bending moment and shear force diagrams for span AB fully loaded and span BC with minimum load are shown in Fig. 12.21(a) and (b), respectively. From these, and Fig. 12.17(a) and (b):

$M_{BA}=783-105=678$ kNm; $V_{BA}=601+13=614$ kN
$M_{BC}=413-105=308$ kNm; $V_{BC}=200+13=213$ kN.

(a)

(b)
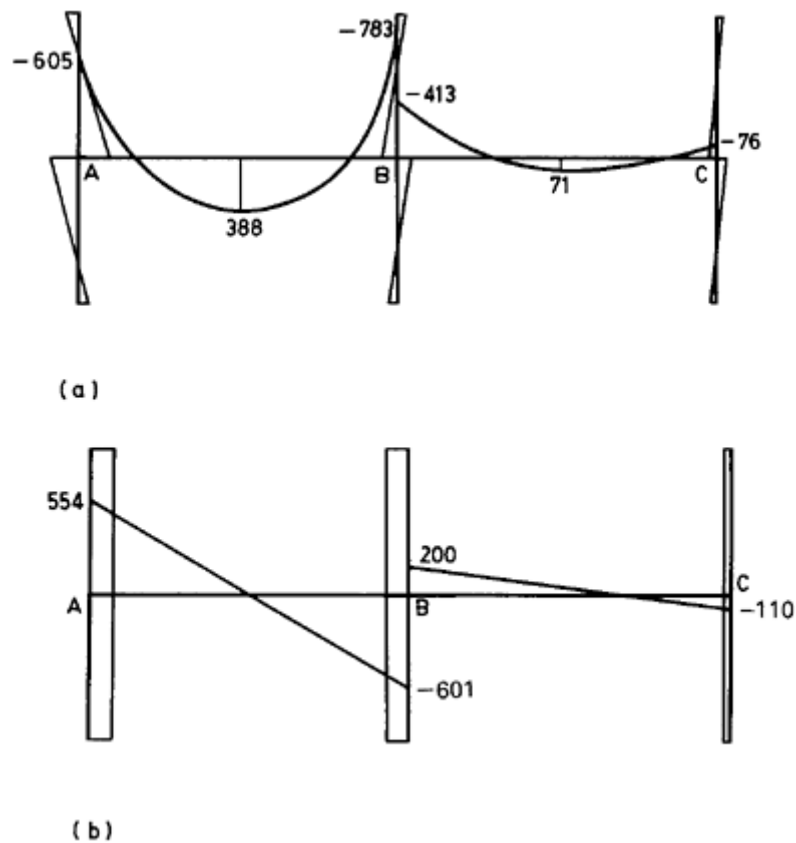
Figure 12.21 Ultimate (a) bending moment (kNm) and shear force (kN) diagrams.

Thus, from Equation 12.3:

$(V_{cr})_{BA}$=0.29×1343×281×10^{-3}+289.6×614/678
=371.7 kN

$(V_{cr})_{BC}$=0.29×1343×281×10^{-3}+289.6×213/308
=309.7 kN.

In the longitudinal direction, for column B3 it can be shown that:

M_0=173.8 kNm; M_{32}=205 kNm; V_{32}=153 kN
M_{34}=480 kNm; V_{34}=574 kN.

Thus:

$(V_{cr})_{32}$=0.29×1343×281×10^{-3}+173.8×153/205
=239.2 kN

$(V_{cr})_{34}$=0.29×1343×281×10^{-3}+173.8+574/480
=317.3 kN,

and the total shear resistance

    =371.7+309.7+239.2+317.3
    =1237.9 kN.

From Equation 12.6:

    V_{eff}=801 [1+1.5×370/(801×1.343)]
    =1214.3 kN,

and thus no shear reinforcement is required.
    Finally, the shear resistance of the slab should be checked at the edge of the drop panel, where the effective depth is reduced.
    ■■

REFERENCES

American Concrete Institute (1977) *Building Code Requirements for Reinforced Concrete,* ACI 318–77, Detroit.

Birkenmaier, M., Welbergen, G.H. and Winkler, N. (1986) *Post-Tensioned Concrete Flat Slabs,* BBR Ltd, Berne.

Concrete Society (1994), *Post-tensioned Concrete Floors—Design Handbook,* Technical Report No. 43, London.

Cope, R.J. and Clark, L.A. (1984) *Concrete Slabs, Analysis and Design,* Elsevier Applied Science, London.

Regan, P.E. (1985) *The Punching Resistance of Prestressed Concrete Slabs.* Proceedings of the Institution of Civil Engineers, Part 2, 79.

13

Design examples

13.1 INTRODUCTION

This chapter presents typical designs of the two types of prestressed concrete member, cracked and uncracked, in the form of computer spreadsheets. These are now widely available and provide an excellent means of performing repetitive calculations quickly and accurately. Once the design is complete the pages can be printed out and inserted in a file as with handwritten calculations.

The spreadsheet used here is Microsoft® Excel™. Microsoft is a registered trademark and Excel is a trademark of Microsoft Corporation. The individual cell formulas listed at the end of each example can be used with little amendment in most of the many other spreadsheets available. The layout of the spreadsheets can be altered to suit individual requirements; it is only important to maintain the relationships between the cells. Diagrams, where required, can be drawn on the printed sheets by hand or by importing graphics drawn using a computer aided drafting program.

The full sets of design inequalities have been shown in Example 13.1 for completeness and the critical ones marked with ***. For a given type of section it will soon become clear which are the most critical and the spreadsheets can be simplified accordingly.

In the listings of cell formulas, (H) after the cell location indicates that the contents are used as intermediate calculations and are not to form part of the completed spreadsheet.

Example 13.2 contains some iterative procedures for cracked section analyses. These require selection of values of ε_c and x until the forces in both steel and concrete match and the resulting moment of resistance equals the applied bending moment at the section.

	A	B	C	D	E	F	G	H
1	Ref.			EXAMPLE 13.1	Uncracked beam			13.1/1
2								
3		Pretensioned double-T floor beams are required to span 15 m.						
4								
5	Table 3.7	Assume exposure class 2(a): Decompression required						
6								
7	Table 3.6	Cover =		40	mm for tendons			
8				35	mm for reinforcement			
9								
10		Loading						
11					kN/m2			
12			Finishes		1.20			
13			Services + ceiling		0.50			
14			Partitions		1.00			
15			Imposed Load		3.00			
16								
17								
18		Material Properties						
19					N/mm2			
20		Concrete	(28 days)	fck	40			
21			(7 days)	f'ck	30			
22								
23		Steel	tendons:	fpk	1860			
24			links:	fyk	250			
25			reinf't:	fyk	460			
26								
27		Allowable Stresses						
28					N/mm2		N/mm2	
29	Sect. 3.7		Transfer:	f'min	-2.9	f'max	18.0	
30	Table 3.3		Service:	fmin	-3.5	(fmax)qp	18.0	
31						(fmax)ra	24.0	
32								
33		Initial Estimate of Beam Depth						
34								
35		L/h =	18					
36								
37		L =	15	m	Thus h =	0.83	m	
38								
39		Chosen Section:						
40					2400 mm	50 mm		
41								
42								
43						Yb 815 mm		
44								
45								

	A	B	C	D	E	F	G	H
46	Ref.			**EXAMPLE 13.1**	Uncracked beam			13.1/2
47								
48		Beam Section Properties:						
49								
50	Beam	B'm d'pth		815	mm	B'm w'dth	2400	mm
51	section	Rib w'dth		160	mm	yb =	539	mm
52	tables	Zt =	8.42E+07	mm3		Ac =	3.66E+05	mm2
53		Zb =	4.29E+07	mm3		Ic =	2.31E+10	mm4
54								
55		Minimum Section Size:						
56								
57		wo =		8.8	kN/m	Mo =	246.9	kNm
58	Table 3.2	wqp =		17.4	kN/m	Mqp =	489.9	kNm
59		wfr =		19.6	kN/m	Mfr =	550.7	kNm
60		wra =		22.5	kN/m	Mra =	631.7	kNm
61								
62		Assume alpha =	0.9		and beta =	0.65		
63								
64	Equ. 9.3(a)	Zt >=	1.55E+07	mm3				
65	Equ. 9.3(b)	Zt >=	1.74E+07	mm3	***			Section
66								size
67	Equ. 9.3(c)	Zb >=	2.75E+07	mm3	***			adequate
68								
69		Prestress Force						
70								
71		Effective depth of tendons =			729	mm		
72				e max =	453	mm		
73								
74	Equ. 9.4(a)	Po <=	2454.0	kN	(denominator negative)			
75	Equ. 9.4(b)	Po <=	1985.6	kN	***			
76	Equ. 9.4(c)	Po >=	-7099.1	kN	(denominator negative)			
77	Equ. 9.4(d)	Po >=	-9614.6	kN	(denominator negative)			
78	Equ. 9.4(e)	Po >=	1300.6	kN	***			
79								
80		No. of 12.9 mm dia. super strands			=	14		
81								
82		Po =	1822.8	kN	Ap =	1400	mm2	
83								
84		**Check for Decompression**						
85								
86		At 25 mm below lowest tendon, using 0.9 Po:						
87								
88		zb25 =	4.46E+07	mm3				
89								Decompr.
90		(fb25)fr =		1.39	N/mm2	(> 0)		satisfied

	A	B	C	D	E	F	G	H
91	Ref.		EXAMPLE 13.1		Uncracked beam			13.1/3
92								
93		(fb)ra =		-0.56	N/mm2	(>fmin)		Section
94								uncracked
95		Estimate of Losses						
96								
97		(i) Elastic shortening						
98								
99				fpo =	1302.0	N/mm2		
100				m =	6.3			
101				r =	251	mm		
102								
103	Equ. 4.5	At midspan:		fcg =	14.4	N/mm2		
104								
105		At supports, assume that no. of tendons						
106		to be debonded	=	6				
107								
108				fcg =	11.4	N/mm2		
109								
110			Average	fcg =	12.9	N/mm2		Midspan
111								alpha =
112	Equ. 4.1			Delta Po =	112.9	kN		0.94
113								
114		(ii) Long-term losses						
115								
116	Table 2.2	Creep coefficient	=	1.5				
117								
118	Table 2.3	Shrinkage strain	=	3.00E-04				
119								
120	Fig 2.7	Low-relaxation steel,		delta fpr =		39.1	N/mm2	
121	Table 4.3							
122		At midspan:		fcg =	10.24	N/mm2		
123								
124				fcpo=	19.85	N/mm2		
125								
126	Equ. 4.10			Long-term losses =	311.6	N/mm2		
127								
128		At the supports:		fcg = fcpo =	11.34	N/mm2		
129								
130	Equ. 4.10			Long-term losses =	254.8	N/mm2		
131								
132			Average long-term losses =		283.2	N/mm2		Midspan
133								beta =
134				Delta Po=	396.5	kN		0.72
135								

	A	B	C	D	E	F	G	H
136	Ref.		EXAMPLE 13.1		Uncracked beam			13.1/4
137								
138		Cable Zone						
139								
140		Limits are given by:						
141								
142			m	0	2.5	5	7.5	
143			Mo	0.0	137.2	219.5	246.9	
144			Mqp	0.0	272.2	435.5	489.9	
145			Mra	0.0	350.9	561.5	631.7	
146	Equ 9.6(a)	***	e<=	373	453	501	518	
147	Equ 9.6(b)		e<=	334	414	462	478	
148	Equ 9.6(c)		e>=	-924	-717	-592	-551	
149	Equ 9.6(d)		e>=	-1309	-1042	-881	-828	Debonding
150	Equ 9.6(e)	***	e>=	-231	36	196	250	required
151								
152	Equ 9.6(a)	Distance to theoretical debonding point			=	2.47	m	
153								
154		No. of tendons debonded		=	6			
155								
156		Remaining prestressing force		=	1041.6	kN		
157								
158		Limits in debonded zone are given by:						
159								
160			m	0	1.24	1.86	2.47	
161			Mo	0.0	74.7	107.0	136.0	
162			Mra	0.0	191.2	273.8	347.9	
163	Equ 9.6(a)		e<=	480	557	590	619	
164	Equ 9.6(e)		e>=	-317	-62	48	147	
165								
166	Table 8.1	Transmission length		=	0.774	m		
167	Equ 8.1							
168		Actual debonding length		=		1.545	m from support	
169								
170		Ultimate Strength						
171								
172		Assuming that neutral axis lies within the flange:						
173								
174		x =	46.4	mm				NA in
175								flange
176		ep =	0.0562	(> 0.00651)				Steel has
177								yielded
178		Mu =	1442.3	kNm				
179								
180		wult =	32.9	kN/m				

	A	B	C	D	E	F	G	H
181	Ref.		EXAMPLE 13.1		Uncracked beam			13.1/5
182								Ultimate
183		Mult =	924.8	kNm				strength
184								adequate
185		Shear						
186								
187		At support, effective depth d to tendons			=	696	mm	
188		(lowest 6 no. tendons debonded)						
189								
190		At distance d away from support, Vsd			=	223.7	kN	
191								
192					Msd =	163.6	kNm	
193		ro(l) =	0.36%					
194								
195		k =	0.90		nu =	0.5		
196								
197	Table 7.1	Basic shear str'ngth =			0.41	N/mm2		
198								Shear
199	Equ. 7.1	VRd1 =	230.8	kN				reinf't.
200								required
201	Equ. 7.3	VRd2 =	1870.4	kN				
202	Equ. 7.4							
203	Equ. 7.2	Asw/s =	-0.05					
204								
205		Link dia =	12	mm				
206								
207		s =	-4333	mm				
208								
209	Equ. 7.5	Td =	112.1	kN				
210								
211		As =	280	mm2				
212								
213								
214		Deflection						
215								
216		(a) Initial camber						
217								
218		Ecm =	32	kN/mm2				
219								
220		do =	-21.6	mm				
221								
222								
223								
224								
225								

	A	B	C	D	E	F	G	H
226	Ref.		EXAMPLE 13.1		Uncracked beam			13.1/6
227								
228		(b) Quasi-permanent load						
229								
230		Ecm =		12.8 kN/mm2				
231								
232		dqp =	-17.7	mm				
233								Deflection
234		Span/deflec. ratio	=	-846				satisfactory
235								
236								
237								
238								
239								
240								
241								
242								
243								
244								
245								
246								
247								
248								
249								
250								
251								
252								
253								
254								
255								
256								
257								
258								
259								
260								
261								
262								
263								
264								
265								
266								
267								
268								
269								
270								

Example 13.1 Uncracked beam ■■

Cell	Formula
G29	0.6*E21
G30	0.45*E20
G31	0.6*E20
F37	C37/C35
C57	24*F52/1E6
C58	C57+F50*(E12+E13+E14+0.3*E15)/1E3
C59	C58+F50*0.3*E15/1E3
C60	C59+0.4*F50*E15/1E3
F57	C57*C37$\wedge$2/8
F58	C58*C37$\wedge$2/8
F59	C59*C37$\wedge$2/8
F60	C60*C37$\wedge$2/8
C64	(D62*F58−F62*F57)*1E6/(D62*G30−F62*E29)
C65	(D62*F60−F62*F57)*1E6/(D62*G31−F62*E29)
C67	(D62*F60−F62*F57)*1E6/(F62*G29−D62*E30)
E71	C50−(C8+C205+1.5*12.9+20)
E72	F51−(C50−E71)
C74	(C52*E29−F57*1E6)/(D62*1E3*(C52/F52−E72))
C75	(C53*G29+F57*1E6)/(D62*1E3*(C53/F52+E72))
C76	(C52*G30−F58*1E6)/(F62*1E3*(C52/F52−E72))
C77	(C52*G31−F60*1E6)/(F62*1E3*(C52/F52−E72))
C78	(C53*E30+F60*1E6)/(F62*1E3*(C53/F52+E72))
C82	0.7*E23*F82/1E3
F82	F80*100
C88	F53/(F51−C8+25−C205−12.9/2)
C90	0.9*F62*C82*1E3*(1/F52+E72/C88)−F59*1E6/C88
C93	0.9*F62*C82*1E3*(1/F52+E72/C53)−F60*1E6/C53
E99	C82*1E3/F82
E100	200/C218
E101	(F53/F52)$\wedge$0.5
E103	E99/(E100+F52/(F82*(1+(E72/E101)$\wedge$2)))−F57*1E6*E72/F53
E108	E99/(E100+F52/(F82*(F80−D106)/F80*(1+(E72/E101)$\wedge$2)))
E110	(E103+E108)/2
E112	E100*E110*F82/1E3
H112	(C82−E112)/C82
E120	0.025*1.2*0.7*E23
E122	C82*H112*1E3*(1/F52+E72$\wedge$2/F53)−F58*1E6*E72/F53
E124	C82*H112*1E3*(1/F52+E72$\wedge$2/F53)
E126	(D118*200*1E3+E120+E100*D116*(E122+E123))/ (1+E100*F82/F52*(1+F52*E72$\wedge$2/F53)*(1+0.8*D116))
E128	E124*(F80−D106)/F80
E130	(D118*200*1E3+E120+E100*D116*2*E128/(1+E100*F82/ F52*(1+F52*E72$\wedge$2/F53)*(1+0.8*D116))

E132	(E126+E130)/2
E134	E132*F82/1E3
H134	(C82−E112−E134)/C82
D143	C57*D142*(C37−D142)/2
D144	C58*D142*(C37−D142)/2
D145	C60*D142*(C37−D142)/2
D146	(−C52*E29+D143*1E6)/(H112*C82*1E3)+C52/F52
D147	(C53*G29+D143*1E6)/(H112*C82*1E3)−C53/F52
D148	(−C52*G30+D144*1E6)/(H134*C82*1E3)+C52/F52
D149	(−C52*G31+D145*1E6)/(H134*C82*1E3)+C52/F52
D150	(C53*E30+D145*1E6)/(H134*C82*1E3)−C53/F52
F152	(−F153−(F153∧2–4*G153)∧0.5)/(2*1E3)
F153(H)	−C37*1E3
G153(H)	((E72−C52/F52)*H112*C82*1E3+C52*E29)*2/C57
E156	(F80−E154)*C82/F80
D163	(−C52*E29+D161*1E6)/(H112*E156*1E3)+C52/F52
D164	(−C53*E30+D162*1E6)/(H134*E156*1E3)−C53/F52
E166	60*12.9/1E3
E168	F152−E166*1.2
C174	0.78*E23*F82/(0.456*E20*F50)
C176	C82*H134/(F82*200)+(E71−C174)*0.0035/C174
C178	0.78*E23*F82*(E71−0.4*C174)/1E6
C180	1.35*(C57+(E12+E13+E14)*F50/1E3+1.5*E15*F50/1E3
C183	C180*C37∧2/8
F187	E71−(20+12.9)
F190	C180*(C37/2−F187/1E3)
F192	C180*F187*(C37−F187/1E3)/(2*1E3)
C193	(F80−E154)*F82/(2*F187*C51*F80)
C195	1.6−F187/1E3
F195	0.7−E20/200
C199	(D197*C195*(1.2+40*C193)+0.15*C82*H134*1E3/ F52)*2*C51*F187/1E3
C201	0.3*F195*E20*2*C51*F187*67*(1−1.5*1.2*C82*H134*1E3/ (F52*E20))/1E3
C203	(F190−C199)*1E3/(0.78*E24*F187)
C207	D205∧2*PI()/(2*C203)
C209	F192/(0.9*F187)+F190/2
C211	C209*1E3/(0.87*E25)
C220	−C37∧2*C82*H112*E72*1E6/(8*C218*F53)+ 5*C57*C37∧4*1E9/(384*C218*F53)
C230	C218/(1+D116)
C232	−C37∧2*C82*H134*E72*1E6/(8*C230*F53)+ 5*C58*C37∧4*1E9/(384*C230*F53)
D234	C37/C232*1E3

■■

	A	B	C	D	E	F	G	H
1	Ref.			EXAMPLE 13.2 - Cracked beam				13.2/1
2								
3		Pretensioned floor beams at 450 mm centres are required						
4		to span 5 m, supporting hollow-core tiles.						
5								
6	Table 3.7	Assume exposure class 1:			wk = 0.2 mm			
7								
8	Table 3.6	Cover =		25	mm for tendons			
9				20	mm for reinforcement			
10								
11		Loading						
12					kN/m2			
13			Hollow-core tiles		2.80			
14			Finishes		1.20			
15			Services + ceiling		0.75			
16			Partitions		1.00			
17			Imposed Load		4.00			
18								
19								
20		Material Properties						
21					N/mm2			
22		Concrete	(28 days)	fck	30			
23			(7 days)	f'ck	25			
24								
25		Steel	tendons:	fpk	1770			
26			reinf't:	fyk	460			
27								
28								
29		Allowable Stresses						
30					N/mm2		N/mm2	
31	Sect 3.7		Transfer:	f'min	-2.6	f'max	15.0	
32	Table 3.3		Service:	fmin	-2.9	(fmax)qp	13.5	
33						(fmax)ra	18.0	
34								
35		Ultimate Strength (Preliminary)						
36								
37		Span =		5	m			
38								
39		Floor beams:		h =	225	mm		
40				b =	150	mm		
41				Spacing =	450	mm		
42								
43		Wire dia.=		5	mm Effect. depth =	195	mm	
44								
45								

	A	B	C	D	E	F	G	H
46	Ref.			EXAMPLE 13.2 - Cracked beam				13.2/2
47								
48		wo =		0.81	kN/m	wult =	7.29	kN/m	
49								
50		Mult =		22.8	kNm				
51								
52		Assume beta	=	0.8				
53								
54	Sect. 9.8	For equilibrium in section:			$x =$	66	mm	
55		(assuming steel has yielded)						
56					Ap req'd =	98	mm2	
57								Steel has
58		epk =	0.00620		ep =	0.01176		yielded
59								
60								
61		Beam Section Properties:						
62								
63		Z_t =	1.27E+06	mm3				
64		Z_b =	1.27E+06	mm3				
65		Ac =	3.38E+04	mm2				
66		Ic =	1.42E+08	mm4				
67		yb =	112.5	mm				
68					Mo =	2.5	kNm	
69		wqp =		3.9	kN/m	Mqp =	12.3	kNm	
70		wfr =		4.5	kN/m	Mfr =	14.0	kNm	
71		wra =		5.2	kN/m	Mra =	16.2	kNm	
72								
73		Prestress Force						
74								
75		Adopt criterion of zero tension under quasi-permanent load:						
76								
77		e =		82	mm	Po req'd =	128.7	kN	
78								
79		Provide :		4	no. 5mm dia. cold-drawn wires			
80								Untens'd
81		Po =	97.1	kN	Ap =	78.4	mm2	steel
82								required
83	Sect. 9.8	For equilibrium in section:			$x =$	66	mm	
84		(assuming steel has yielded)						
85					As =	68	mm2	
86		Try:						
87		2	T	8	As prov.=	101	mm2	
88								Steel has
89		Check:	ep =	0.01176				yielded
90								

	A	B	C	D	E	F	G	H
91	Ref.			EXAMPLE 13.2 - Cracked beam				13.2/3
92								
93		Estimate of Losses						
94								
95		(i) Elastic shortening						
96								
97			fpo =	1239.0	N/mm2			
98			m =	6.6				
99			r =	65	mm			
100								
101	Equ. 4.5	At midspan:		fcg =		5.2 N/mm2		
102								
103		At support:		fcg =		7.2 N/mm2		
104								
105			Average	fcg =		6.2 N/mm2		Midspan
106								alpha =
107	Equ. 4.1			Delta Po =	3.2	kN		0.97
108								
109								
110		(ii) Long-term losses						
111								
112	Table 2.2	Creep coefficient	=	1.5				
113								
114	Table 2.3	Shrinkage strain	=	3.00E-04				
115								
116	Fig. 2.7	Low-relaxation steel, delta fpr	=		37.2 N/mm2			
117	Table 4.3							
118		At midspan:		fcg =		0.13 N/mm2		
119								
120				fcpo =		7.22 N/mm2		
121								
122	Equ. 4.10			Long-term losses =		164.0 N/mm2		
123								
124		At the supports:		fcg = fcpo =		7.22 N/mm2		
125								
126	Equ. 4.10			Long-term losses =		231.5 N/mm2		
127								
128			Average long-term losses =			197.7 N/mm2		Midspan
129								beta =
130				Delta Po =	15.5	kN		0.81
131								
132								
133								
134								
135								

	A	B	C	D	E	F	G	H
136	Ref.			EXAMPLE 13.2 - Cracked beam				13.2/4
137								
138		Cracking						
139								
140		Check for cracked section:						
141								Section
142		(fb)ra =		-6.17	N/mm2	< fmin		cracked
143								
144		Ecm =		32.00	kN/mm2			
145								
146		Frequent load:				Mfr =	14.0	kNm
147								
148		ec	x	Fc	Fp	Fs	(Fsp+Fs)	Mr
149		0.000387	90	83.6	77.0	9.0	86.0	14.00
150		0.000387	91	84.5	76.8	8.8	85.7	13.99
151	***	0.000387	92	85.4	76.7	8.7	85.4	13.99
152		0.000387	93	86.4	76.6	8.5	85.1	13.99
153		0.000387	94	87.3	76.4	8.3	84.8	13.99
154								
155		fs =		86	N/mm2			
156								
157		Cracking load:				Mcr =	12.1	kNm
158								
159		ec	x	Fc	Fp	Fs	(Fsp+Fs)	Mr
160		0.000283	112	76.1	73.6	4.2	77.7	12.09
161		0.000283	113	76.7	73.5	4.1	77.6	12.11
162	***	0.000283	114	77.4	73.4	4.0	77.4	12.12
163		0.000283	115	78.1	73.4	3.9	77.3	12.13
164		0.000283	116	78.8	73.3	3.9	77.2	12.15
165								
166	Equ. 5.3	fsr =		40	N/mm2	esm =	0.0003385	
167								Cracking
168	Equ. 5.2	srm =		120	mm	wk =	0.07	mm	satisf'ry
169								
170		Concrete Stresses						
171								
172		Transfer:						
173			Midspan:	ft =	-1.30	N/mm2	> f'min	
174								
175				fb =	6.87	N/mm2	< f'max	
176		Quasi-permanent load:						
177								
178			Midspan:	(ft)qp =	7.56	N/mm2	<(fmax)qp	
179								
180			Support:	ft =	-2.76	N/mm2	> fmin	

	A	B	C	D	E	F	G	H
181	Ref.			EXAMPLE 13.2 - Cracked beam				13.2/5
182								
183				fb =	7.41	N/mm2	< fmax	
184								
185		Shear						
186								
187		At distance d away from support, Vsd			=	16.8	kN	
188								
189		ro(l) =	0.61%					
190								
191		k =	1.41		nu =	0.55		
192								
193	Table 7.1	Basic shear strength =				0.35	N/mm2	
194								No shear
195	Equ. 7.1	VRd1 =	27.8	kN				reinf't.
196								required
197		Minimum links:						
198								
199	Table 7.2	Asw/s =	0.36		Link dia. =		8	mm
200								
201		s =	279	mm				
202								
203		Vsd < 2/3 VRd2; smax =				117	mm	
204								
205								
206		Deflection						
207								
208		(a) Initial camber			Ecm =		30.5	kN/mm2
209								
210		do =	7.1	mm	(assuming uncracked section)			
211								
212		(b) Quasi-permanent load			Ecm =		12.2	kN/mm2
213								
214	Equ. 6.1	At midspan, 1/r1(uncracked)		=	7.08E-06	mm-1		
215								
216		dqp(uncracked)		=	18.4	mm		
217								
218		For cracked section:			Mqp =		12.3	kNm
219								
220		ec	x	Fc	Fp	Fs	(Fsp+Fs)	Mr
221		0.000620	148	84.0	81.5	3.9	85.4	12.26
222		0.000620	149	84.5	81.4	3.8	85.2	12.27
223	***	0.000620	150	85.1	81.3	3.7	85.0	12.29
224		0.000620	151	85.7	81.3	3.6	84.8	12.31
225		0.000620	152	86.2	81.2	3.5	84.7	12.34

	A	B	C	D	E	F	G	H
226	Ref.		EXAMPLE 13.2 - Cracked beam					13.2/6
227								
228		fs =		37 N/mm2	Distribution coeff.	=	0.153	
229								
230			dqp (cracked) =	10.7 mm				
231								Deflection
232	Equ. 6.5	dqp =	11.9	mm	Span/deflec. ratio	=	419	satisf'ry
233								
234								
235								
236								
237								
238								
239								
240								
241								
242								
243								
244								
245								
246								
247								
248								
249								
250								
251								
252								
253								
254								
255								
256								
257								
258								
259								
260								
261								
262								
263								
264								
265								
266								
267								
268								
269								
270								

Example 13.2 Cracked beam ■■

Cell	Formula
G31	0.6*E23
G32	0.45*E22
G33	0.6*E22
F43	E39–C9–F199–C43/2
C48	E39*E40*24/1E6
F48	1.35*(C48+E41*(E13+E14+E15+E16)/1E3)+1.5*E41*E17/ 1E3
C50	F48*C37$\wedge$2/8
F54	(−H54−(H54$\wedge$2–4*H55)$\wedge$0.5)/2
H54(H)	−F43*2.5
H55(H)	5.485*C50*1E6/(E40*E22)
F56	0.585*E22*E40*F54/E25
C58	0.7*E25/(200*1E3)
F58	D52*C58+(F43−F54)*0.0035/F54
C63	C66/C67
C64	C66/(E39−C67)
C65	E39*E40
C66	E40*E39$\wedge$3/12
C67	E39/2
F68	C48*C37$\wedge$2/8
F69	C69*C37$\wedge$2/8
F70	C70*C37$\wedge$2/8
F71	C71*C37$\wedge$2/8
C69	C48+E41*(E13+E14+E15+E16)/1E3+0.3*E41*E17/1E3
C70	C69+0.3*E41*E17/1E3
C71	C70+0.4*E41*E17/1E3
C77	F43−(E39−C67)
F77	F69*1E3/(C64*D52*(1/C65+C77/C64))
C81	0.7*E25*F81/1E3
F81	C79*19.6
F83	F54
F85	(0.456*E40*E22*F83–0.78*E25*F81)/(0.87*E26)
F87	B87*D87$\wedge$2*PI()/4
D89	D52*C58+(F43−F83)*0.0035/F83
D97	0.7*E25
D98	200/F208
D99	(C66/C65)$\wedge$0.5
E101	D97/(D98+C65/(F81*(1+(C77/D99)$\wedge$2)))−F68*C77*1E6/C66
E103	D97/(D98+C65/(F81*(1+(C77/D99)$\wedge$2)))
E105	(E101+E103)/2
E107	(D98*E105)*F81/1E3

H107   (C81−E107)/C81

E116   0.025*1.2*0.7*E25

E118   C81*H107*1E3*(1/C65+C77∧2/C66)−F69*1E6*C77/C66

E120   C81*H107*1E3*(1/C65+C77∧2/C66)

E122   (D114*200*1E3+E116+D98*D112*(E118+E120)/ (1+D98*F81/C65*(1+C65*C77
        ∧2/C66*(1+0.8*D112)))

E124   E120

E126   (D114*200*1E3+E116+D98*D112*2*E124/(1+D98*F81/ C65*(1+C65*C77∧
        2/C66*(1+0.8*D112))

E128   (E122+E126)/2

E130   E128*F81/1E3

H130   (C81−E107−E130)/C81

C142   0.9*H130*C81*1E3*(1/C65+C77/C64)−F70*1E6/C64

F146   F70

B150   B149

C150   C149+1

D150   B150*C150*C144*E40/2

E150   ((F43−C150)/C150*B150+H130*C58*200*F81*0.9

F150   (F43−C150)/C150*B150*200*F87

G150   E150+F150

H150   (D150*C150*2/3+G150*(F43−C150))/1E3

C155   (F43−C151)/C151*B151*200*1E3

F157   0.9*H130*C81*1E3*((1/C65+C77/C64)−E32)*C64/1E6

C166   ((F43−C162)/C162*B162*200*1E3

F166   C155*(1−(C166/C155)∧2)/(200*1E3)

C168   50+0.25*0.5*(2.0*C79*5+0.8*B87*D87)/(C79+B87)/
        ((F81+F87)/(2.5*E40*(E39−F43)))

F168   1.7*C168*F166

E173   H107*C81*1E3*(1/C65−C77/C63)+F68*1E6/C63

E175   H107*C81*1E3*(1/C65+C77/C64)−F68*1E6/C64

E178   B223*F212*1E3

E180   H130*C81*(1/C65−C77/C63)

E183   H130*C81*(1/C65+C77/C64)

F187   F48*(C37/2−F43/1E3)

C189   (F81+F87)/(E40*F43)

C191   1.6−F43/1E3

F191   0.7−E22/200

C195   (E193*C191*(1.2+40*C189)+0.15*H130*C81*1E3/ C65)*F43*E40/1E3

C199   0.0024*E40

C201   F199∧2*PI()/(2*C199)

E203   0.6*F43

C210   −C37∧2*H107*C81*C77*1E6/(8*F208*C66)+ 5*C48*C37∧
        4*1E9/(384*F208*C66)

F212	F208/(1+D112)
E214	F69*1E3/(F212*C66)
D216	E214*0.104*C37∧2*1E6
F218	F69
B222	B221
C222	C221+1
D222	B222*C222*F212*E40/2
E222	((F43−C222)/C222*B222+H130*C58)*200*F81
F222	(F43−C222)/C222*B222*200*F87
G222	E222+F222
H222	(D222*C222*2/3+G222*(F43−C222))/1E3
C228	(F43−C223)/C223*B223*200*1E3
G228	1−(C228/C166)∧2
D230	B223/C223*0.104*C37∧2*1E6
C232	F228*D21 6+(1−F228)*D230
G232	C37*1E3/C232

Solutions to problems

1.1 54 kgf

1.2 26.6 kg

1.3 102.9 N/mm^2; 10.3 N/mm^2

1.4 19.5 mm

1.6 490 kN; 0.29 mm

1.7 3.06m

4.1 0.9%

4.2 r_{ps1}=105.47 m; r_{ps2}=20.09 m: 576 mm

4.3 2.9%

4.4 1.9mm

5.1 16.51 N/mm^2; −2.42 N/mm^2

5.2 A=2.63 N/mm^2; B=−1.91 N/mm^2

5.3 4.6%; σ_t=−0.56 N/mm^2; σ_b=9.38 N/mm^2; introduce lower chord of concrete framework, not connected to tendon

5.4 Cantilever support: σ_t=−2.58 N/mm^2; σ_b=12.06 N/mm^2
Midspan: σ_t=9.20 N/mm^2; σ_b=−2.92 N/mm^2

5.5 σ_c=6.34 N/mm^2; σ_s=1057 N/mm^2

5.6 14 208 kNm

5.7 $M_u/(bd^2f_{ck})$=0.78 (1–0.416 x/d)(A_pf_{pk}/bdf_{ck})

6.1 PL^2/Ebh^3 (0.148 e_1+0.0625 e_2)

6.2 −25.9 mm

9.1 6 no.; 4 no.

9.2 40.3 kN/m; 2548.0 kN.

10.1 2393.6 kN.

10.2 3286.5 kNm

10.3 (i) −1.97 N/mm^2 (ii) −3.45 N/mm^2 (iii) −1.60 N/mm^2 (iv) −3.43 N/mm^2

11.1 −1408/EI m.

11.2 (i) R_A=−15.7 kN; $_{RB}$=15.7 kN; R_C=15.7 kN; R_D=−15.7 kN
(ii) R_A=14.3 kN; $_R$B=−44.4 kN; R_C=45.8 kN; R_D=−15.7 kN

11.3 The line of pressure is a linear transformation of the original profile. Therefore the new profile and its line of pressure are coincident.

11.4 (i) -9.73 N/mm^2 (ii) -3.54 N/mm^2; max. 16.95 N/mm^2, min. 11.38 N/mm^2.

11.5
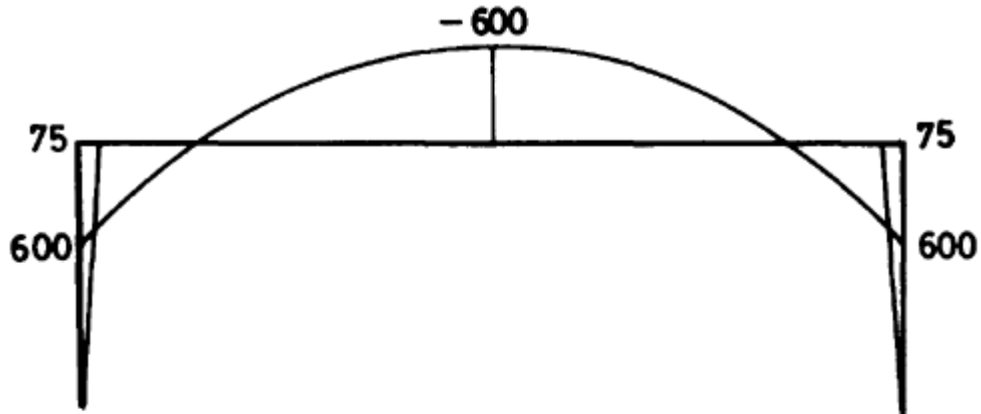
(a) Primary moments (kNm)
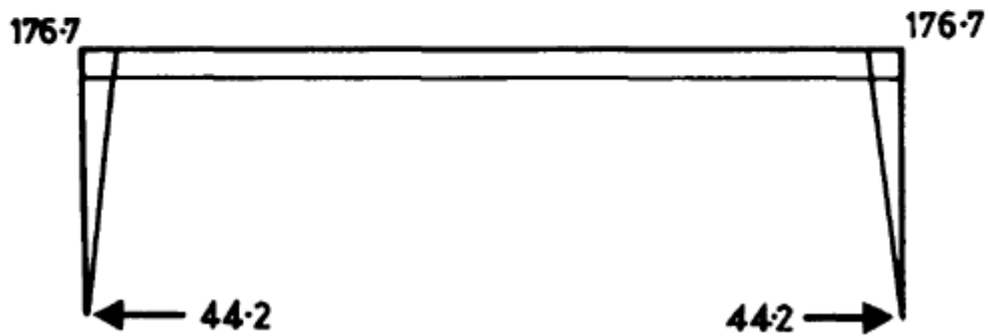
(b) Secondary moments and reactions (kNm, kN)

Bibliography

GENERAL

Abeles, P.W. and Bardhan-Roy, B.K. (1981) *Prestressed Concrete Designer's Handbook,* Viewpoint, Slough.

Allen, A.H. (1981) *An Introduction to Prestressed Concrete,* Cement and Concrete Association, Slough.

Bate, S.C.C. and Bennett, E.W. (1976) *Design of Prestressed Concrete,* Wiley, New York.

Beeby, A.W. and Narayanan, R.S. (1995) *Designer's Handbook to Eurocode 2, Part 1.1: Design of Concrete Structures ,* Thomas Telford, London.

British Cement Association (1994) *'Worked Examples for the Design of Concrete Buildings',* London.

British Cement Association (1993) *'Concise Eurocode for the Design of Concrete Buildings',* London.

Gerwick, B.C. (1971) *Construction of Prestressed Concrete Structures,* Wiley, New York.

Guyon, Y. (1974) *Limit State Design of Prestressed Concrete,* Applied Science, London.

Krishna Raju, N. (1981) *Prestressed Concrete,* Tata McGraw-Hill, New Delhi.

Leonhardt, F. (1964) *Prestressed Concrete: Design and Construction,* Wilhelm Ernst, Berlin.

Libby, J.R. (1977) *Modern Prestressed Concrete,* Van Nostrand Reinhold, New York.

Lin, T.Y. and Burns, N.H. (1981) *Design of Prestressed Concrete Structures,* Wiley, New York.

Mosley, W.H., Hulse, R. and Bungey, J.H. (1996) *Reinforced Concrete Design to Eurocode 2,* Macmillan, London.

Naaman, A.E. (1981) *Prestressed Concrete Analysis and Design,* McGraw-Hill, New York.

Nilson, A.H. (1978) *Design of Prestressed Concrete,* Wiley, New York.

Ramaswamy, G.S. (1976) *Modern Prestressed Concrete Design,* Pitman, London.

Rowe, R.E. *et al.* (1987) *Handbook to British Standard BS8110:1985 Structural Use of Concrete,* Viewpoint, London.

Sawko, F. (ed.) (1978) *Developments in Prestressed Concrete,* Vols 1 and 2, Applied Science, London.

Warner, R.F. and Faulkes, K.A. (1979) *Prestressed Concrete,* Pitman, Sydney.

BRIDGES

Clark, L.A. (1982) *Concrete Bridge Design to BS5400,* Cement and Concrete Association, London.

Green, J.K. (1973) *Detailing for Standard Prestressed Concrete Bridge Beams,* Cement and Concrete Association, London.

Hambly, E.C. (1991) *Bridge Deck Behaviour* (2nd edn), E&FN Spon, London.

Liebenberg, A.C. (1992) *Concrete Bridges: Design and Construction,* Longman Scientific and Technical, Harlow.

Mathivot, J. (1983) *The Cantilever Construction of Prestressed Concrete Bridges,* Cement and Concrete Association, London.

Pennells, E. (1978) *Concrete Bridge Designer's Manual,* Cement and Concrete Association, London.

Podolny, W. (1982) *Construction and Design of Prestressed Concrete Segmental Bridges,* Wiley, New York.

Strasky, J. (1995) Pedestrian Bridge at Lake Vranov, Czech Republic, *Proceedings of the Institution of Civil Engineers,* 108, August 1995.

Woolley, M.V. and Clark, G.M. (1993) Post-Tensioned Concrete Bridges, *The Structural Engineer,* 71 Nos 23 and 24.

SPECIAL TOPICS

American Society of Civil Engineers, *Fatigue Life of Prestressed Concrete Beams,* Bulletin No. 19 of Reinforced Concrete Research Council.

Concrete Society (1977) *Segmental Precast Prestressed Concrete Piles,* Technical Report No. 12.

Concrete Society (1983), *Partial Prestressing,* Technical Report No. 23.

Cowan, H.J. (1965) *Reinforced Concrete and Prestressed Concrete in Torsion,* London.

Curtin, W.G. and Howard, J. (1991) Research on Prestressed Cantilever Diaphragm Walls, *The Structural Engineer,* **69**, No. 6.

Green, J.K. and Perkins, P.H. (1980) *Concrete Liquid Retaining Structures,* Applied Science, London.

Taylor, H.P.J. (1993) The Railway Sleeper: 50 Years of Pretensioned, Prestressed Concrete, *The Structural Engineer,* **71**, No. 16.

COMPUTING

Hulse, R. and Mosley, W.H. (1987) *Prestressed Concrete Design by Computer,* Macmillan, London.

Index